UNIVERSIDAD AUTONOMA DE MADRID

Procesos y patrones evolutivos en anfibios de la península ibérica: una perspectiva comparada y multiescala

JORGE GUTIÉRREZ RODRÍGUEZ
Museo Nacional de Ciencias Naturales

TESIS DOCTORAL
Madrid, 2017

Universidad Autónoma de Madrid
Dpto. Biología

Museo Nacional de Ciencias Naturales
Dpto. Biodiversidad y Biología Evolutiva

Procesos y patrones evolutivos en anfibios de la península ibérica: una perspectiva comparada y multiescala

Evolutionary patterns and processes in amphibians from the Iberian peninsula: a comparative and multi-scale perspective

Memoria presentada por el licenciado Jorge Gutiérrez Rodríguez para optar al grado de Doctor en Genética y Biología Celular por la Universidad Autónoma de Madrid

DIRECTOR:

Íñigo Martínez-Solano González
Museo Nacional de Ciencias Naturales
Dpto. Biodiversidad y Biología Evolutiva

TUTOR ACADEMICO:

Joaquina de la Torre Escudero
Universidad Autónoma de Madrid
Dpto. Biología

TESIS DOCTORAL
Madrid, 2017

La presente tesis doctoral ha dado lugar a las siguientes publicaciones científicas:

Artículo I

Gutiérrez-Rodríguez J, Gonzalez EG, Martínez-Solano Í (2014) Development and characterization of twelve new polymorphic microsatellite loci in the Iberian ribbed newt, *Pleurodeles waltl* (Caudata: Salamandridae), with data on cross-amplification in *P. nebulosus*. *Amphibia-Reptilia* 35: 129–134.

Artículo II

Gutiérrez-Rodríguez J, Martínez-Solano Í (2013) Isolation and characterization of sixteen polymorphic microsatellite loci in the Western Spadefoot, *Pelobates cultripes* (Anura: Pelobatidae) via 454 pyrosequencing. *Conservation Genetics Resources* 5: 981–984.

Artículo III

Gutiérrez-Rodríguez J, Barbosa AM, Martínez-Solano Í (2017) Integrative inference of population history in the Ibero-Maghrebian endemic *Pleurodeles waltl* (Salamandridae). *Molecular Phylogenetics and Evolution* 112: 122–137.

Artículo IV

Gutiérrez-Rodríguez J, Barbosa AM, Martínez-Solano Í (2017) Present and past climatic effects on the current distribution and genetic diversity of the Iberian spadefoot toad (*Pelobates cultripes*): an integrative approach. *Journal of Biogeography* 44: 245–258.

Artículo V

Gutiérrez-Rodríguez J, Gonçalves J, Civantos E, Martínez-Solano Í (2017) Comparative landscape genetics of pond-breeding amphibians in Mediterranean temporal wetlands: the positive role of structural heterogeneity in promoting gene flow. *Molecular Ecology*. En revisión.

Articulo VI

Gutiérrez-Rodríguez J, Sánchez-Montes G, Martínez-Solano Í (2017) Effective to census population size ratios in two Near Threatened Mediterranean amphibians: *Pleurodeles waltl* and *Pelobates cultripes*. *Conservation Genetics*. En prensa.

Jorge Gutiérrez Rodríguez fue financiado por una beca JAEpredoc del Consejo Superior de Investigaciones Científicas (CSIC) y del European Social Fund (ESF). La tesis fue financiada por los proyectos CGL2008-04271-C02-01/BOS, y CGL2011-28300 (Ministerio de Ciencia e Innovación -MICINN-, Ministerio de Economía y Competitividad -MEC-, y FEDER).

Índice

Agradecimientos

En primer lugar, quiero dar las gracias a mi familia, especialmente a mi madre, mi padre y mi hermano. A mi madre por haberme acompañado siempre al campo cuando lo necesitaba y dejarme organizar nuestras vacaciones para ir a coger los bichitos que me apasionaban. A mi hermano principalmente por dejarse engañar en esas vacaciones y colaborar para poder capturar el mayor número de especies posibles. A mi padre por trasmitirme esta afición desde que era pequeño y haberme acompañado y ayudado persiguiendo gallipatos en Valdemanco.

En segundo lugar, ha sido un placer formar parte de esta institución. He pasado grandes momentos con todos mis compañeros, ya amigos, en donde me he sentido como si estuviera en mi casa.

Quiero agradecer a Iñigo por todos los años que hemos pasado juntos a pesar de la distancia física que casi siempre nos ha separado. Por estar pendiente siempre de cada pregunta chorra que se me ocurría y por todos esos momentos en el campo, algunos horribles (congelado o intoxicado por mis queridos anfibios) y otros bien buenos, como esos viajecitos a Portugal.

También quiero recordar a Marina por darme una estupenda bienvenida, principalmente en mis grandes momentos de timidez a la llegada al museo, ahora esto parece poco creíble. Por preocuparse por mí, explicarme todo el laboratorio y siempre estar dispuesta a dar su tiempo para solucionar cualquier duda o problema.

A Mario por haberme dado la oportunidad de empezar en el museo, alimentar mi afición y orientarme (andaba yo bien perdido y queriéndome dedicar a la cría de sapos). También quiero agradecerle por permitirme gastar parte del dinero de sus proyectos en secuenciar todos los tetigónidos que me he ido encontrando todos estos años.

A Rafa por todas sus firmitas “sin pedir nada a cambio”, por todas sus “barbacoas” y por los mejores “lab meetings”.

Quiero agradecer a Joaquina por estar siempre pendiente de mí y estar siempre dispuesta a ayudarme.

A Mercedes y Vicenta por darme acceso y ayudarme en la colección de ortópteros. A Pablo por fomentar mi afición con los tetigónidos. A Guaci por esas primeras enseñanzas con los microsatélites en veterinaria (cuando aún la respetaba, al pensar que sería mi codirectora). A Nacho por traernos comida rica del norte y permitirme robarle las nasas. A Carolina y Annie por alimentarme durante la tesis y darme energías para escribir. A Piluchi por aguantar mis propuestas matrimoniales con su hija, por haberme hecho cientos de extracciones y por hacerme más ameno el laboratorio.

A Karen por despertarme todas las mañana para no llegar tarde al trabajo, presionándome y diciéndome "apúrate", y por esas vacaciones tan especiales que me dieron fuerzas para acabar.

A Paloma por aguantar todas mis bonicas observaciones y por esos momentos tan grandes que hemos pasado procrastinando, muestreando, durmiendo, etc. A mi novia "Juanita" por ser tan comprensiva conmigo y siempre llevarme a tomar cervecitas los domingos y algún que otro día.. . A Silvia por escucharme siempre, pasar tal cantidad de ratos juntos, leer mis párrafos aburridos y esas míticas salidas nocturnas. A Patri por tantas tardes en su sofá, o no tan tardes, y por esos viajes que nos vamos a hacer. A Ernesto por acompañarme siempre en mis viajecitos y demostrar devoción por mis "gafanhotos". A Lourdes por todos esos momentos en la puerta de la jirafa.

Y a otros muchos tantos del museo que pasaron o están en el museo y que me hicieron pasar tan grandes ratos como Miriam, Paula, David, Samu, Chiara, Goyo, Guille, Cristina, Raquel, Iker, Fer, Merel, Miguel, Paty, Andrea, Carlos P, Carlos T, Sofía, Domingo, Ainhoa, Isabel, Tania, P. Lattig, Fede, Alejandro, Michel, Adelmo, Pilar, Buckley, Sebastián, Teresa, Bere, Rosita, Dragan, Alberto, Diushi, Anca, Chio, Rodo, Fafa, Eva, Neus, Jose, Keltoum y Judit.

Y que no se me olvide el mejor camarero del mundo, a Jorge por ponerme esas tapas, sopitas y patxaranes tan ricos que me han alimentado durante la parte final de mi tesis.

A mis compañeros de las estancias en Oporto y Connecticut como el Prof. Pereira, Simona, Daniele, Frank, Diana, Jolita, Javi, Maria Helena, Javi, Hugo, Bruno, Guille, Sara, Elizabeth y Sandra por haberme hecho más amenos los días en la distancia.

A mis amigos de toda la vida: Alex, Juan, Marina, Guille, Laura, Javi P., Javi M., Poca, Polonio y María. Especialmente a Guille y Alex (alias "mi vecino") por hacerse los engañados en nuestras vacaciones, haciendo paradas para hacer pis y en el fondo era para buscar saltamontes. A María por haber vuelto de Inglaterra y por pasar tantos momentos juntos después de salir del museo. A Laura por compartir todos los veranos mis primeras experiencias herpetológicas con ella, que no siempre salieron bien y por ser una de las mejores personas que conozco. A Juan por salvarme en mi estancia de los bosques de Norteamérica, sacarme de ese agujero y acogerme en su casa.

Y todos mi amigos de la universidad por la cantidad de tiempo que hemos pasado juntos para llegar a esto Marcos, Lucia, Celia, Mapatxe, Sofía, Jaime J., Jaime R., Valva y en especial a Marta por soportarme y sufrir las experiencias de Valdemanco.

Resumen

Uno de los principales objetivos de la biología evolutiva es describir los patrones de diversidad biológica y explicar cómo se han originado. Además de dar respuesta a preguntas acerca del origen de las especies, de los factores que determinan su distribución geográfica, o los patrones de diversidad intraespecífica, este conocimiento permite establecer las bases para mitigar o revertir procesos de extinción local y establecer programas de conservación basados en la evidencia científica. Existe un desfase entre el progreso de la catalogación de la biodiversidad y el de su explicación en términos de procesos y mecanismos, que en general avanza a menor ritmo. Para paliar esta diferencia, en los últimos años se ha fomentado la integración de información a diferentes escalas espaciales y temporales y niveles de análisis con objeto de esclarecer el papel de diferentes mecanismos evolutivos en la generación de patrones de diversidad biológica. En la presente tesis doctoral se ha adoptado esta aproximación para profundizar en el conocimiento de la historia evolutiva de dos especies de anfibios de la península ibérica, el gallipato, *Pleurodeles waltl* Michahelles, 1830, y el sapo de espuelas, *Pelobates cultripes* (Cuvier, 1829), mediante un estudio comparado realizado a tres escalas espaciales y temporales. En concreto, se han realizado estudios filogeográficos, de genética del paisaje y de demografía a escala local para adquirir una comprensión integral de los patrones filogeográficos observados e inferir los procesos evolutivos responsables de estos patrones en las dos especies. Para ello, se han empleado datos moleculares, modelos de distribución de especies (SDMs), variables ambientales en sistemas de información geográfica (SIG) y métodos de captura-marcaje-recaptura (CMR). En primer lugar se caracterizaron microsatélites polimórficos para *P. waltl* y *P. cultripes*. Gracias a ello y con el uso adicional de marcadores mitocondriales se han identificado patrones espaciales comunes de subdivisión genética en sentido "Este-Oeste". Sin embargo, los procesos de diversificación son más antiguos (Plio-Pleistoceno) en *P. waltl* que en *P. cultripes* (500 ka). La diversidad genética actual de *P. waltl* y *P. cultripes* está significativa y positivamente correlacionada con las áreas que han permanecido favorables climáticamente para ambas especies desde el último interglaciar (LIG, 140-120 ka). Estas áreas se concentran fundamentalmente en el sur de la

península ibérica y han funcionado como reservorios de diversidad genética a través del tiempo. Por otro lado, se ha documentado que en ambas especies, las poblaciones localizadas cerca de su límite norte de distribución presentan baja diversidad genética y ocupan zonas marginalmente favorables y caracterizadas por una menor estabilidad climática a lo largo del tiempo, especialmente en *P. cultripes*, lo que las hace más vulnerables frente a cambios climáticos a largo plazo. A una escala regional, se han identificado los principales factores asociados a la conectividad poblacional a través del análisis de tres conjuntos de variables a diferentes niveles de resolución espacial que potencialmente afectan al flujo génico. Se han encontrado diferentes patrones de estructura genética, siendo más marcados y a una escala más fina de diferenciación en *P. waltl*. Además, se han observado similitudes en el efecto de la topografía a escala regional y diferencias marcadas en el papel de la heterogeneidad y del contenido en agua de la cubierta vegetal en la estructura genética de las dos especies a una escala fina. Los resultados sugieren que ciertos tipos de vegetación, principalmente zonas estructuralmente heterogéneas de matorral mediterráneo y dehesas, favorecen la conectividad poblacional. A una escala local y mediante el uso de técnicas de CMR, las tasas de dispersión observadas resultaron ser bajas para las dos especies, aunque mayores en *P. cultripes*. Estos datos de dispersión son consistentes con las diferencias observadas en la estructura genética de ambas especies a diferentes escalas. Por otro lado, no se hallaron diferencias significativas en los patrones de dispersión entre sexos en *P. cultripes*, mientras que en *P. waltl* existen evidencias tanto directas como indirectas que sugieren una mayor tasa de dispersión en hembras. Por último, se estimó el ratio entre el tamaño efectivo (Ne, y su variante Nb) y el tamaño de censo de la población (Nc). Este ratio es uno de los parámetros más importantes para la gestión de poblaciones silvestres, porque combina información sobre la abundancia de la población y su diversidad genética, y ayuda por tanto a predecir la viabilidad de la población a largo plazo. Se obtuvieron las primeras estimas de los ratios Ne/Nc y Nb/Nc en *P. waltl* y *P. cultripes* mediante la combinación de observaciones directas de campo y aproximaciones moleculares. Ambas especies mostraron ratios similares, siendo ligeramente inferiores en *Pleurodeles* (0,21-0,24) con respecto a *Pelobates* (0,25-0,30). Los resultados obtenidos en la presente tesis doctoral permiten sustentar

medidas de conservación orientadas al diseño de corredores naturales que tengan en cuenta las características biológicas de las dos especies, sus preferencias en la selección de hábitat y su historia evolutiva, con objeto de garantizar la conservación de su diversidad genética y potencial evolutivo.

Summary

One of the main goals of evolutionary biology is to describe patterns of biological diversity and explain how they have originated. In addition to answering questions about the origin of species, the factors shaping their geographical distribution, or patterns of intraspecific diversity, this knowledge can be applied for mitigating or reversing local extinction processes and establishing conservation programs based on scientific evidence. There is a mismatch between the progress in cataloging biodiversity and its explanation in terms of processes and mechanisms, which generally advances at a slower rate. In order to close this gap, recent studies have called for the integration of information at different spatial and temporal scales and levels of analysis to clarify the role of different evolutionary mechanisms in the generation of patterns of biological diversity. In this PhD dissertation, we have adopted this approach to study the evolutionary history of two amphibian species from the Iberian Peninsula, the Iberian ribbed newt, *Pleurodeles waltl* Michahelles, 1830, and the western spadefoot toad, *Pelobates cultripes* (Cuvier, 1829), conducting a comparative study at three spatial and temporal scales. Specifically, we have carried out phylogeographic, landscape genetics and local-scale demographic studies to produce an integral perspective on the observed phylogeographic patterns and infer the evolutionary processes responsible for these patterns in both species. For this purpose, we used molecular data, species distribution models (SDMs), environmental variables in geographic information systems (GIS) and capture-mark-recapture (CMR) methods. Firstly, novel sets of polymorphic microsatellites were characterized for *P. waltl* and *P. cultripes*. With the addition of mtDNA sequences, we found a common spatial pattern of genetic subdivision (East-West) in both species. However, intraspecific diversification in *P. waltl* is older (Plio-Pleistocene) than in *P. cultripes* (500 ka). Genetic diversity in *P. waltl* and *P. cultripes* is significantly and positively correlated with regions that have remained environmentally favourable through the last interglacial (LIG, 140-120 ka). These areas are mostly located in southern Iberia and have acted as reservoirs of genetic diversity through time. Additionally, populations of both species at the northern end of their ranges show lower genetic diversity and tend to occupy marginally favourable areas, which are characterized by low climatic

stability through time. This is especially the case of *P. cultripes*, which makes this species more vulnerable to long-term climate change. At the regional scale, we identified major factors associated with population connectivity through the analysis of three sets of variables potentially affecting gene flow at increasingly finer levels of spatial resolution. We found differences in genetic structure across species, with stronger, finer-scale genetic structure in *P. waltl*. In addition, we observed a similar effect of topography but notable differences in the role of fine-scale patterns of heterogeneity in vegetation cover and water content in shaping patterns of regional genetic structure in the two species. We found a positive role of certain vegetation types and structural heterogeneity (mainly habitat patches of Mediterranean scrubland and open oak woodlands, or "dehesas") in facilitating population connectivity in both species. At the local scale, observed displacement rates were low in both species, although higher in *P. cultripes*, which is consistent with observed differences in the genetic structure of both species at different scales. We did not find evidence for sex-biased dispersal in *P. cultripes*, but both direct and indirect evidence suggest a tendency for female-biased dispersal in *P. waltl*. Finally, we estimated effective (Ne, and the related measure Nb) to census population size (Nc) ratios. These are among the most important parameters to take into account for the management of wildlife populations, because they combine information on population abundance and genetic diversity and help predict population viability in the long term. We obtained the first estimates of the Ne/Nc and Nb/Nc ratios in *P. waltl* and *P. cultripes* through the integration of field-based and molecular approaches. Both species showed similar ratios, although slightly lower in *Pleurodeles* (0.21-0.24) than in *Pelobates* (0.25-0.30). Our findings can be used to design corridors connecting populations of both species, taking into account their biological characteristics, preferences in habitat selection and evolutionary history, to help preserve their genetic diversity and evolutionary potential.

Introducción general

Uno de los principales objetivos de la biología evolutiva es describir los patrones de diversidad biológica y explicar cómo se han originado (Okasha, 2016). Los avances en el proceso de catalogación de la Biodiversidad deben ir acompañados de una mejor comprensión acerca de los procesos y mecanismos que generan diversidad (Hardisty y Roberts, 2013). Además de dar respuesta a preguntas acerca del origen de las especies o de los factores que determinan su distribución geográfica, o los patrones de diversidad intraespecífica, este conocimiento permite además establecer las bases para mitigar o revertir procesos de extinción local y establecer programas de conservación basados en evidencia científica (Hoban *et al*., 2013; Frankham *et al*., 2014).

No obstante, existe un desfase entre el proceso de catalogación y el de explicación en términos de procesos y mecanismos, que en general avanza a menor ritmo. Para paliar esta diferencia, en los últimos años se ha fomentado la integración de información a diferentes escalas espaciales y temporales y niveles de análisis con objeto de esclarecer el papel de diferentes mecanismos evolutivos en la generación de patrones de diversidad biológica (Buckley, 2009). En la presente tesis doctoral se ha adoptado esta aproximación para profundizar en el conocimiento de la historia evolutiva de dos especies sintópicas de anfibios de la península ibérica, el gallipato, *Pleurodeles waltl* Michahelles, 1830, y el sapo de espuelas ibérico, *Pelobates cultripes* (Cuvier, 1829), mediante un estudio comparado realizado a tres escalas espaciales y temporales. En concreto, se han realizado estudios filogeográficos, de genética del paisaje y de demografía a escala local para adquirir una comprensión integral de los patrones filogeográficos observados e inferir los procesos evolutivos responsables de estos patrones en las dos especies.

Ventajas de realizar estudios comparados

El estudio comparado de especies ampliamente co-distribuidas, como es el caso de las elegidas para este estudio, permite discernir el papel relativo de factores demográficos, ecológicos e históricos en su historia evolutiva (Papadopoulou y Knowles, 2016). Por ejemplo, a escala filogeográfica es posible analizar la congruencia de los patrones de variación genética entre especies y determinar si comparten una historia evolutiva común (Zink, 1996), analizando si los eventos

vicariantes que han afectado a las especies son similares tanto a escala espacial como temporal y determinando si los cambios en su tamaño efectivo poblacional a lo largo del tiempo han sido sincrónicos o no (Arbogast y Kenagy, 2001). Además, a escala de paisaje, la aproximación comparada permite identificar diferencias interespecíficas asociadas al efecto variable de diversas características del paisaje en los patrones de conectividad y flujo génico entre poblaciones y permiten por tanto identificar los factores que actúan como barreras a la dispersión (Schwenk y Donovan, 2011; Keller *et al*., 2014). Comprender cuáles son los procesos implicados en la diferenciación genética entre poblaciones a escala contemporánea ayuda a inferir de una manera más robusta cuáles pudieron ser los mecanismos históricos responsables de los patrones de diversidad genética de las especies a una escala espacial y temporal mayor (filogeográfica). Los estudios de genética del paisaje comparada pueden inferir además el papel de ciertas características ecológicas de las especies (por ejemplo, relacionadas con aspectos de sus historias vitales o "life histories") en su estructura genética, por ejemplo evaluando la relación entre las diferencias en la capacidad de dispersión entre las especies objeto de estudio y su estructura genética (Goldberg y Waits, 2010; Coster *et al*., 2015). Dado que las estimas genéticas de migración pueden subestimar la capacidad real de dispersión de los organismos de estudio, observada directamente en estudios demográficos mediante técnicas de CMR (Lowe y Allendorf, 2010), es importante complementar aproximaciones moleculares con estudios de campo. De este modo es posible comprender cómo los patrones de dispersión y conectividad a pequeña escala generan patrones de diversidad y estructura a escalas temporales y espaciales mayores.

Filogeografía

Esta disciplina fue inicialmente concebida como un puente entre la sistemática molecular y la genética de poblaciones (Chan *et al*., 2011). Se centra en el estudio de las relaciones entre las genealogías de genes y la geografía, a escala intraespecífica o de especies estrechamente relacionadas (Avise *et al*., 1987; Avise, 2000), mediante la inferencia de tasas históricas de migración, expansiones/declives poblacionales, cuellos de botella y eventos de vicarianza y su papel en la historia evolutiva de las especies (Avise, 2000; Avise, 2009). La

filogeografía plantea hipótesis relacionando los patrones genéticos con eventos geológicos, factores ambientales e interacciones entre factores geográficos y aspectos de la ecología e historia natural de las especies (Knowles, 2009). Para ello, se apoya en el hecho de que procesos históricos como la subdivisión de poblaciones, las expansiones poblacionales o los procesos de nueva colonización producen distintos patrones en la distribución y relaciones entre sí de los alelos en poblaciones y especies (Templeton *et al*., 1995; Sexton *et al*., 2014). Dos de los factores más determinantes en la formación y evolución de la estructura filogeográfica de las especies son la distancia media de dispersión y el tamaño efectivo poblacional (Irwin y Gibbs, 2002). En general, las especies con distancias de dispersión más bajas suelen presentar una estructura filogeográfica más marcada, como consecuencia de la acción de barreras geográficas al flujo génico (Avise *et al*., 1994). La presencia de una fuerte estructura filogeográfica también está relacionada con la existencia de tamaños poblacionales bajos (Irwin y Gibbs, 2002). El origen de linajes evolutivos intraespecíficos bien diferenciados genéticamente generalmente está asociado a eventos de vicarianza, en los que la aparición de una barrera biogeográfica o la dispersión activa o pasiva desde los centros ancestrales de origen a nuevas áreas sin colonizar fragmenta una población en un conjunto de poblaciones más o menos aisladas.

El principal proceso responsable de generar diversidad genética en los individuos de una especie es la mutación, mientras que la migración, la deriva genética y la selección natural son mecanismos que alteran las frecuencias génicas en las poblaciones. Generalmente las tasas de mutación son muy bajas, entre 10^{-4} y 10^{-6} por gen y generación (Hartl y Clark, 1997). En el caso de la deriva génica, los cambios en las frecuencias alélicas entre poblaciones se producen de manera aleatoria a lo largo del tiempo, mientras que la selección natural favorece a las variantes que están asociadas a un mayor éxito reproductivo. Por último, la migración también es determinante en los procesos de diferenciación genética, ya que produce un efecto homogeneizador entre las poblaciones (Gagnaire *et al*., 2015). Estas cuatro fuerzas evolutivas (mutación, migración, deriva y selección) son las responsables últimas de los patrones de diversidad genética que encontramos en la naturaleza, y discernir su papel relativo a lo largo de la historia evolutiva de las especies es uno de los principales objetivos de la biología evolutiva.

Para reconstruir la historia evolutiva de las especies a escala filogeográfica, los marcadores moleculares más usados tradicionalmente han sido los genes del ADN mitocondrial (ADNmt). Esto es debido a que presentan una serie de ventajas frente a los genes nucleares. La molécula de ADNmt se caracteriza por carecer de intrones, tiene limitada o nula recombinación, presenta genes ortólogos y su modo de herencia es haploide (Saccone *et al*., 1999). Este modo de herencia hace que su tamaño efectivo sea menor (una cuarta parte) que el del ADN nuclear autosómico (Moore, 1995), lo que a su vez va asociado a tasas de substitución de nucleótidos uno o varios órdenes de magnitud más rápidas que las documentadas en genes nucleares de copia única (Avise, 2009). Como resultado, en ausencia de selección y migración, los genes mitocondriales divergen más rápido por deriva genética que los genes nucleares (Hare, 2001) y el proceso de formación de genealogías con grupos recíprocamente monofiléticos es más rápido que en el caso de los marcadores nucleares (Irwin y Gibbs, 2002). Sin embargo, al tener herencia uniparental, las genealogías de ADNmt no siempre son congruentes con la historia evolutiva de la especie, sobre todo cuando existen diferencias entre sexos en caracteres que afectan al "fitness" o a comportamientos dispersivos (Hoelzer, 1997). Por estos motivos, las aproximaciones filogeográficas que combinan marcadores de los genomas mitocondrial y nuclear ofrecen la oportunidad de reconstruir de una manera más fidedigna los patrones genealógicos en función de la historia y el ambiente que las poblaciones han experimentado (Hare, 2001; Hung *et al*., 2016).

Más recientemente, el uso de marcadores microsatélites ha llegado a ser común en filogeografía (Díaz *et al*., 2017; Vila *et al*., 2017). Estos marcadores se caracterizan por ser repeticiones en tándem generalmente de menos de 5 pares de bases de longitud y con una alta variabilidad asociada a la presencia de un diferente número de repeticiones en individuos de una misma población (Jehle y Arntzen, 2002). Se les considera marcadores neutrales codominantes, con herencia mendeliana simple y que pueden llegar a presentar un número muy alto de alelos en un mismo locus (González, 2003). Los microsatélites presentan altas tasas de mutación, entre 10^{-3} y 10^{-4} por locus y generación (Ellegren, 2000). Generalmente, estos marcadores son especialmente útiles para inferir eventos demográficos recientes (Pearse y Crandall, 2004), mientras que los marcadores

mitocondriales permiten reconstruir de manera más robusta el resultado de procesos más antiguos. Sin embargo, el uso de los microsatélites también puede plantear una serie de complicaciones, ya que en ocasiones pueden presentar diferentes tasas de mutación entre loci o entre alelos de un mismo locus, lo que hace que sean difícilmente comparables entre taxones. Además, pueden existir problemas de homoplasia debido a sus altas tasas de mutación y se han descrito también diferentes artefactos asociados al proceso de genotipado, como los alelos nulos (Brito y Edwards, 2009). A pesar de las limitaciones de ambos tipos de marcadores, ADNmt y microsatélites, su combinación ofrece información complementaria y puede revelar diferentes aspectos de la compleja historia evolutiva de las especies a diferentes escalas temporales (Zhang y Hewitt, 2003). De este modo, permiten desentrañar de una manera más completa los procesos evolutivos responsables de la distribución actual de la variación genética, mediante la inferencia de cambios demográficos o eventos vicariantes asociados a barreras al flujo génico, tanto históricas como contemporáneas. Por ello, además del uso de genes mitocondriales, en esta tesis se ha dedicado un importante esfuerzo a optimizar nuevos marcadores de tipo microsatélite en las dos especies objeto de estudio (ver más abajo). El proceso de optimización se describe en el capítulo I y ha resultado satisfactorio en tanto que los marcadores desarrollados han aportado información relevante a todas las escalas espaciales y temporales investigadas.

Muchas de las preguntas fundamentales en filogeografía se refieren a cómo la variación física y climática en el espacio y el tiempo modelan los patrones de divergencia genética (Kozak *et al*., 2008). En este sentido, incorporar modelos de distribución de especies (SDMs) a estudios filogeográficos permite incorporar técnicas geoespaciales para identificar áreas con alta y baja favorabilidad climática, que representan la tolerancia ecológica de las especies frente a cambios ambientales a macroescala (Chan *et al*., 2011). Generalmente, estos modelos predicen la probabilidad de presencia de las especies en un área geográfica en base a una serie de variables climáticas, como la precipitación anual o la temperatura (Phillips *et al*., 2006). Los SDMs permiten estimar las áreas de distribución en el pasado (hasta el último periodo interglaciar, aproximadamente hace 120-140 miles de años, ka) mediante la proyección de las distribuciones actuales en base a reconstrucciones paleoclimáticas. Estos modelos también presentan algunas

limitaciones, ya que generalmente asumen la estabilidad del nicho, es decir, una relación constante entre el clima y la presencia de las especies, y rara vez tienen en cuenta las limitaciones asociadas a la capacidad de dispersión o las interacciones bióticas entre especies (Waltari *et al*., 2007; Pearman *et al*., 2008). Sin embargo, se ha demostrado que la combinación de datos moleculares y SDMs puede producir hipótesis filogeográficas robustas acerca de la demografía histórica en una gran variedad de taxones (Fitze *et al*., 2011; Hegna *et al*., 2015; Tsuda *et al*., 2015). Por ejemplo, un objetivo fundamental de la filogeografía es evaluar el papel de los ciclos glaciales, asociados a eventos de expansiones y contracciones demográficas, en los patrones actuales de diversidad genética (Kozak *et al*., 2008). Los SDMs permiten identificar áreas que han permanecido climáticamente estables a través de varios ciclos glaciales y mediante el análisis de su correlación con las áreas de mayor diversidad genética actual es posible evaluar su papel como refugios glaciales. Además, la combinación de datos moleculares y SDMs permite asociar los eventos demográficos históricos inferidos en las especies a partir de las señales que dejan en el genoma con los cambios climáticos ocurridos durante los periodos glaciares, revelando los mecanismos ecológicos y evolutivos responsables de los procesos de diferenciación poblacional (Chan *et al*., 2011).

En esta tesis se han realizado estudios filogeográficos en las dos especies objeto de estudio combinando información de marcadores mitocondriales y nucleares (genes nucleares y microsatélites) e integrando SDMs proyectados al pasado, como se describe en el capítulo II.

Genética del paisaje

Los estudios filogeográficos suelen estar centrados en una escala en la que los factores que afectan tanto a las distribuciones históricas como a las actuales de las especies son críticos para entender los procesos que estructuran los patrones de variación genética (Knowles, 2009). Tanto la filogeografía como la genética del paisaje tienen como objetivo fundamental comprender la distribución espacial de la diversidad genética (Avise *et al*., 1987; Manel *et al*., 2003). La diferencia fundamental entre la genética del paisaje y la filogeografía es el contexto temporal en el cual se centra cada una de ellas; la primera investiga los procesos contemporáneos, mientras la filogeografía investiga procesos históricos

(Sork y Waits, 2010). La genética del paisaje tiene como objetivo entender cómo las características específicas del paisaje y los procesos microevolutivos como el flujo génico, la deriva genética y la selección interactúan para configurar la cantidad y la distribución espacial de la variación genética (Manel *et al*., 2010), así como identificar las características del paisaje que promueven o limitan la conectividad genética de las poblaciones (Storfer *et al*., 2010).

Para ello, esta disciplina utiliza generalmente marcadores de evolución rápida como los microsatélites, los cuales proporcionan una excelente resolución para inferir procesos contemporáneos, mientras en filogeografía el marcador más usado ha sido el ADN mitocondrial, más adecuado para comprender los procesos históricos (Wang, 2010). Las metodologías de genética del paisaje integran datos topográficos, geográficos y ecológicos en sistemas de información geográfica (SIG), con medidas explícitas de diversidad y diferenciación genética, junto a estimas de tamaño efectivo poblacional, los cuales pueden ayudar a identificar las barreras al flujo génico y entender de una manera más adecuada los factores que limitan la conectividad en un contexto evolutivo (Chan *et al*., 2011). La filogeografía y genética del paisaje representan una combinación idónea para entender los procesos microevolutivos tanto recientes como históricos (Wang, 2010), ya que los factores contemporáneos que afectan a la estructura genética de las poblaciones pueden ayudar a entender los procesos históricos que ocurrieron en el pasado. En general las variables más utilizadas para inferir conectividad a nivel de paisaje están asociadas a la topografía, hidrología y usos del suelo, aunque más recientemente se han incorporado también diferentes índices de humedad y cobertura y heterogeneidad de la vegetación mediante técnicas de teledetección, los cuales permiten caracterizar hábitats terrestres a una escala fina para organismos con baja capacidad de dispersión (Wulder *et al*., 2004; Greenberg *et al*., 2005; Peterman *et al*., 2014).

Para investigar los factores que determinan la estructura genética de las especies a escala de paisaje, en esta tesis se ha llevado a cabo un estudio comparado analizando variables describiendo el hábitat de las dos especies de anfibios seleccionadas a diferentes grados de resolución, incluyendo la cobertura vegetal o los distintos usos del suelo, como se describe en el capítulo III.

Demografía

El efecto de la selección, la deriva genética o la migración está fuertemente condicionado por factores demográficos (Metcalf y Pavard, 2007). Por ejemplo, las tasas de migración están relacionadas con la estructura de edad de las poblaciones, ya que en general los juveniles son más proclives a colonizar nuevas áreas, y el tamaño efectivo de las poblaciones afecta directamente a la deriva genética, ya que en poblaciones de mayor tamaño el tiempo de fijación de los alelos debido al azar es mayor. Tanto la distancia de dispersión como el tamaño efectivo poblacional interactúan para determinar la estructura filogeográfica de una especie (Irwin y Gibbs, 2002; Weckworth *et al*., 2013).

En general, el papel de la dispersión en la formación patrones filogeográficos ha sido más ampliamente documentado que el del tamaño efectivo. Tanto la estructura genética de las poblaciones de una especie como el origen y establecimiento final de linajes evolutivos independientes dependen de los patrones de flujo génico entre poblaciones (Schaal *et al*., 1998; Arnold, 2015). La dispersión determina la escala espacial en la cual se produce mezcla genética entre poblaciones y, por tanto, su grado de homogeneidad y endogamia. La divergencia genética entre poblaciones está a menudo correlacionada con el grado de aislamiento geográfico y es consistente con la idea de que el flujo genético reduce la divergencia, en oposición al efecto de la selección natural, que tiende a aumentarla (Lenormand, 2002). Esto puede ser explicado por la acción de la deriva génica o por la variación de la presión de la selección con la distancia (Lenormand, 2002). Sin embargo, en gran parte de las especies que han sido estudiadas desde un punto de vista filogeográfico existe un amplio desconocimiento acerca de los patrones de conectividad espacial entre poblaciones a pequeña escala. Esto se debe a que obtener observaciones directas de dispersión es difícil para muchas especies; sin embargo, estas estimas pueden ser obtenidas mediante técnicas de marcaje-captura-recaptura o de manera indirecta mediante estudios de genética del paisaje, aunque es importante comparar ambas aproximaciones porque pueden ofrecer resultados dispares.

El tamaño efectivo poblacional (Ne) también juega un papel determinante en biología evolutiva, así como en biología de la conservación (Frankham *et*

al., 2014). Se define como el tamaño de una población "ideal" que experimenta la misma tasa de cambio de frecuencias de alelos o heterocigosidad que la población objeto de estudio (Wright, 1931). El tamaño efectivo poblacional determina la tasa de cambio genética en una población debida a deriva génica (Charlesworth, 2009) y es crucial para estimar la variabilidad genética de la población y la efectividad relativa de la selección frente a la deriva génica. Por ello, el valor de Ne está relacionado a su vez con las tasas de evolución del ADN. En poblaciones con tamaño efectivo reducido, la deriva genética dicta el cambio de frecuencias alélicas (Nei *et al*., 1975) y puede llegar a generar procesos rápidos de especiación. Esto se debe a que la probabilidad de fijación de genes coadaptados es mayor en poblaciones pequeñas (Crow y Kimura, 1965). Sin embargo, en poblaciones grandes el efecto de la deriva es leve comparado con el de la selección (Hartl y Clark, 1997). El efecto esperado de la deriva genética está inversamente relacionado con el tamaño efectivo de la población (Caballero, 1994). El tamaño efectivo de la población (Ne) puede estar condicionado por parámetros demográficos, como por ejemplo la proporción de sexos o sex ratio, la variación en la cantidad de progenie generada y la estructura de edad, lo que produce a su vez cambios en el tamaño poblacional y de manera indirecta en la estructura genética y espacial de las especies (Charlesworth, 2009). Por ejemplo, el tamaño efectivo de la población se reduce drásticamente con respecto al número de individuos reproductores (N) si la proporción entre hembras y machos está ampliamente sesgada hacia uno de los dos sexos, o cuando la varianza en el éxito reproductor es mayor a la esperada en relación al azar. También se reduce el tamaño efectivo en situaciones de endogamia, en poblaciones que están estructuradas por edad y estadios vitales, o si se producen cuellos de botella o extinciones locales en metapoblaciones conectadas entre sí mediante flujo génico. En cambio, el tamaño efectivo de la metapoblación aumenta cuando la migración entre las poblaciones es limitada (Charlesworth, 2009).

Para investigar el efecto de parámetros demográficos locales como la dispersión o el tamaño poblacional en la estructura genética regional y global de las especies, en esta tesis se han llevado a cabo estudios de captura-marcaje-recaptura durante un periodo de al menos 4 años (en algunos casos hasta 8 años de seguimiento) en las dos especies objeto de estudio en una población de la Sierra

de Guadarrama. Los resultados han sido posteriormente interpretados en relación con las estimas indirectas obtenidas a partir de la aplicación de marcadores moleculares, como se describe en el capítulo IV.

Área de estudio

La presente tesis doctoral se ha centrado principalmente en la península ibérica, donde las dos especies seleccionadas para su estudio presentan el núcleo central de su distribución. La península ibérica forma parte de la cuenca Mediterránea, uno de los 25 puntos calientes de biodiversidad a nivel mundial (Myers *et al*., 2000), que se caracteriza por ser una de las áreas con más riqueza de especies y endemismos de Europa, junto con la península itálica y los Balcanes. Esto se debe a un conjunto de factores, entre ellos su compleja historia geológica, con puentes con el norte de África en diferentes momentos históricos, una orientación este-oeste de sus principales cadenas montañosas, que limita movimientos poblacionales latitudinales, y la existencia de una gran diversidad de pisos bioclimáticos. Estos factores hacen de la península ibérica uno de los refugios glaciales pleistocénicos más importantes de Europa (Gómez y Lunt, 2007).

Desde un punto de vista paleogeográfico, el periodo del Mioceno al Pleistoceno ha contribuido de manera fundamental a los procesos de especiación y diversificación de los vertebrados ibéricos actuales. En el Mioceno, la mayor parte de la deformación tectónica de Iberia se produjo debido al choque entre ésta y África, a consecuencia del cual se formaron las cordilleras béticas, el arco de Gibraltar y el Rif (Platt *et al*., 2013). Durante ese periodo existían varios corredores entre el Atlántico y Mediterráneo, como el corredor Nord bético, el corredor del Guadalhorce y los corredores rifeños (Martín *et al*., 2009). Como consecuencia de la crisis del Mesiniense se produjo la desecación del Mediterráneo y se estableció el último puente entre la península y el norte de África (Krijgsman *et al*., 1999). Desde el Plioceno hasta la actualidad, el estrecho de Gibraltar ha sido la única conexión entre el Mediterráneo y el Atlántico. Estas conexiones y desconexiones a lo largo del tiempo han causado sucesivos eventos vicariantes y por tanto han contribuido de manera fundamental a los procesos de diversificación en la península ibérica y el norte de África. Más recientemente, durante el Pleistoceno se produjo una serie de oscilaciones climáticas, con periodos fríos y cálidos

sucediéndose en el tiempo. Estas oscilaciones tuvieron un importante efecto en los patrones de diversidad genética de muchas especies de climas templados, causando contracciones y expansiones demográficas y fenómenos de extinción y dando forma a la distribución actual de las especies (Hewitt, 1996, 2004; Provan y Bennett, 2008). Los cambios climáticos pleistocénicos afectaron de manera desigual a diferentes áreas geográficas, causando fuertes extinciones por ejemplo en el centro y norte de Europa pero favoreciendo la supervivencia de comunidades enteras asociadas a los denominados refugios glaciales en áreas más cálidas, entre las que se cuenta la península ibérica. Estas áreas tienen una mayor riqueza y endemicidad de especies, así como una mayor diversidad genética a nivel intraespecífico (Ursenbacher *et al*., 2015; Wielstra *et al*., 2015). Dentro del refugio ibérico se ha descrito la existencia de múltiples refugios independientes, asociados a subdivisiones genéticas originadas por el aislamiento de grupos de poblaciones en diferentes sectores de la península durante las glaciaciones del Pleistoceno (Gómez y Lunt, 2007). Estos fenómenos de aislamiento y divergencia acontecidos durante las glaciaciones han dado lugar al origen de linajes intraespecíficos o incluso a procesos de especiación en algunos taxones. Las especies adaptadas a climas mediterráneos se suelen caracterizar por una mayor diversidad genética en el sur de su distribución, que incluye áreas históricamente más estables tanto demográfica como climáticamente, en contraste con la homogeneidad genética que se observa en el norte (Hewitt, 1996, 2000).

Desde un punto de vista biogeográfico, en la península ibérica están presentes dos de las regiones corológicas más importantes de Europa Occidental. La región mediterránea ocupa la mayor parte de la península ibérica, y está dominada por bosque y matorral mediterráneos con inviernos suaves y lluviosos y veranos cálidos. Por otro lado, la región eurosiberiana está restringida al norte y noroeste de la península y se caracteriza por la existencia de bosques caducifolios, con inviernos húmedos, fríos y lluvias durante el verano. La península ibérica se caracteriza por presentar una gran heterogeneidad topográfica, con múltiples cadenas montañosas orientadas mayoritariamente de oeste a este. Esta accidentada topografía tiene como consecuencia fuertes gradientes altitudinales, asociados a su vez a la existencia de varios pisos bioclimáticos dentro de cada una de las regiones corológicas. De este modo es posible la presencia de un gran

número de hábitats diferentes en áreas relativamente reducidas, que favorecen la coexistencia de especies. Todo ello resulta en la gran riqueza específica que caracteriza a la península ibérica, que presenta además una gran heterogeneidad en cuanto a patrones de distribución, con un gran número de endemismos en múltiples grupos taxonómicos.

Grupo de estudio

Los anfibios son el grupo de vertebrados con mayor número de especies amenazadas, con casi un tercio de sus especies catalogadas bajo alguna categoría de amenaza (IUCN *et al*., 2008). Actualmente sus poblaciones están en declive en todas las regiones del mundo (Stuart *et al*., 2008); esto se debe principalmente a la destrucción y fragmentación de sus hábitats, la mortalidad asociada a enfermedades infecciosas, los efectos negativos de especies exóticas y el cambio climático (Hof *et al*., 2011). Se caracterizan por tener baja capacidad de dispersión (Bowne y Bowers, 2004; Graeter *et al*., 2008), tamaños efectivos poblacionales bajos (Funk *et al*., 1999) y en general por la fragmentación natural de sus hábitats de reproducción (Jehle *et al*., 2005).

En la cuenca mediterránea, los anfibios presentan un alto riesgo de extinción a medio y largo plazo (Araújo *et al*., 2006). Muchas de las especies presentan distribuciones fragmentadas, debido a la dependencia de puntos de agua para la reproducción, cuya disponibilidad disminuirá en las próximas décadas debido al incremento de la aridez, cambios de los usos del suelo y efectos impredecibles en el hidroperiodo (Doulgeris *et al*., 2016).

En la presente tesis doctoral se han seleccionado dos especies endémicas de la peninsula ibérica con requerimientos ecológicos similares, *Pleurodeles waltl* y *Pelobates cultripes*. En un análisis basado en doce factores ambientales, ambas especies mostraron los mayores índices de similaridad (Índice de Jaccard) entre dos especies de anfibios ibéricos (Sillero *et al*., 2009), y de hecho a menudo se encuentran en sintopía. Sus poblaciones se encuentran en declive debido a la perdida de hábitats acuáticos, la fragmentación de sus hábitats y la introducción de especies invasoras (Montori *et al*., 2002; Tejedo y Reques, 2002), por lo que han sido catalogadas como especies Casi Amenazadas (NT) por la IUCN (Beja *et al*., 2009; Beja *et al*., 2016). A continuación se resumen algunos aspectos básicos

Figura 1. Ejemplar adulto de *P. waltl* en la Laguna de Valdemanco (Madrid).

de su historia evolutiva, distribución y biología.

***Pleurodeles waltl* Michahelles, 1830 (Fig. 1)**

Es una especie de tritón perteneciente a la familia Salamandridae conocida comúnmente como gallipato. El género está formado por tres especies, que se distribuyen por el oeste de la región mediterránea. *Pleurodeles nebulosus* (Guichenot, 1850) se extiende por el norte de Argelia y Túnez, mientras que *Pleurodeles poireti* (Gervais, 1836) se distribuye exclusivamente en la península de Edough en Argelia (Carranza y Wade, 2004; Escoriza *et al*., 2016). Por último, *P. waltl* está distribuida por la mayor parte de la península ibérica y noroeste de Marruecos (Fig. 2), ocupando principalmente el piso bioclimático mesomediterráneo, aunque también se encuentra en el termomediterráneo y supramediterráneo (Montori *et al*., 2002). Su rango altitudinal comprende desde el nivel del mar hasta los 1540 metros en la Sierra de Guadarrama, en el Sistema Central (Martínez-Solano, 2006), con poblaciones más escasas a partir de los 1000 metros de altitud (García-París *et al*., 2004).

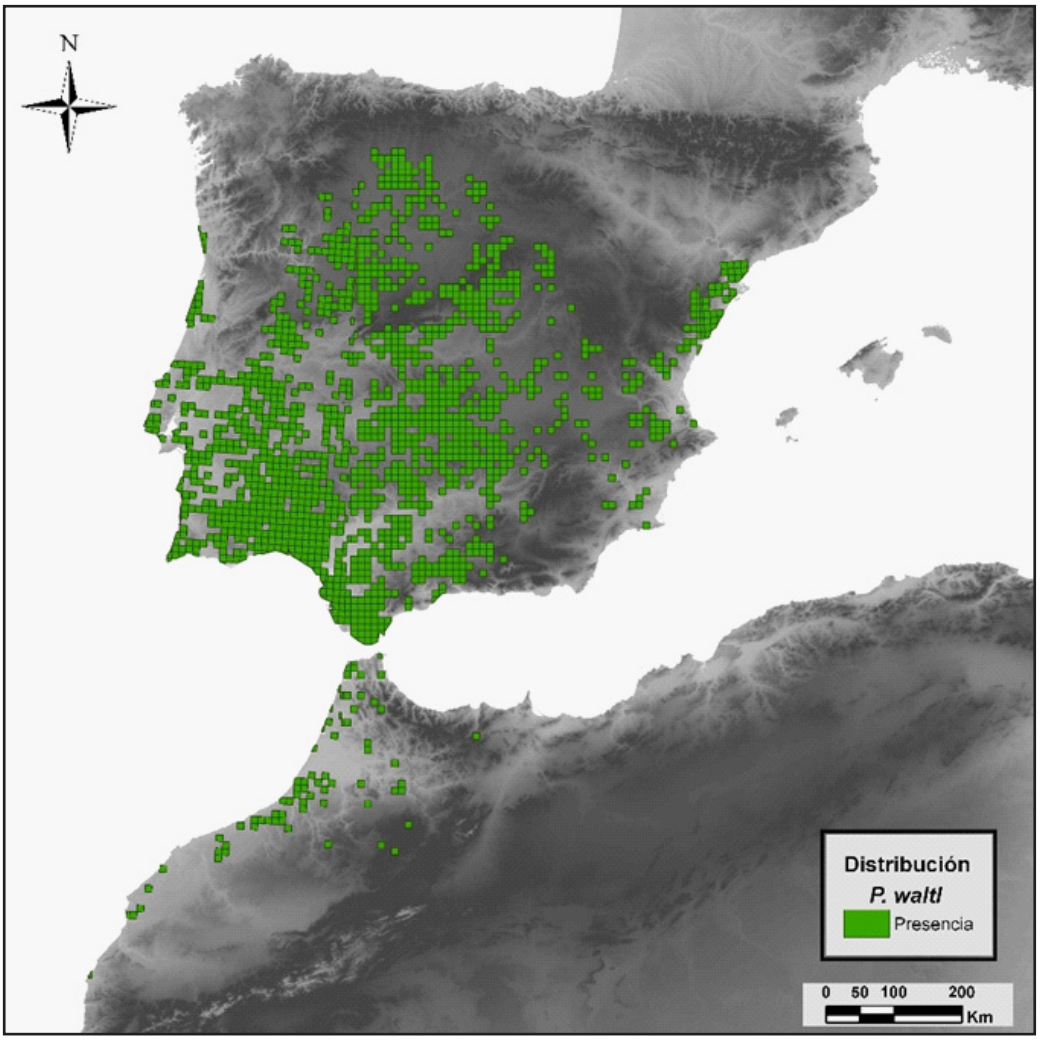

Figura 2. Mapa de distribución de *P. waltl* en cuadrículas de 10x10km, basado en los atlas herpetológicos de Portugal (Loureiro *et al*., 2008), España (MAGRAMA, 2015) y Marruecos (Bons y Geniez, 1996). Además, se han incluido datos de localidades adicionales en Marruecos presentadas por Beukema *et al*. (2013).

Es una especie nocturna, siendo infrecuente observar individuos activos durante el día. Se reproduce en todo tipo de puntos de agua, como pueden ser charcas temporales, lagunas y cursos de agua lenta, ocupando también medios antrópicos como pueden ser canteras abandonadas, canales de riego, pozos, embalses y albercas (García-París, 1985). Habita preferentemente en medios grandes, profundos y con escasa corriente (Díaz-Paniagua, 1983). En general, los individuos de poblaciones más septentrionales presentan una fase acuática más corta que los de la mitad meridional de la península ibérica. La época de

reproducción suele comenzar desde el mes de diciembre y se extiende hasta mayo, con pequeñas variaciones dependiendo del área geográfica (García-París *et al*., 2004). El apareamiento se produce siempre bajo el agua, colocándose el macho bajo la hembra y sujetándola por las axilas de los miembros anteriores. Tras ello, el macho deposita un espermatóforo, que es recogido por la hembra. La fecundación se produce en la cavidad de la cloaca de la hembra, a medida que van saliendo los huevos. El tamaño de puesta oscila entre 150 y 1300 huevos, dependiendo de la talla y edad de la hembra (a mayor tamaño y edad, mayor es la puesta), y las hembras suelen depositar los huevos de manera dispersa sobre la vegetación acuática (García-París *et al*., 2004). Existen pocos datos demográficos acerca de la especie. En un estudio esqueletocronológico de hembras adultas, se estimaron edades comprendidas entre 1 y 10 años, con una media de 4 años (Díaz-Paniagua *et al*., 2005). En cuanto al tamaño poblacional, solo hay datos disponibles de una población en la provincia de Salamanca, en la que se estimó un tamaño menor de 100 individuos que se reducía más de la mitad en periodos de sequía (López-González, 1995). En el mismo estudio se observaron distancias de dispersión en subadultos superiores a 1 km, entre puntos de reproducción (López-González, 1995).

Presentan cierto dimorfismo sexual, las hembras generalmente con el cuerpo más robusto, cabeza más ancha, cola más corta y extremidades posteriores más largas y las anteriores más cortas que los machos (Fontanet y Horta, 1989). En cuanto a la variación morfológica a lo largo de su área de distribución, solo se han documentado cambios en la talla y en el color (García-París *et al*., 2004). Las poblaciones del norte de África se caracterizan por ser de menor tamaño. Esta característica llevó a pensar que podría tratarse de una subespecie diferente (Pasteur y Bons, 1959), sin embargo esta hipótesis no ha sido apoyada por diversos estudios moleculares (Busack, 1986; Carranza y Arnold, 2004; Veith *et al*., 2004).

Los estudios filogenéticos del género *Pleurodeles* realizados por Carranza y Arnold (2004) y Veith *et al*. (2004) permitieron la identificación de dos linajes mitocondriales bien diferenciados en *P. waltl*: uno extendido por el oeste y centro de la península ibérica y otro repartido por el este de la misma y presente también en el norte de África. Se han propuesto diferentes hipótesis para explicar

el evento vicariante entre ambos linajes, con diferencias en la escala temporal y espacial asociada al proceso de divergencia. La primera hipótesis estaría relacionada con la crisis del Mesiniense hace 5,3 millones de años (Ma), con la separación del linaje oeste en la península ibérica y el este en el norte de África (Veith *et al*., 2004). La segunda hipótesis data el evento vicariante en torno a 3,2-2 Ma, con la separación de los dos linajes en la península ibérica (Carranza y Arnold, 2004). Las poblaciones pertenecientes al linaje ibero-marroquí comparten haplotipos mitocondriales a ambos lados del estrecho de Gibraltar (Carranza y Arnold, 2004; Veith *et al*., 2004), aunque también se han encontrado haplotipos exclusivos (Batista *et al*., 2004). Para explicar estos patrones se han propuesto eventos recientes de colonización desde la península al norte de África o viceversa, mediante balsas de vegetación arrastradas por corrientes marinas o bien como resultado de introducciones de carácter antrópico (Busack, 1986; Batista *et al*., 2004; Veith *et al*., 2004). También se han llevado a cabo estudios genéticos basados en aloenzimas, que encontraron ligeras diferencias entre las poblaciones ibéricas y las marroquís, con distancias genéticas del 0.1%. Este resultado ha sido interpretado como evidencia de flujo génico posterior a la crisis del Mesiniense (Busack, 1986). En el linaje oeste, las poblaciones situadas al sur del río Mira en el suroeste de Portugal forman un grupo bien diferenciado del resto de poblaciones (van de Vliet *et al*., 2014).

Los estudios previos sobre la especie han revelado una compleja historia evolutiva, con algunas cuestiones por desentrañar, como el origen de las poblaciones del norte de África o el papel de las glaciaciones del Pleistoceno en la distribución de su diversidad genética. Tampoco se conoce en detalle la distribución de los dos linajes mitocondriales en la península ibérica o si podría existir cierto grado de aislamiento reproductivo entre ellos. Además, se dispone de pocos datos acerca de las variables del paisaje que más afectan a la conectividad entre poblaciones, o de la capacidad de dispersión, tamaños poblacionales o la longevidad de los individuos de la especie.

Pelobates cultripes (Cuvier, 1829) (Fig. 3)

Es una especie de anuro conocida comúnmente como sapo de espuelas. Pertenece a la familia Pelobatidae. El género está integrado por cinco especies, *Pelobates*

Figura 3. Ejemplar adulto de *P. cultripes* en la Laguna de Valdemanco (Madrid).

fuscus (Laurenti, 1768), *Pelobates vespertinus* (Pallas, 1771), *Pelobates syriacus* Boettger, 1889, *Pelobates varaldii* Pasteur & Bons, 1959 y *Pelobates cultripes*. Se distribuyen por el noroeste de África, sur, centro y este de Europa, alcanzando el oeste de Asia. En el caso de *P. cultripes*, se extiende por la mayor parte de la península ibérica, alcanzando la costa mediterránea francesa y estando ausente en la Cordillera Cantábrica (Fig. 4; García-París *et al*., 2004; Loureiro *et al*., 2008). Existen poblaciones aisladas en la costa atlántica francesa (Duguet y Melki, 2003). Su distribución es más o menos continua en áreas con sustratos arenosos silíceos en la mitad oeste de la península ibérica; en cambio se presenta de manera más dispersa en la mitad este de la península, dominada por suelos calcáreos (García-París *et al*., 2004). Su rango altitudinal es similar al de *P. waltl*, encontrándose desde el nivel del mar hasta los 1770 metros (Cejudo, 1990; Tejedo y Reques, 2002; García-París *et al*., 2004).

Es una especie estrictamente nocturna, con un periodo corto de actividad anual, manteniéndose enterrados la mayor parte del año en sustratos blandos y

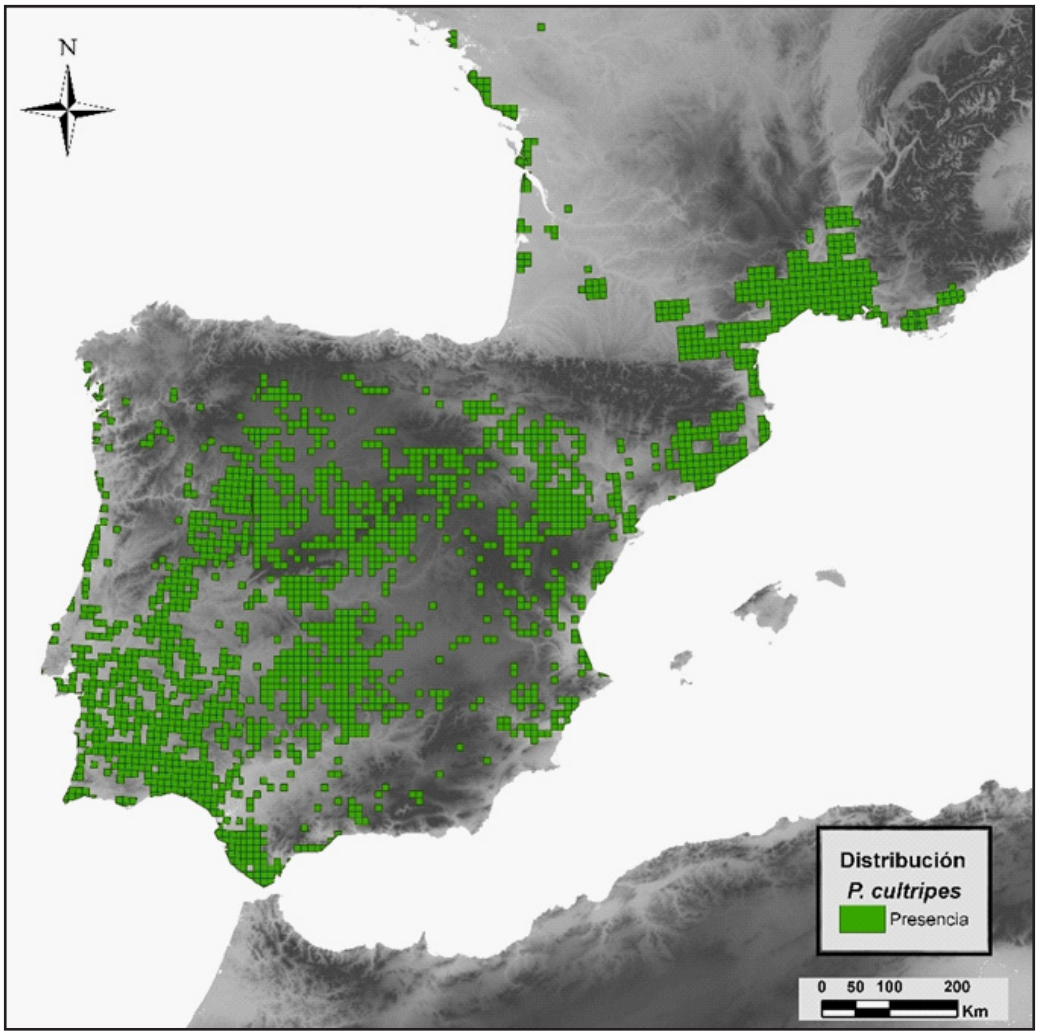

Figura 4. Mapa de distribución de *P. cultripes* en cuadrículas de 10x10km, basado en los atlas herpetológicos de Portugal (Loureiro *et al*., 2008), España (MAGRAMA, 2015) y Francia (MNHN, 2014).

arenosos. Generalmente se reproducen en charcas temporales, lagunas pequeñas poco profundas y ríos y arroyos con poca corriente. Los puntos de agua temporales que emplea para la reproducción se caracterizan por un largo hidroperiodo, lo que les permite completar su extenso desarrollo larvario, que suele tardar en completarse entre dos y seis meses (Talavera y Sanchiz, 1987; Tejedo, 1993). El periodo reproductor varía ampliamente con la latitud y con las variaciones climáticas anuales, siendo de octubre a marzo en áreas de climas más suaves y comenzando a finales de febrero en la Meseta Norte (Recuero, 2014). Las hembras permanecen menos tiempo en los puntos de agua y una vez depositada la puesta

no vuelven a ella hasta el siguiente periodo reproductor (Lizana *et al*., 1994). El amplexus o abrazo nupcial se produce bajo el agua, realizándose la fecundación externamente a medida que las hembras van depositando los huevos de manera irregular en cordones gelatinosos, en áreas abiertas o entre la vegetación en las orillas. El tamaño de puesta oscila entre 1301 y 6882 huevos (González de la Vega, 1988; Lizana *et al*., 1994). Los individuos de ambos sexos alcanzan la madurez sexual a los dos años en la zona centro peninsular (Talavera, 1990), mientras que en el sur peninsular maduran a los tres años (Leclair *et al*., 2005) y en el valle del Ebro a los dos años los machos y a los tres las hembras (Pascual-Pons *et al*., 2017). La edad máxima en estas poblaciones del valle del Ebro es de 5 años para los machos y de 6 para las hembras (Pascual-Pons *et al*., 2017) y en las poblaciones del sur es de 7 años para los machos y 8 para las hembras (Leclair *et al*., 2005), mientras que en el centro peninsular alcanzan 12 años los machos y 11 las hembras (Talavera, 1990). No se dispone de datos acerca de tamaños poblacionales o tasas de dispersión entre puntos de reproducción en esta especie. En cuanto a su variabilidad morfológica se han observado considerables diferencias en su morfología craneal (García-París *et al*., 2004), presentando también grandes diferencias de tamaño corporal asociadas al tipo de sustrato, que afectan al peso y tamaño de la puesta, y al tamaño de los huevos (Marangoni *et al*., 2008).

La historia evolutiva del género ha sido asociada a diferentes eventos geológicos, dependiendo de los métodos de calibración del reloj molecular aplicados en diferentes estudios. Inicialmente, el evento vicariante asociado a la especiación entre *P. cultripes* y su especie hermana, *P. varaldii*, se asoció a la crisis del Mesiniense (Busack *et al*., 1985). Posteriormente, García-París y Jockusch (1999) dataron la separación entre las dos especies en el Mioceno Tardío, mientras que Veith *et al*. (2006) encontraron argumentos a favor y en contra de las dos hipótesis anteriores, sin que en la actualidad exista un consenso. En estudios previos se ha encontrado una baja diversidad genética a lo largo de toda su distribución, sin que exista una estructura filogeográfica clara (Crottini *et al*., 2010; Fitó *et al*., 2011). Esta baja diversidad se ha atribuído a una reducción masiva de sus poblaciones durante las últimas glaciaciones del Pleistoceno, con recolonizaciones más recientes desde refugios glaciales que estarían en áreas

cálidas de la península ibérica, probablemente en el sur (Fitó *et al*., 2011).

En general, los estudios realizados sobre la filogeografía de la especie no han podido profundizar en el conocimiento de su estructura genética y geográfica, ya que la mayor parte de su diversidad genética actual parece haber sido modelada por procesos evolutivos recientes y los marcadores moleculares utilizados en estos estudios, de evolución lenta, no aportaron suficiente resolución. También se desconoce cómo los cambios climáticos ocurridos durante el último ciclo glacial han afectado la distribución y diversidad genética de la especie. Como en el caso de *P. waltl*, existen pocos datos disponibles acerca del papel de diferentes variables ambientales y topográficas en la conectividad entre poblaciones y además, a escala local la disponibilidad de datos demográficos (tamaños poblacionales, capacidad de dispersión) es muy limitada.

Referencias

Araújo MB, Thuiller W, Pearson RG (2006) Climate warming and the decline of amphibians and reptiles in Europe. Journal of Biogeography 33: 1712–1728.

Arbogast BS, Kenagy GJ (2001) Comparative phylogeography as an integrative approach to historical biogeography. Journal of Biogeography 28: 819–825.

Arnold ML (2015) Divergence with genetic exchange. Oxford University Press. Oxford, Reino Unido.

Avise JC (2000) Phylogeography: the history and formation of species. Harvard University Press. Cambridge, EEUU.

Avise JC (2009) Phylogeography: retrospect and prospect. Journal of Biogeography 36: 3–15.

Avise JC, Arnold J, Ball RM, *et al*. (1987) Intraspecific phylogeography: the mitochondrial DNA bridge between population genetics and systematics. Annual Review of Ecology and Systematics 18: 489–522.

Avise JC, Nelson WS, Sibley CG (1994) DNA sequence support for a close phylogenetic relationship between some storks and New World vultures. Proceedings of the National Academy of Sciences 91: 5173–5177.

Batista V, Harris DJ, Carretero MA (2004) Genetic variation in *Pleurodeles waltl* Michahelles, 1830 across the Strait of Gibraltar derived from mitochondrial DNA sequences. Herpetozoa 16: 166–168.

Beja P, Bosch J, Tejedo M, *et al*. (2009) *Pleurodeles waltl*. The IUCN Red List of Threatened Species 2009. http://www.iucnredlist.org

Beja P, Bosch J, Tejedo M, *et al*. (2016) *Pelobates cultripes*. The IUCN Red List of Threatened Species 2016. http://www.iucnredlist.org

Beukema W, De Pous P, Donaire-Barroso D, *et al*. (2013) Review of the systematics, distribution, biogeography and natural history of Moroccan amphibians. Zootaxa 3661.

Bons J, Geniez P (1996) Amphibiens et reptiles du Maroc (Sahara occidental compris): atlas biogéographique. Asociacion Herpetológica Espanola. Madrid, España.

Bowne DR, Bowers MA (2004) Interpatch movements in spatially structured populations: a literature review. Landscape Ecology 19: 1–20.

Brito PH, Edwards SV (2009) Multilocus phylogeography and phylogenetics using sequence–based markers. Genetica 135: 439–455.

Buckley D (2009) Toward an organismal, integrative, and iterative phylogeography. BioEssays 31: 784–793.

Busack SD (1986) Biogeographic analysis of the herpetofauna separated by the formation of the Strait of Gibraltar. National Geographic Research 2: 17–36.

Busack SD, Maxson LR, Wilson MA (1985) *Pelobates varaldii* (Anura: Pelobatidae): a morphologically conservative species. Copeia 1985: 107–112.

Caballero A (1994) Developments in the prediction of effective population size. Heredity 73: 657–679.

Carranza S, Arnold EN (2004) History of West Mediterranean newts, *Pleurodeles* (Amphibia: Salamandridae), inferred from old and recent DNA sequences. Systematics and Biodiversity 1: 327–337.

Carranza S, Wade E (2004) Taxonomic revision of Algero-Tunisian *Pleurodeles* (Caudata: Salamandridae) using molecular and morphological data. Revalidation of the taxon *Pleurodeles nebulosus* (Guichenot, 1850). Zootaxa 488: 1–24.

Cejudo D (1990) Nueva altitud máxima para *Pelobates cultripes*. Boletín de la Asociación Herpetológica Española 1: 20.

Chan LM, Brown JL, Yoder AD (2011) Integrating statistical genetic and geospatial methods brings new power to phylogeography. Molecular Phylogenetics and Evolution 59: 523–537.

Charlesworth B (2009) Effective population size and patterns of molecular evolution and variation. Nature Reviews Genetics 10: 195–205.

Coster SS, Babbitt KJ, Cooper A, Kovach AI (2015) Limited influence of local and landscape factors on finescale gene flow in two pond-breeding amphibians. Molecular Ecology 24: 742–758.

Crottini A, Galán P, Vences M (2010) Mitochondrial diversity of Western spadefoot toads, *Pelobates cultripes*, in northwestern Spain. Amphibia-Reptilia 31: 443–448.

Crow JF, Kimura M (1965) Evolution in sexual and asexual populations. The American Naturalist 99: 439–450.

Díaz-Paniagua C (1983) Influencia de las características del medio acuático sobre las poblaciones de larvas de anfibios en la Reserva Biológica de Doñana (Huelva, España). Doñana, Acta Vertebrata 10: 41–53.

Díaz-Paniagua C, Gómez C, Portheault A, De Vries W (2005) Los anfibios de Doñana. Organismo Autónomo de Parques Nacionales, Ministerio de Medio Ambiente. Madrid, España.

Díaz JA, Verdú-Ricoy J, Iraeta P, *et al*. (2017) There is more to the picture than meets the eye: adaptation for crypsis blurs phylogeographical structure in a lizard. Journal of Biogeography 44: 397–408.

Doulgeris C, Papadimos D, Kapsomenakis J (2016) Impacts of climate change on the hydrology of two Natura 2000 sites in Northern Greece. Regional Environmental Change 16: 1941–1950.

Duguet R, Melki F (2003) Les Amphibiens de France, Belgique et Luxemburg. Collection Parthénope. Editions Biotope. Mèze, Francia.

Ellegren H (2000) Microsatellite mutations in the germline: implications for evolutionary inference. Trends in Genetics 16: 551–558.

Escoriza D, Gutiérrez-Rodríguez J, Ben Hassine J, Martínez-Solano I (2016) Genetic assessment of the threatened microendemic *Pleurodeles poireti* (Caudata, Salamandridae), with molecular evidence for hybridization with *Pleurodeles nebulosus*. Conservation Genetics 17: 1445–1458.

Fitó F, Rivera X, Roca J, *et al*. (2011) Extremely low level of genetic variability in Iberian *Pelobates cultripes* (Cuvier, 1829) (Amphibia; Anura; Pelobatidae). Butlletí de la Societat Catalana d'Herpetologia 19: 21–28.

Fitze P, Gonzalez–Jimena V, San-Jose L, *et al*. (2011) Integrative analyses of speciation and divergence in *Psammodromus hispanicus* (Squamata: Lacertidae). BMC Evolutionary Biology 11: 1–22.

Fontanet X, Horta N (1989) Biometría y dimorfismo sexual en *Pleurodeles waltli* Michahelles, 1830 (Amphibia, Salamandridae) de una población del NE de la Península Ibérica. Miscel•lània Zoològica 13: 202–206.

Frankham R, Bradshaw CJA, Brook BW (2014) Genetics in conservation management: Revised recommendations for the 50/500 rules, Red List criteria and population viability analyses. Biological Conservation 170: 56–63.

Funk WC, Tallmon DA, Allendorf FW (1999) Small effective population size in the long–toed salamander. Molecular Ecology 8: 1633–1640.

Gagnaire P-A, Broquet T, Aurelle D, *et al*. (2015) Using neutral, selected, and hitchhiker loci to assess connectivity of marine populations in the genomic era. Evolutionary Applications 8: 769–786.

García-París M (1985) Los anfibios de España. Ministerio de Agricultura, Pesca y Alimentación. Madrid, España.

García-París M, Jockusch EL (1999) A mitochondrial DNA perspective on the evolution of Iberian *Discoglossus* (Amphibia: Anura). Journal of Zoology 248: 209–218.

García-París M, Montori A, Herrero P (2004) Fauna Iberica. Vol. 24. Amphibia: Lissamphibia. Museo Nacional de Ciencias Naturales, Consejo Superior de Investigaciones Cientificas. Madrid, España.

Goldberg CS, Waits LP (2010) Comparative landscape genetics of two pond-breeding amphibian species in a highly modified agricultural landscape. Molecular Ecology 19: 3650–3663.

Gómez A, Lunt D (2007) Refugia within Refugia: patterns of phylogeographic concordance in the Iberian Peninsula. In: Phylogeography of Southern European Refugia (eds. Weiss S, Ferrand N), pp. 155–188. Springer Netherlands.

González de la Vega JP (1988) Anfibios y reptiles de la provincia de Huelva. Ertisa. Huelva, España.

González EG (2003) Microsatélites: sus aplicaciones en la conservación de la biodiversidad. Graellsia 59: 377–388.

Graeter GJ, Rothermel BB, Gibbons JW (2008) Habitat selection and movement of pond-breeding amphibians in experimentally fragmented pine forests. The Journal of Wildlife Management 72: 473–482.

Greenberg JA, Dobrowski SZ, Ustin SL (2005) Shadow allometry: Estimating tree structural parameters using hyperspatial image analysis. Remote Sensing of Environment 97: 15–25.

Hardisty A, Roberts D (2013) A decadal view of biodiversity informatics: challenges and priorities. BMC Ecology 13: 16.

Hare MP (2001) Prospects for nuclear gene phylogeography. Trends in Ecology & Evolution 16: 700–706.

Hartl DL, Clark AG (1997) Principles of population genetics. Sinauer associates Sunderland.

Hegna RH, Galarza JA, Mappes J (2015) Global phylogeography and geographical variation in warning coloration of the wood tiger moth (*Parasemia plantaginis*). Journal of Biogeography 42: 1469–1481.

Hewitt GM (2000) The genetic legacy of the Quaternary ice ages. Nature 405: 907–913.

Hewitt GM (1996) Some genetic consequences of ice ages, and their role in divergence and speciation. Biological Journal of the Linnean Society 58: 247–276.

Hewitt GM (2004) Genetic consequences of climatic oscillations in the Quaternary. Philosophical Transactions of the Royal Society of London. Series B: Biological Sciences 359: 183–195.

Hoban SM, Hauffe HC, Pérez-Espona S, *et al*. (2013) Bringing genetic diversity to the forefront of conservation policy and management. Conservation Genetics Resources 5: 593–598.

Hoelzer GA (1997) Inferring phylogenies from mtDNA variation: mitochondrial-gene trees versus nuclear–gene trees revisited. Evolution 51: 622–626.

Hof C, Araujo MB, Jetz W, Rahbek C (2011) Additive threats from pathogens, climate and land–use change for global amphibian diversity. Nature 480: 516–519.

Hung C-M, Drovetski SV, Zink RM (2016) Matching loci surveyed to questions asked in phylogeography. Proceedings of the Royal Society B: Biological Sciences 283: 1826

Irwin DE, Gibbs HL (2002) Phylogeographic breaks without geographic barriers to gene flow. Evolution 56: 2383–2394.

IUCN, Conservation International, NatureServe (2008) An analysis of amphibians on the 2008 IUCN Red List. http://www.iucnredlist. org/amphibians.

Jehle R, Arntzen J (2002) Review: microsatellite markers in amphibian conservation genetics. Herpetological Journal 12: 1–9.

Jehle R, Burke T, Arntzen J (2005) Delineating fine-scale genetic units in amphibians: probing the primacy of ponds. Conservation Genetics 6: 227–234.

Keller D, Holderegger R, Strien MJ, Bolliger J (2014) How to make landscape genetics beneficial for conservation management? Conservation Genetics 16: 503–512.

Knowles LL (2009) Statistical phylogeography. Annual Review of Ecology, Evolution, and Systematics 40: 593–612.

Kozak KH, Graham CH, Wiens JJ (2008) Integrating GIS-based environmental data into evolutionary biology. Trends in Ecology & Evolution 23: 141–148.

Krijgsman W, Hilgen FJ, Raffi I, Sierro FJ, Wilson DS (1999) Chronology, causes and progression of the Messinian salinity crisis. Nature 400: 652–655.

Leclair MH, Leclair R, Gallant J (2005) Application of skeletochronology to a population of *Pelobates cultripes* (Anura: Pelobatidae) from Portugal. Journal of Herpetology 39: 199–207.

Lenormand T (2002) Gene flow and the limits to natural selection. Trends in Ecology & Evolution 17: 183–189.

Lizana M, Márquez R, Martín-Sánchez R (1994) Reproductive biology of *Pelobates cultripes* (Anura: Pelobatidae) in central Spain. Journal of Herpetology: 28, 19–27.

López-González FJ (1995) Demografía y biología reproductora del gallipato *Pleurodeles waltl* Michahelles, 1830 en medios acuáticos temporales de Salamanca. Tesina. Universidad de Salamanca.

Loureiro A, Ferrand de Almeida N, Carretero M, Paulo O (2008) Atlas dos anfíbios e répteis de Portugal. Instituto da Conservação da Natureza e da Biodiversidade, Lisboa, 257.

Lowe WH, Allendorf FW (2010) What can genetics tell us about population connectivity? Molecular Ecology 19: 3038–3051.

MAGRAMA (2015) Inventario Español de Especies Terrestres. Fauna de vertebrados: Anfibios y reptiles. Ministerio de Agricultura, Alimentación y Medio Ambiente, website Http://www.magrama.gob.es/es/biodiversidad/temas/conservacion-de-especies-amenazadas/vertebrados [Acceso 2 enero de 2015].

Manel S, Joost S, Epperson BK, *et al*. (2010) Perspectives on the use of landscape genetics to detect genetic adaptive variation in the field. Molecular Ecology 19: 3760–3772.

Manel S, Schwartz MK, Luikart G, Taberlet P (2003) Landscape genetics: combining landscape ecology and population genetics. Trends in Ecology & Evolution 18: 189–197.

Marangoni F, Tejedo M, Gomez-Mestre I (2008) Extreme reduction in body size and reproductive output associated with sandy substrates in two anuran species. Amphibia-Reptilia 29: 541–553.

Martín JM, Braga JC, Aguirre J, Puga–Bernabéu Á (2009) History and evolution of the North-Betic Strait (Prebetic Zone, Betic Cordillera): A narrow, early Tortonian, tidal-dominated, Atlantic-Mediterranean marine passage. Sedimentary Geology 216: 80–90.

Martínez-Solano I (2006) Atlas de distribución y estado de conservación de los anfibios de la Comunidad de Madrid. Graellsia 62: 253–291.

Metcalf CJE, Pavard S (2007) Why evolutionary biologists should be demographers. Trends in Ecology & Evolution 22: 205–212.

Montori A, Llorente GA, Santos X, Carretero MA (2002) *Pleurodeles waltl* Michahelles, 1830. Gallipato. En: Atlas y libro rojo de los anfibios y reptiles de España (eds. Pleguezuelos JM, Márquez R, Lizana M), pp. 51–54. Dirección General de Conservación de la Naturaleza–Asociación Herpetológica Española. Madrid, España.

Moore WS (1995) Inferring phylogenies from mtDNA variation: Mitochondrial–gene trees versus nuclear-gene trees. Evolution 49: 718–726.

Myers N, Mittermeier RA, Mittermeier CG, Da Fonseca GA, Kent J (2000) Biodiversity hotspots for conservation priorities. Nature 403: 853–858.

Nei M, Maruyama T, Chakraborty R (1975) The bottleneck effect and genetic variability in populations. Evolution 29: 1–10.

Okasha S (2016) The relation between kin and multilevel selection: an approach using causal graphs. The British Journal for the Philosophy of Science 67: 435–470.

Papadopoulou A, Knowles LL (2016) Toward a paradigm shift in comparative phylogeography driven by trait-based hypotheses. Proceedings of the National Academy of Sciences 113: 8018–8024.

Pascual–Pons M, Oromi N, Pujol-Buxó E, *et al*. (2017) Life history traits of a spadefood toad (*Pelobates cultripes*) population from a semiarid zone in the north east of the Iberian Peninsula. Herpetological Journal 27: 57–61.

Pasteur G, Bons J (1959) Les batraciens du Maroc. Travaux de l'Institut Scientifique Chérifien, Série Zoologie. Rabat, Marruecos.

Pearman PB, Guisan A, Broennimann O, Randin CF (2008) Niche dynamics in space and time. Trends in Ecology & Evolution 23: 149–158.

Pearse DE, Crandall KA (2004) Beyond FST: Analysis of population genetic data for conservation. Conservation Genetics 5: 585–602.

Peterman WE, Connette GM, Semlitsch RD, Eggert LS (2014) Ecological resistance surfaces predict fine–scale genetic differentiation in a terrestrial woodland salamander. Molecular Ecology 23: 2402–2413.

Phillips SJ, Anderson RP, Schapire RE (2006) Maximum entropy modeling of species geographic distributions. Ecological modelling 190: 231–259.

Platt JP, Behr WM, Johanesen K, Williams JR (2013) The Betic-Rif arc and its orogenic hinterland: a review. Annual Review of Earth and Planetary Sciences 41: 313–357.

Provan J, Bennett KD (2008) Phylogeographic insights into cryptic glacial refugia. Trends in Ecology & Evolution 23: 564–571.

Recuero E (2014) Sapo de espuelas – *Pelobates cultripes* (Cuvier, 1829). En: Enciclopedia Virtual de los Vertebrados Españoles (eds. Salvador A, Martínez-Solano I). Museo Nacional de Ciencias Naturales. Madrid, España.

Saccone C, De Giorgi C, Gissi C, Pesole G, Reyes A (1999) Evolutionary genomics in Metazoa: the mitochondrial DNA as a model system. Gene 238: 195–209.

Schaal B, Hayworth D, Olsen KM, Rauscher J, Smith W (1998) Phylogeographic studies in plants: problems and prospects. Molecular Ecology 7: 465–474.

Schwenk WS, Donovan TM (2011) A multispecies framework for landscape conservation planning. Conservation Biology 25: 1010–1021.

Sexton JP, Hangartner SB, Hoffmann AA (2014) Genetic isolation by environment or distance: which pattern of gene flow is most common? Evolution 68: 1–15.

Sillero N, Brito JC, Skidmore AK, Toxopeus AG (2009) Biogeographical patterns derived from remote sensing variables: the amphibians and reptiles of the Iberian Peninsula. Amphibia-Reptilia 30: 185–206.

Sork VL, Waits L (2010) Contributions of landscape genetics – approaches, insights, and future potential. Molecular Ecology 19: 3489–3495.

Storfer A, Murphy MA, Spear SF, Holderegger R, Waits LP (2010) Landscape genetics: where are we now? Molecular Ecology 19: 3496–3514.

Stuart SN, Hoffmann M, Chanson J, *et al*. (2008) Threatened amphibians of the world. Lynx Edicions. Barcelona, España.

Talavera RR (1990) Evolución de Pelobatidos y Peloditidos (Amphibia: Anura): morfología y desarrollo del sistema esquéletico. Tesis doctoral, Universidad Complutense de Madrid.

Talavera RR, Sanchiz B (1987) Temperature dependence of larval development in *Pelobates cultripes* (preliminary experiments). Societas Europaea Herpetologica, Faculty of Sciences, Nijmegen.

Tejedo M (1993) Size-dependent vulnerability and behavioral responses of tadpoles of two anuran species to beetle larvae predators. Herpetologica 49: 287–294.

Tejedo M, Reques R (2002) *Pelobates cultripes* (Cuvier, 1829). Sapo de espuelas. En: Atlas y libro rojo de los anfibios y reptiles de España (eds. Pleguezuelos JM, Márquez R, Lizana M), pp. 94–96. Dirección General de Conservación de la Naturaleza–Asociación Herpetológica Española. Madrid, España.

Templeton AR, Routman E, Phillips CA (1995) Separating population structure from population history: a cladistic analysis of the geographical distribution of mitochondrial DNA haplotypes in the tiger salamander, *Ambystoma tigrinum*. Genetics 140: 767–782.

Tsuda Y, Nakao K, Ide Y, Tsumura Y (2015) The population demography of *Betula maximowicziana,* a cool-temperate tree species in Japan, in relation to the last glacial period: its admixture-like genetic structure is the result of simple population splitting not admixing. Molecular Ecology 24: 1403–1418.

Ursenbacher S, Guillon M, Cubizolle H, *et al*. (2015) Postglacial recolonization in a cold climate specialist in western Europe: patterns of genetic diversity in the adder (*Vipera berus*) support the central-marginal hypothesis. Molecular Ecology 24: 3639–3651.

van de Vliet MS, Diekmann OE, Machado M, *et al*. (2014) Genetic divergence for the amphibian *Pleurodeles waltl* in Southwest Portugal: dispersal barriers shaping geographic patterns. Journal of Herpetology 48: 38–44.

Veith M, Fromhage L, Kosuch J, Vences M (2006) Historical biogeography of Western Palearctic pelobatid and pelodytid frogs: a molecular phylogenetic perspective. Contributions to Zoology 75: 109–120.

Veith M, Mayer C, Samraoui B, Barroso DD, Bogaerts S (2004) From Europe to Africa and vice versa: Evidence for multiple intercontinental dispersal in ribbed salamanders (Genus *Pleurodeles*). Journal of Biogeography 31: 159–171.

Vila M, Hermida M, Fernández C, *et al*. (2017) Phylogeography and Conservation Genetics of the Ibero-Balearic Three-Spined Stickleback (*Gasterosteus aculeatus*). PLoS ONE 12: e0170685.

Waltari E, Hijmans RJ, Peterson AT, *et al*. (2007) Locating Pleistocene refugia: comparing phylogeographic and ecological niche model predictions. PLoS ONE 2: e563.

Wang IJ (2010) Recognizing the temporal distinctions between landscape genetics and phylogeography. Molecular Ecology 19: 2605–2608.

Weckworth BV, Musiani M, DeCesare NJ, *et al*. (2013) Preferred habitat and effective population size drive landscape genetic patterns in an endangered species. Proceedings of the Royal

Society B: Biological Sciences 280: 1769.

Wielstra B, Babik W, Arntzen JW (2015) The crested newt *Triturus cristatus* recolonized temperate Eurasia from an extra-Mediterranean glacial refugium. Biological Journal of the Linnean Society 114: 574–587.

Wright S (1931) Evolution in Mendelian populations. Genetics 16: 97–159.

Wulder MA, Hall RJ, Coops NC, Franklin SE (2004) High spatial resolution remotely sensed data for ecosystem characterization. BioScience 54: 511–521.

Zhang D-X, Hewitt GM (2003) Nuclear DNA analyses in genetic studies of populations: practice, problems and prospects. Molecular Ecology 12: 563–584.

Zink RM (1996) Comparative phylogeography in North American birds. Evolution: 308–317.

OBJETIVOS

El objetivo general de la presente tesis es profundizar en los procesos evolutivos responsables de los patrones de diversidad y estructura genética de dos especies sintópicas de anfibios endémicas de la península ibérica. Para ello, se ha planteado un estudio comparado, integrando aproximaciones a diferentes escalas espaciales y temporales asociadas a las disciplinas de la filogeografía, genética del paisaje y demografía, en cada una de las cuales se han planteado objetivos específicos:

- **Capítulo I:**

  - Desarrollar y caracterizar un conjunto de loci polimórficos de tipo microsatélite en *Pleurodeles waltl* y *Pelobates cultripes*.
  - Comprobar el éxito de amplificación cruzada en especies afines a *P. waltl* y *P. cultripes*.

- **Capítulo II:**

  - Reconstruir la historia evolutiva de las dos especies.
  - Localizar refugios glaciales y reconstruir la demografía histórica y posibles rutas de recolonización posglacial.
  - Identificar las barreras históricas y contemporáneas al flujo génico y evaluar la concordancia temporal de los procesos de divergencia de ambas especies.

- **Capítulo III:**

  - Comparar los patrones de diversidad y estructura genética regional de las dos especies e identificar los factores del paisaje que más determinan la conectividad poblacional a diferentes escalas espaciales.
  - Evaluar la importancia de las características biológicas y el efecto de la abundancia (tamaño poblacional) en la diversidad y estructura genética de las dos especies.

- **Capítulo IV:**

  - Estimar el tamaño poblacional (Nc), el tamaño efectivo poblacional (Ne) y el número efectivo de individuos reproductores (Nb) a escala local mediante métodos directos (Captura-Marcaje-Recaptura) e indirectos (genéticos) para obtener estimas de los ratios Ne/Nc y Nb/Nc en ambas especies.
  - Obtener estimas directas e indirectas de la capacidad de dispersión en las dos especies y comprobar si existen diferencias entre sexos.

Capítulo I

Desarrollo de marcadores nucleares hipervariables (SSR)

Artículo I: Desarrollo y caracterización de 12 nuevos microsatélites polimórficos en el gallipato, *Pleurodeles waltl* (Caudata: Salamandridae), con datos de amplificación cruzada en *P. nebulosus*

Artículo II: Aislamiento y caracterización de 16 microsatélites polimórficos en el sapo de espuelas, *Pelobates cultripes* (Anura: Pelobatidae) mediante pirosecuenciación 454

Development and characterization of twelve new polymorphic microsatellite loci in the Iberian ribbed newt, *Pleurodeles waltl* (Caudata: Salamandridae), with data on cross-amplification in *P. nebulosus*

J Gutiérrez-Rodríguez, E G. Gonzalez, Í Martínez-Solano

Publicado en

Amphibia-Reptilia 2014 Volume 35, 129 – 134

DOI: 10.1163/15685381-00002926

Abstract

Twelve novel polymorphic microsatellite loci were isolated and characterized for the Iberian ribbed newt, *Pleurodeles waltl* (Caudata, Salamandridae). The distribution of this newt ranges from central and southern Iberia to northwestern Morocco. Polymorphism of these novel loci was tested in 40 individuals from two Iberian populations and compared with previously published markers. The number of alleles per locus ranged from two to eight. Observed and expected heterozygosity ranged from 0.13 to 0.57 and from 0.21 to 0.64, respectively. Cross-species amplification was tested in *Pleurodeles nebulosus*, which is listed as Vulnerable by the IUCN. Eight new and seven previously published loci amplified successfully in that species and thus represent a valuable conservation tool. The novel microsatellites will be useful for a better understanding of the population dynamics, demography, genetic structure, and evolutionary history of *Pleurodeles waltl* and *P. nebulosus*.

Resumen

Se han aislado y caracterizado 12 nuevos microsatélites polimórficos en el gallipato, *Pleurodeles waltl* (Caudata, Salamandridae). Esta especie se distribuye por el centro y sur de la península ibérica y en el noroeste de Marruecos. Se evaluó el polimorfismo de estos marcadores en 40 individuos de dos poblaciones de la península ibérica y se comparó con el de otros marcadores previamente publicados. El número observado de alelos por locus estuvo entre 2 y 8. Los valores de heterocigosidad observada y esperada estuvieron entre 0,13 y 0,57 y entre 0,21 y 0,64, respectivamente. Estos nuevos marcadores, junto con los previamente publicados, fueron aplicados a la especie *Pleurodeles nebulosus*. Esta especie habita en el noroeste de Argelia y Túnez, y está catalogada como Vulnerable (VU) por la UICN. De los marcadores analizados, ocho de los nuevos y siete de los publicados previamente amplificaron con éxito en esta especie. Estos nuevos marcadores serán útiles para profundizar en el conocimiento de la dinámica poblacional, demografía, estructura genética e historia evolutiva de *P. waltl* y *P. nebulosus.*

The Iberian ribbed newt, *Pleurodeles waltl* Michahelles, 1830, is a large (up to 30 cm) salamandrid that is widely distributed throughout most of the Iberian Peninsula and northwestern Morocco (Beukema *et al*., 2013). Currently, it is listed as Near Threatened by the IUCN, given that populations probably are in significant decline (Beja *et al*., 2009). The main threats are aquatic habitat loss, road mortality and the introduction of invasive species like the crayfish *Procambarus clarkii* (Montori *et al*., 2002). However, habitat fragmentation may also play a negative role in the ribbed newt's regional dynamics, especially at the southern end of the range. Potentially available conservation measures such as identification and protection of corridors connecting populations are limited by the lack of data on their biology and demography (Salvador, 2002).

Previous phylogeographic studies have identified two distinct mitochondrial lineages (Carranza & Arnold, 2004; Veith *et al*., 2004). A western lineage is distributed across the west and center of the Iberian Peninsula, while an eastern lineage spreads across eastern Iberia and northern Morocco. According to Carranza and Arnold (2004), the process of vicariance between the two lineages would have occurred between 3.2 and 2 million years ago, in the Late Pliocene or Early Pleistocene. Populations of Morocco and the Iberian Peninsula are genetically very similar and even share mtDNA haplotypes (Veith *et al*., 2004), which has led some authors to propose alternative hypotheses to explain the low genetic differentiation between populations on both sides of the Gibraltar Strait. The first hypothesis is a recent anthropogenic introduction in northern Morocco, and the second suggests the origin of Moroccan populations through passive transport on vegetation rafts carried by ocean currents (Busack, 1986; Veith *et al*., 2004). These hypotheses have not been tested with fast-evolving molecular markers, like microsatellites, which are well suited for the study of such recent events. Microsatellites are ubiquitous, codominant, noncoding genetic markers consisting of repeats of one to six base pairs with high levels of length polymorphism due to higher rates of mutation than other genomic regions. Because of their high variability and ease of genotyping they are widely used to address questions in Evolutionary and Conservation Biology (Ellegren, 2004).

In this study, we report the development of twelve new polymorphic microsatellite loci in *P. waltl*. Cross-species amplification was also tested in

samples of the closely related, north African endemic species *P. nebulosus*, which is listed as Vulnerable by the IUCN. We compare levels of polymorphism in the newly developed loci with those previously published (van de Vliet *et al*., 2009) and discuss potential applications.

An enriched partial genomic library was generated from DNA of a single individual of *Pleurodeles waltl* collected from Valdemanco, Madrid, Spain. The library was prepared at the Sequencing Genotyping Facility, Cornell Life Sciences Core Laboratory Center (CLC). Genomic DNA was extracted with Qiagen DNeasy Blood and Tissue Kits, digested with the restriction enzymes BsaA I and Hinc II, and ligated to SNX linkers (Hamilton *et al*., 1999). The cut DNA was enriched by hybridization with a mix of biotin-labelled oligonucleotide probes (motifs: GT_8, $TC_{9.5}$, TA_{15}, TTA_{11}, $GTT_{6.33}$, TTC_7, $GCT_{4.33}$, GAT_7, $GTA_{8.33}$, $GTG_{8.33}$, $GTG_{4.67}$, $GTC_{4.67}$,TCC_5, $TTTA_{8.5}$, $TTTG_{5.25}$, $TTTC_6$, $GATA_7$, $GTAT_{6.25}$, $GAAT_{5.5}$, $GATT_{5.5}$, $GTTA_{6.25}$, $TTAC_{6.75}$, $GATG_{4.25}$, $GGTT_4$, $GCTT_{3.75}$, $GTAG_{4.25}$, $GTCA_{4.25}$, $GTTC_4$, $TCAC_{4.25}$, $TTCC_{4.25}$) and incubated at 56°C for 20 minutes. The enriched product was carefully isolated from the rest of the genomic DNA fragments using streptavidin-coated magnetic beads (NEB) and amplified by PCR using the SNX linkers. PCR products were purified and ligated with vector pUC19 (NEB) and transformed into *Escherichia coli* electrocompetent DH5α-E cells (Invitrogen). The recombinant clones obtained were directly transferred onto nylon filter membranes (Osmonics), and once fixed, they were hybridized at 50°C overnight with 33P-labelled probes taken from the same motifs used previously. The nylon membranes were transferred to film plastic wrap and exposed to film for chemiluminiscent signal detection. Positive colonies containing microsatellites were cultivated, amplified with M13 forward or reverse primers and sequenced using an ABI PRISM 3100 automated sequencer (Applied Biosystems).

A total of 34 clones containing microsatellite motifs were selected for further screening. Primer pairs were designed with the program Primer3plus (Untergasser *et al*., 2007). Genomic DNA was extracted from tail tips of larvae with NucleoSpin Tissue-Kits (Macherey-Nagel). PCR reactions were performed in a total volume of 15 µl, including 25 ng of template DNA, 5× GoTaq Flexi buffer (PROMEGA), 1.5 mM $MgCl_2$, 0.1 mM dNTP, 0.1 µM fluorescent primer, 0.1 µM primer and 0.5 U GoTaq Flexi DNA polymerase (PROMEGA). The PCR

cycling profile consisted of an initial denaturation at 95°C for 5 minutes, followed by 35 cycles of denaturation at 95°C for 45 seconds, annealing between 57-62°C for 45 seconds, and extension at 72°C for 45 seconds, with a final extension at 72°C for 10 minutes. PCR products were visualized on 2.5% agarose gels. PCR primer fail rate (65%) was similar to that reported by van de Vliet *et al*. (2009) (60%).

Of the 34 initially selected loci, 26 showed unambiguous bands and were chosen to score genetic variation in samples from two populations of *P. waltl* (Valdemanco: Madrid, n: 20; and Chiclana: Cádiz, n: 20) and one of *P. nebulosus* (Jendouba, Tunisia, n: 8). The two populations of *P. waltl* represent the two major mtDNA lineages previously described (eastern: Chiclana; western: Valdemanco), although in Valdemanco there are eastern mtDNA haplotypes in low frequencies too (around 10%, unpublished data). Fluorescent dyes 6-FAM, PET, NED, and VIC were used to label forward primers for use in multiplex reactions, which were designed with MULTIPLEX MANAGER v1.2 (Holleley & Geerts, 2009). PCR reactions were performed using Type-it Microsatellite PCR kits (Qiagen). All reactions were performed in a total volume of 15 µl, containing 7.5 µl of Master Mix, 1.2 µl of primer mix (0.2 µM of each primer) and 25 ng of template DNA. The PCR cycling profile consisted of an initial denaturation at 95°C for 5 minutes, followed by 30 cycles of denaturation at 95°C for 30 seconds, annealing between 57-62°C for 90 seconds, and extension at 72°C for 30 seconds, with a final extension at 60°C for 10 minutes. PCR products were genotyped on an ABI PRISM 3730 sequencer with the GeneScan 500 LIZ size standard (Applied Biosystems), and fragments were scored and binned using GENEMAPPER v4.0 (Applied Biosystems). In order to compare levels of polymorphism, we genotyped the same samples using eleven previously published microsatellites (van de Vliet *et al*., 2009). For this purpose, three additional multiplex reactions were designed: multiplex 1 (loci Ppl2, Ppl3, Ppl5), multiplex 2 (Ppl1, Ppl12, Ppl13, Ppl14) and multiplex 3 (Ppl4, Ppl6, Ppl7, Ppl10). The markers Ppl8, Ppl9 and Ppl11 were also tested, however they presented some problems, such as dropout, nonspecific amplification, and no amplification, respectively. PCR reactions were performed using the same conditions described above. Differences in PCR protocols across studies may account for the lower amplification success, since van de Vliet *et al*.

Table I.1. Description of 12 new polymorphic and one monomorphic microsatellite loci isolated for the Iberian Ribbed newt (*Pleurodeles waltl*). The locus name, primer sequences, fluorescent dye, repeat motif, multiplex reaction, annealing temperature (Ta), size of amplified product (bp), and GenBank accession numbers are described for each locus. The number of individuals successfully genotyped (n), number of alleles (N_A), observed (Ho) and expected (He) heterozygosities are also included for each locus and population (Valdemanco/Chiclana), as well as cross-species amplification of each locus in *P. nebulosus* (+: positive, -: negative).

Locus	Primer sequence	Labelling dye	Repeated motif	Multiplex reaction	Ta	Size ranges (bp)	n	N_A	Ho	He	*P. nebulosus*	GenBank accession no.
Pleu2.3	5' TTGGAAACCACAACTGATGAA 3' 5' ATTTCCTGCTCTCCACACCA 3'	NED	$(TC)_{10}$	Multiplex 1	60	226 - 240	20/20	1/4	0/0.5	0/0.42	+	KF647652
Pleu2.19	5' ATGAACCCCTGGAGACACTG 3' 5' ACGCTCAGTCCGTTCATTTT 3'	VIC	$(TG)_{14}$	Multiplex 1	60	228 - 236	20/20	4/3	0.6/0.45	0.49/0.53	-	KF647653
Pleu2.34	5' GAGACATGACTTGCCCAACA 3' 5' CTTTGCCCCGGTAATACTCC 3'	6-FAM	$(CA)_{12}$	Multiplex 1	60	138 -148	20/16	2/1	0.35/0	0.47/0	-	KF647658
Pleu2.16	5' CTATTGTGGTGACCCGCATT 3' 5' GCCTTATGAGGGTTTCATGC 3'	PET	$(TG)_{16}(AG)_{19}$	Multiplex 2	57	219 - 251	20/20	2/7	0.5/0.6	0.46/0.68	+	KF647655
Pleu2.31	5' AGCCTCTTGGTTGGTCTCAG 3' 5' CATGTCCCGTTCTTTGTCCT 3'	VIC	$(GA)_{10}$	Multiplex 2	57	210 - 216	20/20	2/1	0.4/0	0.5/0	-	KF647657
Pleu3.2	5' GACCGCTGCTGCAAGTATCT 3' 5' AGAGCGCTTTACACCAGAGC 3'	6-FAM	$(TTC)_{21}$	Multiplex 2	57	184 - 223	20/20	2/7	0.4/0.75	0.5/0.78	+	KF647661
Pleu3.5	5' CAAGCAGGGTTTTGCCTTTA 3' 5' CCTGCTTTGCAACTCTCTCC 3'	6-FAM	$(TGA)_3$ GGAAGCTGTTGGGGC $(TGA)_9$	Multiplex 3	60	178 - 199	20/20	1/4	0/0.55	0/0.58	+	KF647662
Pleu4.1	5' CTAGTGAGCAGCACGTCCAC 3' 5' ATGAAAACTCCGCTTGAAGG 3'	VIC	$(ATTG)_2ACTG(ATTG)_5$	Multiplex 3	60	194 - 198	20/20	2/2	0.2/0.15	0.48/0.14	+	KF647660
Pleu2.35	5' GACCTATCCTAGTTTCTCATCCTCAC 3 ' 5' TTGTTATGCAAAATTCAGGAGA 3'	6-FAM	$(TC)_{14}$	Multiplex 4	62	139 -151	20/19	1/4	0/0.26	0/0.42	+	KF647659
Pleu3.14	5' CAGCTGGATAAACATGGCAAC 3' 5' TTTCGAATGCAAATCAAAGC 3'	6-FAM	$(ATT)_5(GTT)_9$	Multiplex 4	62	257 - 266	20/19	2/4	0.05/0.53	0.05/0.59	-	KF647664

Pleu3.11	5' GGGAAATCTCAGTCCGAACA 3' 5' ACCTCTTTCCCAGCTCCACT 3'	VIC	$(CTT)_9$	Multiplex 4	62	225 -237	20/20	2/3	0.55/0.4	0.49/0.48	+	KF647663
Pleu2.21	5' TTGGAATGCAGCTATGTTGG 3' 5' TTACCATCTTGGAAAGGCTCT 3'	NED	$(TG)_{13}$	Multiplex 4	62	195 - 223	20/19	3/2	0.7/0.11	0.55/0.5	-	KF647654
Pleu2.29	5' GGACACCTGCTTGACCCTTA 3' 5' CTTCCTGCGACCTTGGTAAA 3'	NED	$(TC)_{10}$ TGTCTG$(TC)_4$	-	57	165	20/20	1	-	-	+	KF647656

(2009) used touch-down profiles for all but one loci.

MICROCHECKER v2.2.3 (van Oosterhout *et al*., 2004) was used to test for evidence of stuttering, large allele dropout and presence of null alleles in each population, using a 99% confidence interval and 1000 randomizations. We calculated the number of alleles (N_A), observed (Ho) and expected (He) heterozygosity for each locus and population with GENALEX v6.5b5 (Peakall & Smouse, 2006). Deviations from Hardy-Weinberg equilibrium (HWE) and evidence of linkage disequilibrium (LD) were tested with the Markov chain method (Guo & Thompson, 1992) implemented in GENEPOP v4.2 (Rousset, 2008). The Markov chain was run with 10 000 dememorization steps, 1000 batches and 10 000 iterations per batch. A sequential Bonferroni correction (Rice, 1989) was applied to adjust for multiple comparisons.

Among the 26 new loci tested, only 12 were polymorphic in the samples of *P. waltl*. Therefore, multiplex reactions were redesigned, and reduced to four reactions (Table I.1). Potential null alleles were detected at locus Pleu2.21 (estimated frequency: 33.7%) in the population of Chiclana, which was the only instance of significant deviation from HWE. There was no evidence of significant LD in any population. This is in contrast to van de Vliet *et al*. (2009), who found significant LD between Ppl12/Ppl13, and significant deviation from HWE in Ppl10. The number of alleles per locus ranged from two (Pleu2.31, Pleu2.34 and Pleu4.1) to eight (Pleu3.2). The average observed heterozygosity was 0.31 (range: 0.13-0.57) and the average expected heterozygosity was 0.35 (range: 0.21-0.64). The average number of alleles per locus and population ranged from two (Valdemanco) to 3.5 (Chiclana). Observed and expected heterozygosities were 0.31/0.33 and 0.36/0.42 in the populations Valdemanco and Chiclana, respectively. In general, previously published markers were more polymorphic (number of alleles/observed/expected heterozygosities = 6.0/0.73/0.68 and 13.6/0.92/0.88 in Valdemanco and Chiclana, respectively). Reasons for this are unclear, although the use of different motifs in library construction may explain at least part of the differences.

Cross-species amplification with eight samples of *Pleurodeles nebulosus* was successful for eight of the thirteen new loci, although only six were polymorphic (number of alleles ranging from two to six, Table I.2). With

Table I.2. Polymorphism in loci isolated from *P. waltl* in *P. nebulosus* (n = 8): Locus name, number of alleles (N_A), expected (He) and observed (Ho) heterozygosities. * = loci from van de Vliet et *al*. (2009).

Locus	N_A	Size range (bp)	He	Ho
Pleu2.3	2	220 - 226	0.125	0.305
Pleu2.16	6	210 - 242	0.875	0.672
Pleu2.29	3	165 - 169	0.375	0.461
Pleu3.2	2	157 - 172	0.25	0.219
Pleu3.5	1	131	-	-
Pleu4.1	3	190 - 198	0.375	0.57
Pleu2.35	4	118 - 140	0.5	0.609
Pleu3.11	1	231	-	-
Ppl3*	10	139 - 185	1	0.883
Ppl5*	7	146 - 184	0.75	0.844
Ppl7*	9	167 - 195	0.875	0.789
Ppl10*	3	138 - 142	0.125	0.32
Ppl12*	7	110 - 168	0.625	0.813
Ppl13*	11	184 - 278	1	0.875
Ppl14*	5	306 - 322	0.625	0.773

respect to previously published markers, seven out of the eleven loci tested also amplified in *P. nebulosus* samples (number of alleles: three to eleven) and showed higher levels of polymorphism (average number of alleles: 3.3 vs. 7.6, observed/expected heterozygosities: 0.42/0.47 vs. 0.71/0.76, in new vs. published loci, respectively). The overall similar values of polymorphism of the markers across species and the high cross-amplification success in *P. nebulosus* (despite at least 5.3 million years of independent evolution, see Carranza & Arnold, 2004; Veith *et al*., 2004) are in contrast to general expectations, given the overall low transferability of microsatellites in amphibians (Nair *et al*., 2012). The reasons for this are unclear, although biogeographic factors (for instance, lower diversity is expected in populations in recently expanding parts of the range) are unlikely, since historical refugia for the species seem to have been located in the south (unpublished data), where one of the study populations (Chiclana) was sampled.

These new markers complement those previously published and will help to address a variety of questions on the population dynamics and demography (mating system, low-scale dispersal, effective population size), genetic structure

(identification of potential barriers to gene flow), and evolutionary history (delineation of lineages and their contact zones) of *P. waltl*. In addition, the success of cross-amplification tests in the closely related species *P. nebulosus* is important from a conservation perspective. This species is listed as Vulnerable by the IUCN, because its distribution area in northern Algeria and Tunisia is less than 2000 km^2 and is very fragmented (Donaire-Barroso *et al*., 2013) and thus these markers will provide valuable information on the spatial genetic structure of its populations. Further tests should be conducted on the third extant species in the genus, *P. poireti*, which has the smallest range (less than 500 km^2, restricted to the Edough Peninsula in northern Algeria) and is listed as Endangered by the IUCN (Geniez & Mateo, 2006).

Acknowledgements

We thank D. Buckley, E. Recuero, S. Nouira and J. Ben Hassine for help collecting samples and S. Bogdanowicz at Cornell University for help with the microsatellite library. All samples were collected with permits issued by legal authorities in Spain and Tunisia. The manuscript was improved with the comments of two anonymous reviewers and the Associate Editor. This research was funded by grants CGL2008-04271-C02-01/BOS and CGL2011-28300 (Ministerio de Ciencia e Innovación [MICINN], Ministerio de Economía y Competitividad [MEC], Spain, and FEDER) and PPII10-0097-4200 (Junta de Comunidades de Castilla-La Mancha) to IMS. JGR is supported by the Consejo Superior de Investigaciones Científicas of Spain (CSIC) and the European Social Fund (ESF) (JAE-pre PhD fellowship), EGG is a "Juan de la Cierva" postdoctoral fellow supported by the MEC, and IMS was supported by a "Ramón y Cajal" postdoctoral fellowship (MICINN and Universidad de Castilla-La Mancha).

References

Beja P, Bosch J, Tejedo M,, *et al*. (2009) *Pleurodeles waltl*. In: IUCN 2012. IUCN Red List of Threatened Species. Version 2012.2. http://www.iucnredlist.org. Accessed 3 June 2013.

Beukema W, De Pous P, Donaire-Barroso D,, *et al*. (2013) Review of the systematics, distribution, biogeography and natural history of Moroccan amphibians. Zootaxa 3661: 1–60.

Busack SD (1986) Biogeographic analysis of the herpetofauna separated by the formation of the Strait of Gibraltar. National Geographic Research 2: 17–36.

Carranza S, Arnold EN (2004) History of West Mediterranean newts, *Pleurodeles* (Amphibia: Salamandridae), inferred from old and recent DNA sequences. Systematics and Biodiversity 1: 327–337.

Donaire-Barroso D, Salvador A, Slimani T, *et al*. (2006) *Pleurodeles nebulosus*. In: IUCN 2012. IUCN Red List of Threatened Species. Version 2012.2. http://www.iucnredlist.org. Accessed 19 June 2013.

Ellegren H (2004) Microsatellites: simple sequences with complex evolution. Nature Reviews Genetics 5: 435–445.

Geniez P, Mateo JA (2006) *Pleurodeles poireti*. In: IUCN 2012. IUCN Red List of Threatened Species. Version 2012.2. http://www.iucnredlist.org. Accessed 19 June 2013.

Guo SW, Thompson EA (1992) A Monte Carlo method for combined segregation and linkage analysis. American Journal of Human Genetics 51: 1111–1126.

Hamilton MB, Pincus EL, Di Fiore A, Fleischer RC (1999) Universal linker and ligation procedures for construction of genomic DNA libraries enriched for microsatellites. BioTechniques 27: 500–507.

Holleley CE, Geerts PG (2009): Multiplex Manager 1.0: a cross-platform computer program that plans and optimizes multiplex PCR. BioTechniques 46: 511–517.

Montori A, Llorente GA, Santos X, Carretero MA (2002) *Pleurodeles waltl* Michahelles, 1830. Gallipato. In: Atlas y Libro Rojo de los Anfibios y Reptiles de España, p. 51–53. Pleguezuelos JM, Márquez R, Lizana M, Eds, Dirección General de Conservación de la Naturaleza-Asociación Herpetológica Española, Madrid, Spain.

Nair A, Gopalan SV, George S, Kumar KS, Merilä J (2012) Cross-species testing and utility of microsatellite loci in *Indirana* frogs. BMC Research Notes 5: 389.

Peakall R, Smouse PE (2006) Genalex 6: genetic analysis in Excel. Population genetic software for teaching and research. Molecular Ecology Notes 6: 288–295.

Rice WR (1989) Analyzing s of statistical tests. Evolution 43: 223–225.

Rousset F (2008) Genepop'007: a complete reimplementation of the genepop software for Windows and Linux. Molecular Ecology Resources 8: 103–106.

Salvador A (2002) Gallipato – *Pleurodeles waltl*. In: Enciclopedia Virtual de los Vertebrados Españoles. Carrascal LM, Salvador A, Eds, Museo Nacional de Ciencias Naturales, Madrid. http://www.vertebradosibericos.org. Accessed 19 June 2013.

Untergasser A, Nijveen H, Rao X, *et al*. (2007) Primer3Plus, an enhanced web interface to Primer3. Nucleic Acids Research 35: 71–74.

van de Vliet MS, Diekmann OE, Serrão EA, Beja P (2009) Isolation of highly polymorphic microsatellite loci for a species with a large genome size: sharp-ribbed salamander (*Pleurodeles waltl*). Molecular Ecology Resources 9: 425–428.

van Oosterhout C, Hutchinson WF, Wills DPM, Shipley P (2004) Micro-checker: software for identifying and correcting genotyping errors in microsatellite data. Molecular Ecology Notes 4: 535–538.

Veith M, Mayer C, Samraoui B, Barroso DD, Bogaerts S (2004) From Europe to Africa and vice versa: evidence for multiple intercontinental dispersal in ribbed salamanders (Genus *Pleurodeles*). Journal of Biogeography 31: 159–171.

Isolation and characterization of sixteen polymorphic microsatellite loci in the Western Spadefoot, *Pelobates cultripes* (Anura: Pelobatidae) via 454 pyrosequencing

J. Gutiérrez-Rodríguez, I. Martínez-Solano

Publicado en

Conservation Genetics Resources 2013 Volume 5, 981–984

DOI: 10.1007/s12686-013-9948-y

Abstract

The Western Spadefoot, *Pelobates cultripes* (Anura, Pelobatidae), is endemic to the Iberian Peninsula and southeastern France, with isolated populations in the Atlantic coast of France. Its populations are fragmented and it is considered Near Threatened by the IUCN. Here we describe the development of sixteen polymorphic microsatellite loci in this species. Polymorphism was assessed in 95 individuals from five Iberian populations. The number of alleles and expected heterozygosity ranged from 3 to 14 and 0.20 to 0.76, respectively. Eight loci cross-amplified in the closely related and Endangered Moroccan Spadefoot toad, *Pelobates varaldii*. These markers will be useful to address questions about the ecology, population genetics and evolutionary history of *P. cultripes*, including information on effective population size, habitat use and dispersal patterns, which are essential for the efficient management of the fragmented populations characteristic of most of its range.

Resumen

El sapo de espuelas, *Pelobates cultripes* (Anura, Pelobatidae), es una especie endémica de la península ibérica y del sureste de Francia, con poblaciones aisladas en la costa atlántica francesa. Sus poblaciones están fragmentadas y está catalogada como Casi Amenazada (NT) por la UICN. En este trabajo se describe la caracterización de 16 microsatélites polimórficos en *Pelobates cultripes*. Se evaluó el polimorfismo en 95 individuos de cinco poblaciones en la península ibérica. El número observado de alelos por locus estuvo entre 3 y 14, y la heterocigosidad observada entre 0,20 y 0,75. Además, se probaron estos marcadores en el sapo de espuelas marroquí, *Pelobates varaldii*, que está catalogado como En Peligro (EN). De los 16 loci analizados solo amplificaron 8, de los cuales solo 2 resultaron polimórficos. Estos marcadores resultarán útiles para abordar cuestiones acerca de la ecología, genética de poblaciones e historia evolutiva de *P. cultripes*, incluida información sobre el tamaño efectivo poblacional, el uso del hábitat y los patrones de dispersión, que resulta indispensable para el manejo eficaz de las poblaciones fragmentadas características de esta especie.

Amphibians are the most endangered group of vertebrates, with nearly a third of the species threatened or extinct (IUCN *et al*., 2008). Currently their populations are declining in all regions of the world (Stuart *et al*., 2008). The most important causes of these declines are habitat destruction and fragmentation, infectious disease (chytridiomycosis) and climate change (Hof *et al*., 2011). In Europe, projection of species potential distributions under plausible future global change scenarios forecast an increase in suitable habitat for a great proportion of species, except in south-western Europe, where several species will experience a decline in the extent of suitable habitat (Araújo *et al*., 2006).

One of this species is the Western Spadefoot toad, *Pelobates cultripes* (Cuvier, 1829), which is distributed throughout most of the Iberian Peninsula, along the Mediterranean coast of France and in some disjunct areas in the French Atlantic coast (Duget & Melki 2003; García-París *et al*., 2004; Loureiro *et al*., 2008). Its populations are declining range-wide (Tejedo & Reques, 2002) due to habitat loss and the negative impact of invasive species and consequently, the species is listed as Near Threatened by the IUCN (Beja *et al*., 2009).

Here we describe the isolation and characterization of sixteen polymorphic microsatellite loci in *P. cultripes* that will help address a suite of questions ranging from the ecology, demographics, population and landscape genetics, to the phylogeography of the species and provide valuable information for the management of its populations.

A genomic library was constructed at the Sequencing Genotyping Facility, Cornell Life Sciences Core Laboratory Center (CLC) (Andrés & Bogdanowicz, 2011). It was developed from one tadpole (voucher: IMS1224, El Pedroso, Sevilla, Spain). Sequences containing microsatellites were scanned with iQDD 1.3 (Meglécz *et al*., 2010), and forty primer pairs flanking regions with microsatellite motifs were designed with a minimum length of flanking region of 20 bp and a range size between 90 and 320 bp, with an optimal melting temperature of 60 ºC to facilitate multiplexing.

PCR reactions were performed in a total volume of 15 µl, including 25 ng of template DNA, 5x GoTaq Flexi buffer (PROMEGA), 1.5 mM $MgCl_2$, 0.3 mM dNTP, 0.3 µM of each primer and 0.5 U GoTaq Flexi DNA polymerase

(PROMEGA). PCR cycling consisted of initial denaturation (95 ºC, 5 min), 35 cycles of denaturation (95 ºC, 45 s), annealing (60 ºC, 45 s), and extension (72 ºC, 45 s), and a final extension (72 ºC, 10 min).

PCR products were visualized in 2.5 % agarose gels. Of the 40 pairs of primers tested, 24 showed unambiguous bands and were selected for further screening, although only sixteen amplified consistently in all samples. We scored variation in 95 individuals from five populations distributed across the range of the species (Table II.1). Additionally, we tested for cross-amplification in a sample of 17 individuals from three localities of the closely related, North African species *Pelobates varaldii*. This species is cataloged as Endangered by the IUCN due to its restricted and fragmented range and continuing decline in the extent and quality of habitat (Salvador *et al*., 2004).

Forward primers were labeled with fluorescent dyes (6-FAM, PET, NED, and VIC) for use in five multiplex reactions, which were designed with Multiplex Manager 1.2 (Holleley & Geerts, 2009) and performed using Type-it Microsatellite PCR kits (Qiagen) (Table II.2). All reactions were performed in a total volume of 15 µl, containing 7.5 µl of Master Mix, 1.2 µl of primer mix (0.2 µM of each primer), and 5.3 µl of RNase-free H2O. Genotyping was performed on an ABI PRISM 3730 sequencer with the GeneScan 500 LIZ size standard (Applied Biosystems). Peaks were scored manually in GeneMapper 4.0 (Applied Biosystems).

The presence of null alleles, stuttering and large allele dropout in each population was tested using Microchecker 2.2.3 (van Oosterhout *et al*., 2004). Allele dropouts or stuttering were detected in loci Pc4.7 (all populations with the exception of BOC) and Pc4.3 (all populations, except BOC and DON) and thus some caution is required if using these markers.

We estimated the number of alleles (Na), observed (Ho) and expected heterozygosity (He) for each locus and population with GenAlEx 6.5b5 (Peakall & Smouse, 2006) and Genetix (Belkhir *et al*., 2000). The observed number of alleles ranged from 3 to 14 and their size from 119 to 300 bp. The average expected heterozygosity was 0.41 (range: 0.20–0.76) and the average observed heterozygosity, 0.44 (range: 0.20–0.73).

Table II.1. Populations of *P. cultripes* screened for variation with the microsatellites developed in the present study, including locality information, population code, number of samples per population (n), geographic coordinates (latitude and longitude) and estimates of genetic diversity (number of alleles, observed and expected heterozygosity).

Locality	Code	n	Latitude	Longitude	Na	Ho	He
Spain, Valencia, Sinarcas	SIN	19	39° 45' N	1° 14' W	3.5625	0.4605	0.4844
Spain, Madrid, Valdemanco	VAL	19	40° 51' N	3° 38' W	4.0000	0.4020	0.4519
Spain, Huelva, Doñana	DON	19	36° 59' N	6º 27' W	2.6875	0.4322	0.4484
Portugal, Setúbal, Boticos	BOT	19	38° 00' N	8° 29' W	5.1875	0.4281	0.5203
Portugal, Aveiro, Paramos	PAR	19	40° 58' N	8° 38' W	2.6250	0.3158	0.3026

Deviation from Hardy–Weinberg equilibrium (HWE) and evidence of linkage disequilibrium (LD) were tested as implemented in Genepop version 4.2 (Rousset, 2008). A sequential Bonferroni correction (Rice, 1989) was applied to adjust for multiple comparisons. Deviations from HWE were detected in loci Pc4.3 (populations BOC and DON) and Pc4.7 (all populations, except BOC). Significant LD was detected in population DON for loci Pc3.1 and Pc4.5.

Eight out of the sixteen loci tested amplified consistently in *P. varaldii*, although only two of them (Pc3.2 and Pc3.9) were polymorphic (four alleles each).

These novel polymorphic microsatellite markers will add to those described by van de Vliet *et al*. (2009) and provide valuable resources to address questions about the ecology, population genetics and evolutionary history of *P. cultripes*, including information on effective population size, habitat use and dispersal patterns, which are essential for the efficient management of the fragmented populations characteristic of most of its range.

Acknowledgments

We thank M. Barbosa, D. Buckley, I. Gómez Mestre, E. Recuero, G. Sánchez and V. Sancho for help collecting samples and S. Bogdanowicz at Cornell University for help with the microsatellite library. This research was funded by grants CGL2008-04271-C02-01/BOS and CGL2011-28300 (Ministerio de Ciencia e Innovación, Ministerio de Economía y Competitividad, Spain, and FEDER) and PPII10-0097- 4200 (Junta de Comunidades de Castilla la Mancha) to IMS. JGR is supported by the Consejo Superior de Investigaciones Científicas of Spain

Table II.2. Characterization of 16 polymorphic microsatellite loci in the Western Spadefoot (*P. cultripes*), including locus designation, primer sequences, fluorescent dye, repeat motif, multiplex reaction, annealing temperature (ºC), size of amplified product (bp), number of individuals successfully genotyped (n), number of alleles (Na), observed (Ho) and expected (HE) heterozygosities, probability of deviation from Hardy–Weinberg equilibrium (PHW) and GenBank accession number.

Locus	Primer sequence	Labelling dye	Repeat motif	Multiplex reaction	T^a (ºC)	Size range (bp)	n	Na	Ho	He	PHW	GenBank accession no.
Pc3.25	5' GCGTTGGTACACATTGCATC 3' 5' GGCAGCTGTGTAATCGACCT 3'	PET	$(GTT)_7$	Multiplex 1	60	191 - 206	95	6	0.453	0.488	0.435	KF030682
Pc4.1	5' CAAAATGTCCAGTTGGAGTGAG 3' 5' GGAATTTAAGGTGGAAGAGGG 3'	NED	$(TAGA)_5$	Multiplex 1	60	151 - 209	95	14	0.484	0.485	0.006	KF030683
Pc3.2	5' GCTTGTTTGACCTCGTCTCTG 3' 5' CCTCAATGACACCTCTCATGAAC 3'	6-FAM	$(TAA)_{12}$	Multiplex 1	60	178 - 205	95	10	0.758	0.727	0.131	KF030684
Pc3.9	5' GTGTTTCCTGCCAATTGCTT 3' 5' CGTTCACTGATGTCCCAATG 3'	VIC	$(TAA)_6$	Multiplex 1	60	132 -144	95	5	0.316	0.282	0.229	KF030685
Pc3.1	5' TTTGACTAGGGTCCATGCAA 3' 5' GGAAAGTTTTGGGTAAAGCG 3'	PET	$(TAT)_6$	Multiplex 2	60	128 - 137	95	4	0.326	0.312	0.873	KF030686
Pc4.4	5' GGCACACCAAAACACATTGA 3' 5' GACTGTTTATCTATCCATCCACCC 3'	NED	$(TGGA)_5$	Multiplex 2	60	125 -145	95	6	0.379	0.403	0.453	KF030687
Pc3.23	5' CCCTGTAAAGGGCATCATCT 3' 5' TAGGGTGGGAACATCAGGAG 3'	6-FAM	$(CCT)_5$	Multiplex 2	60	178 - 203	95	5	0.253	0.302	0.596	KF030688
Pc4.5	5' TTGCAACTGTATAGAGAGGTGATT 3' 5' TTTCTTTCCCTGTCCGAATG 3'	6-FAM	$(AGAA)_6$	Multiplex 3	60	155 - 187	95	9	0.663	0.643	0.135	KF030689
Pc3.3	5' TCATTGGGAGATCTGAAGCA 3' 5' TAACTGGCGTCCATCATTCA 3'	VIC	$(TGG)_6$	Multiplex 3	60	207 - 225	95	3	0.200	0.196	0.210	KF030690
Pc4.3	5' TTAGGGGAAATGCAAACCAA 3' 5' GAAATGCACCACCATTTTCC 3'	PET	$(GTTT)_7$	Multiplex 3	60	157 - 178	93	9	0.300	0.466	<0.001	KF030691

Pc3.7	5' ATACTCACCATCCCACCCAA 3' 5' TGGTAATCTGCATGTCCCCT 3'	PET	$(TAG)_{14}$	Multiplex 4	60	125 - 158	95	11	0.547	0.530	0.589	KF030692
Pc4.11	5' TCTGCTTGGCCCCTATAGTC 3' 5' TGCAACAAGTTTGGACCAATTA 3'	NED	$(GATA)_{5}$	Multiplex 4	60	119 - 139	93	6	0.242	0.291	0.277	KF030693
Pc4.9	5' TGTTCACACCGTAGACAGCA 3' 5' CGCAATGTACAATTGACAACAG 3'	VIC	$(ATTT)_{5}$	Multiplex 4	60	133 - 149	94	5	0.628	0.580	0.594	KF030694
Pc3.24	5' AATCCCACCATCGTCAATGT 3' 5' TCCTACTACCCCAAGGCTGA 3'	PET	$(CCA)_{6}$	Multiplex 5	60	224 - 239	95	4	0.200	0.198	0.071	KF030695
Pc4.7	5' TTCAATCTGGGCTGAAGAGG 3' 5' AGGCCAAACGACTGAATTTG 3'	6-FAM	$(GATA)_{7}$	Multiplex 5	60	159 - 207	94	11	0.287	0.678	<0.001	KF030696
Pc3.4	5' AGCATACTCCCTACTTGAACCA 3' 5' AGCTAATTCCCCATTCGGTT 3'	6-FAM	$(ACA)_{6}$	Multiplex 5	60	288 - 300	94	5	0.488	0.483	0.214	KF030697

(CSIC) and the European Social Fund (ESF) (JAE-pre PhD fellowship), and IMS is a 'Ramón y Cajal' postdoctoral fellow supported by the Spanish Ministerio de Ciencia e Innovación and the Universidad de Castilla la Mancha.

References

Andrés JA, Bogdanowicz SM (2011) Isolating microsatellite loci: looking back, looking ahead. In: Orgogozo V, Rockman MV (eds) Molecular methods for evolutionary genetics. Springer, New York (USA), pp 211–232.

Araújo MB, Thuiller W, Pearson RG (2006) Climate warming and the decline of amphibians and reptiles in Europe. Journal of Biogeography 33: 1712–1728.

Beja P, Bosch J, Tejedo M, *et al*. (2009) *Pelobates cultripes*. In: IUCN 2012. IUCN Red List of Threatened Species. Version 2012.2. http://www.iucnredlist.org. Accessed 10 April 2013.

Belkhir K, Borsa P, Chikhi L, Raufaste N, Bonhomme F (2000) GENETIX 4.04, Logiciel sous Windows TM pour la Génétique des Populations. Laboratoire Génome, Populations, Interactions. CNRS UMR 5000, Université de Montpellier II, Montpellier, France

Duget R, Melki F (eds) (2003) Les Amphibiens de France, Belgique et Luxemburg, Collection Parthénope. Editions Biotope, Mèze (France)

García-París M, Montori A, Herrero P (2004) Fauna Iberica. Vol. 24. Amphibia: Lissamphibia. Museo Nacional de Ciencias Naturales, Consejo Superior de Investigaciones Científicas, Madrid (Spain)

Hof C, Araújo MB, Jetz W, Rahbek C (2011) Additive threats from pathogens, climate and land-use change for global amphibian diversity. Nature 480: 516–519.

Holleley CE, Geerts PG (2009) Multiplex Manager 1.0: a crossplatform computer program that plans and optimizes multiplex PCR. Biotechniques 46: 511–517.

IUCN, Conservation International, NatureServe (2008) An analysis of amphibians on the 2008 IUCN Red List. http://www.iucnredlist. org/amphibians. Accessed 6 October 2008

Loureiro A, Carretero MA, Ferrand N, Paulo O (2008) Atlas dos Anfíbios e Répteis de Portugal Continental. Instituto da Conservação da Natureza, Lisboa (Portugal)

Meglécz E, Costedoat C, Dubut V *et al* (2010) QDD: a user-friendly program to select microsatellite markers and design primers from large sequencing projects. Bioinformatics 26: 403–404

Peakall R, Smouse PE (2006) GenAlEx 6: genetic analysis in Excel. Population genetic software for teaching and research. Molecular Ecology Notes 6: 288–295.

Rice WR (1989) Analyzing tables of statistical tests. Evolution 43: 223–225.

Rousset F (2008) Genepop'007: a complete re-implementation of the genepop software for Windows and Linux. Molecular Ecology Resources 8: 103–106.

Salvador A, Donaire-Barroso D, Slimani T, El Mouden EH, Geniez P (2004) *Pelobates varaldii*. In: IUCN 2012. IUCN Red List of Threatened Species. Version 2012.2. http://www.iucnredlist.org. Accessed 19 April 2013

Stuart SN, Hoffmann M, Chanson JS, *et al*. (2008) Threatened amphibians of the world. Lynx Edicions, Barcelona, Spain; IUCN, Gland, Switzerland; and Conservation International,

Arlington, VA, USA

Tejedo M, Reques R (2002) *Pelobates cultripes* (Cuvier, 1829). Sapo de espuelas. In: Pleguezuelos JM, Márquez R, Lizana M (eds) Atlas y Libro Rojo de los Anfibios y Reptiles de España. Dirección General de Conservación de la Naturaleza-Asociación Herpetológica Española, Madrid (Spain), pp 94–96.

van de Vliet M, Diekmann O, Serrão E, Beja P (2009) Development and characterization of highly polymorphic microsatellite loci for the Western Spadefoot toad, *Pelobates cultripes*. Conservation Genetics 10: 993–996.

van Oosterhout C, Hutchinson WF, Wills DPM, Shipley P (2004) Micro-checker: software for identifying and correcting genotyping errors in microsatellite data. Molecular Ecology Notes 4: 535–538.

Capítulo II

Escala Filogeográfica

Artículo III: Una perspectiva integradora sobre la historia evolutiva de *Pleurodeles waltl* (Salamandridae), un endemismo ibero-magrebí

Artículo IV: Efectos climáticos del presente y pasado sobre la distribución y diversidad genética actual del sapo de espuelas (*Pelobates cultripes*): un enfoque integrador

Integrative inference of population history in the Ibero-Maghrebian endemic *Pleurodeles waltl* (Salamandridae)

J. Gutiérrez-Rodríguez, M. Barbosa, I. Martínez-Solano

Publicado en

Molecular Phylogenetics and Evolution 2017 Volumen 112, 122–137

DOI: 10.1016/j.ympev.2017.04.022

Abstract

Inference of population histories from the molecular signatures of past demographic processes is challenging, but recent methodological advances in species distribution models and their integration in time-calibrated phylogeographic studies allow detailed reconstruction of complex biogeographic scenarios. We apply an integrative approach to infer the evolutionary history of the Iberian ribbed newt (*Pleurodeles waltl*), an Ibero-Maghrebian endemic with populations north and south of the Strait of Gibraltar. We analyzed an extensive multilocus dataset (mitochondrial and nuclear DNA sequences and ten polymorphic microsatellite loci) and found a deep east-west phylogeographic break in Iberian populations dating back to the Plio-Pleistocene. This break is inferred to result from vicariance associated with the formation of the Guadalquivir river basin. In contrast with previous studies, North African populations showed exclusive mtDNA haplotypes, and formed a monophyletic clade within the Eastern Iberian lineage in the mtDNA genealogy. On the other hand, microsatellites failed to recover Moroccan populations as a differentiated genetic cluster. This is interpreted to result from post-divergence gene flow based on the results of IMA2 and MIGRATE analyses. Thus, Moroccan populations would have originated after overseas dispersal from the Iberian Peninsula in the Pleistocene, with subsequent gene flow in more recent times, implying at least two trans-marine dispersal events. We modeled the distribution of the species and of each lineage, and projected these models back in time to infer climatically favourable areas during the mid-Holocene, the last glacial maximum (LGM) and the last interglacial (LIG), to reconstruct more recent population dynamics. We found minor differences in climatic favourability across lineages, suggesting intraspecific niche conservatism. Genetic diversity was significantly correlated with the intersection of environmental favourability in the LIG and LGM, indicating that populations of *P. waltl* are genetically more diverse in regions that have remained environmentally favourable through the last glacial cycle, particularly southern Iberia and northern Morocco. This study provides novel insights into the relative roles of geology and climate on the biogeography of a biodiversity hotspot.

Resumen

Inferir la historia de poblaciones a través de la señal genética que dejan los procesos demográficos históricos resulta todo un desafío. Sin embargo, los recientes avances metodológicos en modelos de distribución de especies y su integración en estudios filogeográficos calibrados permiten una reconstrucción detallada de escenarios biogeográficos complejos. En este trabajo empleamos una aproximación integral para inferir la historia evolutiva del gallipato (*Pleurodeles waltl*), una especie endémica de la región ibero-magrebí con poblaciones al norte y al sur del Estrecho de Gibraltar. El análisis de un conjunto de datos multilocus (secuencias de ADN mitocondrial y nuclear, y diez microsatélites polimórficos) permitió la identificación de dos linajes evolutivos muy antiguos en las poblaciones ibéricas, originados durante el Plio-Pleistoceno y distribuidos en sentido "Este-Oeste". El evento vicariante que produjo esta división pudo ser el resultado de la formación de la cuenca del río Guadalquivir. En contraste con estudios previos, las poblaciones del norte de África mostraron haplotipos mitocondriales exclusivos, y formaron un grupo monofilético incluido dentro del linaje "Este" ibérico. Por otra parte, de acuerdo con los datos de los microsatélites las poblaciones marroquíes no forman un grupo bien diferenciado. Según los resultados obtenidos con IMA2 y MIGRATE, esto sería el resultado de flujo génico post-divergencia entre poblaciones a ambos lados del Estrecho. De este modo, las poblaciones marroquíes se habrían originado por dispersión a través del mar desde la península ibérica durante el Pleistoceno, con flujo génico más reciente desde el norte de África a la península, lo que implica al menos dos eventos de dispersión transmarina. Se elaboraron modelos de la distribución actual de la especie y de cada linaje por separado para reconstruir la dinámica poblacional más reciente. Para ello, se proyectaron estos modelos al pasado para inferir las áreas climáticas favorables durante el Holoceno Medio, el último máximo glaciar (LGM) y el último interglaciar (LIG). Entre los dos linajes se encontraron pocas diferencias en la favorabilidad climática, lo que sugiere una conservación del nicho ecológico a nivel intraespecífico a lo largo del tiempo. La diversidad genética actual se correlaciona positiva y significativamente con la intersección de la favorabilidad ambiental entre el LIG y el LGM, lo que indica que las poblaciones de *P. waltl* son genéticamente más diversas en aquellas

áreas que han permanecido favorables climáticamente durante el último ciclo glaciar, particularmente en el sur de Iberia y el norte de Marruecos. Este estudio proporciona nuevas evidencias sobre el papel relativo de la geología y el clima en la biogeografía de un punto caliente de biodiversidad.

Introduction

Phylogeography aims to reconstruct the evolutionary history of taxa, both as a chronicle -- a narrative detailing major events and their relative chronological order -- and as a history, inferring the causal connections linking those events (Buckley, 2009). Different aspects of past population histories, such as population fragmentation, expansion/contraction, dispersal, or selection, can be inferred from the molecular signatures of past evolutionary processes in the genome (Nielsen, 2005; Arenas *et al*., 2011). However, in species with deep evolutionary histories, unraveling the relative order of events occurring at different temporal depths from their molecular signatures is often challenging, because different processes can produce a similar trace on the genome, and demographic processes often erase the signals of past events (Ellegren & Galtier, 2016).

Reconstructing an objective, robust narrative and inferring the underlying history requires an integrative, iterative research program in which the study of organismal biology has a central role (Buckley, 2009). In this respect, phylogeography has proven very successful in integrating information from a variety of sources, most recently including environmental data. This, coupled with recent methodological advances in species distribution models (SDMs) such as the application of fuzzy logic (Barbosa & Real, 2012; Barbosa, 2015), has greatly improved our understanding of ecological and climate correlates of species occurrence (Soberón & Peterson, 2005; Svenning *et al*., 2011; Takahashi *et al*., 2014). Projected backwards in time via models of past climate, SDMs have been used to produce estimates of potential species ranges during the Last Interglacial (LIG, ~130 thousand years ago (ka) BP) and the Last Glacial Maximum (LGM, ~21 ka BP) (Varela *et al*., 2010; Acevedo *et al*., 2012; Smith *et al*., 2013). Until recently, paleodistributions of animal species could only be inferred from scarce and often incomplete fossil records, but paleodistributions can now be used to validate projections of SDMs to the past, opening new and exciting avenues in historical biogeography (Malaney *et al*., 2012; Gavin *et al*., 2014). Furthermore, in combination with genetic data, SDMs can help address problematic issues in phylogeographic inference, such as the detection of lineage extinction or the characterization of the routes and geographic extent of species range shifts (Weisrock & Janzen, 2000; Schmitt *et al*., 2014). The integration of

SDMs in phylogeographic studies allows the identification of climatically stable areas through time, which may have served as reservoirs of genetic diversity (glacial refugia), thus producing more robust hypotheses of the evolutionary history of entire biotas (Demos *et al*., 2014).

The Mediterranean Basin is one of the major global biodiversity hotspots (Myers *et al*., 2000), and a significant part of its extraordinarily high level of endemism has been attributed to the action of geological and climatic changes through time, especially since the Miocene, when many of the extant taxa originated. For instance, the migration of the Corsica-Sardinia microplate and the fragmentation of the Betic-Rifean Massif had profound impacts on the origin of new taxa (Bidegaray-Batista & Arnedo, 2011; Maia-Carvalho *et al*., 2014). Later, during the Quaternary, successive climatic oscillations produced cycles of range contraction and expansion in the populations of many species in temperate areas, triggering speciation and extinction (Hewitt, 2000; Bennett & Provan, 2008). In Europe, major glacial refugia have been identified within each of the main southern peninsulas. These areas tend to have not only higher species richness and endemicity, but also higher intraspecific genetic diversity, reflected by parameters such as allelic richness and nucleotide diversity (Ursenbacher *et al*., 2015; Wielstra *et al*., 2015).

Reconstructing the evolutionary history of species originating in the Miocene implies unraveling the relative order of events from their molecular signatures over a deep temporal framework, and thus requires comprehensive geographic sampling and the use of multiple unlinked genetic markers, with different modes of inheritance and mutation rates, to detect genetic signatures of demographic events and processes occurring at multiple temporal scales. For instance, mtDNA can reflect relatively deep phylogeographic breaks, whereas microsatellites are useful to describe more recent population structure. In addition, a growing number of studies are combining SDMs and phylogeographic inference to identify climatically stable areas that may have acted as refugia over the last glacial cycles. However, relatively few such integrative studies have focused on the Iberian Peninsula, which is otherwise well known from a comparative phylogeographic perspective (Gómez & Lunt, 2007).

In this study, we combine SDMs and molecular data to identify glacial

refugia and reconstruct the population history of the Iberian ribbed newt *Pleurodeles waltl* Michahelles, 1830 (Amphibia, Caudata, Salamandridae), an Ibero-Maghrebian endemic with populations north and south of the Strait of Gibraltar. Previous phylogeographic studies have identified two divergent mitochondrial lineages within this species: one distributed across western and central Iberia, and another in eastern Iberia and northern Morocco (Batista *et al*., 2004; Carranza & Arnold, 2004; Veith *et al*., 2004). Different hypotheses differing in the estimated temporal depth of the split have been proposed to explain this phylogeographic break. Furthermore, the origin of north African populations, which are genetically very similar to southern Iberian populations, is unclear, which has led to the proposal of competing hypotheses, including recent human-mediated dispersal vs a natural, overseas dispersal colonization event (Batista *et al*., 2004; Carranza & Arnold, 2004; Veith *et al*., 2004). Here we analyze data from the nuclear and mitochondrial genomes in a geographically comprehensive sample, covering the complete distribution range of this species, and readdress biogeographic hypotheses through time-calibrated genealogies, continuous diffusion phylogeographic models, and estimates of historical rates of gene flow between southern Iberia and north Africa. In addition, we characterize the environmental niche and population structure of the species, explicitly testing for ecological differentiation across mtDNA lineages. Finally, we identify potential refugial areas as the intersection between climatically favorable areas through last glacial and interglacial periods, and test for their correlation with different estimates of genetic diversity (nucleotide diversity, allelic richness, mean number of private alleles, and heterozygosity), in order to reconstruct the historical demography and postglacial recolonization history of this species throughout its deep evolutionary history.

Methods

Sampling and DNA extraction, amplification and sequencing

We sampled 478 individuals of *P. waltl* from 55 localities across the species' range (Fig. III.1A, Table III.1). Samples included tail tips of adults or larvae, which were released back in the place of capture. Tissues were preserved in absolute

Table III.1. Locality information for the samples used in this study, including latitude and longitude, sample size (n) for microsatellite (SSR) and mtDNA analyses, sample codes, number of haplotypes, mtDNA lineages, and nucleotide diversity (π). Locality ID corresponds to Figure 1.

ID	Locality	Longitude	Latitude	n SSR	MtDNA				
					n	Sample Codes	Haplotypes	Lineage	(π)
1	Albires, León, Spain	-5.280	42.276	10	4	IMS3032-IMS3035	H1	Western	0.00000
2	Revilla de Campos, Palencia, Spain	-4.710	42.006	10	4	IMS3097-IMS3100	H1	Western	0.00000
3	Valdefinjas, Zamora, Spain	-5.467	41.435	10	3	IMS3182, IMS3184-IMS3185	H1	Western	0.00000
4	Navales-Valdecarros, Salamanca, Spain	-5.450	40.785	10	4	PW565-PW568	H1, H23	Western	0.00117
5	Ciudad Rodrigo, Salamanca, Spain	-6.576	40.569	10	4	PW663- PW666	H1	Western	0.00000
6	Fermoselle, Zamora, Spain	-6.367	41.328	20	4	IMS2841-IMS2844	H1	Western	0.00000
7	Santo Tomé del Puerto, Segovia, Spain	-3.589	41.200	19	4	IMS1827- IMS1830	H1	Western	0.00000
8	Valdemanco-La Cabrera, Madrid, Spain	-3.645	40.853	10	5	PW09001-PW09004, PW09006	H1	Western	0.00000
9	Faro, Faro, Portugal	-7.979	37.051	9	4	PW738-PW741	H26	Western	0.00000
10	Sedas, Beja, Portugal	-7.599	37.537	10	4	PW442, PW444-PW446	H23	Western	0.00000
11	Abela, Setúbal, Portugal	-8.558	38.042	10	4	PW470-PW473	H23, H24	Western	0.00117
12	Évora, Évora, Portugal	-7.928	38.555	10	4	PW493-PW496	H23	Western	0.00000
13	Coruche, Santarém, Portugal	-8.519	38.999	10	4	PW685- PW688	H1, H3	Western	0.00058
14	Tocha, Coimbra, Portugal	-8.807	40.375	10	4	PW705- PW708	H4	Western	0.00000
15	Jerez de los Caballeros, Badajoz, Spain	-6.696	38.340	10	3	PW513- PW514, PW516	H23, H25	Western	0.00234
16	Campanario, Badajoz, Spain	-5.613	38.840	10	4	PW541-PW544	H1	Western	0.00000
17	Peñarroya-Pueblonuevo, Córdoba, Spain	-5.092	38.285	10	4	PW380-PW383	H1	Western	0.00000
18	Membrío, Cáceres, Spain	-7.048	39.532	9	4	IMS2833- IMS2836	H15, H16, H17	Western	0.00312

19	Navalmoral de la Mata, Cáceres, Spain	-5.547	39.908	9	4	IMS2789-IMS2791, IMS2793	H1, H14	Western	0.00058
20	Menasalbas, Toledo, Spain	-4.357	39.662	10	3	PW595-PW597	H1	Western	0.00000
21	El Toboso, Toledo, Spain	-2.982	39.485	10	7	PW620- PW623, Toboso1-Toboso3	H2	Eastern	0.00000
22	Malagón, Ciudad Real, Spain	-3.907	39.178	10	6	PW651- PW654, La_ Nava1- La_Nava2	H1	Western	0.00000
23	Cabezarrubias del Puerto, Ciudad Real, Spain	-4.257	38.569	10	5	IMS3410-IMS3414	H1	Western	0.00000
24	Tanger Asilah, Tanger-Tetuan, Morocco	-5.979	35.624	15	9	IMS1153- IMS1157, PW769- PW772	H8, H18	Eastern	0.00163
25	Larache-Ksar el Kebir, Tanger-Tetuan, Morocco	-6.039	35.040	8	4	PW849-PW852	H28, H18	Eastern	0.00190
26	Moulay Bousselhaim, Garb-Chrarda-Beni Hsen, Morocco	-6.086	34.770	10	4	PW786-PW789	H22, H18	Eastern	0.00190
27	Kenitra, Garb-Chrarda-Beni Hsen, Morocco	-6.576	34.208	10	3	PW808-PW810	H22, H27	Eastern	0.00187
28	Had Soualem, Chauía-Uardiga, Morocco	-7.829	33.406	10	4	PW837- PW840	H22	Eastern	0.00000
29	Doñana, Huelva, Spain	-6.455	36.989	10	4	PW718- PW721	H5, H6, H7	Eastern	0.00109
30	Chiclana, Cádiz, Spain	-6.032	36.434	20	20	IMS1194 -IMS1213	H5, H9, H10, H11	Eastern	0.00131
31	Cabra, Córdoba, Spain	-4.368	37.507	10	4	PW362- PW365	H5	Eastern	0.00117
32	El Pedroso, Sevilla, Spain	-5.785	37.828	10	6	IMS1220- IMS1221, PW400-PW403	H12	Eastern	0.00109
33	Villanueva de San Juan, Sevilla, Spain	-5.289	37.060	10	3	PW424, PW427-PW428	H5	Eastern	0.00000
34	Bienservida, Albacete, Spain	-2.712	38.550	10	5	IMS3308-IMS3312	H2	Eastern	0.00123
35	Navalcudia, El Bonillo, Albacete, Spain	-2.489	38.939	10	5	IMS3399-IMS3403	H2	Eastern	0.00123
36	El Perelló, Tarragona, Spain	0.670	40.858	10	10	IMS2357-IMS2366	H2	Eastern	0.00000
37	Morella, Castellón, Spain	-0.071	40.502	10	4	IMS3247-IMS3250	H2	Eastern	0.00000
38	Toll Nou, Beneixama, Alicante, Spain	-0.737	38.750	10	5	IMS3369-IMS3373	H2	Eastern	0.00000

ID	Locality	Longitude	Latitude	n SSR	MtDNA				
					n	Sample Codes	Haplotypes	Lineage	(π)
39	Cabañas de El Salobral, Albacete, Spain	-1.965	38.791	10	5	IMS3268-IMS3272	H2	Eastern	0.00123
40	Las Nogueras, Valencia, Spain	-1.082	39.588	11	11	IMS1989-IMS1999	H2	Eastern	0.00000
41	Sinarcas, Valencia, Spain	-1.239	39.763	10	5	IMS3288-IMS3292	H2	Eastern	0.00000
42	Los Palancares, Cuenca, Spain	-1.959	40.010	10	5	IMS3379-IMS3383	H2	Eastern	0.00000
43	Gárgoles, Guadalajara, Spain	-2.631	40.757	-	4	IMS2623-IMS2625, IMS2627	H13	Eastern	0.00000
44	Los Escoriales, Jaén, Spain	-3.924	38.180	-	7	PW345- PW351	H5	Eastern	0.00000
45	Sierra de Loja, Granada, Spain	-4.173	37.114	-	2	PW875-PW876	H5, H29	Eastern	0.00117
46	Moulay Abdesalam, Tanger-Tetuan, Morocco	-5.488	35.271	-	1	GVA214	H21	Eastern	0.00190
47	Mazarambroz, Toledo, Spain	-4.096	39.653	-	3	Castanar2, Castanar4-Castanar5	H1	Western	0.00000
48	La Mierla, Guadalajara, Spain	-3.261	40.923	-	3	La_Mierla1- La_ Mierla3	H1	Western	0.00000
49	Pelahustán, Toledo, Spain	-4.585	40.180	-	1	MNCN10075	H1	Western	0.00000
50	Ksar el Kebir, Tanger-Tetuan, Morocco	-5.916	35.004	-	1	MNCN7184	H18	Eastern	0.00190
51	14 km S Asilah, Tanger-Tetuan, Morocco	-6.017	35.323	-	2	MVZ231893, MVZ186103	H21, H18	Eastern	0.00163
52	5.5km SE Rabat, Rabat-Salé-Zemmour-Zaer, Morocco	-6.824	33.960	-	1	MVZ162384	H19	Eastern	0.00187
53	10 km E Rabat-Sale Bridge, Rabat-Salé-Zemmour-Zaer, Morocco	-6.702	34.012	-	1	MVZ186090	H22	Eastern	0.00187
54	2.5 km E Puerto Real, Cádiz, Spain	-6.115	36.561	-	1	MVZ231894	H20	Eastern	0.00131
55	Tanger, Tanger-Tetuan, Morocco	-5.833	35.792	-	1	MVZ230275	H8	Eastern	0.00163

ethanol and kept in a freezer at -20 °C. Genomic DNA was later extracted with NucleoSpin Tissue-Kits (Macherey-Nagel).

We amplified and sequenced a mitochondrial fragment (856 bp) of the NADH dehydrogenase subunit 4 gene and adjacent tRNAs in 240 specimens from the 55 localities sampled (Fig. III.1A, Table III.1). We refer to this combined fragment (ND4+tRNAs) as ND4 throughout the text. We used primers ND4 and Leu (Arévalo *et al*., 1994), with PCR cycling conditions including an initial denaturation (94°C, 5 min), 40 cycles of denaturation (94°C, 30 s), annealing (53°C, 30 s), and extension (72°C, 1.30 min), and a final extension step (72ºC, 10 min). PCRs were performed in a 25 µl volume containing 25 ng of template DNA, 0.2 µM of each primer, 0.4 mM dNTP, 1 mM $MgCl_2$ and 2.5 µl of 5x GoTaq Flexi buffer (PROMEGA) and 0.5 U GoTaq Flexi DNA polymerase (PROMEGA). PCR products were visualized in 1% agarose gels to verify amplification and possible contaminations through the use of negative controls. Positive bands were precipitated with sodium acetate and ethanol, and then re-suspended in 20 µl of ultrapure water prior to sequencing in an automatic sequencer ABI PRISM 3730. Since some relevant nodes remained unresolved in the ND4 genealogy (see Results), we amplified and sequenced four additional mitochondrial regions: 16S (561 bp, using primers 16Sar and 16Sbr, Palumbi, 1996), D-loop (778 bp, with primers PRO and PHE, Pereira *et al*., 2016), cytochrome oxydase subunit I (604 bp, with primers AnF1 and AnR1, Jungfer *et al*., 2013) and cytochrome b (1,069 bp, with primers MNCN-Glu F and Amp-P10 R, San Mauro *et al*., 2004), in a subsample of 11 *P. waltl* representing all major lineages in the ND4 genealogy plus one representative of the related *P. poireti* from Algeria. Sequences from the only other extant species in the genus, *P. nebulosus*, were downloaded from GenBank to complete this five-gene dataset (Accession: EU880329, this sample was incorrectly attributed to *P. poireti* in Zhang *et al*., 2008, but can be assigned to *P. nebulosus* based on collection locality data, see Escoriza *et al*., 2016).

Four nuclear DNA regions were amplified and sequenced for *P. poireti*, *P. nebulosus* and several representatives of the two major mitochondrial lineages in *P. waltl* (see Table III.S1 for details): chemokine receptor 4 gene (CXCR4, 507 bp, with the primers Cxcr4 F and Cxcr4 R, see sequences and PCR conditions in Nadachowska & Babik, 2009), recombination-activating protein 1 (RAG1, 900

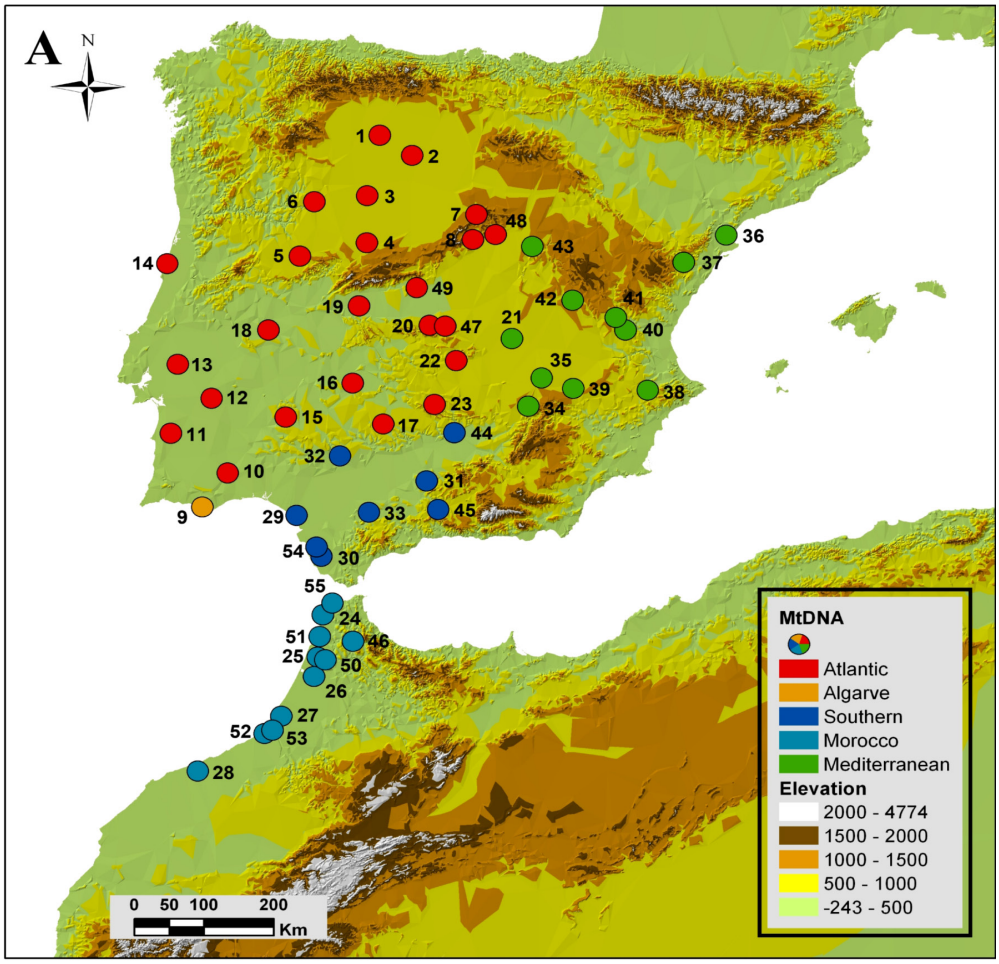
A
N
1
2
3
4
5
6
7
8
48
43
36
37
14
49
42
41
19
20
47
21
40
18
22
35
13
16
39
38
12
23
34
15
17
44
11
32
10
31
9
29
33
45
54
30
55
24
51
46
25
50
26
27
52
53
28
MtDNA
Atlantic
Algarve
Southern
Morocco
Mediterranean
Elevation
2000 - 4774
1500 - 2000
1000 - 1500
500 - 1000
-243 - 500
0 50 100 200
Km

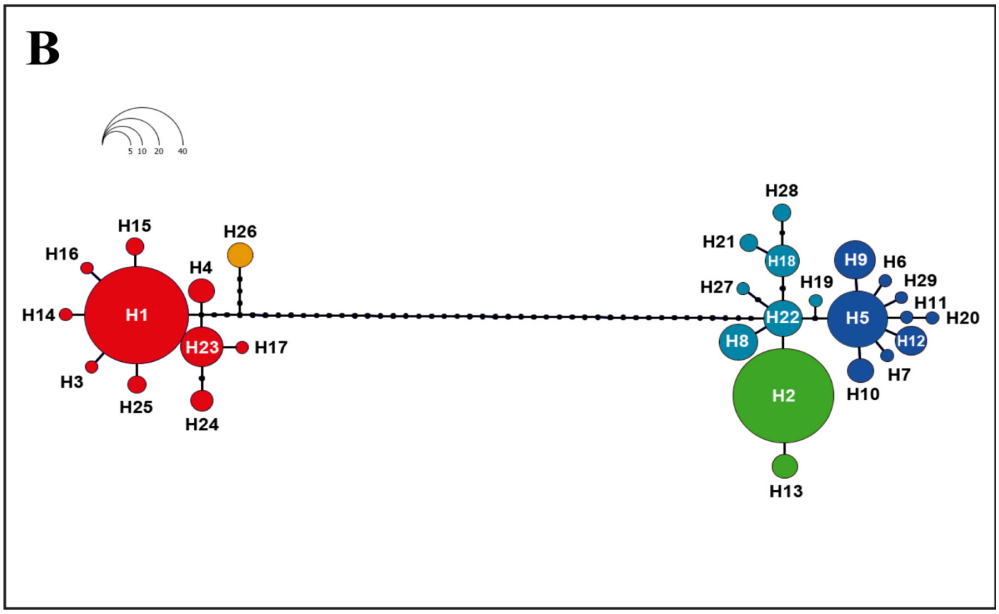
B
5 10 20 40
H15
H16
H26
H4
H14
H1
H23
H17
H3
H25
H24
H28
H21
H18
H9
H6
H27
H19
H29
H22
H5
H11
H20
H8
H12
H7
H2
H10
H13

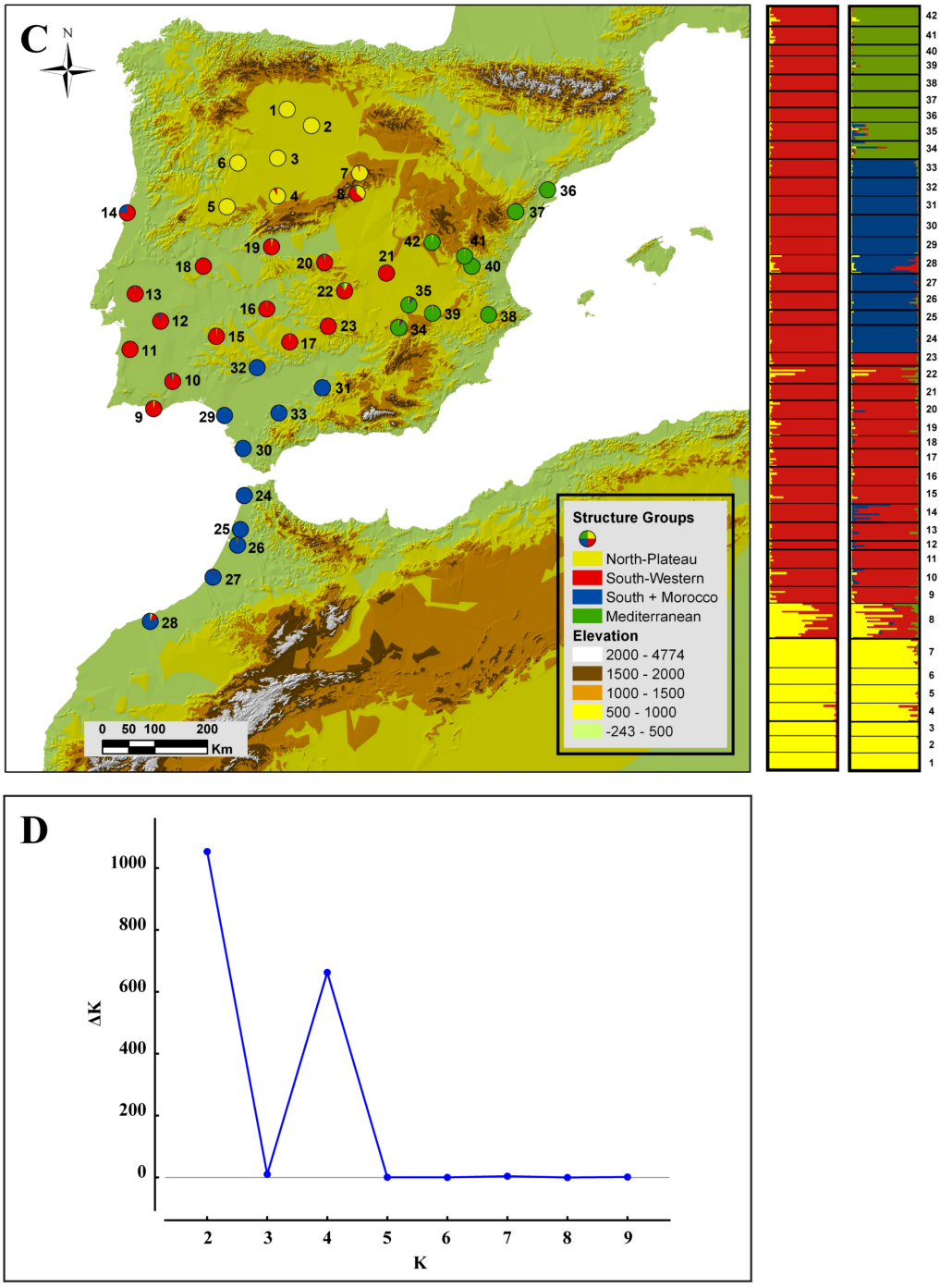

Figure III.1. A) Geographic distribution of the sampled populations, showing the distribution of the two major mtDNA haplogroups (Eastern and Western). The Eastern haplogroup comprises three groups: Mediterranean (green), Southern (dark blue), and Morocco (light blue). The Western haplogroup comprises two groups: Algarve (orange), and Atlantic (red). B) Haplotype network of mtDNA (ND4) sequences in *P. waltl*. Two main mtDNA haplogroups were identified, separated by 43 mutations. C) Results of Structure, showing the spatial distribution of genetic clusters based on values of K=2 and K=4. D) Values of ΔK, showing peaks at K=2 and K=4.

bp, with the primers Amp-RAG1 F and Amp-RAG1 R1, San Mauro *et al*., 2004), solute carrier family 8 (sodium/calcium exchanger) member 3 (SLC8A3, 536 bp, with the newly designed primers SLC8A3F: 5'-GCA GAC AGG CGG TTA CTT TT-3' and SLC8A3R 5'-AGG ATG GCT CTG CCA ATG3', R. Pereira, unpublished) and sodium-calcium exchanger 1 (NCX1, 672 bp, with the primers Naca-L and Naca-P, Roelants & Bossuyt, 2005).

Microsatellites (SSR)

We genotyped 459 samples from 42 populations (Fig. III.1C; Table III.1) with ten previously published highly polymorphic microsatellites (van de Vliet *et al*., 2009). These were grouped into three multiplex reactions: multiplex 1 (loci Ppl2, Ppl3, Ppl5), multiplex 2 (Ppl1, Ppl12, Ppl13, Ppl14) and multiplex 3 (Ppl6, Ppl7, Ppl10). Multiplex reactions were performed with Type-it Microsatellite PCR kits (Qiagen) following protocols described in Gutiérrez-Rodríguez *et al*. (2014). Genotyping was performed on an ABI PRISM 3730 sequencer with the GeneScan 500 LIZ size standard (Applied Biosystems), and peaks were scored manually using GENEMAPPER v4.0 (Applied Biosystems).

Analysis of mtDNA data

Sequences were edited with SEQUENCHER v4.10.1 and aligned manually in MEGA v6.06 (Tamura *et al*., 2013). The number of haplotypes was estimated using DNASP v5 (Librado & Rozas, 2009). Haplotype networks were generated with HAPLOVIEWER (available from: http:// www.cibiv.at/~greg/haploviewer), using a neighbor-joining tree reconstructed with PAUP* v4.0 (Swofford, 2003). Nucleotide diversity (π) was calculated by grouping populations with a buffer of 30 km in the Iberian Peninsula and 20 km in Morocco, to increase sample size while maintaining a regular spatial sampling scheme. This analysis was carried out using SPADS v1.0 (Dellicour & Mardulyn, 2014), and the results were interpolated in ARCGIS 10 (ESRI Inc., Redlands, CA, USA) with the universal kriging function and a spherical semivariogram model. Average genetic distances (p-uncorrected) between and within lineages were calculated with MEGA. We tested for signs of demographic expansion in *P. waltl* and all major mtDNA clades recovered in the five-gene dataset (see Results): Atlantic, Mediterranean,

Southern, and Morocco, by calculating mismatch distributions, Fu's F_s (Fu, 1997), Tajima's D (Tajima, 1989)), Ramos-Onsins and Rozas' R_2 (Ramos-Onsins and Rozas, 2002) and Harpending's raggedness index (Harpending, 1994) in DNASP. Significance was assessed through coalescent simulations with 10,000 replicates.

BEAST analyses

We used *BEAST v1.8 (Drummond *et al*., 2012) to infer speciation times in *Pleurodeles*, including the deep intraspecific split in *P. waltl* (see Results), and estimate nucleotide substitution rates in the different genomic regions analyzed (five mitochondrial and four nuclear DNA genes), in particular in the ND4 partition for subsequent use in continuous diffusion analyses (see below). *BEAST simultaneously infers the species tree and the underlying gene trees based on the multispecies coalescent model (Heled & Drummond, 2010). In order to calibrate the species tree, and considering that the closest extant relative of *Pleurodeles* is the clade formed by *Tylototriton* and *Echinotriton* (e.g., Marjanović & Laurin, 2014) and the limited availability of genetic data for the latter taxa, we used *Tylototriton* as the outgroup. GenBank accession numbers of newly generated sequences as well as those downloaded from GenBank for the analyses are listed in Table III.S1. The cladogenesis between *Pleurodeles* and *Tylototriton* + *Echinotriton* can be assigned a minimum age by assuming that the fossil taxon *Chelotriton* is a member of the group *Tylototriton* + *Echinotriton* (Marjanović & Laurin, 2014). Specifically, the minimum age would be the middle Eocene age of *Chelotriton robustus* at around 41 million years ago (Mya) (Marjanović & Laurin, 2014; Marjanović & Witzmann, 2015). While there is considerable uncertainty about the maximum age of this split, because the fossil record of the Cretaceous and Paleocene is not dense enough, we tentatively considered the split between Salamandrinae and Pleurodelinae at 66 Mya based on Marjanović and Laurin (2014, Fig. 2). To apply this calibration, we specified a lognormal prior for the age of the root of the species tree, encompassing values between 41 and 66 Mya (mean: 53.0 Mya; st. dev.: 0.12; offset: 0; mean in real space=true). We selected the optimal nucleotide substitution model for each of the nine gene partitions based on JMODELTEST v2.5 (Darriba *et al*., 2012), choosing the best-ranked model that was also available in BEAST. We did not explore codon-

partitioning strategies in this analysis to avoid overparametrization. Analyses were run under a strict molecular clock and the Yule speciation model. We also ran analyses assuming a relaxed (uncorrelated-lognormal) molecular clock for all genetic regions, but for all partitions the corresponding 95% highest posterior density intervals for the parameter "coefficient of Variation" included zero, suggesting that a strict clock model provides a better fit to the data. Convergence was assessed through inspection of the logfile in TRACER v1.6 (Rambaut *et al*., 2014), and a Maximum Clade Credibility Tree was reconstructed with TreeAnnotator (distributed as part of the BEAST package).

We used phylogeographic continuous diffusion models as implemented in BEAST to reconstruct range dynamics through time in *P. waltl* based on mtDNA sequences. This analysis simultaneously reconstructs gene trees, ancestral population sizes, and the geographic ranges of inferred nodes, which can be visualized through time provided appropriate calibrations or substitution rates are supplied. For this analysis, we used all 240 ND4 *P. waltl* sequences and selected the optimal partitioning scheme and optimal nucleotide substitution models with PARTITIONFINDER v1.1.1 (Lanfear *et al*., 2012). Geographic coordinates for each sequence were included, with a jitter module generating random coordinates (window size: 0.1) for individuals from the exact same location. We chose this window size to be small enough that it was robust to the low overall dispersal and high genetic structure in the species and at the same time didn't impose computational constraints associated with extremely low values. Analyses were run under a strict molecular clock, with the clock rate specified based on the results of the previous analysis (lognormal distribution; mean=0.006 substitutions/site/million years; st. dev.: 0.3; offset: 0; mean in real space=true), and using the Bayesian Skyline plot (linear, number of groups=5) as the coalescent prior. The Brownian model was used to describe the geographic diffusion process through time across branches of the inferred gene tree (Lemey *et al*., 2010). Convergence was assessed through inspection of the log file in TRACER v1.6, and a MCCT was reconstructed with TreeAnnotator. This tree was used to generate time-calibrated reconstructions of the diffusion process using the modules "Continuous Tree" and "Time Slicer" in SPREAD3 (Bielejec *et al*., 2016). BEAST analyses were run in the Cipres Science Gateway (Miller *et al*., 2010).

Analysis of microsatellite data

The presence of null alleles, stuttering and large allele dropout in each population was tested using MICROCHECKER v2.2.3 (van Oosterhout *et al*., 2004), with a 99% confidence interval and 1,000 randomizations. We also carried out a genetic parentage analysis to eliminate possible full-siblings in each population using COLONY v2.0.5.1 (Jones & Wang, 2010). Colony analyses were performed assuming a mating system with monogamous females and polygamous males, implementing the full-likelihood method of Wang (2004) with 10 independent, medium-length runs. Deviations from Hardy-Weinberg equilibrium (HWE) and evidence of linkage disequilibrium (LD) were tested between all pairs of loci using GENEPOP on the web (http://genepop.curtin.edu.au; Raymond & Rousset, 1995). Significance values for all multiple tests were evaluated by applying a sequential Bonferroni correction (Rice, 1989).

We estimated the mean number of alleles (Na), and both observed (Ho) and expected heterozygosity (He) for each locus and population with GENALEX v6.5b5 (Peakall & Smouse, 2012). Allelic richness (Ar) and mean number of private alleles (P) for each population were calculated with ADZE (Szpiech *et al*., 2008). This program uses a rarefaction approach to allow the comparison of populations with different sample sizes. Ar, P, Ho and π were spatially interpolated using ARCINFO (ESRI, Redlands, CA, USA) with the universal kriging function and a spherical semivariogram model. Subsequently, we performed a principal components analysis on the four genetic diversity variables with PAST v3 (Hammer *et al*., 2001). Values for the first axis (PC1) were checked to correlate positively with all individual measures of genetic diversity, and then interpolated across the species' range following the steps above.

We used the individual-based Bayesian clustering method implemented in STRUCTURE v2.3.4 (Pritchard *et al*., 2000) to describe range-wide patterns of genetic structure based on microsatellite data. STRUCTURE analyses consisted of ten independent runs for K=1-20 clusters (each run consisting of a burn-in of 500,000 generations followed by 1,000,000 MCMC iterations), assuming the admixture model with correlated allele frequencies between populations and the LOCPRIOR option off (Falush *et al*., 2003). The optimal number of genetic clusters was estimated through the ΔK method (Evanno *et al*., 2005) using

STRUCTURE HARVESTER 0.6.94 (Earl & vonHoldt, 2012), although other K values showing consistent, biologically significant results were also considered for further discussion. Average admixture coefficients of optimal clusters were calculated with CLUMPP v1.1 (Jakobsson & Rosenberg, 2007). Graphs of assignment probabilities were produced with DISTRUCT v1.1 (Rosenberg, 2004).

We tested for evidence of recent demographic changes in each of the five major microsatellite clusters identified in previous analyses using the k and g tests (Reich *et al*., 1999). The k-test is based on the observed distribution of allele size within locus, while the g-test is based on allele length variance across loci (Reich *et al*., 1999). Analyses were carried using the kgtests Excel macro program (Bilgin, 2007).

Historical migration between North Africa and the Iberian Peninsula

In order to elucidate the evolutionary history of populations currently separated by the Strait of Gibraltar, historical migration analyses were carried out to confront the "retention of ancestral polymorphism" vs "gene flow" hypotheses between populations on opposite sides of the Strait. Historical migration rates ($M = m/\mu$) and effective population sizes ($\Theta = 4Ne\mu$) were estimated using MIGRATE-N v3.6.4 (Beerli, 2009). Three different migration models were tested: 1) unidirectional migration from southern Iberia to Morocco; 2) unidirectional migration from Morocco to southern Iberia; and 3) panmixia. These analyses were performed by grouping microsatellite genotypes from all Moroccan samples into one population (Morocco), whereas the Iberian population included all individuals in the Iberian South microsatellite cluster (the most closely related group, see BEAST Results in Fig. III.2A). Analyses were run under the Bayesian approach (Beerli, 2006; Beerli & Felsenstein, 2001), assuming the Brownian motion mutation model with constant mutation across all loci. Uniform priors were chosen for Θ (Min. = 0, Max. = 1000, Delta = 100) and M (Min. = 0, Max. = 1000, Delta = 100). Ten replicates were run for each of the three models, starting with a random UPGMA tree and calculating the initial values of M and Θ from FST estimates. The runs consisted of one long chain with 2,500,000 steps, discarding 100,000 as a burn-in, with a static heating scheme using four chains. The best model was chosen

based on Bezier marginal likelihoods and applying the Bayes factor approach (Beerli & Palczewski, 2010; Kass & Raftery, 1995).

An alternative approach to estimating gene flow and effective population sizes among groups was also performed based on the isolation with migration model (IM: Hey & Nielsen, 2004) using IMA2 (Hey, 2010; Hey & Nielsen, 2007). We used the same groups as in the Migrate analyses, but with a combined microsatellite + mitochondrial dataset. The stepwise-mutation model (SMM: Kimura & Ohta, 1978) was used for microsatellites (mean mutation rate: $5x10^{-4}$), and the HKY model of DNA substitution (Hasegawa *et al*., 1985) was used for ND4 sequences. Two independent runs with different seed numbers and 20 heated metropolis-coupled Markov chains (a= 0.96 and b= 0.9) were perfomed. These runs consisted of a varying burn-in period of at least 5 million steps, followed by 15 million steps, with sampling every 100 steps. The effective population size of the ancestral (q0), Morocco (q1) and southern Iberian Peninsula (q2) groups, the population migration rate (m1-2 and m2-1), and the time of divergence (t) between groups were estimated. The maximum prior values for the parameters were q = 200, m = 1.0 and t = 200. Finally, a likelihood-ratio test was carried out to determine the statistical significance of inferred migration rates between groups.

Climatic favourability models

To infer climatically favourable areas (potential refugia and diversification/ dispersal centres) under current and past climate, we built SDMs based on the current occurrence patterns of *P. waltl* and of each of its major mitochondrial lineages separately. Predictor variables were obtained from the WorldClim data set (Hijmans *et al*., 2005) for current climate, for the LIG, and for the three climatic simulations currently available for both the LGM and the Mid Holocene based on the same variables used for model building: CCSM4, MIROC-ESM, and MPI-ESM-P. The dataset included 19 bioclimatic variables with potential direct or indirect relationships with species occurrence (Table III.S2).

The modelling area included the entire distribution range of the species, spanning three countries (Portugal, Spain and Morocco; Fig. III.1). The modelling units were 10 km x 10 km UTM cells, matching most national atlases

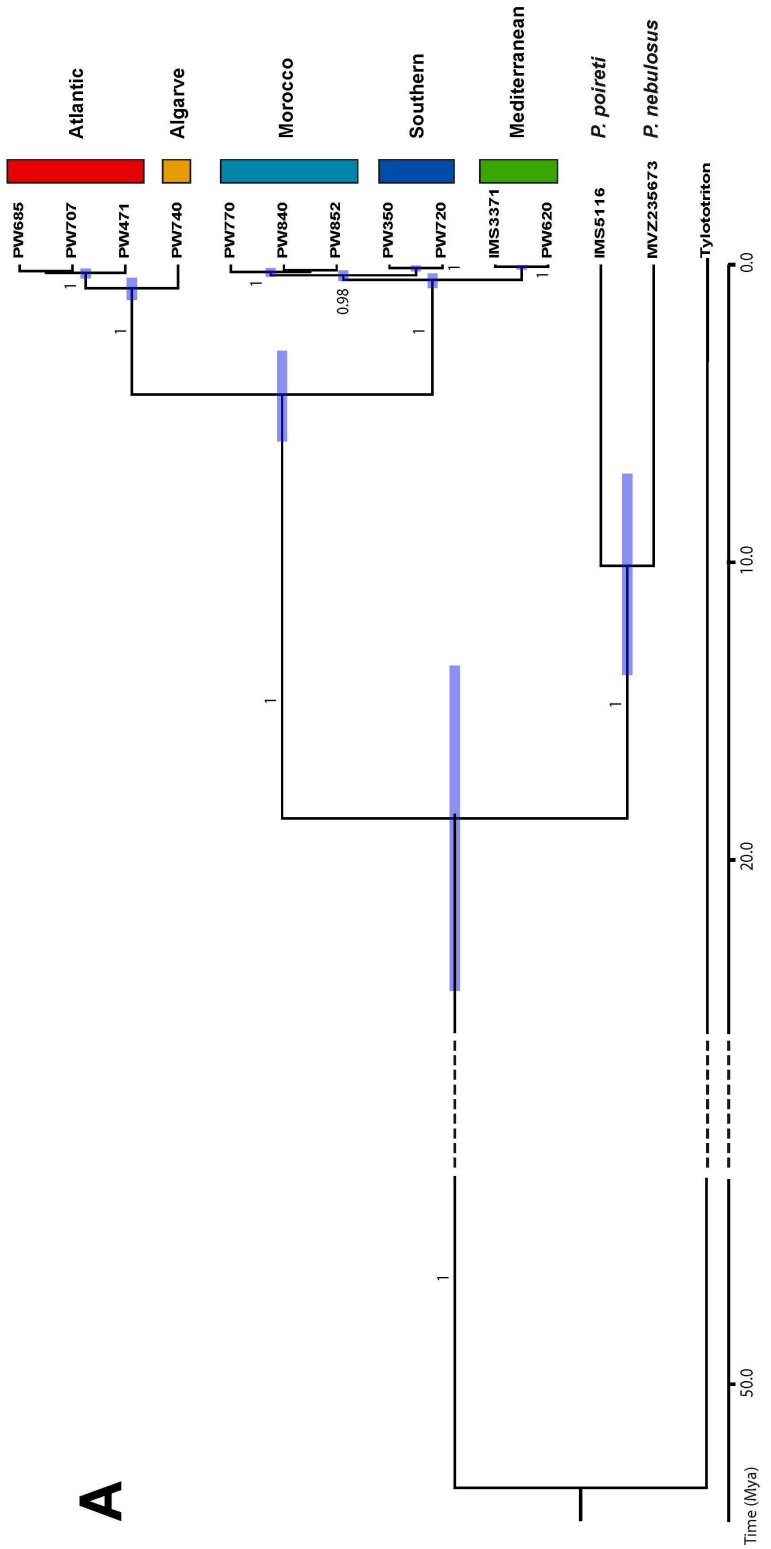
A
Atlantic
Algarve
Morocco
Southern
Mediterranean
P. poireti
P. nebulosus
PW685
PW707
PW471
PW740
PW770
PW840
PW852
PW350
PW720
IMS3371
PW620
IMS5116
MVZ235673
Tylototriton
1
0.98
0.0
10.0
20.0
50.0
Time (Mya)

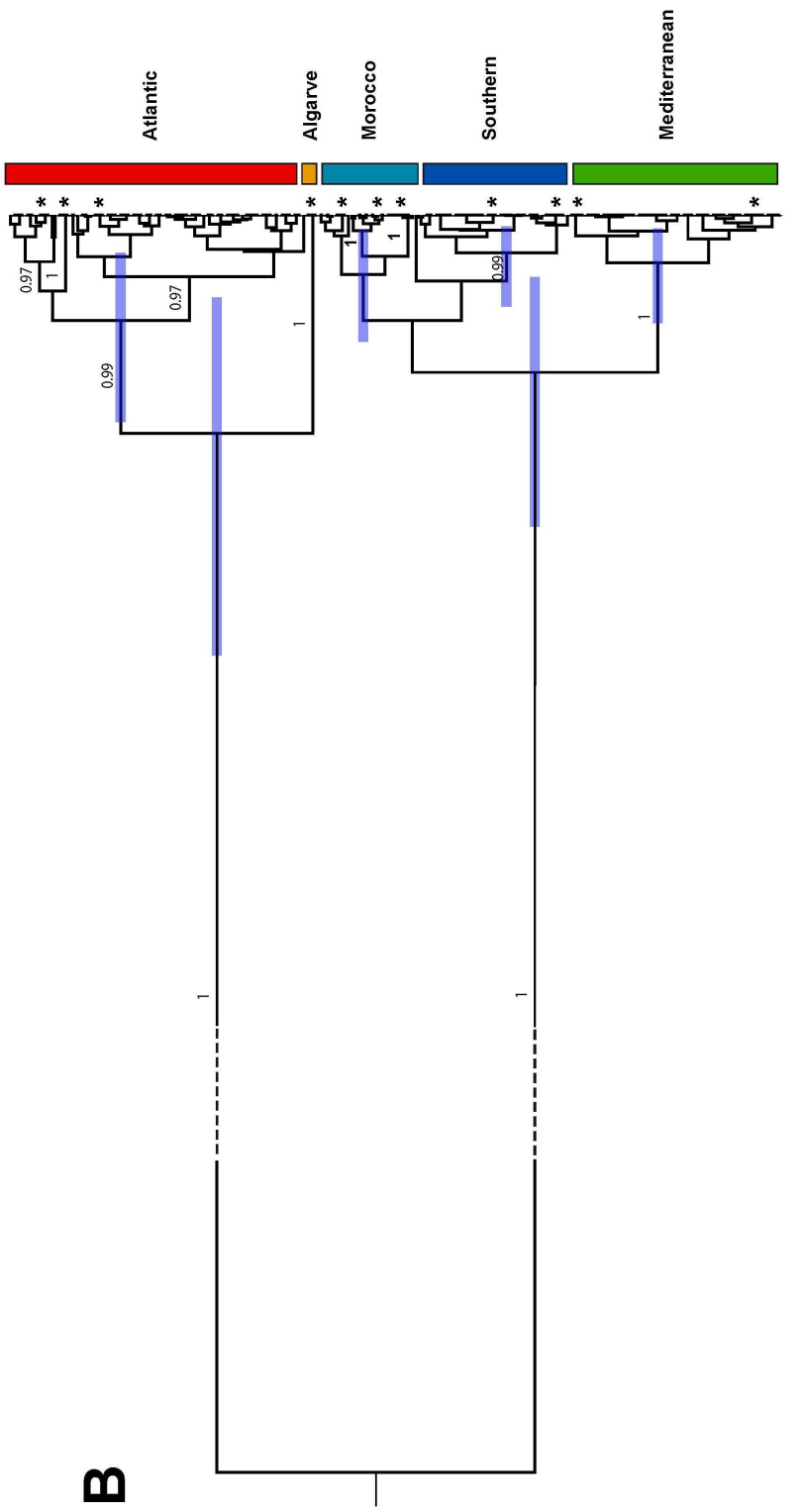

Figure III.2. A. Time-calibrated mtDNA tree resulting from the *BEAST analysis. Values above branches represent Bayesian Posterior Probabilities (BPPs) higher than 0.95. Bars show 95% Highest Posterior Density Intervals (HPDis) of time estimates. Scale bar in millions of years. B. Time-calibrated tree from ND4 sequences of *P. waltl* recovered in continuous diffusion analyses. Asterisks indicate samples included in the *BEAST analysis.

of amphibian distributions (e.g., Pleguezuelos *et al*., 2002; Loureiro *et al*., 2008). While this spatial resolution is relatively coarse given the limited mobility of the studied species, it is appropriate for the spatial extent and the climatic data under analysis, and the best compromise for minimizing positional error in occurrence records while encompassing the species' distribution range. Vector maps of countries and of the UTM grids were downloaded from the EDIT geoplatform (Sastre *et al*., 2009) and clipped to the study area. Distribution data from Portugal (Loureiro *et al*., 2008) and Spain (MAGRAMA, 2015) were imported directly from the source databases. Occurrence points in the Moroccan herpetological atlas (Bons & Geniez, 1996) were digitized, geo-referenced and intersected with the UTM grid. Additional occurrence data from Morocco were obtained from Beukema *et al*. (2013). We further completed the dataset by adding the locations of our own samples (Table III.1).

For modelling the distribution of each lineage while taking advantage of the previously published, though not genetically identified distribution data (Bons & Geniez, 1996; Loureiro *et al*., 2008; Beukema *et al*., 2013; MAGRAMA, 2015), we needed to assign available presence records to a lineage wherever possible. We used the *phylin* R package (Tarroso *et al*., 2015) to compute a genetic semi-variogram based on our sampled populations (31 Eastern and 26 Western lineage occurrences), fit a spherical model, and calculate the potential distribution of each lineage, taking into account spatial autocorrelation and both the geographic and genetic distance between samples. *P. waltl* records with at least 0.8 probability (i.e., odds of at least 4:1) of belonging to one of the lineages were then assigned to that lineage.

Models were built in R v3.0.2 (R Core Team, 2013) with the *fuzzySim* package (Barbosa, 2015), using the favourability function (Real *et al*., 2006), which allows obtaining prevalence-independent values directly comparable across taxa (Acevedo & Real, 2012). Variables with a significant bivariate relationship with the distribution of the species or lineage were first selected based on the false discovery rate (Benjamini & Hochberg, 1995), and then included in multivariate models with a forward-stepwise procedure based on Akaike's Information Criterion. Non-significant variables left in the model were further removed (Crawley, 2007). Model performance was then evaluated with

the *modEvA* R package (Barbosa *et al*., 2013). We measured both discrimination (using 0.5 as the threshold value, which for favourability models equates to using prevalence; Real *et al*., 2006; Acevedo & Real, 2012) and calibration, i.e. the fit of predicted probabilities to oberved occurrence frequencies (see Jiménez-Valverde *et al*., 2013).

The models were extrapolated to hindcast climatically favourable areas based on the WorldClim paleoclimatic simulations. Given that favourability values can be handled directly with fuzzy logic (Real *et al*., 2006; Acevedo & Real, 2012), we used the *fuzzySim* package to calculate the fuzzy intersection of LIG and LGM favourability (Zadeh, 1965), to infer how favourable each cell remained along the glacial cycle. We then calculated the correlations between these sustained favourability values and current genetic diversity.

We mapped and quantified favourability changes between past and current climates, for *P. waltl* and for each mitochondrial lineage, using the fuzzy range change measures (including overall proportional gain, loss and stability) available in *fuzzySim* package. We also compared the favourability patterns obtained for the main lineages, using niche similarity measures such as Schoener's D and Warren's I (Warren *et al*., 2008), as well as fuzzy similarity indices adapted from classical binary similarity, including Jaccard's and Baroni-Urbani and Busers's indices (Barbosa, 2015). The latter two have the advantage of having associated significance values.

Results

Mitochondrial Analyses

Partial sequences of the ND4 gene plus adjacent tRNAs (856 bp) were obtained for 240 individuals from 55 populations (GenBank accession numbers in Table III.S1). Twenty-nine different haplotypes were found (Table III.1), defined by 72 variable sites, of which 64 were parsimony-informative. Nucleotide diversity ranged from 0 to 0.0031 (Table III.1). The reconstructed haplotype network showed two main haplogroups, diagnosing two major lineages in *P. waltl*, henceforth referred to as Western and Eastern (Fig. III.1B). The Western lineage is distributed across the Iberian west and center, whereas the Eastern lineage extends

across eastern Iberia and northern Morocco (Fig. III.1A). Each haplogroup can be subdivided into several geographically consistent sub-haplogroups (Fig. III.1A, B). The highest values of nucleotide diversity were found in northern Morocco (Eastern haplogroup) and south-western Iberia (Western haplogroup, populations Membrío and Jerez), and the lowest values occurred across northern, central and eastern Iberia (Fig. III.S1). Average genetic distance (p-uncorrected) between haplogroups was 5.4%, while average distances within haplogroups were 0.26% (Eastern, range: 0.01-0.8%) and 0.18% (Western, range: 0.1-1.2%). Scenarios of historical demographic expansion were not consistently supported by mismatch distributions or neutrality tests (Fu's F_s, Tajima's D and R_2) for the species or for any of the main four haplogroups considered separately (Table III.2 and Fig. III. S2).

*BEAST analyses produced a fully resolved tree with high support in all nodes (Bayesian Posterior Probabilities, BPPs = 1; Fig. III.S3). According to these results, the split between *P. waltl* and *P. nebulosus* + *P. poireti* took place in the Miocene (median: 18.00 million years ago -Mya-, 95% highest posterior density interval -HPDi-: 12.66-23.57 Mya). The vicariant event between *P. poireti* and *P. nebulosus* occurred during the Miocene (median: 9.21 Mya, 95% -HPDi-: 5.11-13.67 Mya). Finally, the inferred split between the Western and Eastern lineages of *P. waltl* dates back to the Pliocene (median: 3.51 Mya, 95% -HPDi-: 0.75-5.39 Mya).

The topology of the 5-gene mtDNA dataset recovered in the *BEAST analysis includes two major clades and several well-supported intraspecific subclades in *P. waltl* (Fig. III.2A). The Western clade includes two well-supported subclades, corresponding to the Atlantic and Algarve haplogroups. The TMRCA of these subclades dates back to the Pleistocene (median: 0.78 Mya, 95% HPDi: 0.44-1.18 Mya). The Eastern clade is divided into three well-supported subclades (BPP:1): Mediterranean, Southern and Morocco (Fig. III.2A). The TMRCA of these clades dates back to the Pleistocene (median: 0.5 Mya, 95% HPDi: 0.29-0.77 Mya). The Southern and Morocco subclades are recovered as sister groups (BPP:0.98). The TMRCA of these clades dates back to the Pleistocene (median: 0.35 Mya, 95% HPDi: 0.19-0.54 Mya). Finally, the four independent nDNA genealogies recovered in the *BEAST analysis recovered the monophyly of *P.*

Table III.2. Results of tests for demographic expansion in *P. waltl* (Pw), including the Atlantic (A), Mediterranean (Md), Southern (S), and Moroccan (M) haplogroups. Values of Fu's F_s, Tajima's D, R_2 and the raggedness index (R) from mismatch distributions are provided, including their associated p values.

	Fu's F_s	**p**	**Tajima's D**	**p**	**R_2**	**p**	**R**	**p**
Pw	15.803	0.970	2.8453	0.998	0.1604	0.999	0.1131	1.0
A	-4.1894	**0.029**	-1.4277	**0.042**	0.0451	0.089	0.2432	0.633
Md	-0.3342	0.433	-0.5643	0.189	0.0578	0.207	0.6044	0.619
S	-4.359	**0.005**	-1.2637	0.090	0.0616	0.070	0.1594	0.328
M	-0.4011	0.451	-0.3521	0.409	0.1091	0.372	0.0182	**0.005**

waltl and of *P. poireti* + *P. nebulosus* (BPP = 1.0, Figs. III.S4-III.S7). The Eastern and Western clades in *P. waltl* were also recovered as monophyletic, though with low support (BPP<0.90).

Continuous diffusion analyses produced robust results, with ESSs values >200 for all parameters. The ND4 tree is largely consistent with the 5-gene mtDNA topology, except with lower support values at some nodes (Fig. III.2B and Fig. III.S8). The ancestral area of the Western lineage was inferred to be located in the southwestern Iberian Peninsula, with subsequent expansions to the south and the north, reaching the North Plateau in the LIG (88 ka.; Fig. III.S9). In the Eastern lineage, the inferred ancestral area included southern Iberia and North Africa. The Eastern lineage would have colonized Morocco by 270 ka, and subsequently expanded in Iberia to the north and east (Fig. III.S9).

Microsatellite Analyses

Potential null alleles were detected in the loci Ppl2 at Peñarroya-Pueblonuevo and Ppl10 at Moulay Bousselhaim. Forty-six individuals were removed after the sibship analysis in COLONY, leaving only one representative per sibship group (Table III.3). The observed number of alleles ranged from 1 to 10 per locus and population. Summary statistics of genetic diversity for each population are shown in Table III.3. The lowest observed heterozygosities were found north of the Central System mountains, in the North Plateau populations, and also in northeastern Iberia, whereas the highest values were recorded in southern Iberia and Morocco (Fig. III.S1D). Allelic richness ranged from 1.45 to 6.09, with the highest values found in south-western Iberia and in Morocco (Fig. III.S1B). The

Table III.3. Genetic diversity in 42 populations of *P. waltl* based on 10 microsatellite loci. N=sample size; Nc=sample size after exclusion of potential siblings from the sample; Na=mean number of alleles; Ho and He: observed and expected heterozygosity; Ar: allelic richness standardized to the lowest sample size (4); P: number of private alleles (4). Locality ID corresponds to Figure 1 and to Table 1.

ID	N	Nc	Na	Ho	He	Ar (4)	P (4)
1	10	9	1.297	0.178	0.184	1.516	0.000
2	10	9	1.382	0.238	0.218	1.583	0.006
3	10	8	1.203	0.175	0.142	1.446	0.000
4	10	10	1.884	0.430	0.408	2.308	0.000
5	10	10	1.705	0.450	0.373	2.050	0.000
6	20	9	1.466	0.278	0.258	1.733	0.000
7	19	16	2.461	0.550	0.555	2.843	0.000
8	19	19	3.780	0.725	0.703	3.862	0.001
9	9	9	3.148	0.700	0.659	4.027	0.103
10	10	10	5.769	0.864	0.812	5.217	0.205
11	10	10	4.761	0.882	0.771	4.690	0.102
12	10	5	4.853	0.915	0.764	5.162	0.202
13	10	10	4.207	0.830	0.749	4.425	0.358
14	10	10	3.412	0.590	0.627	3.753	0.019
15	10	10	4.277	0.809	0.755	4.384	0.042
16	10	10	4.259	0.790	0.745	4.467	0.034
17	10	10	3.723	0.668	0.701	4.098	0.167
18	9	7	4.759	0.900	0.777	4.936	0.264
19	9	9	4.354	0.856	0.761	4.480	0.035
20	10	10	3.420	0.790	0.673	3.690	0.005
21	10	9	1.987	0.465	0.405	2.323	0.000
22	10	10	4.140	0.726	0.723	4.317	0.019
23	10	7	3.165	0.886	0.661	3.617	0.004
24	15	15	5.504	0.853	0.800	4.924	0.215
25	8	8	5.365	0.850	0.803	5.295	0.247
26	10	10	7.100	0.850	0.857	5.909	0.271
27	10	10	3.462	0.800	0.699	3.900	0.017
28	10	10	5.104	0.790	0.797	4.961	0.200
29	10	10	7.373	0.926	0.855	5.890	0.442
30	20	12	8.956	0.917	0.876	6.088	0.726
31	10	10	3.385	0.720	0.681	3.676	0.160
32	10	10	4.069	0.828	0.709	4.264	0.258
33	10	10	6.200	0.919	0.832	5.458	0.509
34	10	10	3.238	0.690	0.675	3.800	0.052
35	10	10	3.909	0.750	0.727	4.184	0.028
36	10	8	1.315	0.200	0.163	1.525	0.001
37	10	9	1.426	0.278	0.259	1.876	0.023
38	10	9	1.499	0.267	0.275	1.767	0.000
39	10	10	2.777	0.684	0.605	3.314	0.027
40	11	6	1.532	0.450	0.276	1.739	0.000
41	10	10	2.208	0.450	0.440	2.612	0.001
42	10	10	1.642	0.390	0.340	1.831	0.000

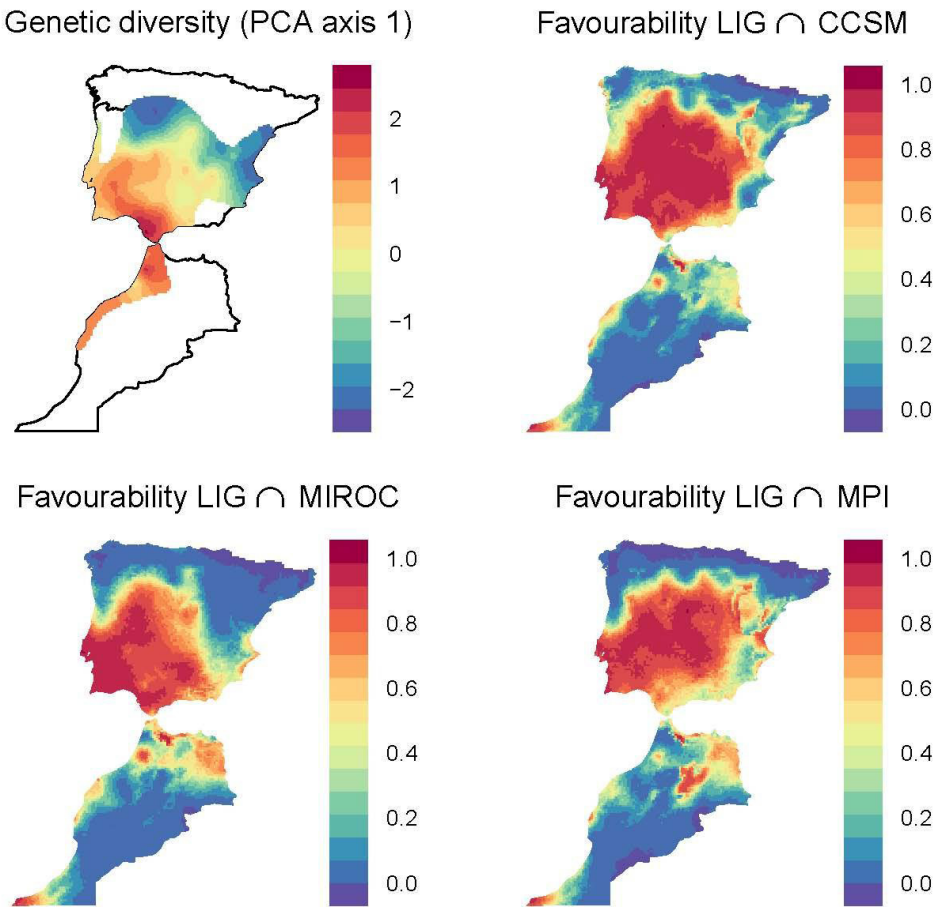

Figure III.3. Genetic diversity of *P. waltl*, based on the first axis of a principal components analysis (PC1) summarizing nucleotide diversity, observed heterozygosity, allelic richness, and mean number of private alleles (positive PC1 scores indicate higher diversity); and the intersection between climatic favourability for this species in the Last Inter-Glacial period (LIG) and in each of the three climatic simulations (CCSM4, MIROC-ESM and MPI-ESM-P) available for the Last Glacial Maximum (LGM).

mean number of private alleles was also highest in the vicinity of the Strait of Gibraltar (Fig. III.S1C).

The first principal component of genetic diversity (PC1) correlated positively with all summarized variables (π, Ho, Ar and P) and accounted for 98.9 % of their variance. Mapping the interpolated values of PC1 across the species' range revealed a decrease of genetic diversity from south to north, with genetically impoverished populations in the North Plateau and the eastern litoral of the Iberian Peninsula (Fig. III.3 and Fig. III.S1).

STRUCTURE analyses supported an optimal clustering level at K=2, according to the Evanno method (Fig. III.1D), with replicate runs producing consistent results (standard deviation of likelihood scores across replicates near zero). At K=2, one cluster is distributed north of the Central System mountains in the North Plateau, whereas the other occupies the rest of the species' range (Fig. III.1C). An additional hierarchical level of genetic structuring was detected at K=4, with a substantial increase in ΔK and all 10 replicates producing congruent, biologically meaningful results. At K=4, the previously recovered second cluster was subdivided into three groups: one in the southwest, in the Tagus and Guadiana river basins; another extending throughout the Guadalquivir river basin and Morocco; and a third one in eastern Iberia (Fig. III.1C). Most populations had high average assignment probabilities to a single cluster, with the exception of population 8 (Valdemanco), which is admixed, suggesting gene flow between two different clusters. At higher values of K, we recovered finer structuring within groups, including an Algarve genetic cluster appearing in most replicates at K values ≥11.

Based on k-test results, we detected significant signatures of demographic expansions in the North-Plateau (P-value=0.001) and Southwestern (P-value=0.045) clusters and in the Morocco group (P-value=0.008). In contrast, results of inter-locus g-tests were not significant for any genetic cluster.

Historical migration between North Africa and the Iberian Peninsula

The Bayes factor approach implemented in MIGRATE provided best support for the second model, i.e., unidirectional migration from Morocco to the southern Iberian Peninsula (Table III.4). Similar results were obtained with IMA2, where the likelihood ratio test (LRT) supports non-zero gene flow from Morocco to the Iberian Peninsula (2Nm = HiPt: 1.893, 95% HPD: 0.8213-3.338). Estimates of effective population sizes largely overlapped between Morocco (q1 = HiPt: 58.10, 95% HPD: 42.90-77.90) and southern Iberia (q2 = HiPt: 57.30, 95% HPD: 42.70-76.10). No precise divergence time estimates could be obtained in the analyses due to lack of convergence.

Table III.4. Comparison of three models of migration between Morocco (M) and the southern Iberian Peninsula (S).

Model	Bezier IML	Ln Bayes factor	Choice (Bezier)	Model Probability
S to M	-21463.13	-6012.53	2	0
M to S	-15450.60	0	1 (best)	1
Panmictic	-104801.28	-89350.68	3	0

Climatic favourability

The obtained distribution models (Table III.S3) had a good overall fit to the current distribution data, especially for *P. waltl* and for the Western lineage (Fig. III.4). Performance measures reached relatively high scores (Fig. III.S10), with e.g. areas under the receiver operating characteristic curve (AUC) considered "excellent" for *P. waltl* and the Western lineage and "good" for the Eastern lineage (Swets, 1988), and with McFadden's pseudo-R^2 values reflecting "excellent fit" in all three cases (McFadden, 1978). The Eastern lineage revealed less clear environmental patterns, with several climatically favourable areas outside and detached from its current distribution, but often inside the current distribution of the Western lineage (Fig. III.4). Fuzzy intersection between climatic favourability values revealed a range of areas that are highly favourable for both lineages simultaneously (Fig. III.4).

Niche similarity measures revealed some affinity between the environmental patterns of the two lineages, with Schoener's D = 0.42 and Warren's I = 0.69 (Warren *et al*., 2008). Fuzzy comparison of favourability values using adapted binary similarity indices (Barbosa 2015) revealed similarity values compatible with chance (i.e., neither larger nor smaller than expected at random) for Jaccard's similarity index (J = 0.28), and higher than expected by chance for Baroni-Urbani and Busers's index (B = 0.61), which accounts for shared absences as well as shared presences.

According to the models applied to paleoclimatic simulations (Fig. III. S11), despite some quantitative differences, past favourability values were significantly correlated with current ones – i.e., the most and least favourable areas, within the available climatic conditions, were largely the same as today, especially during the LGM and the Mid Holocene (Fig. III.S12). The intersections between favourability in the LIG and under each LGM simulation, indicating

the maintenance of favourable conditions through the glacial cycle (Fig. III.3), were significantly although not highly correlated with genetic diversity within the species' range; the strongest correlation was obtained with the MIROC-ESM scenario (Pearson's r = 0.56 under MIROC-ESM, r = 0.11 under CCSM4, and r = 0.05 under MPI-ESM-P; $p < 0.001$ with 5540 degrees of freedom).

Favourability change between time periods included both increases and decreases, with eastern Spain generally showing the sharpest changes in climatic favourability across time (Fig. III.S13). Overall proportional gain, loss, stability and change in favourability between past and current climate are shown in Figure III. 5.

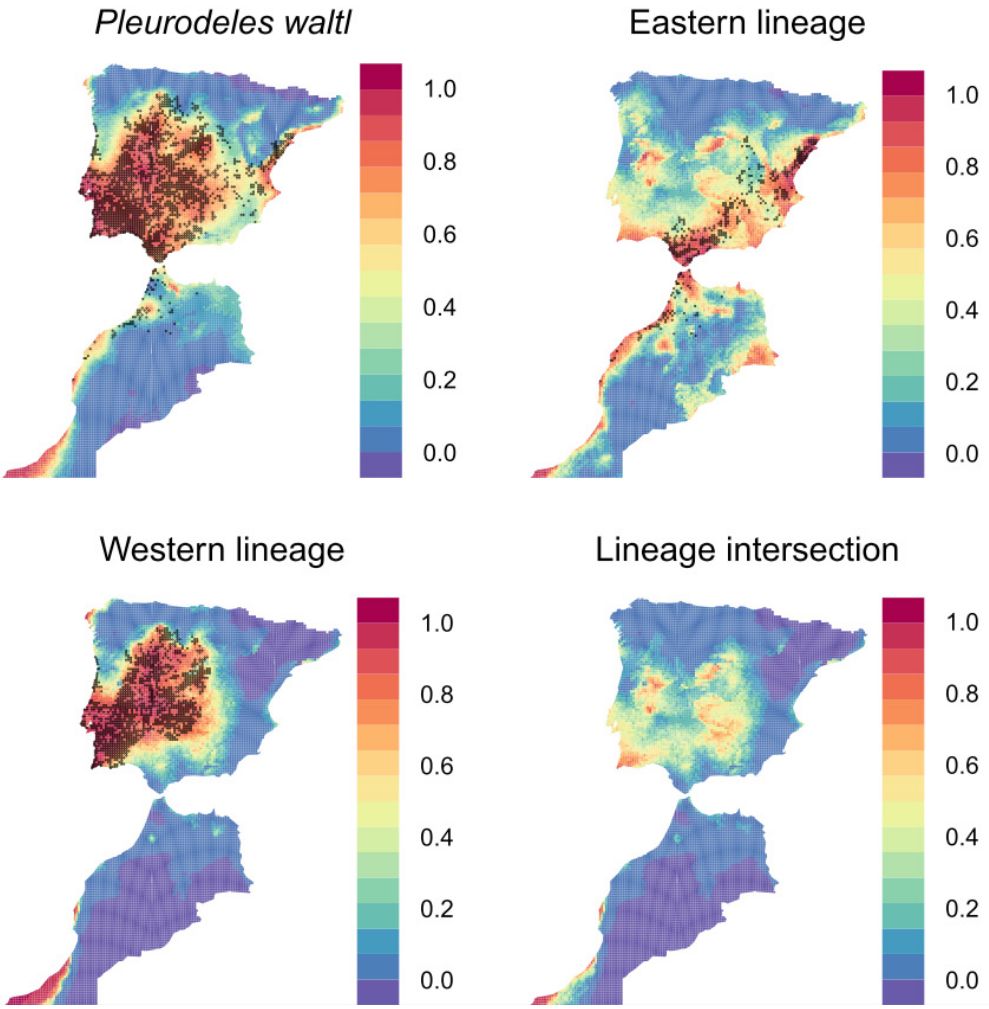

Figure III.4. Species distribution models showing current climatic favourability for *P. waltl* and for each of the two major mtDNA lineages, including areas that are climatically favourable for both lineages (intersection). Black dots represent presence records.

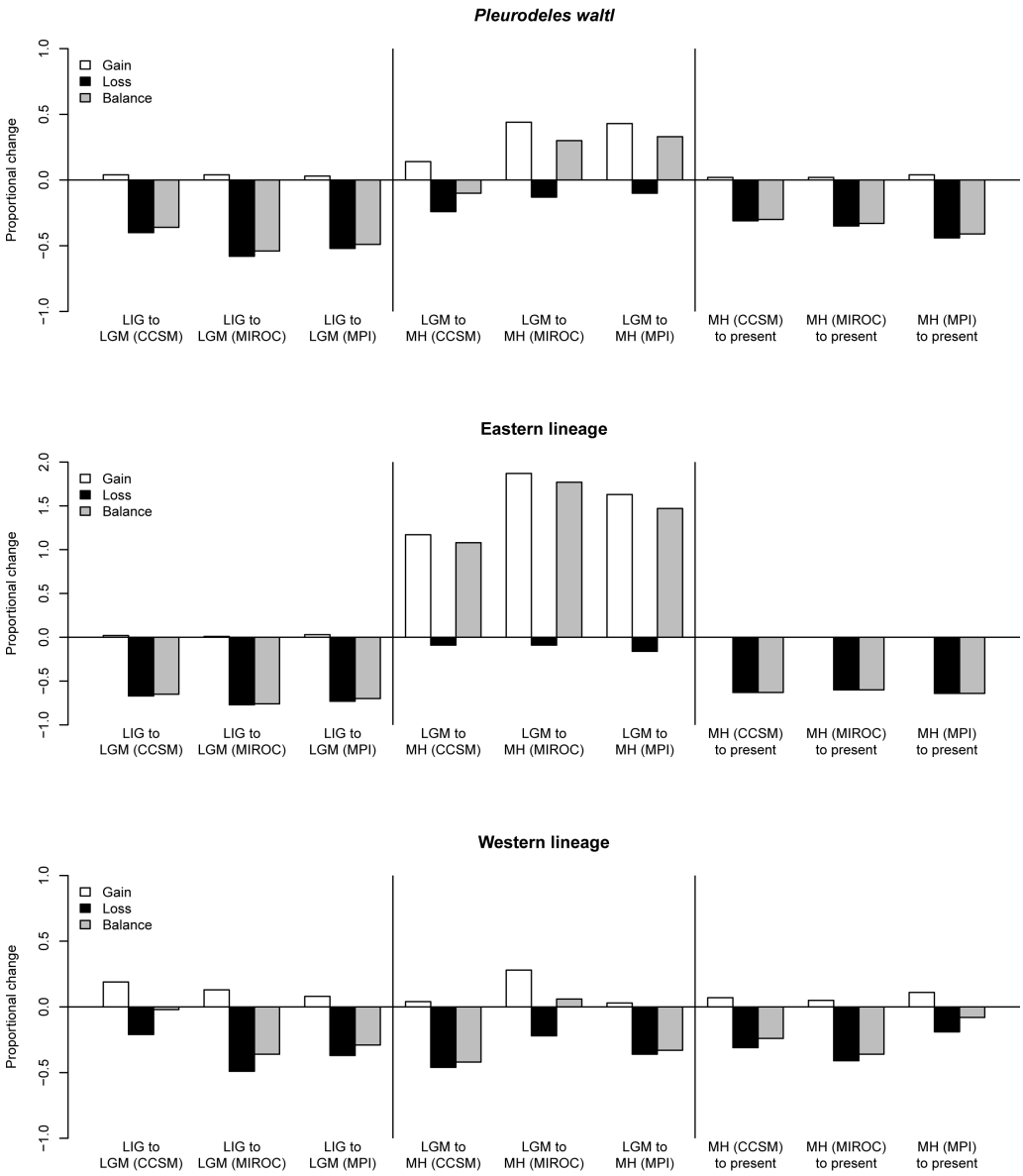

Figure III.5. Fuzzy range change measures (fuzzy equivalents of the proportional gain, loss and overall change in areas favourable for presence) among time periods, from the Last Inter-Glacial (LIG) to the Last Glacial Maximum (LGM), the Mid Holocene (MH) and the present, including the three paleoclimatic simulations currently available across periods on WorldClim (CCSM4, MIROC-ESM and MPI-ESM-P).

Discussion

Inference of population history based on molecular markers is challenging, especially in species with deep evolutionary histories, because different processes can leave similar genetic signatures, and recent processes may erase the signal of older events. Integrative approaches combining molecular and environmental data have great potential for solving these problems, at least in part, and for unravelling the relative importance of different events through the evolutionary history of a species. Our approach, based on a combination of time-calibrated gene tree and ancestral area reconstruction, cluster analysis on genotypic data, estimation of ancestral population sizes and historical patterns of gene flow, and reconstruction of climatic favourability through time, allowed the identification of both paleogeographic and climatic factors involved in the population differentiation of *P. waltl*, with an overall larger importance of the former in shaping current patterns of genetic diversity and structure. Our study provides evidence for key events affecting this species at three major temporal windows. First, a deep vicariant event, dating back to the Pliocene, left a strong genetic signal of population differentiation. Later, in the Pleistocene, trans-marine dispersal events, probably associated with eustatic changes during glacial periods, allowed the colonization of North Africa from the Iberian Peninsula, with at least one additional, more recent event of trans-marine dispersal. Finally, climatic fluctuations in the past 130 ka appear to have had only limited effects on population structure and genetic diversity.

Deep history: Neogene tectonics and relationships between Moroccan and Iberian biotas

The Maghreb has been identified as an important center for species diversification during the Pliocene and Pleistocene, with the area around the Strait of Gibraltar acting as an important biogeographical link between North Africa and Europe at different times (Husemann *et al*., 2013). Previous studies have revealed complex relationships between species on both sides of the Strait of Gibraltar, but North African populations have often been neglected. Species with a deep evolutionary history that are distributed on both sides of this major barrier, such as *P. waltl*, can thus provide valuable information about the biogeography of this region.

Paleogeographic events in the Pliocene are probably associated with the split between the two main mitochondrial lineages (Western and Eastern) in *P. waltl* (Figs. III.1 and III.2). These lineages were identified in previous studies (Carranza & Arnold, 2004; Veith *et al*., 2004) and are largely separated by the Guadalquivir river basin. Based on our calibration, the intraspecific split in *P. waltl* can be tentatively associated with the paleogeographic events associated with the formation of this basin (Doadrio, 1988). This event has also been linked with phylogeographic breaks in other taxa with limited dispersal, including invertebrates (*Carabus*: Andújar *et al*., 2012), amphibians (*Salamandra*: García-París *et al*., 1998; *Discoglossus*: Martínez-Solano, 2004), and reptiles (*Podarcis*: Kaliontzopoulou *et al*., 2011; *Vipera*: Velo-Antón *et al*., 2012). It is worth noting that nucleotide differences among the two main mitochondrial clades of *P. waltl* involved up to ten fixed non-synonymous substitutions.

Within the two major mtDNA lineages, we also identified several sublineages with a marked geographic pattern. In the case of the Western lineage, two sublineages were recovered: one formed by the population of the Algarve (S Portugal) and the other grouping the remaining populations (Atlantic). The split between them occurred in the Pleistocene (TMRCA median: 785 ka, 95%HPDi: 0.44-1.79 Mya). This phylogeographic break is present in many other taxa, including plants (Trindade *et al*., 2012; Caldas, 2013), invertebrates (Mendes, 1992; Serrano, 1995; Barat, 2013), fish (Mesquita *et al*., 2005, 2007), amphibians (Martínez-Solano *et al*., 2006; Gonçalves *et al*., 2009; Reis *et al*., 2011), reptiles (Godinho *et al*., 2008), and mammals (Centeno-Cuadros *et al*., 2009). This shared break has been associated to the formation of the Serra do Caldeirão mountain range during the lower Pliocene (Gonçalves *et al*., 2009). In the case of the Eastern lineage, with a TMRCA estimated at a median age of 504 ka (95%HPDi: 286-773 ka), three sub-clades were recovered (Mediterranean, Southern and Morocco), with their estimated TMRCAS concentrated within the past 240 ka.

Using sequences of the ND4 mitochondrial gene, we found that all haplotypes on either side of the Strait of Gibraltar were exclusive to each area (Fig. III.1B), in contrast with previous findings of shared haplotypes based on more slowly evolving markers. This led to the hypothesis of a recent anthropogenic

introduction from the Iberian Peninsula into Morocco (Carranza & Arnold, 2004) that can be rejected based on the new data, which argue in favor of a relatively old independent history for Moroccan populations. In fact, our time estimates suggest a TMRCA for Moroccan haplotypes of 240 ka (95%HPDi: 122-394 ka), in the Pleistocene. Overall similarity between Moroccan and southern Iberian populations based on microsatellite data can be explained by shared history and post-divergence gene flow, as inferred from MIGRATE and IMA2 analyses. Whereas the timing of this event (or events) of post-divergence gene flow could not be estimated in the present study, some opportunities may have existed during the cooler phases of the Pleistocene, when the 14.4 km distance between both sides of the Strait of Gibraltar was reduced to 3.5 km (Pleguezuelos *et al*., 2008 and references therein) as a consequence of sea level fluctuations. This, together with the reduction of salinity in the Western Mediterranean Sea during the glaciations (Bozec *et al*., 2007), may have facilitated trans-marine dispersal events through rafts of vegetation, as hypothesized for other amphibians (Bell *et al*., 2015; Measey *et al*., 2007; Vences *et al*., 2003).

Concordance between mtDNA haplogroups and microsatellite clusters

Microsatellite data can reveal finer, more recent population structure than slower-evolving markers and, when combined with mtDNA sequences, detect admixture between divergent lineages, illustrating important aspects of the process of population differentiation and speciation (Dufresnes *et al*., 2015; Thomé *et al*., 2016). In *P. waltl*, cluster analyses of microsatellite genotype data are generally consistent with the major mtDNA divisions, with few exceptions. Structure results for K=4 recovered a North-Plateau and a South-Western cluster (both of which have mtDNA haplotypes in the Western mtDNA lineage), and also a Mediterranean and a Southern cluster, the latter including the Moroccan populations (all individuals in these two clusters carry Eastern mtDNA haplotypes). The North Plateau group emerged as a distinct cluster from K=2. This group is characterized by extremely low levels of genetic diversity and was inferred to have colonized its current range relatively recently, perhaps undergoing bottlenecks, to which Structure seems to be particularly sensitive (Manel *et al*., 2003). This pattern of low genetic diversity in this area has also been reported in the co-occurring anuran *Pelobates*

cultripes (Gutiérrez-Rodríguez *et al*., 2017). The Algarve mtDNA lineage was recovered as a genetically distinct group, although at higher values of K, in line with the results of van de Vliet *et al*. (2014), who found significantly reduced cross-amplification success when comparing populations from Algarve (south of the Mira river) with populations further north. The different Iberian groups were largely delimited by major river basins: the North-Plateau group in the Duero Basin, the South-Western group in the Tagus and Guadiana basins, the South group in the Guadalquivir Basin, and the Mediterranean group in the eastern basins. Strikingly, based on Structure analyses, populations from Morocco were not recovered as a distinct group. This contrasts with Busack's (1985, 1986) finding of Nei distances of 0.1 between Moroccan and Iberian populations in his comparative allozyme study, which is also consistent with reported morphological differences between Iberian and Moroccan populations (Pasteur, 1958; but see also Beukema *et al*., 2013). Although sample sizes were low in Busack's study, there were fixed allelic differences at two loci between populations in southern Iberia and Morocco, and calibration of an allozyme-based molecular clock suggested differentiation within the past 2 Mya.

Recent history: the role of glacial events in population structure

The cycling of glacial and interglacial periods during the Pleistocene produced large-scale demographic changes in temperate biotas (Hewitt, 2004). These demographic changes, often involving bottlenecks and founder effects, could potentially erase the signal of deeper evolutionary history, for instance through the random extinction of geographically restricted lineages. This is a limit of traditional phylogeographic inference that can be alleviated with the integration of species distribution models, especially in morphologically and ecologically conservative species. In our study species, the recent evolutionary history, as inferred from the integration of climate-based distribution models and current patterns of genetic diversity, seems to have been characterized by overall stability since the LIG, in contrast with the deeper evolutionary events uncovered by the analyses of molecular data (especially mtDNA). Climatic favourability during the LGM was significantly correlated with current favourability, which, combined with the results of continuous diffusion analyses and population expansion tests,

does not provide clear and consistent signs of recent demographic expansions (Fig. III.S2, Table III.2), but rather suggests overall demographic stability associated with climatically favourable conditions throughout the species' range. However, closer inspection of net changes in climatic favourability across the analysed time periods (Fig. III.5) shows that moderate decreases in the LIG-LGM transition were followed by larger increases in the LGM-MH transition, especially for the Eastern mtDNA haplogroup (Fig. III.S11). Considering the results of tests for signatures of demographic changes based on mtDNA and microsatellites, these increases in favourability through time do not seem to have been tracked by the species or by its major genetic clusters with recent demographic expansions (Table III.2 and Fig. III.S2), with the exception of the North-Plateau cluster. This may be the result of more recent declines in climatic favourability from the MH to the present (Fig. III.5), with successions of favourable and unfavourable periods potentially erasing the genetic signatures of previous demographic events.

The intersection of climatic favourability in the LIG and LGM, which highlights steadily favourable areas for the species along the last glacial cycle, was significantly correlated with current genetic diversity in *P. waltl*. This is in spite of wide differences across available paleoclimatic simulations for the LGM. Although the correlation coefficients were not particularly high, they argue in favor of the existence of southern refugia in the Iberian Peninsula that acted as genetic reservoirs through time, with moderate coefficients probably reflecting a longer timeframe for the role of these areas as refugia (Fig. III.S9).

The current climatic favourability models were well adjusted to the occurrence patterns of the species and major lineages (Fig. III.S10), with little evidence for substantial differences in favourability among lineages, as shown by niche overlap and fuzzy similarity measures. This results in large areas of overlapping favourability, mainly in the central area of the Iberian Peninsula (Fig. III.4), suggesting a high environmental potential for co-occurrence and thus admixture across lineages. Genetic evidence is consistent with this interpretation, as potentially admixed populations (21 (mtDNA-nDNA discordance) and 22 (admixture in Structure analyses); Fig. III.1) are located in areas identified as favourable for both lineages (Fig. III.4).

The application of species distribution modelling to intraspecific genetic lineages holds great promise for clarifying the role of niche evolution in shaping patterns of population divergence and for predicting future responses to climate change (Gotelli & Stanton-Geddes, 2015; Brown *et al*., 2016). However, defining lineage boundaries is often complicated, even when genetic sampling is comprehensive. In this respect, the procedure implemented in the *phylin* package (Tarroso *et al*., 2015) provided a significant improvement over previously available methods for modelling the distributions of intra-specific lineages or cryptic species (e.g., Real *et al*., 2005), as it accounts for the autocorrelation structure of genetic information, interpolates genetic data based on a statistical model, estimates the uncertainty of the predictions, and identifies the most likely occurrence areas of each lineage based on a subset of genetically identified individuals. In turn, the procedures implemented in package *fuzzySim* (Barbosa, 2015) make it possible to 1) use multiple criteria simultaneously for selecting the appropriate variables for each model; 2) obtain environmental favourability values directly comparable across lineages and time periods, independently of sampled prevalence (Real *et al*., 2006); and 3) assess the significance of similarity among favourability patterns without using arbitrary thresholds to separate predicted presences from predicted absences. Thus, it allows direct comparison between continuous model predictions, avoiding the loss of quantitative information (Barbosa, 2015). Package *modEvA* (Barbosa *et al*., 2013) provided a unified framework for evaluating models using multiple metrics, not only of discrimination and classification capacity, but also of calibration or reliability of the continuous predictions, which is just as important in assessing model performance (Pearce & Ferrier, 2000; Jiménez-Valverde *et al*., 2013).

Acknowledgments

We thank I. Acevedo, E. Ayllón, J. Barbadillo, J. Ben Hassine, A. Bermejo, D. Buckley, P. Cabezas, M.J. Fernández, D. Escoriza, I. Gomez-Mestre, E. González, L. Gutiérrez, P. Hernández, M. Lapeña, P. Mas, P. Pavón, E. Recuero, R. Ribeiro, C. Rodríguez, A. Sánchez, V. Sancho, and G. Velo-Antón for help during field work or providing samples. B. Álvarez and I. Rey (DNA and Tissue collection, MNCN-CSIC) provided access to samples under their care. P. Ochoa and L.

Alcaraz helped with laboratory procedures. D. Buckley, E. Jockusch, R. Pereira and two anonymous reviewers provided valuable feedback on a preliminary draft. R. Pereira kindly shared primer information for SLC8A3, developed while funded by the European Science Foundation (Frontiers of Speciation Research, Exchange grant 3318), and by the European Commission (Synthesys grant ES-TAF-1486). K. Roelants provided tips for the amplification of nuclear genes. D. Marjanović and D. Buckley provided valuable feedback on molecular clock calibration strategies and the Salamandridae fossil record. Jesús Marco and Luis Cabellos provided access to the supercomputer Altamira at the Institute of Physics of Cantabria (IFCA-CSIC), member of the Spanish Supercomputing Network, for performing historical migration analyses. JGR was supported by the Consejo Superior de Investigaciones Científicas of Spain (CSIC) and the European Social Fund (ESF) (JAE-pre PhD fellowship). AMB is supported by FCT and FEDER/COMPETE 2020 through contract IF/00266/2013, exploratory project CP1168/CT0001, and funds POCI-01-0145-FEDER-006821 to unit UID/BIA/50027. This research was funded by grants CGL2008-04271-C02-01/BOS, and CGL2011-28300 (Ministerio de Ciencia e Innovación -MICINN-), Ministerio de Economía y Competitividad -MEC-, Spain, and FEDER) to IMS, who was funded by the Severo Ochoa Program (SEV-2012-0262).

References

Acevedo P, Melo-Ferreira J, Real R, Alves PC (2012) Past, Present and Future Distributions of an Iberian Endemic, *Lepus granatensis*: Ecological and Evolutionary Clues from Species Distribution Models. PLoS ONE 7: e51529.

Acevedo P, Real R, (2012) Favourability: concept, distinctive characteristics and potential usefulness. Naturwissenschaften 99, 515–522.

Andújar C, Gómez-Zurita J, Rasplus J-Y, Serrano J (2012) Molecular systematics and evolution of the subgenus *Mesocarabus* Thomson, 1875 (Coleoptera: Carabidae: *Carabus*), based on mitochondrial and nuclear DNA. Zoological Journal of the Linnean Society 166: 787–804.

Arenas M, Ray N, Currat M, Excoffier L (2011) Consequences of range contractions and range shifts on molecular diversity. Molecular Biology and Evolution 29: 207–218.

Arèvalo E, Davis SK, Sites JW (1994) Mitochondrial DNA sequence divergence and phylogenetic relationships among eight chromosome races of the *Sceloporus grammicus* complex (Phrynosomatidae) in central Mexico. Systematic Biology 43: 387–418.

Barat J (2013) Revisión de la identidad de *Neocallicrania serrata* (Bolívar, 1885) y descripción de dos táxones afines: *Neocallicrania serrata pfaui* ssp. n. y *Neocallicrania barrosi* sp.

n.(Orthoptera, Tettigoniidae, Bradyporinae, Ephippigerini). Boletín de la SEA 52, 1–16.

Barbosa AM, Real R (2012) Applying fuzzy logic to comparative distribution modelling: a case study with two sympatric amphibians. The Scientific World Journal 2012: 1–10.

Barbosa AM, Real R, Muñoz AR, Brown JA (2013) New measures for assessing model equilibrium and prediction mismatch in species distribution models. Diversity and Distributions 19: 1333–1338.

Barbosa AM (2015) fuzzySim: applying fuzzy logic to binary similarity indices in ecology. Methods in Ecology and Evolution 6: 853–858.

Batista V, Harris DJ, Carretero MA (2004) Genetic variation in *Pleurodeles waltl* Michahelles, 1830 (Amphibia: Salamandridae) across the Strait of Gibraltar derived from mitochondrial DNA sequences. Herpetozoa 16: 166–168.

Beerli P (2006) Comparison of Bayesian and maximum-likelihood inference of population genetic parameters. Bioinformatics 22: 341–345.

Beerli P (2009) How to use MIGRATE or why are Markov chain Monte Carlo programs difficult to use. In: Population Genetics for Animal Conservation (eds Bertorell G, Bruford MW, Hauffe HC, Rizzoli A, Vernesi C), pp. 42–79. Cambridge University Press, Cambridge.

Beerli P, Felsenstein J (2001) Maximum likelihood estimation of a migration matrix and effective population sizes in n subpopulations by using a coalescent approach. Proceedings of the National Academy of Sciences 98: 4563–4568.

Beerli P, Palczewski M (2010) Unified framework to evaluate panmixia and migration direction among multiple sampling locations. Genetics 185: 313–326.

Bell RC, Drewes RC, Zamudio KR (2015) Reed frog diversification in the Gulf of Guinea: Overseas dispersal, the progression rule, and in situ speciation. Evolution 69: 904–915.

Benjamini Y, Hochberg Y (1995) Controlling the false discovery rate: A practical and powerful approach to multiple testing. Journal of the Royal Statistical Society. Series B, Statistical methodology 57: 289–300.

Bennett KD, Provan J (2008) What do we mean by 'refugia'? Quaternary Science Reviews 27: 2449–2455.

Beukema W, De Pous P, Donaire-Barroso D, *et al*. (2013). Review of the systematics, distribution, biogeography and natural history of Moroccan amphibians. Zootaxa 3661.

Bidegaray-Batista L, Arnedo MA (2011) Gone with the plate: the opening of the Western Mediterranean basin drove the diversification of ground-dweller spiders. BMC Evolutionary Biology 11: 317.

Bielejec F, Baele G, Vrancken B, *et al*. (2016) SpreaD3: interactive visualisation of spatiotemporal history and trait evolutionary processes. Molecular Biology and Evolution 33: 2167-2169.

Bilgin R (2007) Kgtests: a simple Excel Macro program to detect signatures of population expansion using microsatellites. Molecular Ecology 7: 416–417.

Bons J, Geniez P (1996) Anfibios y reptiles de Marruecos. Asociación Herpetológica Española, Barcelona. 319 pp

Bozec A, Kageyama M, Ramstein G, Crépon M (2007) Impact of a Last Glacial Maximum sea-level drop on the circulation of the Mediterranean Sea. Geophysical Research Abstracts 9, 03935.

Brown JL, Weber JJ, Alvarado-Serrano DF, *et al*. (2016) Predicting the genetic consequences of future climate change: The power of coupling spatial demography, the coalescent, and historical landscape changes. American Journal of Botany 103, 153–163.

Busack SD (1985) A biogeographical analysis of a vicariant event: the herpetofauna of the Gibraltar Strait. Ph. D. dissertation., University of California, Berkeley.

Busack SD (1986) Biogeographic analysis of the herpetofauna separated by the formation of the Strait of Gibraltar. National Geographic Research 2: 17–36.

Buckley D (2009) Towards an organismal, integrative, and iterative Phylogeography. BioEssays: 31, 784–793.

Caldas, F.B., 2013. *Thymus lotocephalus*. The Red List of Threatened Species 2013: e.T161974A5522381. Downloaded on 07 March 2016.

Carranza S, Arnold EN (2004) History of West Mediterranean newts, *Pleurodeles* (Amphibia: Salamandridae), inferred from old and recent DNA sequences. Systematics and Biodiversity 1: 327–337.

Centeno-Cuadros A, Delibes M, Godoy JA (2009) Phylogeography of Southern Water Vole (*Arvicola sapidus*): evidence for refugia within the Iberian glacial refugium? Molecular Ecology 18: 3652–3667.

Crawley MJ (2007) The R Book. John Wiley & Sons, Chichester.

Darriba D, Taboada GL, Doallo R, Posada D (2012) jModelTest 2: more models, new heuristics and parallel computing. Nature Methods 9: 772–772.

Dellicour S, Mardulyn P (2014) SPADS 1.0: a toolbox to perform spatial analyses on DNA sequence data sets. Molecular Ecology Resources 14, 647–651.

Demos TC, Kerbis Peterhans JC, Agwanda B. Hickerson MJ (2014) Uncovering cryptic diversity and refugial persistence among small mammal lineages across the Eastern Afromontane biodiversity hotspot. Molecular Phylogenetics and Evolution 71: 41–54.

Doadrio I (1988) Delimitation of areas in the Iberian peninsula on the basis of freshwaterfishes. Bonner zoologische Beiträge 39, 113–128.

Drummond AJ, Suchard MA, Xie D, Rambaut A (2012) Bayesian Phylogenetics with BEAUti and the BEAST 1.7. Molecular Biology and Evolution 29: 1969–1973.

Dufresnes C, Brelsford A, Crnobrnja-Isailović J, *et al*. (2015) Timeframe of speciation inferred from secondary contact zones in the European tree frog radiation (*Hyla arborea* group). BMC Evolutionary Biology 15: 155.

Earl D, vonHoldt B (2012) STRUCTURE HARVESTER: a website and program for visualizing STRUCTURE output and implementing the Evanno method. Conservation Genetics Resources 4: 359–361.

Ellegren H, Galtier N (2016) Determinants of genetic diversity. Nature Reviews Genetics 17: 422–433.

Escoriza D, Gutiérrez-Rodríguez J, Ben Hassine J, Martínez-Solano I (2016) Genetic assessment of the threatened microendemic *Pleurodeles poireti* (Caudata, Salamandridae), with molecular evidence for hybridization with *Pleurodeles nebulosus*. Conservation Genetics 17, 1445-1458.

Evanno G, Regnaut S, Goudet J (2005) Detecting the number of clusters of individuals using the software STRUCTURE: a simulation study. Molecular Ecology 14: 2611–2620.

Falush D, Stephens M, Pritchard JK (2003) Inference of population structure using multilocus genotype data: linked loci and correlated allele frequencies. Genetics 164: 1567–1587.

Fu Y-X (1997) Statistical tests of neutrality of mutations against population growth, hitchhiking and background selection. Genetics 147: 915–925.

García-París M, Alcobendas M, Alberch P (1998) Influence of the Guadalquivir River basin on mitochondrial DNA evolution of *Salamandra salamandra* (Caudata: Salamandridae) from southern Spain. Copeia 1998: 173–176.

Gavin DG, Fitzpatrick MC, Gugger PF *et al*. (2014) Climate refugia: joint inference from fossil records, species distribution models and phylogeography. New Phytologist 204: 37–54.

Godinho R, Crespo EG, Ferrand N (2008) The limits of mtDNA phylogeography: complex patterns of population history in a highly structured Iberian lizard are only revealed by the use of nuclear markers. Molecular Ecology 17: 4670–4683.

Gómez A, Lunt D (2007) Refugia within refugia: patterns of phylogeographic concordance in the Iberian Peninsula. In: Phylogeography of Southern European Refugia (eds Weiss S, Ferrand N), pp. 155–188. Springer Netherlands.

Gonçalves H, Martínez-Solano I, Pereira RJ, *et al*. (2009) High levels of population subdivision in a morphologically conserved Mediterranean toad (*Alytes cisternasii*) result from recent, multiple refugia: evidence from mtDNA, microsatellites and nuclear genealogies. Molecular Ecology 18: 5143–5160.

Gotelli NJ, Stanton-Geddes J (2015) Climate change, genetic markers and species distribution modelling. Journal of Biogeography 42: 1577–1585.

Gutiérrez-Rodríguez J, Gonzalez EG, Martínez-Solano I (2014) Development and characterization of twelve new polymorphic microsatellite loci in the Iberian ribbed newt, *Pleurodeles waltl* (Caudata: Salamandridae), with data on cross-amplification in *P. nebulosus*. Amphibia-Reptilia 35: 129–134.

Gutiérrez-Rodríguez J, Barbosa AM, Martínez-Solano I (2017) Present and past climatic effects on the current distribution and genetic diversity of the Iberian spadefoot toad (*Pelobates cultripes*): an integrative approach. Journal of Biogeography 44: 245–258.

Harpending RC (1994) Signature of ancient population growth in a low-resolution mitochondrial DNA mismatch distribution. Human Biology 66: 591–600.

Hasegawa M, Kishino H, Yano T-a (1985) Dating of the human-ape splitting by a molecular clock of mitochondrial DNA. Journal of Molecular Evolution 22: 160–174.

Hammer Ø, Harper DAT, Ryan PD (2001) PAST: Paleontological statistics software package for education and data analysis. Palaeontologia Electronica 4: 9.

Heled J, Drummond AJ (2010) Bayesian inference of species trees from multilocus data. Molecular Biology and Evolution 27: 570–580.

Hewitt G (2000) The genetic legacy of the Quaternary ice ages. Nature 405: 907–913.

Hewitt G (2004) Genetic consequences of climatic oscillations in the Quaternary. Philosophical Transactions of the Royal Society B: Biological Sciences 359: 183–195.

Hey J (2010) Isolation with migration models for more than two populations. Molecular Biology and Evolution 27: 905–920.

Hey J, Nielsen R (2004) Multilocus methods for estimating population sizes, migration rates and divergence time, with applications to the divergence of *Drosophila pseudoobscura* and

D. persimilis. Genetics 167: 747–760.

Hey J, Nielsen R (2007) Integration within the Felsenstein equation for improved Markov chain Monte Carlo methods in population genetics. Proceedings of the National Academy of Sciences 104: 2785–2790.

Hijmans R, Cameron S, Parra J, Jones P, Jarvis A (2005) Very high resolution interpolated climate surfaces for global land areas. International Journal of Climatology 25: 1965–1978.

Husemann M, Schmitt T, Zachos FE, Ulrich W, Habel JC (2013) Palaearctic biogeography revisited: evidence for the existence of a North African refugium for Western Palaearctic biota. Journal of Biogeography 41: 81–94.

Jakobsson M, Rosenberg NA (2007) CLUMPP: a cluster matching and permutation program for dealing with label switching and multimodality in analysis of population structure. Bioinformatics 23: 1801–1806.

Jiménez-Valverde A, Acevedo P, Barbosa AM, Lobo JM, Real R (2013) Discrimination capacity in species distribution models depends on the representativeness of the environmental domain. Global Ecology and Biogeography 22: 508–516.

Jones OR, Wang J (2010) COLONY: a program for parentage and sibship inference from multilocus genotype data. Molecular Ecology Resources 10: 551–555.

Jungfer KH, Faivovich J, Padial J, *et al*. (2013) Systematics of spiny-backed treefrogs (Hylidae: *Osteocephalus*): an Amazonian puzzle. Zoologica Scripta 42: 351–380.

Kaliontzopoulou A, Pinho C, Harris DJ, Carretero MA (2011) When cryptic diversity blurs the picture: a cautionary tale from Iberian and North African *Podarcis* wall lizards. Biological Journal of the Linnean Society 103: 779–800.

Kass RE, Raftery AE (1995) Bayes Factors. Journal of the American Statistical Association 90: 773–795.

Kimura M, Ohta T (1978) Stepwise mutation model and distribution of allelic frequencies in a finite population. Proceedings of the National Academy of Sciences 75: 2868–2872.

Lanfear R, Calcott B, Ho SYW, Guindon S (2012) Partitionfinder: combined selection of partitioning schemes and substitution models for phylogenetic analyses. Molecular Biology and Evolution 29: 1695–1701.

Lemey P, Rambaut A, Welch JJ, Suchard MA (2010) Phylogeography takes a relaxed random walk in continuous space and time. Molecular Biology and Evolution 27: 1877–1885.

Librado P, Rozas J (2009) DnaSP v5: a software for comprehensive analysis of DNA polymorphism data. Bioinformatics 25: 1451–1452.

Loureiro A, Carretero MA, Ferrand N, Paulo O (2008) Atlas dos Anfíbios e Répteis de Portugal Continental. Instituto da Conservação da Natureza, Lisboa (Portugal). 257 pp.

MAGRAMA (2015) Inventario Español de Especies Terrestres. Fauna de vertebrados: Anfibios y reptiles. Ministerio de Agricultura, Alimentación y Medio Ambiente, website Http://www.magrama.gob.es/es/biodiversidad/temas/conservacion-de-especies-amenazadas/vertebrados [accessed 2 January 2015].

Maia-Carvalho B, Gonçalves H, Ferrand N, Martínez-Solano I (2014) Multilocus assessment of phylogenetic relationships in *Alytes* (Anura, Alytidae). Molecular Phylogenetics and Evolution 79: 270–278.

Malaney JL, Frey JK, Cook JA (2012) The biogeographic legacy of an imperilled taxon provides a foundation for assessing lineage diversification, demography and conservation genetics, Diversity and Distribution 18: 689–703.

Manel S, Schwartz MK, Luikart G, Taberlet P (2003) Landscape genetics: combining landscape ecology and population genetics. Trends in Ecology & Evolution 18: 189–197.

Marjanović D, Laurin M (2014) An updated paleontological timetree of lissamphibians,with comments on the anatomy of Jurassic crown-group salamanders (Urodela). Historical Biology 26: 535–550.

Marjanović D, Witzmann F (2015) An extremely peramorphic newt (Urodela: Salamandridae: Pleurodelini) from the latest Oligocene of Germany, and a new phylogenetic analysis of extant and extinct salamandrids. PLoS ONE 10, e0137068.

Martínez-Solano I (2004) Phylogeography of Iberian *Discoglossus* (Anura: Discoglossidae). Journal of Zoological Systematics and Evolutionary Research 42: 298–305.

Martínez-Solano I, Teixeira J, Buckley D, García-París M (2006) Mitochondrial DNA phylogeography of *Lissotriton boscai* (Caudata, Salamandridae): evidence for old, multiple refugia in an Iberian endemic. Molecular Ecology 15: 3375–3388.

McFadden DL (1978) Quantitative methods for analyzing travel behaviour of individuals: some recent developments. In: Hensher D, Stopher P (Eds.), Behavioural travel modelling. Croom Helm, London, 279–318.

Measey GJ, Vences M, Drewes RC, *et al*. (2007) Freshwater paths across the ocean: molecular phylogeny of the frog *Ptychadena newtoni* gives insights into amphibian colonization of oceanic islands. Journal of Biogeography 34: 7–20.

Mendes L (1992) New data on the Thysanuran (Microcoryphia and Zygentoma: Insecta) from the Guadiana River Valley in Algarve (Portugal). Arquivos do Museu Bocage. Nova série 2: 275–286.

Mesquita N, Hänfling B, Carvalho G, Coelho M (2005) Phylogeography of the cyprinid *Squalius aradensis* and implications for conservation of the endemic freshwater fauna of southern Portugal. Molecular Ecology 14: 1939–1954.

Mesquita N, Cunha C, Carvalho GR, Coelho MM (2007) Comparative phylogeography of endemic cyprinids in the south-west Iberian Peninsula: evidence for a new ichthyogeographic area. Journal of Fish Biology 71: 45–75.

Miller MA, Pfeiffer W, Schwartz T (2010) Creating the CIPRES Science Gateway for inference of large phylogenetic trees. 2010 Gateway Computing Environments Workshop (GCE), 1–8.

Myers N, Mittermeier RA, Mittermeier CG, da Fonseca GAB, Kent J (2000) Biodiversity hotspots for conservation priorities. Nature 403: 853–858.

Nadachowska K, Babik W (2009) Divergence in the face of gene flow: the case of two newts (Amphibia: Salamandridae). Molecular Biology and Evolution 26: 829–841.

Nielsen R (2005) Molecular signatures of natural selection. Annual Review of Genetics 39: 197–218.

Palumbi SR (1996) Nucleic acids II: the polymerase chain reaction. In : Molecular Systematics (eds. Hillis DM, Moritz C, Mable BK), pp . 205–247. Sinauer & Associates Inc., Sunderland, Massachusetts.

Pasteur G (1958) Sur la systématique des espèces du genre *Pleurodeles* (Salamandridés). Bulletin de la Société des Sciences Naturelles du Maroc 38: 157–165.

Peakall R, Smouse PE (2012) GenAlEx 6.5: genetic analysis in Excel. Population genetic software for teaching and research—an update. Bioinformatics 28: 2537–2539.

Pearce J, Ferrier S (2000) Evaluating the predictive performance of habitat models developed using logistic regression. Ecological Modelling 133: 225–245.

Pereira RJ, Martínez-Solano I, Buckley D (2016) Hybridization during altitudinal range shifts: nuclear introgression leads to extensive cyto-nuclear discordance in the fire salamander. Molecular Ecology 25: 1551–1565.

Pleguezuelos JM, Márquez R, Lizana M (eds.) (2002) Atlas y Libro Rojo de los Anfíbios y Reptiles de España, 2nd edn. Dirección General de Conservación de la Naturaleza — Asociación Herpetologica Española, Madrid.

Pleguezuelos JM, Fahd S, Carranza S (2008) El papel del Estrecho de Gibraltar en la conformación de la actual fauna de anfibios y reptiles en el Mediterráneo Occidental. Boletín de la Asociación Herpetológica Española 19: 2–17.

Pritchard JK, Stephens M, Donnelly P (2000) Inference of population structure using multilocus genotype data. Genetics 155: 945–959.

Rambaut A, Suchard M, Xie D, Drummond A (2014) Tracer v1.6. Computer program and documentation distributed by the author, website http://beast. bio. ed. ac. uk/Tracer [accessed 27 July 2014].

Ramos-Onsins SE, Rozas J (2002) Statistical properties of new neutrality tests against population growth. Molecular Biology and Evolution 19: 2092–2100.

Raymond M, Rousset F (1995) GENEPOP (Version 1.2): Population genetics software for exact tests and ecumenicism. Journal of Heredity 86: 248–249.

Real R, Barbosa AM, Martínez-Solano I, García-París M (2005) Distinguishing the distributions of two cryptic frogs (Anura: Discoglossidae) using molecular data and environmental modeling. Canadian Journal of Zoology 83: 536–545.

Real R, Barbosa AM, Vargas JM (2006) Obtaining environmental favourability functions from logistic regression. Environmental and Ecological Statistics 13: 237–245.

Reich DE, Feldman MW, Goldstein DB (1999) Statistical properties of two tests that use multilocus data sets to detect population expansions. Molecular Biology and Evolution 16: 453–466.

Reis DM, Cunha RL, Patrão C, Rebelo R, Castilho R (2011) *Salamandra salamandra* (Amphibia: Caudata: Salamandridae) in Portugal: not all black and yellow. Genetica 139: 1095–1105.

Rice WR (1989) Analyzing tables of statistical tests. Evolution 43: 223–225.

Roelants K, Bossuyt F (2005) Archaeobatrachian paraphyly and Pangaean diversification of crown-group frogs. Systematic Biology 54: 111–126.

Rosenberg NA (2004) DISTRUCT: a program for the graphical display of population structure. Molecular Ecology Resources 4: 137–138.

San Mauro D, Gower DJ, Oommen OV, Wilkinson M, Zardoya R (2004) Phylogeny of caecilian amphibians (Gymnophiona) based on complete mitochondrial genomes and nuclear RAG1. Molecular Phylogenetics and Evolution 33: 413–427.

Sastre P, Roca P, Lobo JM, EDIT co-workers (2009) A Geoplatform for improving accessibility to environmental cartography. Journal of Biogeography 36: 568–568.

Schmitt T, Habel JC, Rödder D, Louy D (2014) Effects of recent and past climatic shifts on the genetic structure of the high mountain Yellow-spotted ringlet butterfly *Erebia manto* (Lepidoptera, Satyrinae): a conservation problem. Global Change Biology 20: 2045–2061.

Serrano ARM (1995) Description and natural history of tiger beetles larvae (Coleoptera Cicindelidae) from Castro-Marim-Vila Real de Santo Antonio region (Algarve, Portugal). Arquivos Do Museu Bocage: Nova série 2: 555–606.

Smith SE, Gregory RD, Anderson BJ, Thomas CD (2013) The past, present and potential future distributions of cold-adapted bird species. Diversity and Distributions 19: 352–362.

Soberón J, Peterson AT (2005) Interpretation of models of fundamental ecological niches and species' distributional areas. Biodiversity Informatics 2: 1–10.

Svenning J-C, Fløjgaard C, Marske KA, Nógues-Bravo D, Normand S (2011) Applications of species distribution modeling to paleobiology. Quaternary Science Reviews 30: 2930–2947.

Swets J (1998) Measuring the accuracy of diagnostic systems. Science 240: 1285–1293.

Swofford D (2003) PAUP*. Phylogenetic Analysis Using Parsimony (*and other methods). Version 4. Sinauer Associates, Sunderland, Massachussets.

Szpiech ZA, Jakobsson M, Rosenberg NA (2008) ADZE: a rarefaction approach for counting alleles private to combinations of populations. Bioinformatics 24: 2498–2504.

Tajima F (1989) Statistical method for testing the neutral mutation hypothesis by DNA polymorphism. Genetics 123: 585–595.

Takahashi MK, Eastman JM, Griffin DA, *et al*. (2014) A stable niche assumption-free test of ecological divergence. Molecular Phylogenetics and Evolution 76: 211–226.

Tamura K, Stecher G, Peterson D, Filipski A, Kumar S (2013) MEGA6: molecular evolutionary genetics analysis version 6.0. Molecular Biology and Evolution 30: 2725–2729.

Tarroso P, Velo-Antón G, Carvalho SB (2015) phylin: an r package for phylogeographic interpolation. Molecular Ecology Resources 15: 349–357.

Thomé MTC, Sequeira F, Brusquetti F, *et al*. (2016) Recurrent connections between Amazon and Atlantic forests shaped diversity in Caatinga four-eyed frogs. Journal of Biogeography 43: 1045–1056.

Trindade H, Sena I, Gonçalves S, Romano A (2012) Genetic diversity of wild populations of *Tuberaria major* (Cistaceae), an endangered species endemic to the Algarve region (Portugal), using ISSR markers. Biochemical Systematics and Ecology 45: 49–56.

Ursenbacher S, Guillon M, Cubizolle H, *et al*. (2015) Postglacial recolonization in a cold climate specialist in western Europe: patterns of genetic diversity in the adder (*Vipera berus*) support the central–marginal hypothesis. Molecular Ecology 24: 3639–3651.

van de Vliet MS, Diekmann OE, Machado M, *et al*. (2014) Genetic divergence for the amphibian *Pleurodeles waltl* in Southwest Portugal: dispersal barriers shaping geographic patterns. Journal of Herpetology 48: 38–44.

van de Vliet MS, Diekmann OE, Serrão EA, Beja P (2009) Isolation of highly polymorphic microsatellite loci for a species with a large genome size: sharp-ribbed salamander

(*Pleurodeles waltl*). Molecular Ecology Resources 9: 425–428.

van Oosterhout C, Hutchinson WF, Wills DPM, Shipley P (2004) MICRO-CHECKER: software for identifying and correcting genotyping errors in microsatellite data. Molecular Ecology Resources 4: 535–538.

Varela S, Lobo JM, Rodríguez J, Batra P (2010) Were the Late Pleistocene climatic changes responsible for the disappearance of the European spotted hyena populations? Hindcasting a species geographic distribution across time. Quaternary Science Reviews 29: 2027–2035.

Veith M, Mayer C, Samraoui B, Barroso DD, Bogaerts S (2004) From Europe to Africa and vice versa: Evidence for multiple intercontinental dispersal in ribbed salamanders (Genus *Pleurodeles*). Journal of Biogeography 31: 159–171.

Velo-Antón G, Godinho R, Harris DJ, *et al*. (2012) Deep evolutionary lineages in a Western Mediterranean snake (*Vipera latastei*/*monticola group*) and high genetic structuring in Southern Iberian populations. Molecular Phylogenetics and Evolution 65: 965–973.

Vences M, Vieites DR, Glaw F, *et al*. (2003) Multiple overseas dispersal in amphibians. Proceedings of the Royal Society B: Biological Sciences 270: 2435–2442.

Wang J (2004) Sibship reconstruction from genetic data with typing errors. Genetics 166, 1963–1979.

Warren DL, Glor RE, Turelli M (2008) Environmental niche equivalency versus conservatism: quantitative approaches to niche evolution. Evolution 62: 2868–2883.

Weisrock DW, Janzen FJ (2000) Comparative molecular phylogeography of North American softshell turtles (*Apalone*): implications for regional and wide-scale historical evolutionary forces. Molecular Phylogenetics and Evolution 14: 152–164.

Wielstra B, Babik W, Arntzen JW (2015) The crested newt *Triturus cristatus* recolonized temperate Eurasia from an extra-Mediterranean glacial refugium. Biological Journal of the Linnean Society 114: 574–587.

Zadeh LA (1965) Fuzzy sets. Information and Control 8: 338–353.

Zhang P, Papenfuss TJ, Wake MH, Qu L, Wake DB (2008) Phylogeny and biogeography of the family Salamandridae (Amphibia: Caudata) inferred from complete mitochondrial genomes. Molecular Phylogenetics and Evolution 49: 586–597.

Supplementary

Table III.S1. GenBank accession numbers of sequences analyzed in this study. Sample codes and ID as in Table 1.

		GenBank Accession numbers								
Sample Codes	**ID**	**ND4**	**Dloop**	**16s**	**Cytb**	**Cox1**	**CXCR4**	**NCX1**	**RAG1**	**SLC8A3**
IMS3032	1	KY938267								
IMS3033	1	KY938268								
IMS3034	1	KY938269								
IMS3035	1	KY938270								
IMS3097	2	KY938271								
IMS3098	2	KY938272								
IMS3099	2	KY938273								
IMS3100	2	KY938274								
IMS3182	3	KY938275								
IMS3184	3	KY938276								
IMS3185	3	KY938277								
PW565	4	KY938278								
PW566	4	KY938279								
PW567	4	KY938280								
PW568	4	KY938281								
PW663	5	KY938282								
PW664	5	KY938283								
PW665	5	KY938284								
PW666	5	KY938285								
IMS2841	6	KY938286								
IMS2842	6	KY938287								
IMS2843	6	KY938288								
IMS2844	6	KY938289								

IMS1827	7	KY938290								
IMS1828	7	KY938291								
IMS1829	7	KY938292								
IMS1830	7	KY938293								
PW09001	8	KY938294								
PW09002	8	KY938295								
PW09003	8	KY938296								
PW09004	8	KY938297								
PW09006	8	KY938298								
PW738	9	KY938299								
PW739	9	KY938300								
PW740	9	KY938301	KY938256	KY938219	KY938244	KY938232				
PW741	9	KY938302								
PW442	10	KY938303								
PW444	10	KY938304								
PW445	10	KY938305								
PW446	10	KY938306								
PW470	11	KY938307								
PW471	11	KY938308	KY938257	KY938220	KY938245	KY938233				
PW472	11	KY938309								
PW473	11	KY938310								
PW478	11						KY938179	KY938189	KY938199	KY938209
PW479	11						KY938180	KY938190	KY938200	KY938210
PW493	12	KY938311								
PW494	12	KY938312								
PW495	12	KY938313								
PW496	12	KY938314								

		GenBank Accession numbers								
Sample Codes	**ID**	**ND4**	**Dloop**	**16s**	**Cytb**	**Cox1**	**CXCR4**	**NCX1**	**RAG1**	**SLC8A3**
PW685	13	KY938315	KY938258	KY938221	KY938246	KY938234				
PW686	13	KY938316								
PW687	13	KY938317								
PW688	13	KY938318								
PW705	14	KY938319								
PW706	14	KY938320								
PW707	14	KY938321	KY938259	KY938222	KY938247	KY938235	KY938181	KY938191	KY938201	KY938211
PW708	14	KY938322								
PW513	15	KY938323								
PW514	15	KY938324								
PW516	15	KY938325								
PW541	16	KY938326								
PW542	16	KY938327								
PW543	16	KY938328								
PW544	16	KY938329								
PW380	17	KY938330								
PW381	17	KY938331								
PW382	17	KY938332								
PW383	17	KY938333								
IMS2833	18	KY938334								
IMS2834	18	KY938335								
IMS2835	18	KY938336								
IMS2836	18	KY938337								
IMS2789	19	KY938338								
IMS2790	19	KY938339								

IMS2791	19	KY938340				
IMS2793	19	KY938341				
PW595	20	KY938342				
PW596	20	KY938343				
PW597	20	KY938344				
PW620	21	KY938345	KY938260	KY938223	KY938248	KY938236
PW621	21	KY938346				
PW622	21	KY938347				
PW623	21	KY938348				
Toboso1	21	KY938349				
Toboso2	21	KY938350				
Toboso3	21	KY938351				
PW651	22	KY938352				
PW652	22	KY938353				
PW653	22	KY938354				
PW654	22	KY938355				
La_Nava1	22	KY938356				
La_Nava2	22	KY938357				
IMS3410	23	KY938358				
IMS3411	23	KY938359				
IMS3412	23	KY938360				
IMS3413	23	KY938361				
IMS3414	23	KY938362				
IMS1153	24	KY938363				
IMS1154	24	KY938364				
IMS1155	24	KY938365				
IMS1156	24	KY938366				

		GenBank Accession numbers								
Sample Codes	**ID**	**ND4**	**Dloop**	**16s**	**Cytb**	**Cox1**	**CXCR4**	**NCX1**	**RAG1**	**SLC8A3**
IMS1157	24	KY938367								
PW769	24	KY938368								
PW770	24	KY938369	KY938261	KY938224	KY938249	KY938237				
PW771	24	KY938370								
PW772	24	KY938371								
PW849	25	KY938372								
PW850	25	KY938373								
PW851	25	KY938374								
PW852	25	KY938375	KY938262	KY938225	KY938250	KY938238				
PW786	26	KY938376								
PW787	26	KY938377								
PW788	26	KY938378								
PW789	26	KY938379								
PW808	27	KY938380								
PW809	27	KY938381								
PW810	27	KY938382								
PW837	28	KY938383								
PW838	28	KY938384								
PW839	28	KY938385								
PW840	28	KY938386	KY938263	KY938226	KY938251	KY938239				
PW718	29	KY938387								
PW719	29	KY938388								
PW720	29	KY938389	KY938264	KY938227	KY938252	KY938240				
PW721	29	KY938390								
IMS1194	30	KY938391					KY938182	KY938192	KY938202	KY938212

IMS1195	30	KY938392				
IMS1196	30	KY938393				
IMS1197	30	KY938394				
IMS1198	30	KY938395				
IMS1199	30	KY938396				
IMS1200	30	KY938397				
IMS1201	30	KY938398				
IMS1202	30	KY938399				
IMS1203	30	KY938400				
IMS1204	30	KY938401				
IMS1205	30	KY938402				
IMS1206	30	KY938403				
IMS1207	30	KY938404				
IMS1208	30	KY938405				
IMS1209	30	KY938406				
IMS1210	30	KY938407	KY938183	KY938193	KY938203	KY938213
IMS1211	30	KY938408				
IMS1212	30	KY938409				
IMS1213	30	KY938410				
PW362	31	KY938411				
PW363	31	KY938412				
PW364	31	KY938413				
PW365	31	KY938414				
IMS1220	32	KY938415				
IMS1221	32	KY938416				
PW400	32	KY938417				
PW401	32	KY938418				

		GenBank Accession numbers								
Sample Codes	**ID**	**ND4**	**Dloop**	**16s**	**Cytb**	**Cox1**	**CXCR4**	**NCX1**	**RAG1**	**SLC8A3**
PW402	32	KY938419								
PW403	32	KY938420								
PW424	33	KY938421								
PW427	33	KY938422								
PW428	33	KY938423								
IMS3308	34	KY938424								
IMS3309	34	KY938425								
IMS3310	34	KY938426								
IMS3311	34	KY938427								
IMS3312	34	KY938428								
IMS3399	35	KY938429								
IMS3400	35	KY938430								
IMS3401	35	KY938431								
IMS3402	35	KY938432								
IMS3403	35	KY938433								
IMS2357	36	KY938434								
IMS2358	36	KY938435								
IMS2359	36	KY938436								
IMS2360	36	KY938437								
IMS2361	36	KY938438								
IMS2362	36	KY938439								
IMS2363	36	KY938440								
IMS2364	36	KY938441								
IMS2365	36	KY938442								
IMS2366	36	KY938443								

IMS3247	37	KY938444								
IMS3248	37	KY938445								
IMS3249	37	KY938446								
IMS3250	37	KY938447								
IMS3369	38	KY938448								
IMS3370	38	KY938449								
IMS3371	38	KY938450	KY938265	KY938228	KY938253	KY938241	KY938184	KY938194	KY938204	KY938214
IMS3372	38	KY938451								
IMS3373	38	KY938452								
IMS3268	39	KY938453								
IMS3269	39	KY938454								
IMS3270	39	KY938455								
IMS3271	39	KY938456								
IMS3272	39	KY938457								
IMS1989	40	KY938458					KY938185	KY938195	KY938205	KY938215
IMS1990	40	KY938459					KY938186	KY938196	KY938206	KY938216
IMS1991	40	KY938460								
IMS1992	40	KY938461								
IMS1993	40	KY938462								
IMS1994	40	KY938463								
IMS1995	40	KY938464								
IMS1996	40	KY938465								
IMS1997	40	KY938466								
IMS1998	40	KY938467								
IMS1999	40	KY938468								
IMS3288	41	KY938469								
IMS3289	41	KY938470								

		GenBank Accession numbers								
Sample Codes	**ID**	**ND4**	**Dloop**	**16s**	**Cytb**	**Cox1**	**CXCR4**	**NCX1**	**RAG1**	**SLC8A3**
IMS3290	41	KY938471								
IMS3291	41	KY938472								
IMS3292	41	KY938473								
IMS3379	42	KY938474								
IMS3380	42	KY938475								
IMS3381	42	KY938476								
IMS3382	42	KY938477								
IMS3383	42	KY938478								
IMS2623	43	KY938479								
IMS2624	43	KY938480								
IMS2625	43	KY938481								
IMS2627	43	KY938482								
PW345	44	KY938483								
PW346	44	KY938484								
PW347	44	KY938485								
PW348	44	KY938486								
PW349	44	KY938487								
PW350	44	KY938488	KY938266	KY938229	KY938254	KY938242				
PW351	44	KY938489								
PW875	45	KY938490								
PW876	45	KY938491								
GVA214	46	KY938492								
Castanar2	47	KY938493								
Castanar4	47	KY938494								
Castanar5	47	KY938495								

La_Mierla1	48	KY938496								
La_Mierla2	48	KY938497								
La_Mierla3	48	KY938498								
MNCN10075	49	KY938499								
MNCN7184	50	KY938500								
MVZ231893	51	KY938501								
MVZ186103	51	KY938502								
MVZ162384	52	KY938503								
MVZ186090	53	KY938504								
MVZ231894	54	KY938505								
MVZ230275	55	KY938506								
IMS5116		KY938507		KY938230	KY938255	KY938243	KY938187	KY938197	KY938207	KY938217
IMS5139				KY938231			KY938188	KY938198	KY938208	KY938218
P. nebulosus		EU880329	EU880329	EU880329	EU880329	EU880329				
Tylototriton		KR154461	KR154461	KR154461	KR154461	KR154461	EF107493	EF107273	EF107332	EF107437

Table III.S2. Variables used for modelling the distributions of *Pleurodeles waltl* and each of its Eastern and Western mtDNA lineages.

Code	Definition
bio1	Annual Mean Temperature
bio2	Mean Diurnal Range (Mean of monthly (max temp - min temp))
bio3	Isothermality (bio2/bio7) (* 100)
bio4	Temperature Seasonality (standard deviation * 100)
bio5	Max Temperature of Warmest Month
bio6	Min Temperature of Coldest Month
bio7	Temperature Annual Range (bio5-bio6)
bio8	Mean Temperature of Wettest Quarter
bio9	Mean Temperature of Driest Quarter
bio10	Mean Temperature of Warmest Quarter
bio11	Mean Temperature of Coldest Quarter
bio12	Annual Precipitation
bio13	Precipitation of Wettest Month
bio14	Precipitation of Driest Month
bio15	Precipitation Seasonality (coefficient of variation)
bio16	Precipitation of Wettest Quarter
bio17	Precipitation of Driest Quarter
bio18	Precipitation of Warmest Quarter
bio19	Precipitation of Coldest Quarter

Table III.S3. Variables included in the climatic favourability models for *Pleurodeles waltl* and for the Eastern and Western lineages separately, along with their coefficient estimates, standard errors (SE), z test values and significance (p). Variable codes as in Table S2; *p<0.05; **p<0.01; ***p<0.001.

P. waltl					
	Coefficient	**SE**	**z**	**p**	
(Intercept)	-6.599353	3.734339	-1.767	0.077193	
bio6	0.196133	0.018976	10.336	<2e-16	***
bio11	-0.255249	0.018258	-13.980	<2e-16	***
bio14	-0.262195	0.026058	-10.062	<2e-16	***
bio19	-0.058982	0.003495	-16.875	<2e-16	***
bio16	0.060567	0.005473	11.066	<2e-16	***
bio9	0.016889	0.002322	7.275	3.47e-13	***
bio3	0.321319	0.084746	3.792	0.000150	***
bio5	0.092528	0.017442	5.305	1.13e-07	***
bio10	-0.069322	0.018379	-3.772	0.000162	***
bio15	0.072086	0.012741	5.658	1.53e-08	***
bio17	0.034979	0.008987	3.892	9.93e-05	***
bio2	-0.107958	0.032367	-3.335	0.000852	***
bio13	-0.022993	0.010399	-2.211	0.027031	*
Western					
(Intercept)	-35.648982	5.147085	-6.926	4.33e-12	***
bio6	-0.118259	0.017115	-6.910	4.86e-12	***
bio3	0.619970	0.114145	5.431	5.59e-08	***
bio18	-0.019891	0.005282	-3.766	0.000166	***
bio8	0.036727	0.003889	9.443	<2e-16	***
bio2	-0.171911	0.043583	-3.944	8.00e-05	***
bio9	0.014731	0.002447	6.019	1.76e-09	***
bio15	0.075880	0.015457	4.909	9.15e-07	***
bio4	0.018516	0.001677	11.041	<2e-16	***
bio7	-0.066789	0.023258	-2.872	0.004083	**
bio1	-0.566914	0.052911	-10.714	<2e-16	***
bio11	0.885187	0.068831	12.860	<2e-16	***
bio13	0.019367	0.003751	5.164	<2.42e-07	***
bio10	-0.241413	0.082363	-2.931	0.003378	**

Eastern					
(Intercept)	-1.988e+01	6.364e+00	-3.123	0.001789	**
bio6	6.806e-01	2.623e-02	25.947	<2e-16	***
bio11	-8.255e-01	5.613e-02	-14.705	<2e-16	***
bio18	1.422e-01	1.517e-02	9.376	<2e-16	***
bio2	-4.924e-01	5.427e-02	-9.074	<2e-16	***
bio12	-1.036e-02	9.269e-04	-11.174	<2e-16	***
bio4	-1.370e-02	1.447e-03	-9.468	<2e-16	***
bio7	4.736e-01	3.219e-02	14.715	<2e-16	***
bio14	-5.128e-01	4.126e-02	-12.431	<2e-16	***
bio3	9.543e-01	1.449e-01	6.584	4.58e-11	***
bio9	1.126e-01	4.545e-02	2.476	0.013273	*
bio15	7.487e-02	1.937e-02	3.865	0.000111	***

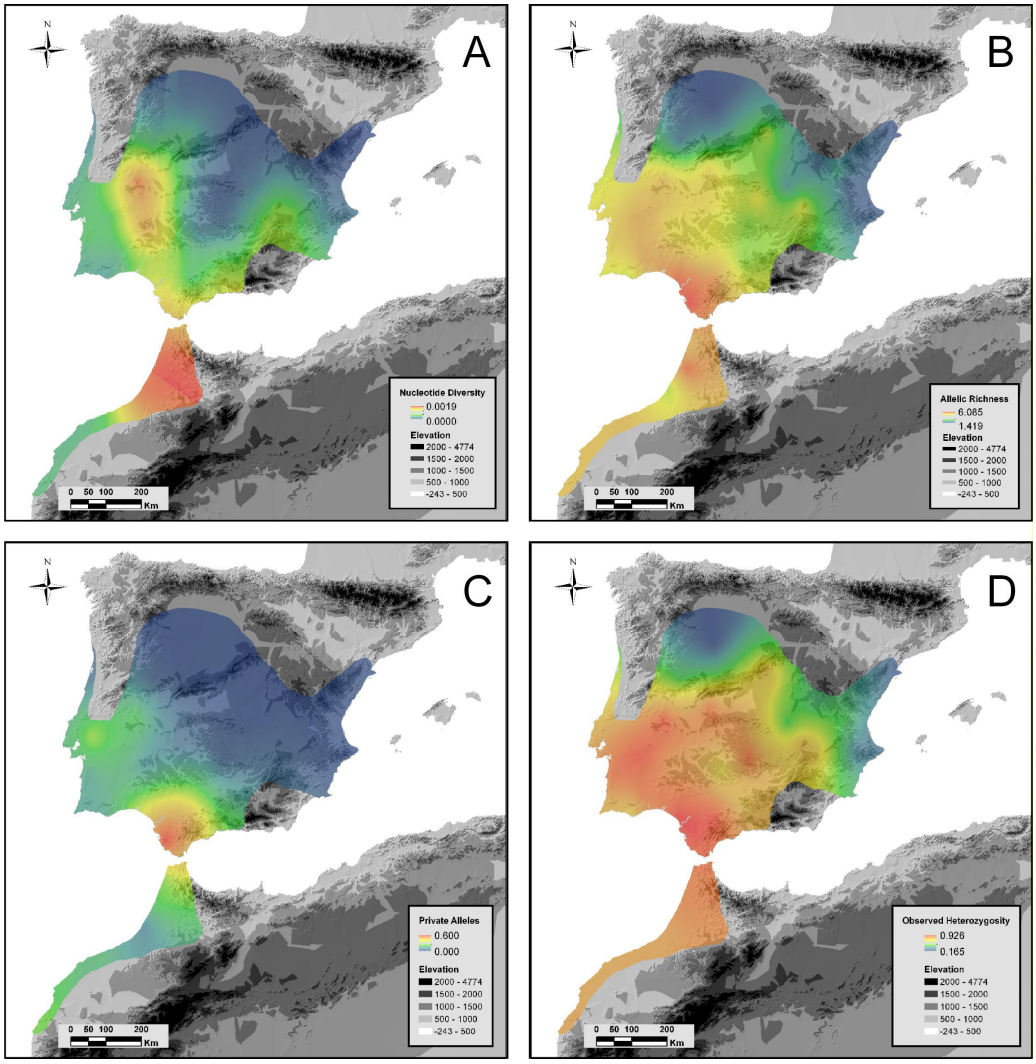

Figure III.S1. Geographic patterns of different measures of genetic diversity in *P. waltl*. A) Nucleotide diversity, B) Allelic richness, C) Private alleles, and D) Observed heterozygosity.

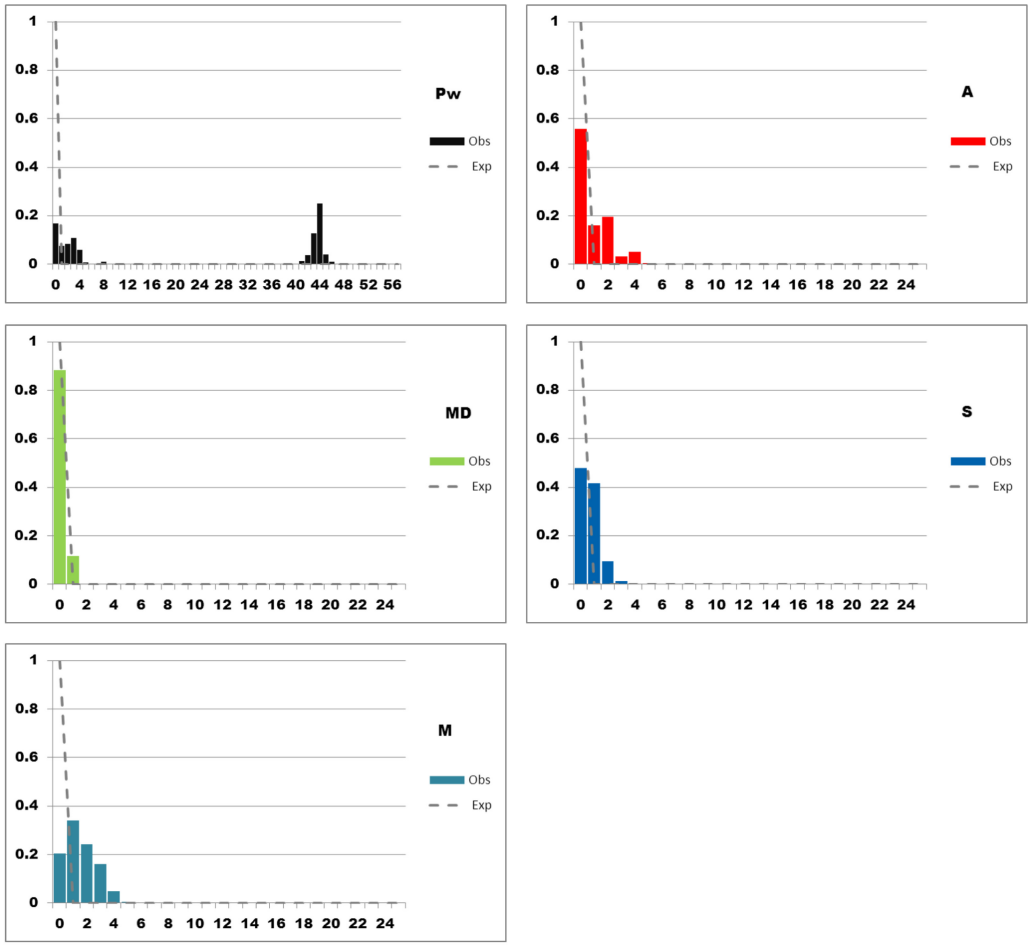

Figure III.S2. Mismatch distributions (expected vs. observed) for the species (Pw, *Pleurodeles waltl*) and the Atlantic (A), Mediterranean (MD), Southern (S) haplogroups and the populations from Morocco (M). The number of pairwise differences and their frequencies are shown on the horizontal and vertical axes, respectively.

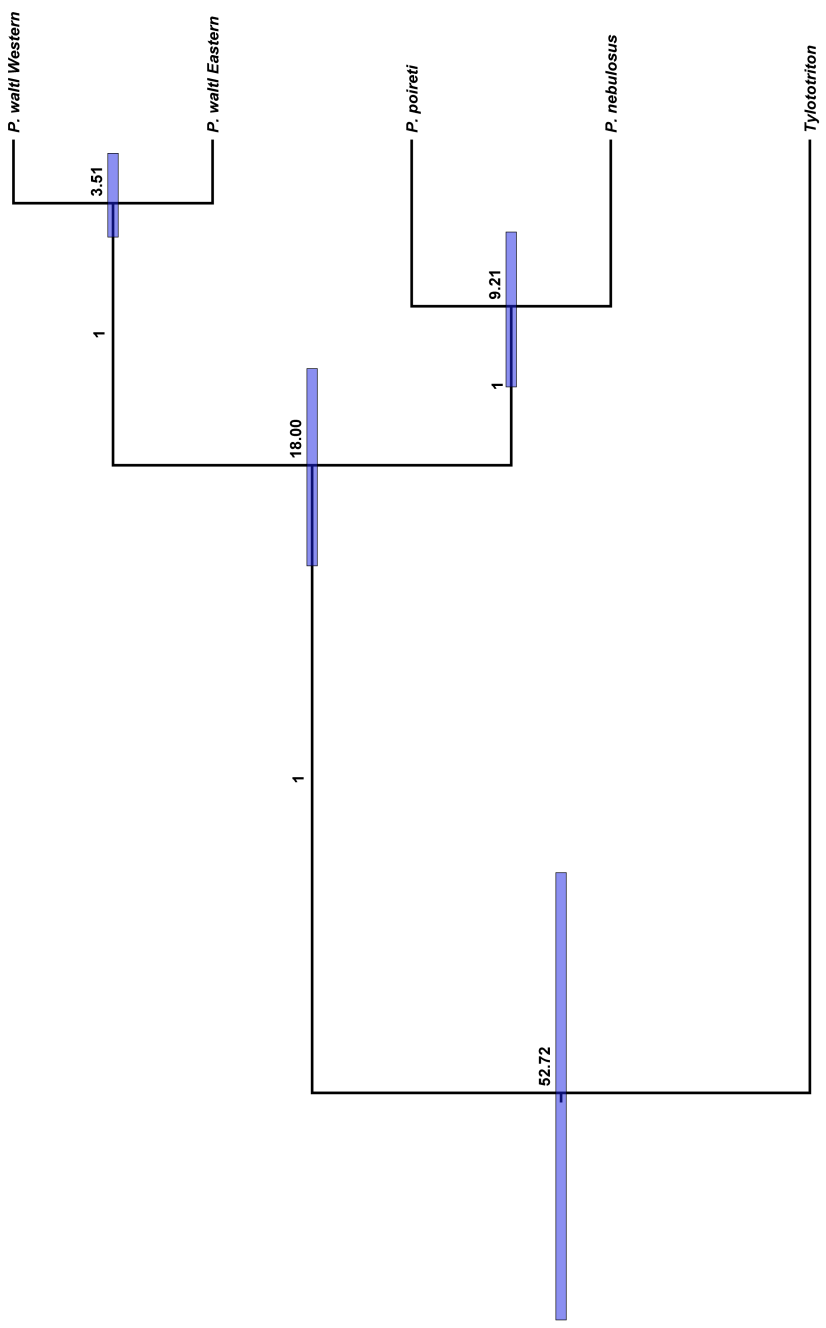

Figure III.S3. *Pleurodeles* species tree, including the two major intraspecific lineages in *P. waltl*, based on the multispecies coalescent analysis of sequences of five mtDNA and four nuclear DNA regions in *BEAST. Values above branches are Bayesian Posterior Probabilities (BPPs). Blue bars represent 95% highest posterior density intervals for split times (median values besides nodes). Scale bar in millions of years ago (Mya).

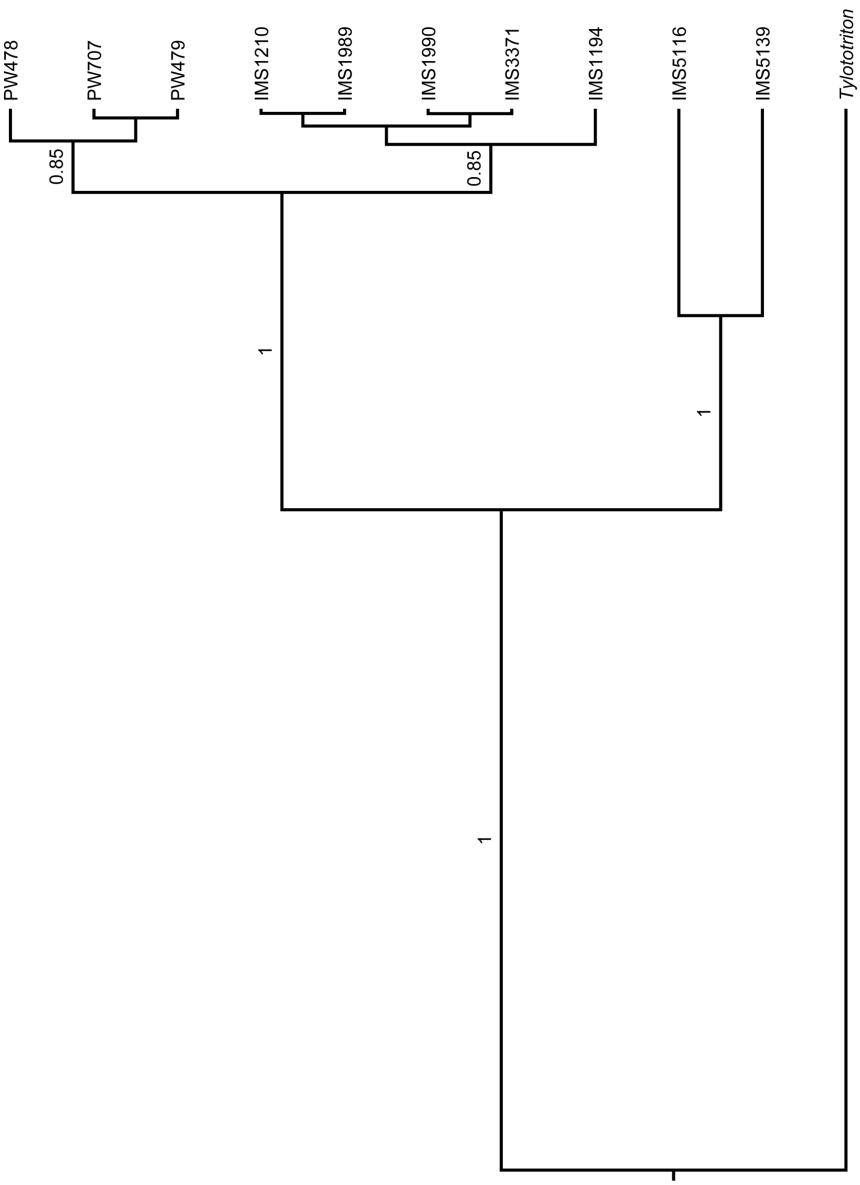

Figure III.S4. Nuclear genealogy of gene CXCR4 based on the *BEAST analysis. Maximum clade credibility tree with BPPs above branches. Scale in substitutions per site per million years.

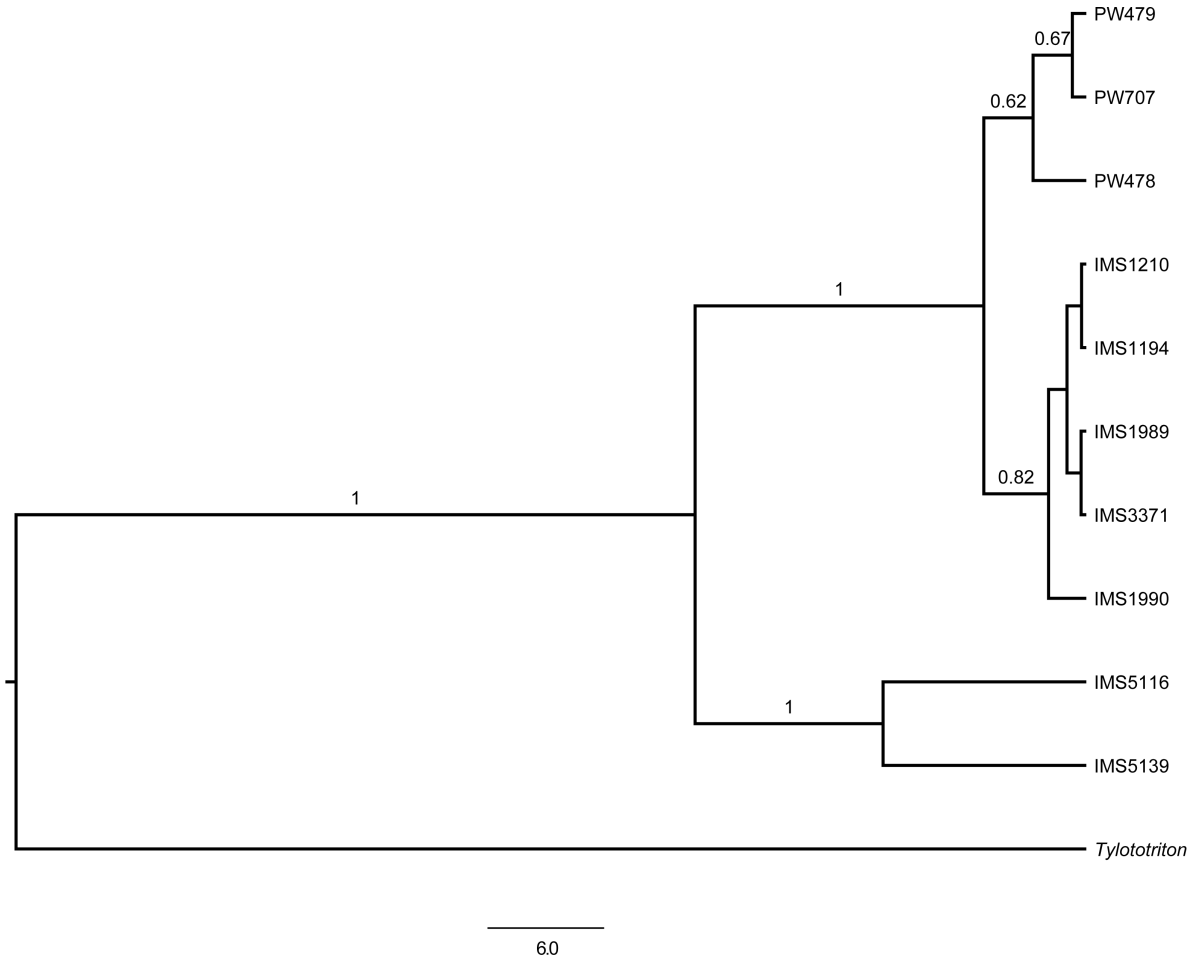

Figure III.S5. Nuclear genealogy of gene NCX1 based on the *BEAST analysis. Maximum clade credibility tree with BPPs above branches. Scale in substitutions per site per million years.

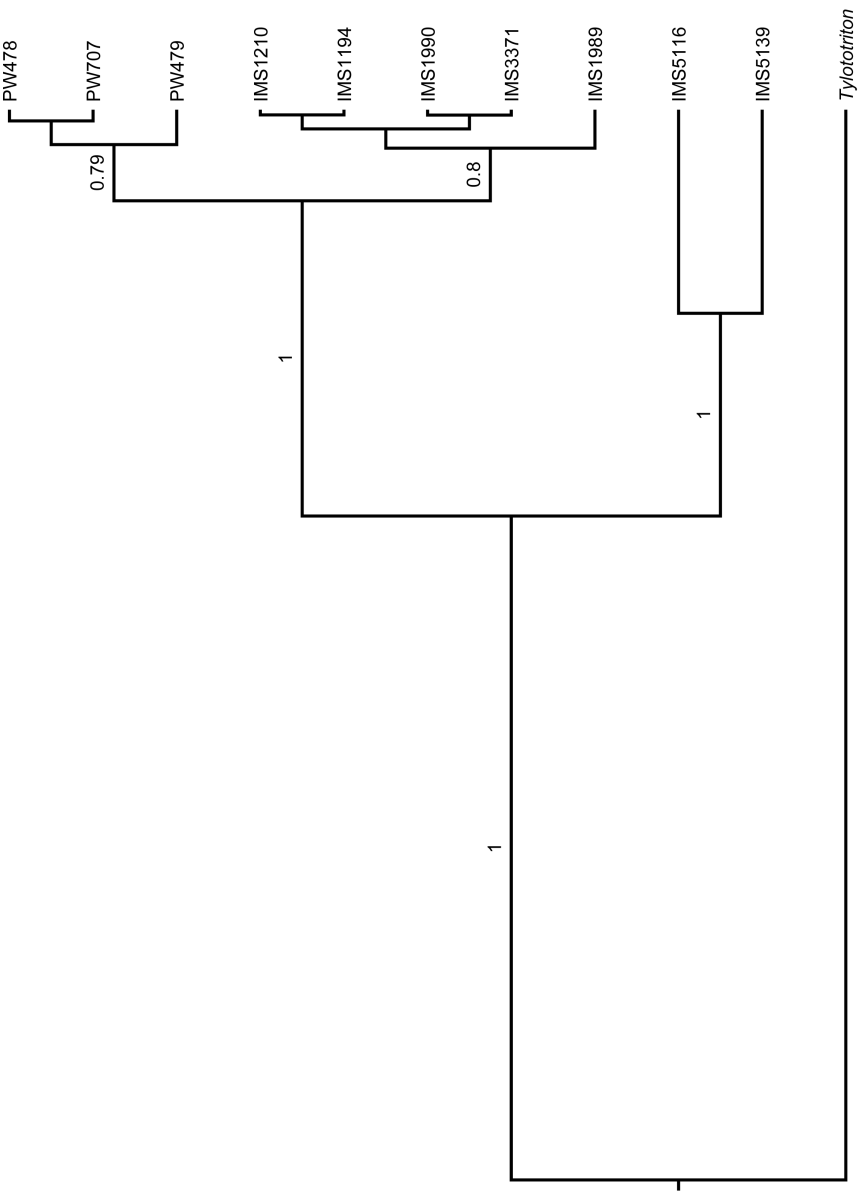

Figure III.S6. Nuclear genealogy of gene RAG1 based on the *BEAST analysis. Maximum clade credibility tree with BPPs above branches. Scale in substitutions per site per million years.

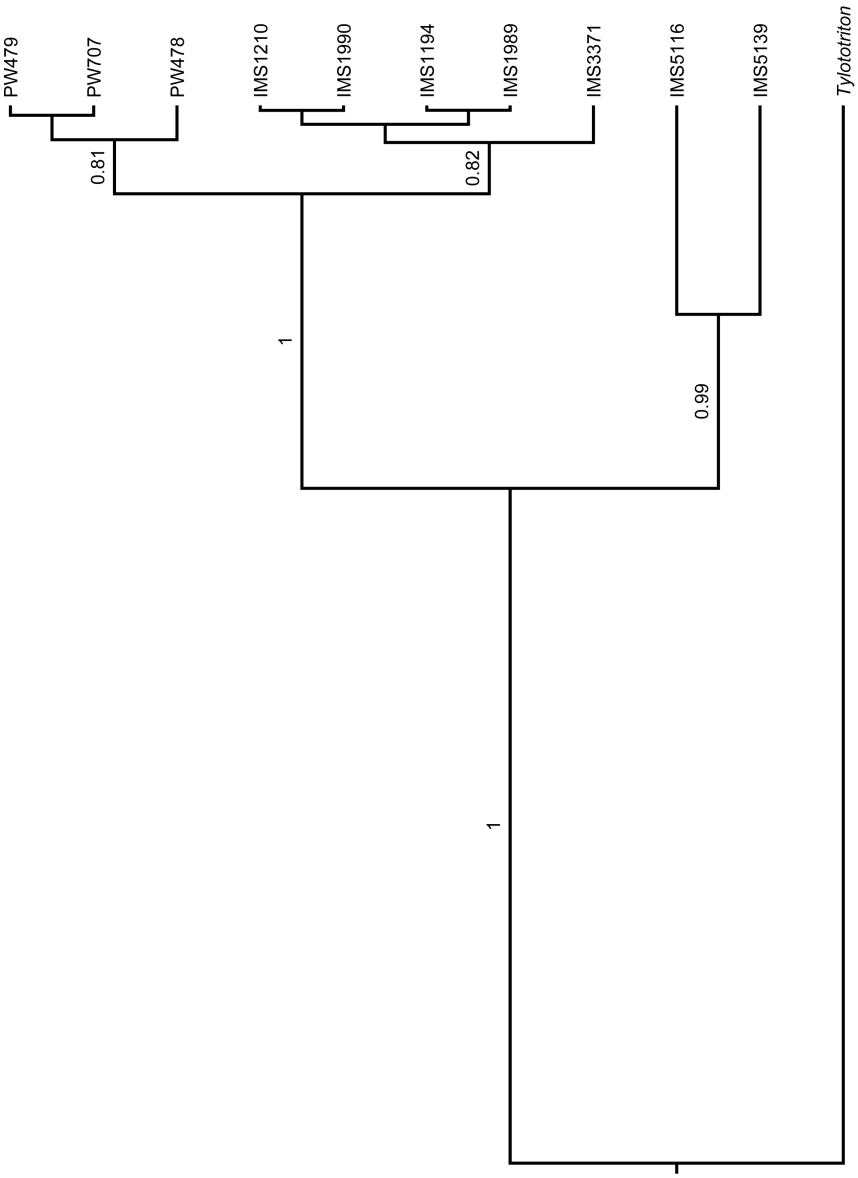

Figure III.S7. Nuclear genealogy of gene SLC8A3 based on the *BEAST analysis. Maximum clade credibility tree with BPPs above branches. Scale in substitutions per site per million years.

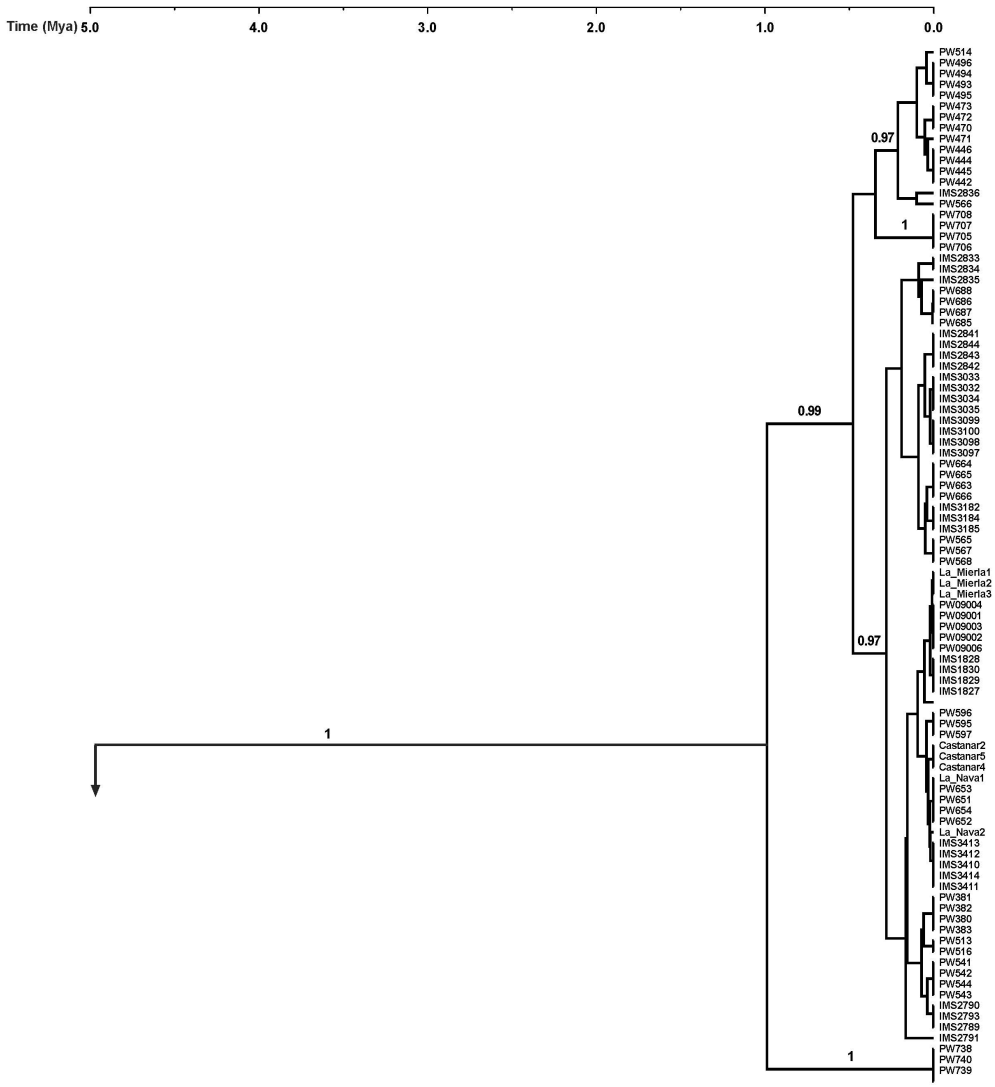

Figure III.S8. Time-calibrated tree from ND4 sequences of *P. waltl* recovered in continuous diffusion analyses.

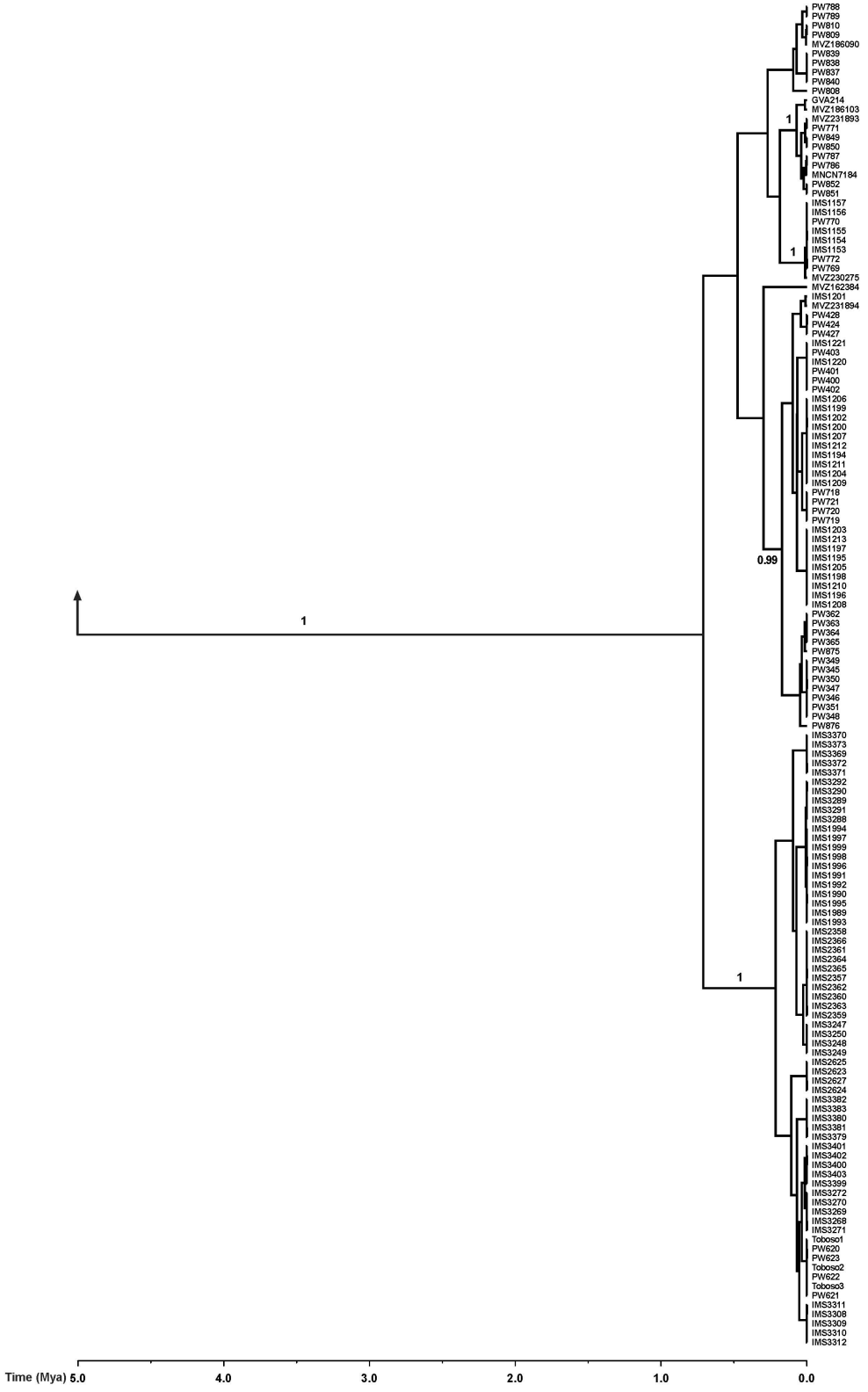
PW788
PW789
PW810
PW809
MVZ186090
PW839
PW838
PW837
PW840
PW808
GVA214
MVZ186103
MVZ231893
PW771
PW849
PW850
PW787
PW786
MNCN7184
PW852
PW851
IMS1157
IMS1156
PW770
IMS1155
IMS1154
IMS1153
PW772
PW769
MVZ230275
MVZ162384
IMS1201
MVZ231894
PW428
PW424
PW427
IMS1221
PW403
IMS1220
PW401
PW400
PW402
IMS1206
IMS1199
IMS1202
IMS1200
IMS1207
IMS1212
IMS1194
IMS1211
IMS1204
IMS1209
PW718
PW721
PW720
PW719
IMS1203
IMS1213
IMS1197
IMS1195
IMS1205
IMS1198
IMS1210
IMS1196
IMS1208
PW362
PW363
PW364
PW365
PW875
PW349
PW345
PW350
PW347
PW346
PW351
PW348
PW876
IMS3370
IMS3373
IMS3369
IMS3372
IMS3371
IMS3292
IMS3290
IMS3289
IMS3291
IMS3288
IMS1994
IMS1997
IMS1999
IMS1998
IMS1996
IMS1991
IMS1992
IMS1990
IMS1995
IMS1989
IMS1993
IMS2358
IMS2366
IMS2361
IMS2364
IMS2365
IMS2357
IMS2362
IMS2360
IMS2363
IMS2359
IMS3247
IMS3250
IMS3248
IMS3249
IMS2625
IMS2623
IMS2627
IMS2624
IMS3382
IMS3383
IMS3380
IMS3381
IMS3379
IMS3401
IMS3402
IMS3400
IMS3403
IMS3399
IMS3272
IMS3270
IMS3269
IMS3268
IMS3271
Toboso1
PW620
PW623
Toboso2
PW622
Toboso3
PW621
IMS3311
IMS3308
IMS3309
IMS3310
IMS3312
1
1
1
1
0.99
Time (Mya)
5.0
4.0
3.0
2.0
1.0
0.0

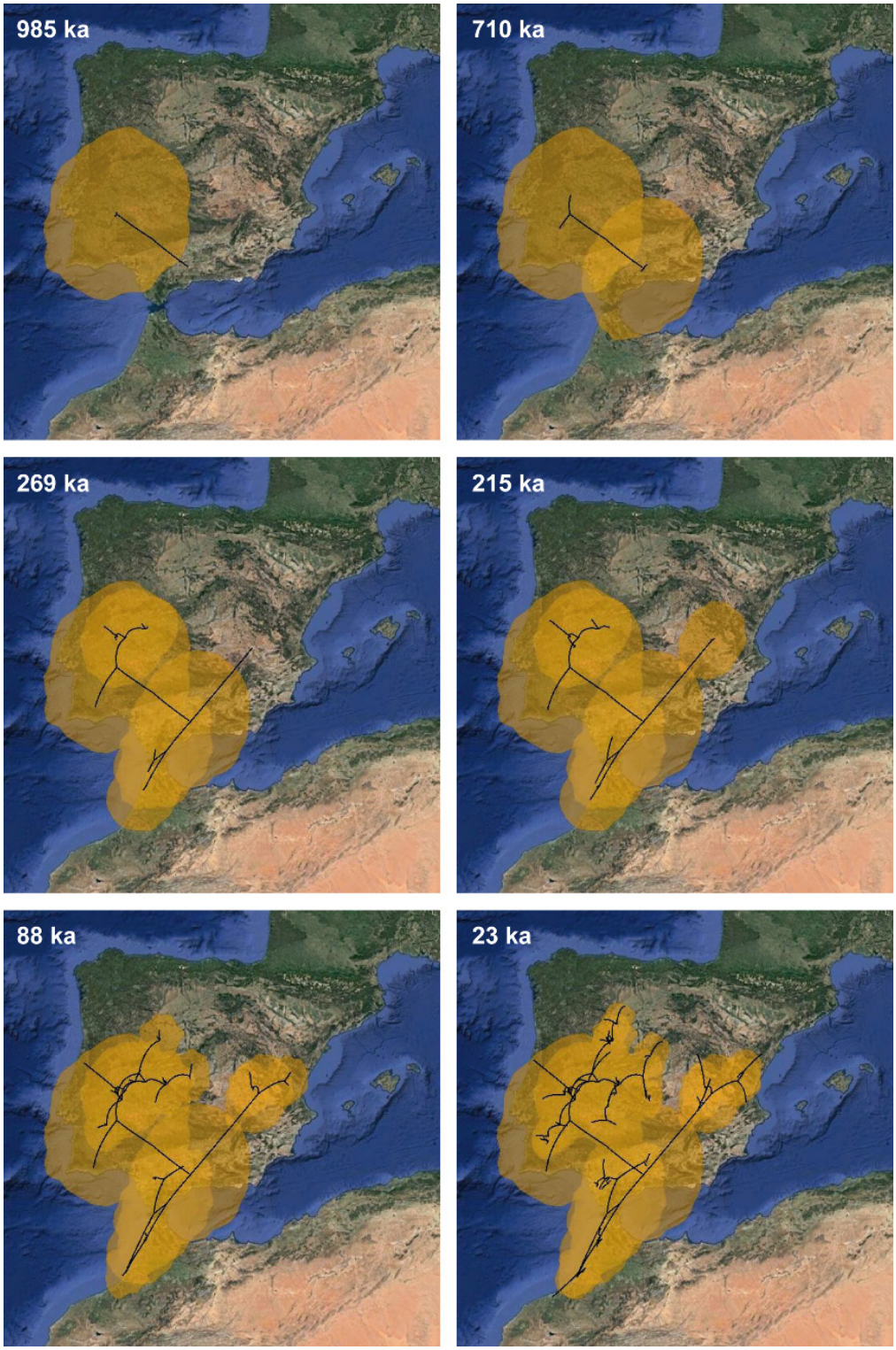

Figure III.S9. Continuous diffusion phylogeographic reconstruction in *P. waltl* at six time slices: 985, 710, 269, 215, 88 and 23 ka.

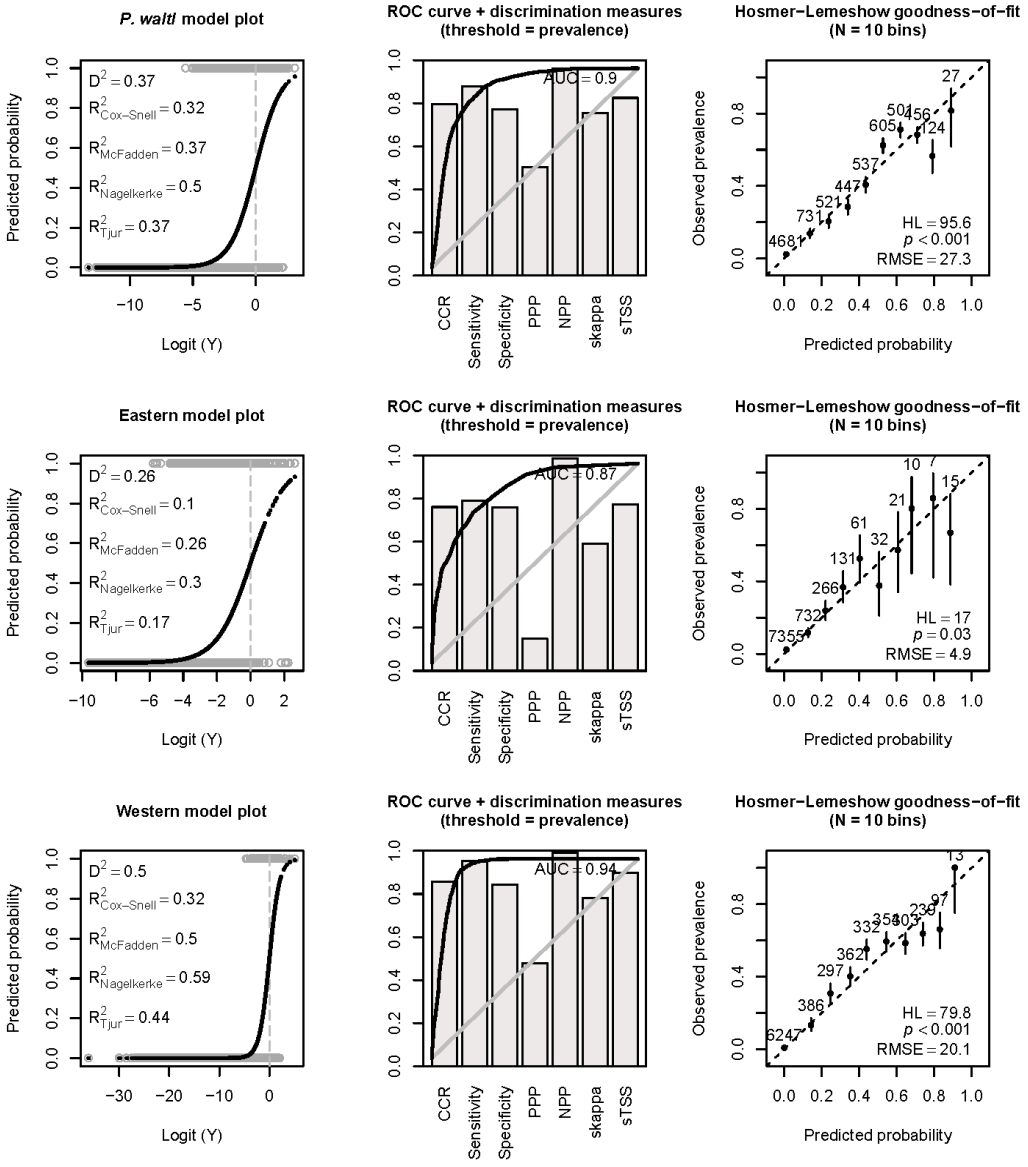

Figure III.S10. Evaluation of the distribution models built for *P. waltl* (top) and for the Eastern (middle) and the Western lineage (bottom), based on presence-absence on UTM 10x10 km cells of mainland Portugal, Spain and Morocco (N = 15912). Measures and plots were obtained with the *modEvA* R package (Barbosa *et al*., 2013).

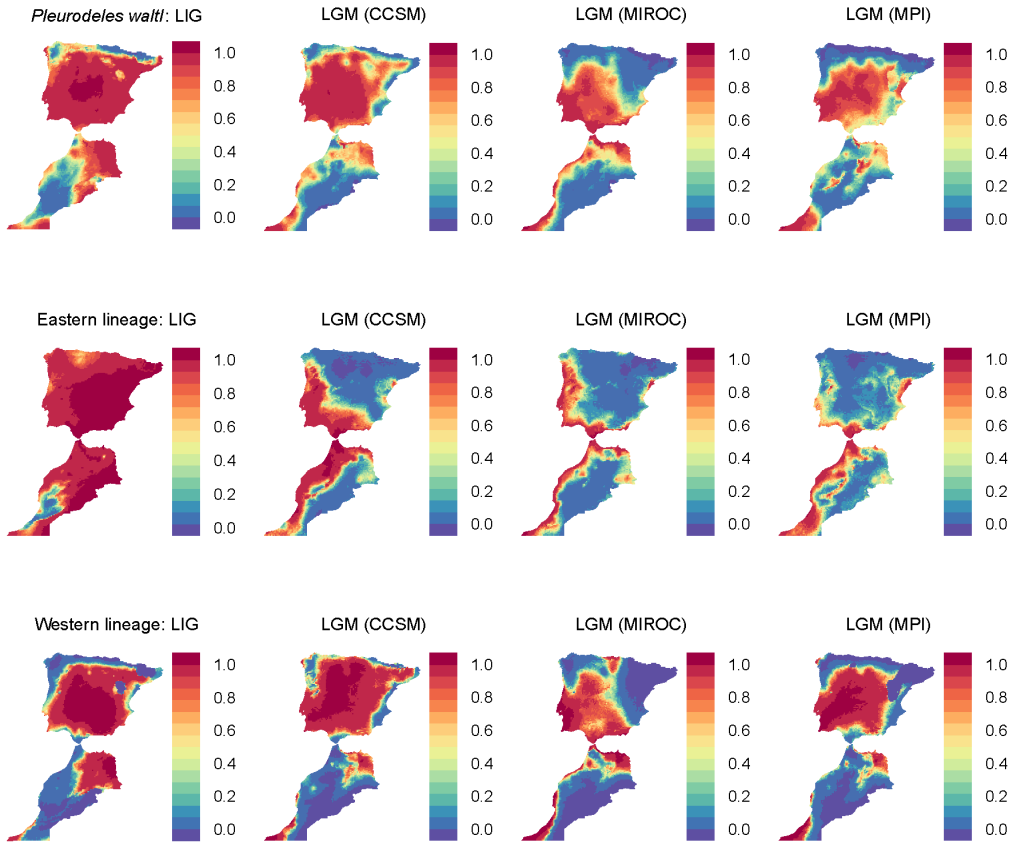

Figure III.S11. Hindcasts of climatic favourability for *P. waltl* (top) and for the Eastern (middle) and Western lineages (bottom) according to the models obtained from current distribution records. LIG: Last Inter-Glacial period, LGM: Last Glacial Maximum, MH: Mid Holocene, the latter two including the three climatic simulations currently available on Wordlclim: CCSM4, MIROC-ESM and MPI-ESM-P.

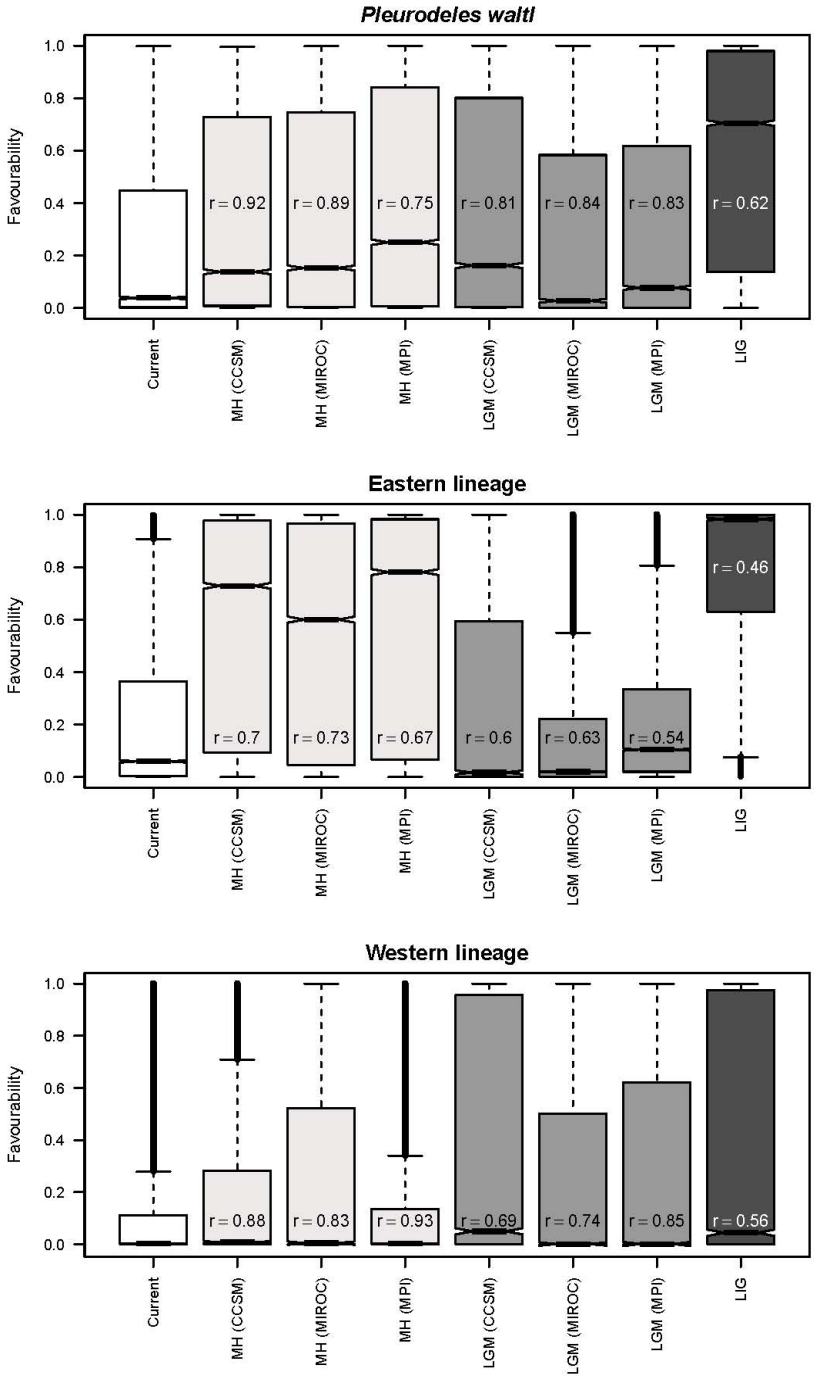

Figure III.S12. Boxplots of climatic favourability for *P. waltl* (top) and for the Eastern (middle) and Western lineage (bottom) under current climate, under the three climatic simulations (CCSM4, MIROC-ESM and MPI-ESM-P) available for the Last Glacial Maximum (LGM) and the Mid Holocene (MH), and under the Last Inter-Glacial period (LIG). The values indicate the coefficients of Pearson's correlation (r) between current and past favourability for each simulation ($p < 0.001$ with 15908 degrees of freedom).

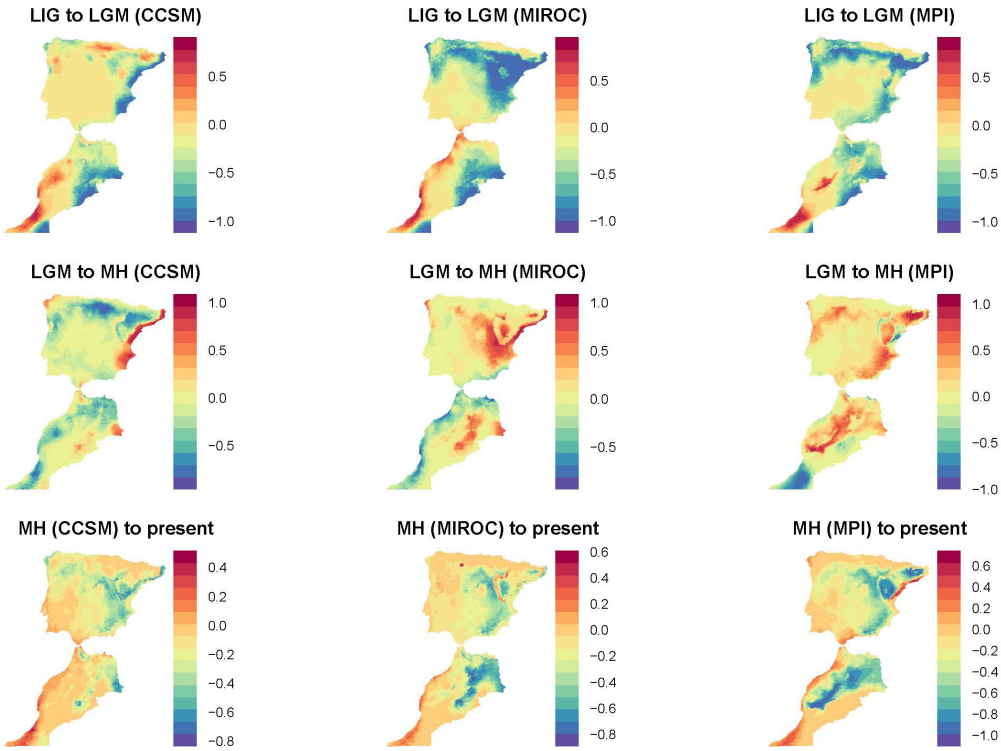

Figure III.S13. Change (difference) in climatic favourability between time periods, considering the three available climatic simulations (CCSM4, MIROC-ESM and MPI-ESM-P) for the Last Glacial Maximum (LGM), the Mid Holocene (MH) and the Last Inter-Glacial period (LIG). Red and blue indicate increase and decrease in climatic favourability across periods, respectively.

Present and past climatic effects on the current distribution and genetic diversity of the Iberian spadefoot toad (*Pelobates cultripes*): an integrative approach

J. Gutiérrez-Rodríguez, M. Barbosa, I. Martínez-Solano

Publicado en

Journal of Biogeography 2017 Volume 44, Issue 2, 245–258

DOI: 10.1111/jbi.1279

Abstract

Aim: Predicting species responses to global change is one of the most pressing issues in conservation biogeography. A key part of the problem is understanding how organisms have reacted to climatic changes in the past. Here, we use species distribution modelling to infer the effects of climate changes since the Last Interglacial (LIG, c. 130,000 yr bp) on patterns of genetic structure and diversity in the Iberian spadefoot toad (*Pelobates cultripes*) in combination with spatially explicit phylogeographical analyses.

Location: Iberian Peninsula and mainland France.

Methods: Five hundred and twenty-four individuals from 54 populations across the species range were sampled to document patterns of genetic diversity and infer their evolutionary history based on data from mtDNA and 14 polymorphic microsatellites. Generalized linear models based on distribution data were used to infer climatic favourability for the species in the present and in palaeoclimatic simulations for the LIG, the mid-Holocene and the Last Glacial Maximum (LGM).

Results: Estimates of genetic diversity show a decreasing trend from south to north, suggesting persistence of high historical population sizes in the southern Iberian Peninsula. Species distribution models show differences in climatic favourability through time, with significant correlations between historically stable favourable areas and current patterns of genetic diversity. These results are corroborated by Bayesian skyline plots and continuous diffusion phylogeographical analyses.

Main conclusions: The results indicate the presence of southern refugia, with moderate recent expansions at the northern end of the species' range. Toads at the northern range margin exhibit the lowest genetic diversity and occupy areas of high past climate variability, classified as marginal in terms of favourability, rendering these populations most vulnerable to climate-mediated changes in the long term.

Resumen

Predecir la respuesta de las especies al cambio global es uno de los objetivos fundamentales de la biología de la conservación. Una de las principales cuestiones es entender cómo los organismos han reaccionado frente a cambios climáticos del pasado. En este estudio hemos aplicado modelos de distribución de especies (SDMs) y análisis filogeográficos espacialmente explícitos para inferir el efecto del cambio del clima desde el último interglaciar (LIG) en los patrones de diversidad y estructura genética en el sapo de espuelas (*Pelobates cultripes*). Esta especie es endémica de la península ibérica y de las costas mediterráneas y atlánticas francesas. Se obtuvieron datos de ADNmit y de 14 microsatélites polimórficos para 524 individuos de 54 poblaciones a lo largo de toda su distribución para caracterizar los patrones de diversidad genética e inferir su historia evolutiva. Además, en base a los datos disponibles sobre su distribución se elaboraron modelos lineales generalizados para inferir la favorabilidad climática para la especie en el presente y, por medio de simulaciones paleoclimáticas del pasado, para el LIG, último máximo glaciar (LGM) y Holoceno medio. Los resultados obtenidos muestran una disminución de la diversidad genética desde el sur hacia el norte de la distribución de la especie, lo que sugiere la persistencia de tamaños poblacionales históricos altos en el sur de la península ibérica. Los SDMs muestran diferencias en la favorabilidad climática a lo largo del tiempo, con una correlación significativa y positiva entre las áreas estables históricamente y la diversidad genética. Estos resultados son apoyados por la reconstrucción de tamaños poblacionales ancestrales ("Bayesian skyline plots") y análisis filogeográficos de difusión continua, que indican la existencia de refugios en el sur de la península ibérica, con expansiones moderadas recientes hacia el norte del área de distribución. Las poblaciones periféricas del norte presentan baja diversidad genética y ocupan áreas con alta variabilidad climática en el pasado, lo que las hace más vulnerables a largo plazo ante futuros cambios climáticos.

Introduction

One of the most pressing issues in conservation biogeography is predicting species responses to global change. Given projected scenarios of climate warming, the survival of many taxa will be determined by plastic responses, genetic adaptation or range shifts tracking favourable conditions (Williams *et al*., 2008; Duputié *et al*., 2012). Initial approaches to this complex problem have involved characterization of the fundamental niche of species and projection under a variety of future scenarios (Araújo *et al*., 2006). These attempts have been fundamentally based on correlative models of individual species (Thuiller *et al*., 2008), which have several limitations, such as coarse spatial resolution (Moritz & Agudo, 2013) or static niche stability (Gavin *et al*., 2014). Thus, more realistic models need to take into account other factors, such as the evolutionary history of the organisms under study (Gavin *et al*., 2014). Critical information can be obtained using the past to predict the future, that is, by understanding how organisms have reacted to climatic changes in the past in order to predict how they are likely to be affected by changes in the future. For example, the combination of species distribution modelling and spatially explicit phylogeographical analyses is emerging as a powerful means to predict how species will react to future climatic changes (Dawson *et al*., 2011; Schmidt *et al*., 2014).

The Quaternary Period, encompassing the past 2.6 Myr, is characterized by a succession of marked, well-studied climatic changes, with 'cold' and 'warm' periods repeated in cyclic intervals. These oscillations have affected patterns of genetic diversity across species through the processes of demographic contraction, expansion and extinction, ultimately shaping current species ranges (Hewitt, 1996, 2004; Provan & Bennett, 2008). From the perspective of several independent disciplines, scientists have documented range shifts in the flora and fauna of this period based on the fossil record, palaeoclimatic reconstructions, and patterns of species distributions (Devender *et al*., 1976; Hoffmann, 1981; Ashworth, 1996; Sket, 1997; Morales Pérez & Serra, 2009). More recently, disciplines like phylogeography and tools like species distribution models (SDMs) have been applied to reconstruct historical processes. Phylogeography identifies refugial areas based on the presence of exclusive lineages or patterns of higher genetic diversity (Médail & Diadema, 2009; Keppel *et al*., 2012). Refugial areas

are important in predicting species responses to climate change, because they represent the fractions of the distribution range where species have persisted for longer in the face of geological and climatic events. This approach is, however, prone to some bias due to incomplete sampling and/or the random extinction of lineages (Weisrock & Janzen, 2000; Cusimano *et al*., 2012). SDMs allow the prediction of the extent of past distribution ranges based on palaeoclimatic reconstructions [with simulations available back to the Last Interglacial (LIG), up to c. 120–140 ka]. The combination of phylogeographical data and SDMs has been shown to produce robust inferences about past demographic changes in a variety of taxa (Fitze *et al*., 2011; Todisco *et al*., 2012; Wilson & Pitts, 2012; Hegna *et al*., 2015; Martínez-Freiría *et al*., 2015; Tsuda *et al*., 2015). Understanding how these demographic changes have affected patterns of population structure and genetic diversity in relation with past climatic changes is key to predicting how future changes will affect population viability.

Southern European peninsulas have been long studied as textbook examples of glacial refugia that have allowed the survival of species and well-differentiated intraspecific lineages across a variety of taxa. However, many phylogeographical studies in this region have focused on the role of these refugia in preserving deeper phylogenetic history, with many taxa originating in the Pliocene-Miocene and surviving as more or less isolated population groups until the present (Englbrecht *et al*., 2000; Martínez-Solano *et al*., 2006; Velo-Antón *et al*., 2012; Recuero *et al*., 2014). Comparative approaches have also emphasized the existence of 'refugia within refugia', with several areas functioning as allopatric refugia within each major peninsula (Gómez & Lunt, 2007). These studies have focused mainly on the possibility of incipient or cryptic speciation. However, within each major peninsula, there are examples of taxa that have evolved in situ for millions of years without showing any genetic signature of deep phylogeographical structure. These species have also been affected by geological and climatic changes throughout the Pliocene and Pleistocene, and thus their study can provide clues about how species cope with such wide-range environmental perturbations.

Here, we use an integrative approach, including population genetics, phylogeographical analyses and modelling of current and past [Holocene, Last

Glacial Maximum (LGM) and LIG] climatic favourability, to quantify changes in favourability through time and analyse the relationship between climatic stability and current patterns of genetic diversity and structure. As a model species, we focused on the Iberian spadefoot toad, *Pelobates cultripes* (Cuvier, 1829). This species belongs to the family Pelobatidae (order Anura) and is a typical inhabitant of Mediterranean habitats across the Iberian Peninsula (IP), extending along the Mediterranean coast of France, with some disjunct, isolated populations in the French Atlantic coast (Duguet & Melki, 2003; García-París *et al*., 2004; Loureiro *et al*., 2008). Its range is mostly continuous in areas with sandy siliceous substrate, dominant in the western half of the IP, and fragmented in calcareous areas in the eastern IP (García-París *et al*., 2004). The species breeds mostly in long-hydroperiod seasonal ponds, which allow the completion of its relatively long larval development (up to 6 months) (Talavera & Sanchiz, 1987; Tejedo, 1993; Buchholz & Hayes, 2002; Díaz-Paniagua *et al*., 2005). This dependence makes it vulnerable to changes in future water availability under global climate change (Corn, 2005). Similarly, past hydroclimatic variation in the Holocene (Magny *et al*., 2013) may have affected this species' historical demography and population structure through changes in seasonal rainfall patterns limiting water availability. Currently, the species is listed as Near Threatened by the IUCN (Beja *et al*., 2009), as its populations are declining range-wide due to habitat loss and the negative impact of invasive species (Tejedo & Reques, 2002).

Previous phylogeographical studies based on limited data and sampling have shown low mitochondrial diversity across this species' range (Crottini *et al*., 2010; Fitó *et al*., 2011). These authors have hypothesized a range reduction during the Pleistocene glaciations to explain this pattern, with glacial refugia inferred to have been located in the southern IP. In that case, we would expect to detect a genetic signature of demographic decline, followed by recent population growth, a pattern of increasing genetic diversity along a south–north axis, and little genetic structure across the species range. Corroboration of this hypothesis would indicate that the species can recover from climatically induced demographic declines, tracking newly available habitats when environmental conditions ameliorate. Here we test this hypothesis, document range-wide patterns of genetic diversity and structure based on a geographically comprehensive multilocus data

set, reconstruct historical demography and describe changes in environmental favourability through time, in order to infer how past climatic changes have affected patterns of genetic structure and diversity in this species.

Material and Methods

Sampling and DNA extraction

Tissue samples from 524 individuals of *P. cultripes* were collected from 54 localities covering all of the species' range (Fig. IV.1B, see Table IV.S1 in Supporting Information). Samples were obtained from tail tips of larvae and toes of adults, preserved in absolute ethanol, and subsequently kept in a freezer at -20 °C. Genomic DNA was extracted using NucleoSpin Tissue-Kits (Macherey-Nagel, Düren, Germany) and later stored at 4 °C.

Mitochondrial DNA

A fragment of mitochondrial DNA (872 bp) including the NADH dehydrogenase subunit 4 gene and flanking tRNAs was amplified and sequenced using primers ND4 and Leu (Arévalo *et al*., 1994). A total of 197 individuals from 54 populations were sequenced. This subsampling is justified by the low level of genetic divergence in mtDNA, including cases in which all individuals sampled in a locality share the same mtDNA haplotype (i.e. nucleotide diversity = 0), which makes sample aggregation a good solution for representation purposes. PCR conditions consisted of an initial denaturation step at 94 °C for 5 min, followed by 40 cycles of denaturation at 94 °C for 30s, annealing at 53 °C for 30 s and extension at 72 °C for 1.30 min, with a final extension step at 72 °C for 10 min. Each reaction was performed in a final volume of 25 µl containing 0.2 µM of each primer, 0.4 mM dNTP, 1 mM $MgCl_2$ and 2.5 µl of 5x GoTaq Flexi buffer (PROMEGA, Madison, WI, USA), 0.5 U GoTaq Flexi DNA polymerase (PROMEGA) and 25 ng of template DNA. PCR amplifications were run on 1% agarose gels to check for successful amplification and possible contaminations using negative controls. PCR products were purified using sodium acetate and ethanol, and then resuspended in 20 µl of ultrapure water prior to sequencing in an automatic sequencer (ABI PRISM 3730, Applied Biosystems, Foster City, CA, USA).

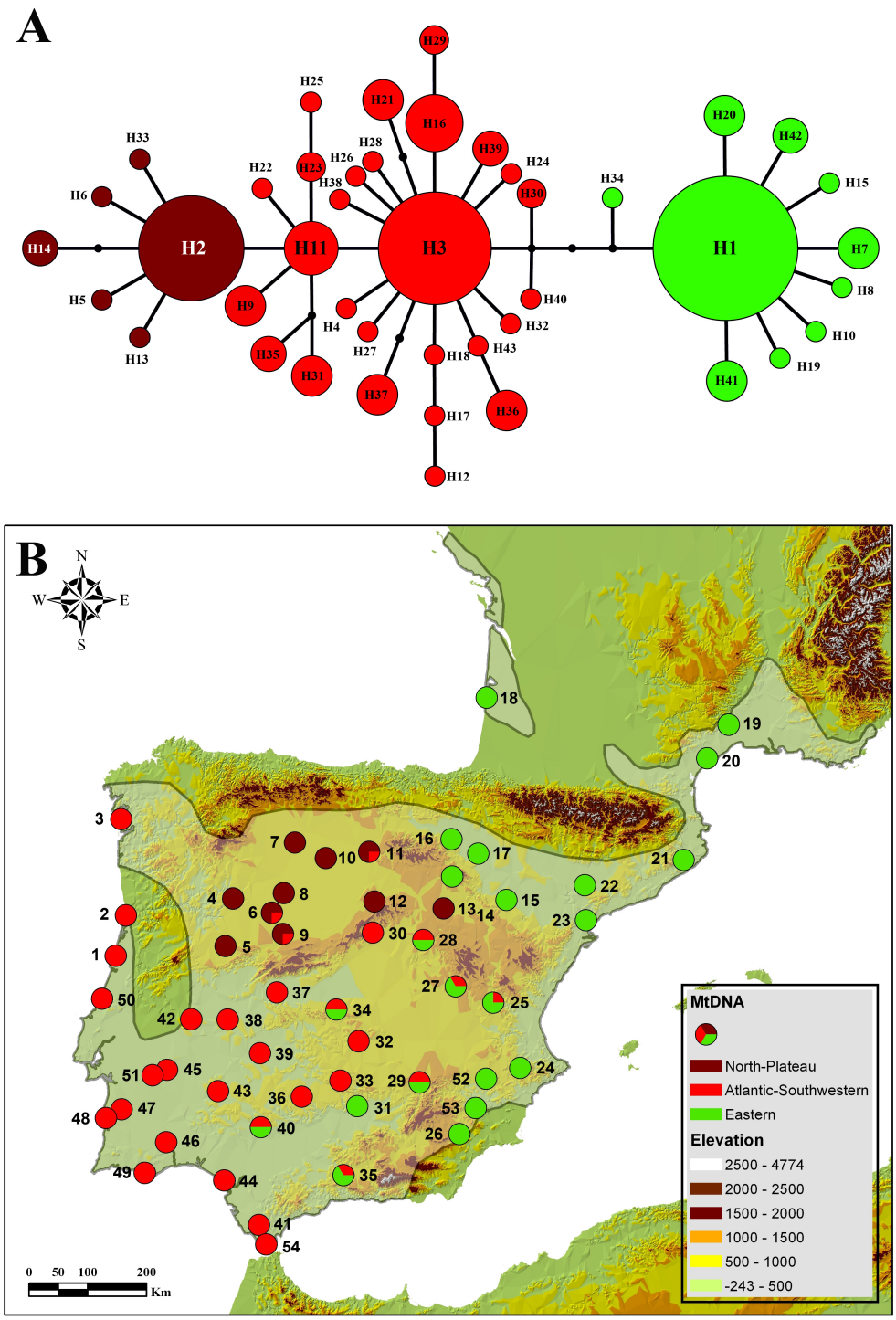

Figure IV.1. A) Haplotype network of mtDNA sequences in *P. cultripes*. Three main haplogroups were identified, each of them including one haplotype found in high frequency and several closely related haplotypes. B) Geographical distribution of the three major haplogroups identified in the analyses, including their relative frequencies when co-occurring in the same locality.

Sequences of mtDNA were edited with Sequencher 4.10.1 (GeneCodes Corp., Ann Arbor, MI, USA) and aligned by eye with Mesquite 3.03 (Maddison & Maddison, 2015). DnaSP 5.10 (Librado & Rozas, 2009) was used to estimate haplotype and nucleotide diversity (p) for each population. Localities within 25 km of each other were grouped together to estimate nucleotide diversity using the software Spads 1.0 (Dellicour & Mardulyn, 2014). These values were subsequently interpolated in a map, using the universal kriging function and a spherical semivariogram model in ArcGIS 10 (ESRI Inc., Redlands, CA, USA).

A haplotype network was generated with Haploviewer (Available from: http://www.cibiv.at/~greg/haploviewer). We also tested for molecular signatures of demographic expansion by calculating mismatch distributions, and several statistics: Fu's Fs (Fu, 1997), Tajima's D (Tajima, 1989) and Ramos-Onsins and Rozas' R_2 (Ramos-Onsins & Rozas, 2002). Significance of these statistics was assessed through coalescent simulations with 10,000 replicates using DnaSP 5.10 (Librado & Rozas, 2009). Mean genetic distances (Kimura-2 parameter, K2p-corrected) between and within lineages were calculated with Mega 6.06 (Tamura *et al*., 2013).

We used phylogeographical continuous diffusion models as implemented in Beast 1.8 (Drummond *et al*., 2012) to reconstruct range dynamics through time in *P. cultripes* based on mtDNA sequences. This analysis simultaneously reconstructs gene trees, ancestral population sizes, and the geographical ranges of inferred nodes, which can be visualized through time provided appropriate calibrations or substitution rates are supplied. As no reliable estimates of substitution rates or calibrations based on fossils or geological events are available for *Pelobates*, we estimated a substitution rate for the mtDNA fragment used (ND4+ adjacent tRNAs) in a family-level phylogenetic analysis including representatives of the families Scaphiopodidade (*Scaphiopus couchii* Baird, 1854, accession: JX564894, and *Spea bombifrons* (Cope, 1863): JX564896, Zhang *et al*., 2013), Pelodytidae (*Pelodytes caucasicus* Boulenger, 1896: KP166769, *P. ibericus* Sánchez Herráiz, Barbadillo-Escrivá, Machordom & Sanchiz, 2000: KP166779, and *P. punctatus* (Daudin, 1802): KP166116, Díaz-Rodríguez *et al*., 2015), Megophryidae (*Leptobrachium montanum* Fischer, 1885: EU180967, *Scutiger* cf *mammatus* (Günther, 1896): EU180974, and *Oreolalax jingdongensis*

Ma, Yang & Li, 1983: EU180972, Rao & Wilkinson, 2008), and Pelobatidae (including one sequence of *P. cultripes* – voucher PC935-, and another one of its sister taxon *P. varaldii* Pasteur & Bons, 1959 – voucher IMS1148-). Based on the estimates of Roelants *et al*. (2007) (153.7 Myr for the split between *Pelobates* and *Spea*) and Wiens (2007) (127 Myr for the same split), we specified a prior for the age of the root of the tree with a lognormal distribution (offset: 125 Myr; log(mean): 1.5; log(SD): 1.0), encompassing values between 125 and 157 Myr. We selected the optimal nucleotide substitution model based on jModeltest 2.5 (Darriba *et al*., 2012) results, choosing the best-ranked model available in Beast, in this case HKY+G (3rd ranked model based on the Bayesian information criterion). Analyses were run under a strict molecular clock and using the Yule speciation model as the coalescent prior. All families were constrained to be monophyletic in the analyses. Convergence was assessed through inspection of the logfile in Tracer 1.6 (Rambaut *et al*., 2014) and a maximum clade credibility tree (MCCT) was reconstructed with TreeAnnotator (distributed as part of the Beast package).

For the continuous diffusion analysis, we used all 197 *P. cultripes* sequences and selected the optimal partitioning strategy and corresponding nucleotide substitution models with PartitionFinder 1.1.1 (Lanfear *et al*., 2012). Geographical coordinates for each sequence were included, with a jitter module generating random coordinates (window size: 0.1) for individuals from the exact same location. Analyses were run for 300 hundred million generations under a strict molecular clock (with the clock rate specified based on the results of the previous analysis, with a normal distribution with mean = 0.005 substitutions/site/million years, and a SD of 0.001, and using the Bayesian skyline plot (linear, number of groups = 5) as the coalescent prior. The Cauchy model was used to describe the geographical diffusion process through time across branches of the inferred gene tree (Lemey *et al*., 2010). Convergence was assessed through inspection of the log file in Tracer and a MCCT was reconstructed with TreeAnnotator. This tree was used to generate time-calibrated reconstructions of the diffusion process using the modules 'Continuous Tree' and 'Time Slicer' in Spread 1.0.7 (Bielejec *et al*., 2011). Beast analyses were run in the Cipres Science Gateway (Miller *et al*., 2010).

Microsatellites (SSR)

A set of 16 recently characterized microsatellite markers (Gutiérrez-Rodríguez & Martínez-Solano, 2013) were used to genotype 517 samples from 49 localities (Table IV.S1). Microsatellites were amplified with PCR conditions described in Gutiérrez-Rodríguez & Martínez-Solano (2013). Amplified fragments were run in an ABI PRISM 3730 sequencer with the GeneScan 500 LIZ size standard (Applied Biosystems). Alleles were visualized and scored manually using GeneMapper 4.0 (Applied Biosystems).

We used Microchecker 2.2.3 (van Oosterhout *et al*., 2004) to test for null alleles, stuttering and large allele dropout in the data set, using a 99% confidence interval and 1000 randomizations. Additionally, we performed a genetic parentage analysis with the software Colony 2.0.5.1 (Jones & Wang, 2010) to remove full-siblings from the sample collected at each locality, to minimize possible biases (Goldberg & Waits, 2010). We assumed a mating system with monogamous females and polygamous males, acknowledging the possibility of multiple mating by males, and implemented the full-likelihood method of Wang (2004), with 10 independent runs and updated allele frequencies. Evidence of linkage disequilibrium (LD) and deviations from Hardy–Weinberg equilibrium (HWE) were tested using Genepop on the web (http://genepop.curtin.edu.au; Raymond & Rousset, 1995). Significance values for multiple tests were adjusted applying a sequential Bonferroni correction (Rice, 1989).

The mean number of alleles (Na), observed (Ho) and expected heterozygosity (He), and Fis (inbreeding coefficient) for each population were estimated in GenAlEx 6.5b5 (Peakall & Smouse, 2012). Private alleles (P) and allelic richness (Ar) were calculated with Adze (Szpiech *et al*., 2008) for each population and mapped using ArcInfo (ESRI, Redlands, CA, USA) with the interpolation universal kriging function and a spherical semivariogram model. Adze uses a rarefaction approach to allow comparison of populations with different sample sizes. A principal components analysis was carried out using Past 3 (Hammer *et al*., 2001), to summarize the variation of nucleotide diversity, observed heterozygosity, private alleles and allelic richness. The first principal component (PC1) was then mapped following the steps above.

We used two Bayesian clustering algorithms to describe population

structure based on microsatellite data: Structure 2.3.4 (Pritchard *et al*., 2000) and Tess 2.3.1 (Chen *et al*., 2007). Structure assigns each multilocus genotype to different clusters, minimizing departures from Hardy–Weinberg and LD, while Tess includes a spatially explicit prior distribution based on a hierarchical mixture model (Chen *et al*., 2007; Durand *et al*., 2009). In Structure, analyses were run assuming correlated allele frequencies between populations (Falush *et al*., 2003) and the admixture model. Ten runs were conducted for each value of K, testing values between 1 and 10, with each run consisting of a burn-in of 500,000 generations followed by 1,000,000 MCMC iterations. The best value of K was selected based on the log probability of the data (Ln(Pr(X'K)) and the ΔK method (Evanno *et al*., 2005) using Structure Harvester 0.6.94 (Earl & vonHoldt, 2012), although other K values showing consistent, biologically significant results were also considered for further discussion. Clumpp 1.1 (Jakobsson & Rosenberg, 2007) was used to summarize results from different runs for the best values of K and graphs of assignment probabilities were produced with Distruct 1.1 (Rosenberg, 2004). Spatially explicit cluster analyses were performed with Tess. The analyses assumed the conditional autoregressive Gaussian model of admixture with linear trend surface (Durand *et al*., 2009), and set the admixture parameter to 1 and the interaction parameter (α) to 0.6 as starting values. Ten independent runs were carried out with K values between 2 and 10, each run with a burn-in of 50,000 iterations followed by 250,000 additional iterations.

Distribution modelling

An environmental favourability model (Real *et al*., 2006) was built with the *fuzzySim* package (Barbosa, 2015) under R 3.1 (R Core Team, 2014), based on presence/absence data on the UTM 10 x 10 km cells of mainland Portugal (Loureiro *et al*., 2008), Spain (MAGRAMA, 2014) and France (MNHN, 2014), and on the 19 bioclimatic variables available in the WorldClim database (Hijmans *et al*., 2005), which had an apropriate temporal and spatial scale for our study. Variables were preselected based on their direct (bivariate) relationship with the species' occurrence, using the false discovery rate (Benjamini & Hochberg, 1995). They were then included in a multivariate model, with a forward-stepwise procedure based on Akaike's information criterion. Any non-significant variables

left in the model were further removed (Crawley, 2007).

The model was evaluated using several performance measures, of both discrimination and calibration (Jiménez-Valverde *et al*., 2013), with the *modEvA* R package (Barbosa *et al*., 2013). It was then applied to the climatic conditions projected for the LIG, the LGM and the mid-Holocene, the latter two including the three hypothetical simulations (CCSM4, MIROC-ESM and MPI-ESM-P) that were available based on the same current climate values used for model building.

We used fuzzy logic (Barbosa & Real, 2012) to calculate the intersection between LIG and LGM favourability, which represents the maintenance of relatively favourable conditions throughout the glaciations. We then correlated these intersected favourability values with the current pattern of genetic diversity within the species' distribution range. We also quantified and represented the general changes in favourability between past simulations and current climate, using the fuzzy range change measures (including overall proportional gain, loss and stability) available in the *fuzzySim* package.

Results

Mitochondrial analyses

The final mitochondrial data set included sequences of 872 bp for 197 specimens from 54 localities (GenBank accession numbers: KU670432-KU670630). The sequences contained 45 variable and 28 parsimony-informative sites and were collapsed into 43 unique haplotypes (Table IV.S1). Three haplotypes (H1, H2 and H3) showed relatively high frequency, while the remaining ones were present at relatively low frequency (Fig. IV.1A). The haplotype network shows two main haplogroups (Eastern and Western), corresponding to populations in the eastern and western Iberian Peninsula. Based on the geographical spread of haplotypes, the western haplogroup can be further subdivided into a North-Plateau and an Atlantic Southwestern haplogroup (Fig. IV.1B). Mean (K2-p) genetic distance between the two main haplogroups was 0.4% (SD = 0.2), and intra-group genetic distances were 0.1% (SD = 0.0) and 0.3% (SD = 0.1) for the Eastern and Western haplogroups respectively. Neutrality tests (Fu' Fs, Tajima's D and R_2) and

Table IV.1. Results of tests for demographic expansion in *P. cultripes*, including the Western (W), Eastern (E) and North Plateau (NP) haplogroups. Values of Fu's Fs, Tajima's D and R_2 are provided, including their associated p-values. All results are significant, indicating demographic expansions.

	Fu's Fs	p	Tajima's D	p	R_2	p
Pc	-35.3579	0.000	-1.9018	0.006	0.0291	0.016
W	-27.0992	0.000	-1.9819	0.004	0.0300	0.007
E	-8.0847	0.000	-1.9453	0.000	0.0383	0.033
NP	-3.3125	0.009	-1.6993	0.011	0.0604	0.047

mismatch distributions support scenarios of historical demographic expansion for the species and the two main haplogroups, with all test statistics yielding significant values (see Table IV.1 and Fig. IV.S1 in Supporting Information). Nucleotide diversity ranged from 0 to 0.00382 (Table IV.S1), with a tendency to increase from south to north (see Fig. IV.S2A).

Beast results produced largely unresolved trees, although some nodes were strongly supported (Bayesian posterior probabilities, BPPs>0.90). These included haplogroup East (BPP: 0.99), as well as four clades including haplotypes from haplogroup West (which was not supported as a major clade). Three of these clades had relatively restricted ranges (pops. 41, 43 and 44; pops. 27, 29 and 30; and pops. 32 and 39), but the fourth clade included populations in the North Plateau (BPP: 1.0), with localities 4–13 (see Fig. IV.S3). Continuous diffusion analyses produced good results, with ESSs values >200 for all parameters. The root of the tree was inferred to date back to the Pleistocene, c. 600 ka. An ancestral area was inferred to be located between the basins of the Tajo and Guadiana rivers, with subsequent expansions to the south, east and north. The species would have been present in most of its current range in the LIG, with the exception of coastal Atlantic Galician and French populations, which would have originated in the last 20 ka (Fig. IV.2). The Bayesian Skyline Plot showed a sustained population increase in the last 250 ka, with a recent decline c. 25 ka and subsequent recovery c. 5 ka (see Fig. IV.S1).

Microsatellite analyses

Genotypes were amplified with a success rate of >99%. Based on results of Microchecker, two microsatellite loci (Pc4.3 and Pc4.7) were discarded because of the inferred presence of null alleles in several populations. Besides, some

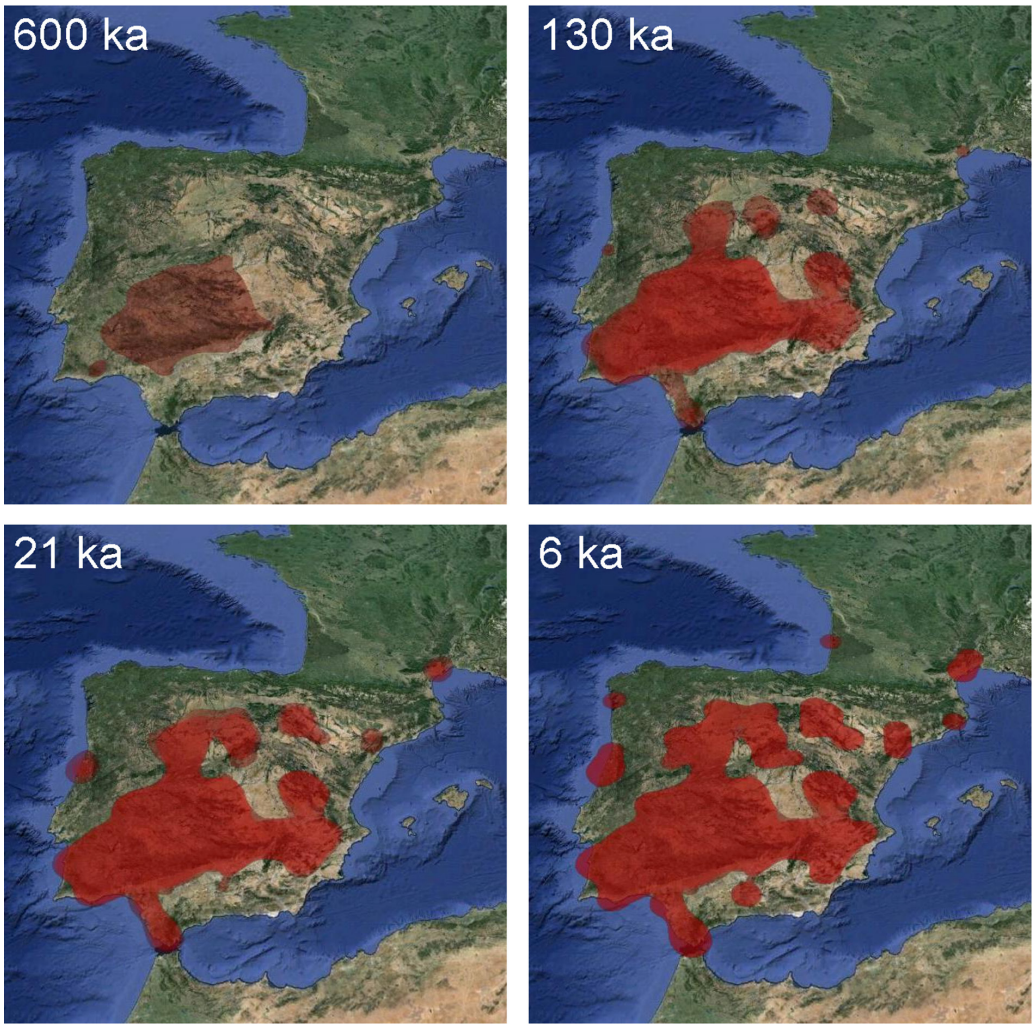

Figure IV.2. Continuous diffusion phylogeographical reconstruction in *Pelobates cultripes* at four time slices: 600, 130, 21 and 6 ka. Areas in red represent the inferred ancestral location at nodes in each temporal 'slice'.

individuals were removed from the data set after the sibship analyses performed in Colony, leaving a single representative per sibship group (Table IV.S1). We found no evidence for significant deviations from HWE or LD.

Descriptive statistics of genetic diversity in *P. cultripes* are shown in Table IV.S1. The average number of alleles and observed heterozygosity per locus and population were 2.71 and 0.37 respectively. The lowest values of observed heterozygosity were found north of the Sistema Central Mountains, as well as in the north-eastern IP and in France (see Fig. IV.S2D). Values of allelic richness across loci showed a decreasing trend from south to north, ranging from 6.09 to

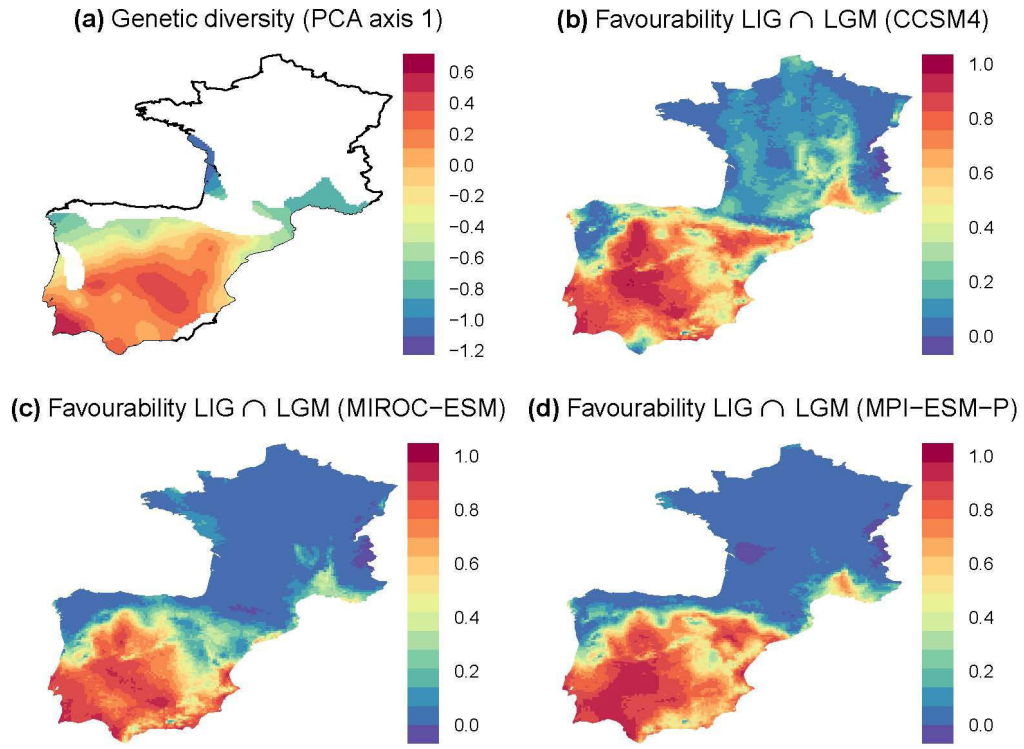

Figure IV.3. A) Genetic diversity of *Pelobates cultripes*, based on the first axis of a principal components analysis (PCA) of nucleotide diversity (π), observed heterozygosity (Ho), allelic richness (Ar), and number of private alleles (P); and the intersection between climatic favourability for this species during the Last Inter-Glacial period (LIG) and each of the three simulations for the Last Glacial Maximum (LGM): B) CCSM4, C) MIROC-ESM and D) MPI-ESM-P.

1.45, whereas the highest values for private alleles were found in south-western IP (see Figs. IV.S2B and IV.S2C).

The first principal component (PC1) of genetic diversity (summarizing the variables π, Ho, Ar and P) accounted for 97.56% of the variance. Mapping PC1 across the species range revealed a clear increasing trend towards the south (see Figs. IV.3 and IV.S2).

The results of the two Bayesian clustering algorithms were congruent. The optimal K value in Structure and Tess runs based on the method of Evanno and the DIC, respectively, was 2. At K = 2, the two genetic clusters correspond to a west-east division. In addition, at K = 3 and K = 6 there were significant increases of ΔK too (Fig. IV.4B). These levels of hierarchical structure showed a strong, clear relationship with geography. For K = 3, the western cluster is subdivided into two clusters, corresponding to populations in the north-west

(coastal northern Portugal and Galicia and North Plateau) and on the Atlantic south-western region (Fig. IV.4). Finally, results of Structure for K = 6 show strong geographical association and consistency across replicate runs (Fig. IV.4). The eastern cluster is subdivided into north and east subgroups, and the western cluster into Atlantic and North Plateau subgroups.

Distribution modeling

Model predictions (see Fig. IV.S4) had good overall evaluation measures (see Fig. IV.S5). For example, they had an area under the receiver operating characteristic curve (AUC) of 0.85, which is generally considered 'good' (Swets, 1988), and a McFadden's pseudo-R^2 of 0.26, which is considered 'excellent fit' (McFadden, 1978).

Overall mean climatic favourability (given by the model based on the species' current distribution) was significantly higher during the LIG than it is currently, and significantly lower during the LGM according to two of the three climatic simulations (MIROC-ESM and MPI-ESM-P). Under the CCSM4 simulation, favourability was slightly higher during the LGM than currently. Regardless of this uncertainty, past favourability values were generally highly correlated with current ones, that is, the most and least favourable areas, within the available climatic conditions, were largely the same as today, especially during the LGM and the mid-Holocene (see Fig. IV.S6).

The intersections between favourability in the LIG and under each LGM simulation, suggesting the maintenance of favourable conditions through the glaciations (Fig. IV.3), were significantly correlated with genetic diversity within the species' range (Pearson's $r = 0.63$ under LGM simulation CCSM4, $r = 0.71$ under MIROC-ESM and $r = 0.78$ under MPI-ESM-P; $P < 0.001$ with 5540 d.f.).

Favourability change between time periods included both increases and decreases, with south-eastern France and north-eastern Spain showing the highest and most consistent increases in favourability since past climate simulations (see Fig. IV.S7). Overall change was more notable with respect to the LIG, with a c. 20% fuzzy range contraction (as given by climatic favourability) towards current favourable areas, whereas a slighter increase occurred after the LGM (Table IV.2).

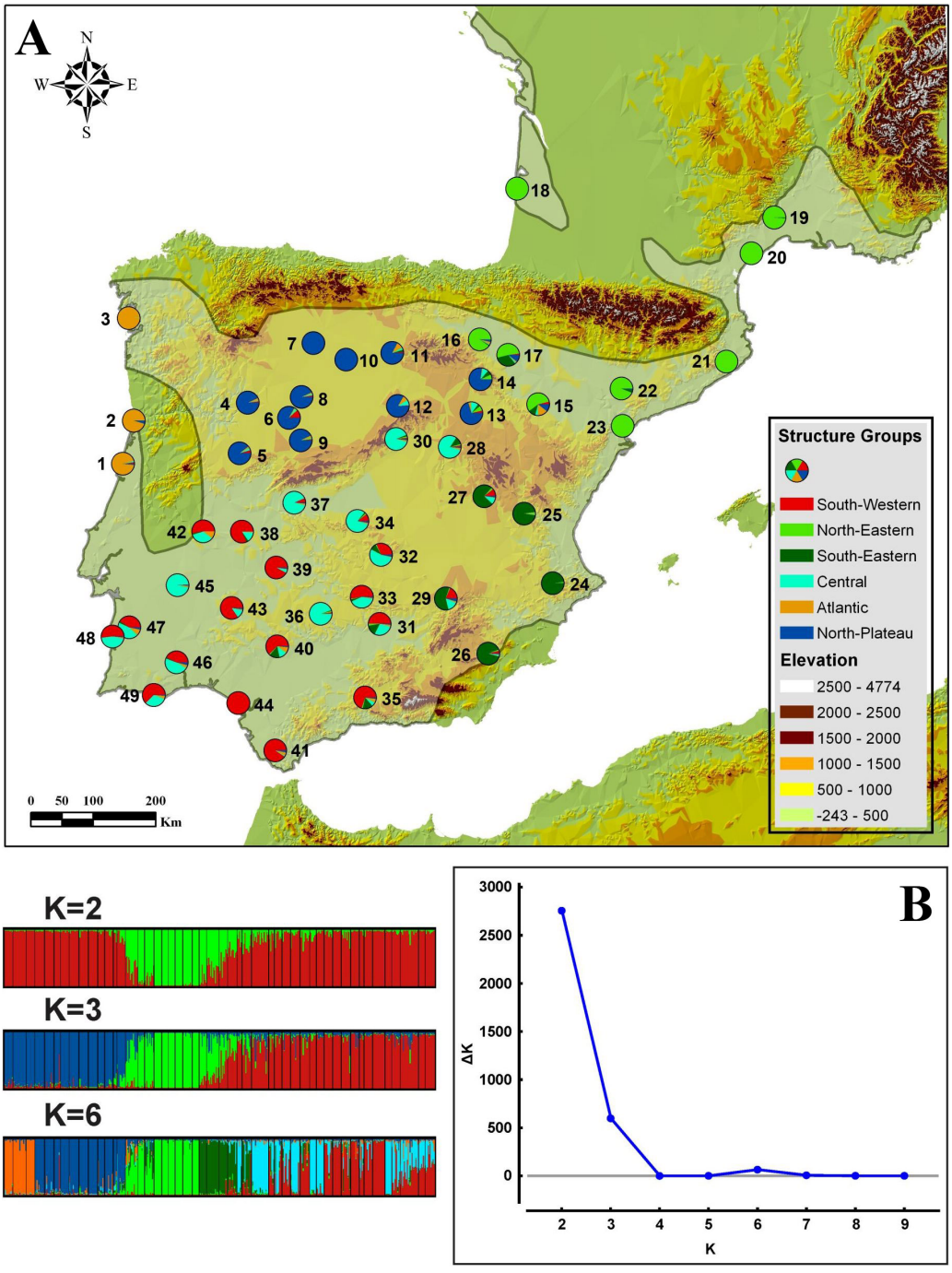

Figure IV.4. A) Results of Structure, showing the spatial distribution of genetic clusters for K = 6 for *Pelobates cultripes*. Alternative values of K are shown for comparison (K = 2 and 3). B) Values of ΔK, showing peaks at K = 2, 3 and 6.

Table IV.2. Fuzzy range change measures (fuzzy equivalents of the proportion of gained, lost, maintained and changed presences) for *Pelobates cultripes* based on climatic favourability in different time periods, from the Last Inter-Glacial (LIG), to the Last Glacial Maximum (LGM), the mid-Holocene and the present, under the three hypothetical climatic simulations currently available across periods on WorldClim.

Time periods	Gain	Loss	Stable	Balance
LIG to LGM (CCSM4)	0.07	0.32	0.06	-0.25
LIG to LGM (MIROC-ESM)	0.01	0.49	0.03	-0.49
LIG to LGM (MPI-ESM-P)	0.06	0.41	0.03	-0.35
LGM to Holocene (CCSM4)	0.13	0.25	0.08	-0.12
LGM to Holocene (MIROC-ESM)	0.45	0.12	0.09	0.32
LGM to Holocene (MPI-ESM-P)	0.22	0.09	0.04	0.13
Holocene (CCSM4) to present	0.11	0.1	0.1	0.01
Holocene (MIROC-ESM) to present	0.1	0.11	0.08	-0.01
Holocene (MPI-ESM-P) to present	0.1	0.19	0.06	-0.09

Discussion

The integration of results from different disciplines such as phylogeography, population genetics and species distribution modelling allowed us to reconstruct demographic changes in *P. cultripes* since the Pleistocene, including an approximation to potential climate-induced range shifts occurring during the last 130,000 years. Overall, we found low genetic variation and relatively shallow genetic structure, but the results obtained by different approaches have provided relevant and congruent insights about the recent evolutionary history of the species that may help predict population responses to future environmental changes.

Our estimates of phylogeographical structure based on mitochondrial DNA data are consistent with previous studies showing low genetic variability and structure across the species' range (Crottini *et al*., 2010; Fitó *et al*., 2011). There is a deep temporal gap between our estimates of the time to the most recent common ancestor (TMRCA) of all extant haplotypes in *P. cultripes* around 500 ka (median value: 535 ka, 95%HPDi: 230–994 ka) and the inferred divergence time from its sister species *P. varaldii* in the Miocene, around 13 Ma (median: 13.26 Ma, 95%HPDi: 9.19–17.91 Ma). This split time is older than those estimated by Busack *et al*. (1985) and García-París *et al*. (2003), at 8–11 Ma and 5.5 Ma, respectively, but all estimates indicate speciation occurred in the Miocene. Our estimate at 13 Ma is consistent with the separation of the Betic-

Rifean Massif during the upper Tortonian period (Martín *et al*., 2009). This split coincides with other diversification events in Iberian amphibians, such as the genus *Alytes* (Maia-Carvalho *et al*., 2014). Despite the inferred long evolutionary history of *P. cultripes* in Iberia, all extant haplogroups share a common ancestor within the last 1 Myr (95%HPDi: 230–994 ka). This contrasts with most other Iberian amphibians, for which geographically structured, old phylogroups provide evidence of survival in allopatric refugia across several Ice Ages (Díaz-Rodríguez *et al*., 2015; Gonçalves *et al*., 2015; Teixeira *et al*., 2015). This may result from massive extinction of lineages during the glaciations of the Pliocene and Pleistocene, although other processes, such as selective sweeps, cannot be ruled out.

In spite of the low mitochondrial variability, two main haplogroups were recovered in our analysis. These groups were not recovered in previous studies using sparser sampling and more slowly evolving markers (Crottini *et al*., 2010; Fitó *et al*., 2011). The main split is across an east–west axis, as previously found in other species, such as *Discoglossus galganoi* Capula, Nascetti, Bullini, Lanza & Crespo, 1985 and *Pleurodeles waltl* Michahelles, 1830 (García-París & Jockusch, 1999; Carranza & Arnold, 2004; Martínez-Solano, 2004; Veith *et al*., 2004). However, whereas in these taxa the vicariant event associated with the eastern-western haplogroup split was inferred to be related to the Guadalquivir basin formation or the Messinian salinity crisis, in the Miocene and Pliocene, vicariance in *P. cultripes* was much more recent, most probably in the Pleistocene.

This east–west division of *P. cultripes* is also apparent from the analyses of SSR data. Structure and Tess both recovered these groups at K = 2. The presence of wide admixture zones between groups suggests high migration rates (Figs. IV.1B and IV.4A). The interpolation of genetic diversity indices shows that genetic diversity is lower in the north, including several groups recovered by Structure: Atlantic, North Plateau and North-Eastern (Figs. IV.3A and IV.4A). This low diversity contrasts with the higher values observed in southern populations and can be explained as resulting from a recent expansion of these populations from the south. The different analyses carried out to detect genetic signatures of demographic expansion, including Fs, D and R_2 statistics and the Bayesian skyline plot, consistently identify a signal of population growth across

all major haplogroups, as well as for the species as a whole (Table IV.1, Fig. IV.S1). However, the different northern groups seem to derive from different source populations. The North Plateau group was recovered in both mtDNA and SSR-based analyses, whereas the others were only identified by the faster evolving SSRs (Figs. IV.1A and IV.4A). This may indicate an older origin for the North Plateau group with respect to the Atlantic and North-Eastern groups, as suggested by continuous diffusion analyses, which infer their presence at that area well before the LIG (Figs. IV.2 and IV.S3).

The fossil record is also consistent with a long but discontinuous presence of the species in the North Plateau, since there are fossil remains in several levels of the Atapuerca formation that date back to the lower Pleistocene (Martín & Sanchiz, 2013; Lobo *et al*., 2016), and are thus older than the estimated TMRCA for the species. This suggests cycles of colonization/extinction in areas north of the Sistema Central Mountains during the Pleistocene. This mountain range probably acted as a significant barrier to gene flow, limiting migration between populations in the south and north. This is in accordance with the species' life history traits: while the species reaches up to 1770 m of elevation in the Sistema Central (Cejudo, 1990), it is generally not abundant above 1000 m (Tejedo & Reques, 2002).

Species distribution models suggested an overall stability of climatically favourable conditions for *P. cultripes* over the last 130 ka, but with some significant changes through time (see Figs. IV.S4, IV.S6 and IV.S7). The geographical extent of climatically favourable areas during the LIG (assuming stable species-environment relationships) was greater than in the present (Table IV.2), whereas significant decreases were detected in south-eastern France and north-eastern Iberia during the LGM (Figs. IV.3, IV.S4 and IV. S7). Climatically stable areas for the species, that is, those resulting from the intersection between favourable areas in the LIG and LGM, are mostly located in the southern half of the Iberian Peninsula, the Northern Plateau and south-eastern France (see Fig. IV.3). Fossil records support our finding, providing evidence for the presence of the species in southern, south-western, central and northeastern Iberia during the upper Pleistocene (Lobo *et al*., 2016).

Our different approaches showed highly consistent results, suggesting the existence of at least three main refugial areas for *P. cultripes* in Iberia, in the south-west, south-east and the Northern Plateau. These areas coincide with climatically stable areas through the LIG and LGM, and were significantly correlated with current patterns of genetic diversity across the species range. A possible fourth refugial area may have existed in south-eastern France, from which both current Atlantic and Mediterranean French populations would descend. This hypothesis is supported by models of climatic favourability based on simulations CCSM4 and MPI-ESM-P (Figs. IV.3 and IV.S4), and by the existence of fossil remains dated 220–130 ka in this region (Hanquet *et al*., 2010). In addition, we found two exclusive haplotypes in Mediterranean French populations (H41, H42; see Table IV.S1). SDMs and molecular evidence, including results of tests of neutrality and mismatch distributions, are thus consistent with the hypothesis that Eastern, Western and Northern Plateau populations have experienced demographic expansions after the LGM, resulting in colonization of northern areas across the current species' range (Table IV.1, Fig. IV.S1). According to these findings, more recently during the Holocene, the Atlantic and North-Eastern groups may have colonized the North Atlantic coast of the Iberian Peninsula and the French Atlantic Coast respectively (Fig. IV.2). The French Atlantic coast may have been colonized from an additional refugium in south-eastern France. In any case, migration through a corridor along the Garonne river from the Mediterranean to the Atlantic coast of France is likely, as previously suggested for another anuran, *P. punctatus* (Díaz-Rodríguez *et al*., 2015). Our mid-Holocene projections, showing some continuity of relatively favourable areas between the Atlantic and Mediterranean coasts, provide support for this hypothesis, although the evidence is not conclusive in terms of the temporal framework involved, as similar continuity was also inferred in previous time intervals (see Fig. IV.S4). In addition, Holocene hydroclimatic variability in the Mediterranean region (Magny *et al*., 2013) may have affected the species' distribution and genetic diversity beyond what mid-Holocene simulations are able to predict.

The major goal of our study was to provide information to help predict the long-term species response to climate-mediated changes. In this respect, our integrative approach supports the idea that populations of *P. cultripes* can recover

from climatically induced demographic declines, and allowed the identification of historically unstable areas in terms of climatic favourability. Among these stand out the Atlantic coasts of France and the north-western Iberian Peninsula, which are also characterized by relatively low values of current favourability. In addition, the low genetic diversity of these populations, along with their location in peripheral areas of the species' range, makes them the most vulnerable to climate-mediated changes in the medium to long term. On the other hand, our results suggest that refugial sites, assuming that they remain climatically stable in the future, ought to be a major conservation priority, since, as long as they are not destroyed by human activities, the species might be able to safely maintain viable populations there in the long run. While past refugia are not guaranteed to remain as favourable in the future, fine-scale environmental heterogeneity and microevolutionary adaptations often allow relict populations to persist under generally harsh climatic conditions, and climate is often a less important threat than direct anthropogenic impacts (Hampe & Jump, 2011). Conservation efforts in historical refugial areas may thus have high potential to ensure the persistence of species in a warmer world.

Acknowledgements

We thank I. Acevedo, J. Alvarez, A. Bermejo, D. Buckley, P. Cabezas, A. Egea, F. Giménez, I. Gomez-Mestre, A. Gosá, E. Pascual, P. Pavón, R. Pereira, E. Recuero, V. Sancho, J. A. Saz, A. Valdeón, G. Velo-Antón and D. B. Wake for help in sample collection. I. Rey and B. Alvarez (Museo Nacional de Ciencias Naturales MNCN-CSIC DNA and Tissue collection) provided some samples. JGR was supported by the Consejo Superior de Investigaciones Científicas of Spain (CSIC) and the European Social Fund (ESF) (JAE-pre PhD fellowship). AMB is supported by FCT and FEDER/COMPETE 2020 through contract IF/00266/2013, exploratory project CP1168/CT0001 and funds POCI-01-0145-FEDER-006821 to unit UID/BIA/50027. This research was funded by grants CGL2008-04271-C02-01/BOS, and CGL2011-28300 (Ministerio de Ciencia e Innovación-MICINN), Ministerio de Economía y Competitividad -MEC-, Spain, and FEDER) to IMS, who is currently supported by funding from the Spanish Severo Ochoa Program (SEV-2012-0262).

References

Araújo MB, Thuiller W, Pearson RG (2006) Climate warming and the decline of amphibians and reptiles in Europe. Journal of Biogeography 33: 1712–1728.

Arévalo E, Davis SK, Sites JW (1994) Mitochondrial DNA sequence divergence and phylogenetic relationships among eight chromosome races of the *Sceloporus grammicus* complex (Phrynosomatidae) in Central Mexico. Systematic Biology 43: 387–418.

Ashworth AC (1996) The response of arctic Carabidae (Coleoptera) to climate change based on the fossil record of the Quaternary Period. Annales Zoologici Fennici 33: 125–131.

Barbosa AM (2015) fuzzySim: applying fuzzy logic to binary similarity indices in ecology. Methods in Ecology and Evolution 6: 853–858.

Barbosa AM, Real R (2012) Applying fuzzy logic to comparative distribution modelling: a case study with two sympatric amphibians. The Scientific World Journal 2012: 10.

Barbosa AM, Real R, Muñoz AR, Brown JA (2013) New measures for assessing model equilibrium and prediction mismatch in species distribution models. Diversity and Distributions 19: 1333–1338.

Beja P, Bosch J, Tejedo M, *et al*. (2009) *Pelobates cultripes*. The IUCN Red List of Threatened Species 2009: e.T58052A11722636. Downloaded on 18 November 2015.

Benjamini Y, Hochberg Y (1995) Controlling the false discovery rate: a practical and powerful approach to multiple testing. Journal of the Royal Statistical Society. Series B (Methodological) 57: 289–300.

Bielejec F, Rambaut A, Suchard MA, Lemey P (2011) SPREAD: spatial phylogenetic reconstruction of evolutionary dynamics. Bioinformatics 27: 2910–2912.

Buchholz DR, Hayes TB (2002) Evolutionary patterns of diversity in spadefoot toad metamorphosis (Anura: Pelobatidae). Copeia 2002: 180–189.

Busack SD, Maxson LR, Wilson MA (1985) *Pelobates varaldii* (Anura: Pelobatidae): a morphologically conservative species. Copeia 1985: 107–112.

Carranza S, Arnold EN (2004) History of West Mediterranean newts, *Pleurodeles* (Amphibia: Salamandridae), inferred from old and recent DNA sequences. Systematics and Biodiversity 1: 327–337.

Cejudo D (1990) Nueva altitud máxima para *Pelobates cultripes*. Boletín de la Asociación Herpetológica Española 1: 20.

Chen C, Durand E, Forbes F, François O (2007) Bayesian clustering algorithms ascertaining spatial population structure: a new computer program and a comparison study. Molecular Ecology Notes 7: 747–756.

Corn PS (2005) Climate change and amphibians. Animal Biodiversity and Conservation 28: 59–67.

Crawley MJ (2007) The R Book. John Wiley & Sons, Chichester.

Crottini A, Galán P, Vences M (2010) Mitochondrial diversity of Western spadefoot toads, *Pelobates cultripes*, in northwestern Spain. Amphibia-Reptilia 31: 443–448.

Cusimano N, Stadler T, Renner SS (2012) A new method for handling missing species in diversification analysis applicable to randomly or nonrandomly sampled phylogenies. Systematic Biology 61: 785–792.

Darriba D, Taboada GL, Doallo R, Posada D (2012) jModelTest 2: more models, new heuristics and parallel computing. Nature Methods 9: 772–772.

Dawson TP, Jackson ST, House JI, Prentice IC, Mace GM (2011) Beyond predictions: biodiversity conservation in a changing climate. Science 332: 53–58.

Dellicour S, Mardulyn P (2014) SPADS 1.0: a toolbox to perform spatial analyses on DNA sequence data sets. Molecular Ecology Resources 14: 647–651.

Devender TRV, Moodie KB, Harris AH (1976) The Desert Tortoise (*Gopherus agassizi*) in the Pleistocene of the Northern Chihuahuan Desert. Herpetologica 32: 298–304.

Díaz-Paniagua C, Gómez-Rodríguez C, Portheault A, de Vries W (2005) Los anfibios de Doñana. Organismo Autónomo de Parques Nacionales, Ministerio de Medio Ambiente, Madrid.

Díaz-Rodríguez J, Gonçalves H, Sequeira F, *et al*. (2015) Molecular evidence for cryptic candidate species in Iberian *Pelodytes* (Anura, Pelodytidae). Molecular Phylogenetics and Evolution 83: 224–241.

Drummond AJ, Suchard MA, Xie D, Rambaut A (2012) Bayesian phylogenetics with BEAUti and the BEAST 1.7. Molecular Biology and Evolution 29: 1969–1973.

Duguet R, Melki F (2003) Les Amphibiens de France, Belgique et Luxemburg, Collection Parthénope. Editions Biotope, Mèze (France), 480.

Duputié A, Massol F, Chuine I, Kirkpatrick M, Ronce O (2012) How do genetic correlations affect species range shifts in a changing environment? Ecology Letters 15: 251–259.

Durand E, Jay F, Gaggiotti OE, François O (2009) Spatial inference of admixture proportions and secondary contact zones. Molecular Biology and Evolution 26: 1963–1973.

Earl D, vonHoldt B (2012) STRUCTURE HARVESTER: a website and program for visualizing STRUCTURE output and implementing the Evanno method. Conservation Genetics Resources 4: 359–361.

Englbrecht CC, Freyhof J, Nolte A, *et al*. (2000) Phylogeography of the bullhead *Cottus gobio* (Pisces: Teleostei: Cottidae) suggests a pre-Pleistocene origin of the major central European populations. Molecular Ecology 9: 709–722.

Evanno G, Regnaut S, Goudet J (2005) Detecting the number of clusters of individuals using the software Structure: a simulation study. Molecular Ecology 14: 2611–2620.

Falush D, Stephens M, Pritchard JK (2003) Inference of population structure using multilocus genotype data: linked loci and correlated allele frequencies. Genetics 164: 1567–1587.

Fitó F, Rivera X, Roca J, *et al*. (2011) Extremely low level of genetic variability in Iberian *Pelobates cultripes* (Cuvier, 1829) (Amphibia; Anura; Pelobatidae). Butlletí de la Societat Catalana d'Herpetologia 19: 21–28.

Fitze P, Gonzalez-Jimena V, San-Jose L, San Mauro D, Aragón P, Suarez T, Zardoya R (2011) Integrative analyses of speciation and divergence in *Psammodromus hispanicus* (Squamata: Lacertidae). BMC Evolutionary Biology 11: 1–22.

Fu Y-X (1997) Statistical tests of neutrality of mutations against population growth, hitchhiking and background selection. Genetics 147: 915–925.

García-París M, Jockusch EL (1999) A mitocondrial DNA perspective on the evolution of Iberian *Discoglossus* (Amphibia: Anura). Journal of Zoology 248: 209–218.

García-París M, Buchholz DR,. Parra-Olea G (2003) Phylogenetic relationships of Pelobatoidea re-examined using mtDNA. Molecular Phylogenetics and Evolution 28: 12–23.

García-París M, Montori A, Herrero P (2004) Fauna Iberica. Vol. 24. Amphibia: Lissamphibia. Museo Nacional de Ciencias Naturales, Consejo Superior de Investigaciones Científicas, Madrid.

Gavin DG, Fitzpatrick MC, Gugger PF *et al* (2014) Climate refugia: joint inference from fossil records, species distribution models and phylogeography. New Phytologist 204: 37–54.

Goldberg CS, Waits LP (2010) Quantification and reduction of bias from sampling larvae to infer population and landscape genetic structure. Molecular Ecology Resources 10: 304–313.

Gómez A, Lunt D (2007) Refugia within refugia: patterns of phylogeographic concordance in the Iberian Peninsula. Phylogeography of southern European refugia (ed. by S Weiss and N Ferrand), pp. 155–188. Springer, Netherlands.

Goncálves H, Maia-Carvalho B, Sousa-Neves T, *et al*. (2015) Multilocus phylogeography of the common midwife toad, *Alytes obstetricans* (Anura, Alytidae): contrasting patterns of lineage diversification and genetic structure in the Iberian refugium. Molecular Phylogenetics and Evolution 93: 363–379.

Gutiérrez-Rodríguez J, Martínez-Solano I (2013) Isolation and characterization of sixteen polymorphic microsatellite loci in the Western Spadefoot, *Pelobates cultripes* (Anura: Pelobatidae) via 454 pyrosequencing. Conservation Genetics Resources 5: 981–984.

Hammer Ø, Harper DAT, Ryan PD (2001) PAST: paleontological statistics software package for education and data analysis. Palaeontologia Electronica 4: 9.

Hampe A, Jump AS (2011) Climate relicts: past, present, future. Annual Review of Ecology, Evolution and Systematics 42: 313–333.

Hanquet C, Valensi P, Bailon S, *et al*. (2010) Caractérisation du climat et de la biodiversité au Pléistocène moyen final, d'après les faunes de vertébrés de la grotte du Lazaret (Nice, France). Quaternaire. Revue de l'Association française pour l'étude du Quaternaire 21: 215–226.

Hegna RH, Galarza JA, Mappes J (2015) Global phylogeography and geographical variation in warning coloration of the wood tiger moth (*Parasemia plantaginis*). Journal of Biogeography 42: 1469–1481.

Hewitt GM (1996) Some genetic consequences of ice ages, and their role in divergence and speciation. Biological Journal of the Linnean Society 58: 247–276.

Hewitt GM (2004) Genetic consequences of climatic oscillations in the Quaternary. Philosophical Transactions of the Royal Society B: Biological Sciences 359: 183–195.

Hijmans R, Cameron S, Parra J, Jones P, Jarvis A (2005) Very high resolution interpolated climate surfaces for global land areas. International Journal of Climatology 25: 1965–1978.

Hoffmann RS (1981) Different voles for different holes: environmental restrictions on refugial survival of mammals. Evolution today: The Second International Congress of Systematic and Evolutionary Biology (ed. by JL Reveal and GGE Scudder), pp. 25–45. British Columbia, Vancouver.

Jakobsson M, Rosenberg NA (2007) CLUMPP: a cluster matching and permutation program for dealing with label switching and multimodality in analysis of population structure. Bioinformatics 23: 1801–1806.

Jiménez-Valverde A, Acevedo P, Barbosa AM, Lobo JM, Real R (2013) Discrimination capacity in species distribution models depends on the representativeness of the environmental

domain. Global Ecology and Biogeography 22: 508–516.

Jones OR, Wang J (2010) COLONY: a program for parentage and sibship inference from multilocus genotype data. Molecular Ecology Resources 10: 551–555.

Keppel G, van Niel KP, Wardell-Johnson GW, *et al*. (2012) Refugia: identifying and understanding safe havens for biodiversity under climate change. Global Ecology and Biogeography 21: 393–404.

Lanfear R, Calcott B, Ho SYW, Guindon S (2012) PartitionFinder: combined selection of partitioning schemes and substitution models for phylogenetic analyses. Molecular Biology and Evolution 29: 1695–1701.

Lemey P, Rambaut A, Welch JJ, Suchard MA (2010) Phylogeography takes a relaxed random walk in continuous space and time. Molecular Biology and Evolution 27: 1877–1885.

Librado P. Rozas J (2009) DnaSP v5: a software for comprehensive analysis of DNA polymorphism data. Bioinformatics 25: 1451–1452.

Lobo JM, Martínez-Solano I, Sanchiz B (2016) A review of the palaeoclimatic inference potential of Iberian Quaternary fossil batrachians. Palaeobiodiversity and Palaeoenvironments 96: 125–148.

Loureiro A, Carretero MA, Ferrand N, Paulo O (2008) Atlas dos Anfíbios e Répteis de Portugal Continental. Instituto da Conservação da Natureza, Lisboa (Portugal).

Maddison W, Maddison D (2015) Mesquite: a modular system for evolutionary analysis. Version 3.03. Available at: http://mesquiteproject.org

Magny M, Combourieu Nebout N, Rousseau D-D, Loutre M-F (2013) (eds.) Holocene changes in environment and climate in the central Mediterranean as reflected by lake and marine records. Climate of the Past, 9 (Special Issue).

MAGRAMA (2014) Inventario Español de Especies Terrestres. Fauna de vertebrados: anfibios y reptiles. Ministerio de Agricultura, Alimentación y Medio Ambiente. Available at: http:// www.magrama.gob.es

Maia-Carvalho B, Gonçalves H, Ferrand N, Martínez-Solano I. (2014) Multilocus assessment of phylogenetic relationships in *Alytes* (Anura, Alytidae). Molecular Phylogenetics and Evolution 79: 270–278.

Martín C, Sanchiz B (2013). Lisanfos KMS. Version 1.2. Museo Nacional de Ciencias Naturales, MNCN-CSIC. Madrid, Spain. Available at: http:// www.lisanfos.mncn.csic.es Accessed 15 October 2015.

Martín JM, Braga JC, Aguirre J, Puga-Bernabéu A (2009) History and evolution of the North-Betic Strait (Prebetic Zone, Betic Cordillera): a narrow, early Tortonian, tidal-dominated, Atlantic-Mediterranean marine passage. Sedimentary Geology 216: 80–90.

Martínez-Freiría F, Velo-Antón G, Brito JC (2015) Trapped by climate: interglacial refuge and recent population expansion in the endemic Iberian adder *Vipera seoanei*. Diversity and Distributions 21: 331–344.

Martínez-Solano I (2004) Phylogeography of Iberian *Discoglossus* (Anura: Discoglossidae). Journal of Zoological Systematics and Evolutionary Research 42: 298–305.

Martínez-Solano I, Teixeira J, Buckley D, García-París M (2006) Mitochondrial DNA phylogeography of *Lissotriton boscai* (Caudata, Salamandridae): evidence for old,

multiple refugia in an Iberian endemic. Molecular Ecology 15: 3375–3388.

McFadden DL (1978) Quantitative methods for analyzing travel behaviour of individuals: some recent developments. In D. Hensher and P. Stopher (Eds.), Behavioural travel modelling (pp. 279–318). Croom Helm.

Médail F, Diadema K (2009) Glacial refugia influence plant diversity patterns in the Mediterranean Basin. Journal of Biogeography 36: 1333–1345.

Miller MA, Pfeiffer W, Schwartz T (2010) Creating the CIPRES Science Gateway for inference of large phylogenetic trees. Gateway Computing Environments Workshop (GCE), 2010, 1–8.

Morales Pérez JV, Serra AS (2009) The Quaternary fossil record of the genus *Testudo* in the Iberian Peninsula. Archaeological implications and diachronic distribution in the western Mediterranean. Journal of Archaeological Science 36: 1152–1162.

Moritz C, Agudo R (2013) The future of species under climate change: resilience or decline? Science 341: 504–508.

Peakall R, Smouse PE (2012) GenAlEx 6.5: genetic analysis in Excel. Population genetic software for teaching and research—an update. Bioinformatics 28: 2537–2539.

Pritchard JK, Stephens M, Donnelly P (2000) Inference of population structure using multilocus genotype data. Genetics 155: 945–959.

Provan J, Bennett KD (2008) Phylogeographic insights into cryptic glacial refugia. Trends in Ecology and Evolution 23: 564–571.

R Core Team (2014) R: a language and environment for statistical computing. R Foundation for Statistical Computing, Vienna. http://www.r-project.org.

Rambaut A, Suchard M, Xie D, Drummond A (2014) Tracer v1.6. Available at: http://beast.bio.ed.ac.uk/Tracer. Accessed 27 July 2014

Ramos-Onsins SE, Rozas J (2002) Statistical properties of new neutrality tests against population growth. Molecular Biology and Evolution 19: 2092–2100.

Rao DQ, Wilkinson JA (2008) Phylogenetic relationships of the mustache toads inferred from mtDNA sequences. Molecular Phylogenetics and Evolution 46: 61–73.

Raymond M, Rousset F (1995) GENEPOP (Version 1.2): population genetics software for exact tests and ecumenicism. Journal of Heredity 86: 248–249.

Real R, Barbosa AM, Vargas JM (2006) Obtaining environmental favourability functions from logistic regression. Environmental and Ecological Statistics 13: 237–245.

Recuero E, Buckley D, García-París M, *et al*. (2014) Evolutionary history of *Ichthyosaura alpestris* (Caudata, Salamandridae) inferred from the combined analysis of nuclear and mitochondrial markers. Molecular Phylogenetics and Evolution 81: 207–220.

Rice WR (1989) Analyzing tables of statistical tests. Evolution 43: 223–225.

Roelants K, Gower DJ, Wilkinson M, *et al*. (2007) Global patterns of diversification in the history of modern amphibians. Proceedings of the National Academy of Sciences USA 104: 887–892.

Rosenberg NA (2004) DISTRUCT: a program for the graphical display of population structure. Molecular Ecology Notes 4: 137–138.

Schmidt GA, Annan JD, Bartlein PJ, *et al*. (2014) Using palaeoclimate comparisons to constrain future projections in CMIP5. Climate of the Past 10: 221–250.

Sket B (1997) Special paper: distribution of *Proteus* (Amphibia: Urodela: Proteidae) and its possible explanation. Journal of Biogeography 24: 263–280.

Swets J (1988) Measuring the accuracy of diagnostic systems. Science 240: 1285–1293.

Szpiech ZA, Jakobsson M, Rosenberg NA (2008) ADZE: a rarefaction approach for counting alleles private to combinations of populations. Bioinformatics 24: 2498–2504.

Tajima F (1989) Statistical method for testing the neutral mutation hypothesis by DNA polymorphism. Genetics 123: 585–95.

Talavera RR, Sanchiz B (1987) Temperature dependence of larval development in *Pelobates cultripes* (preliminary experiments). Societas Europaea Herpetologica, Faculty of Sciences, Nijmegen.

Tamura K, Stecher G, Peterson D, Filipski A, Kumar S (2013) MEGA6: molecular evolutionary genetics analysis version 6.0. Molecular Biology and Evolution 30: 2725–2729.

Teixeira J, Martínez-Solano I, Buckley D, *et al*. (2015) Genealogy of the nuclear β-fibrinogen intron 7 in *Lissotriton boscai* (Caudata, Salamandridae): concordance with mtDNA and implications for phylogeography and speciation. Contributions to Zoology 84: 193–215.

Tejedo M (1993) Size-dependent vulnerability and behavioral responses of tadpoles of two anuran species to beetle larvae predators. Herpetologica 49: 287–294.

Tejedo M, Reques R (2002) *Pelobates cultripes* (Cuvier, 1829). Sapo de espuelas. Atlas y libro rojo de los anfibios y reptiles de España (ed. by JM Pleguezuelos, R Márquez and M Lizana), pp. 94–96. Dirección General de Conservación de la Naturaleza-Asociación Herpetológica Española, Madrid.

Thuiller W, Albert C, Araújo MB, *et al*. (2008) Predicting global change impacts on plant species' distributions: future challenges. Perspectives in Plant Ecology, Evolution and Systematics, 9, 137–152.

Todisco V, Gratton P, Zakharov EV, *et al*. (2012) Mitochondrial phylogeography of the Holarctic *Parnassius phoebus* complex supports a recent refugial model for alpine butterflies. Journal of Biogeography 39: 1058–1072.

Tsuda Y, Nakao K, Ide Y, Tsumura Y (2015) The population demography of *Betula maximowicziana*, a cool-temperate tree species in Japan, in relation to the last glacial period: its admixture-like genetic structure is the result of simple population splitting not admixing. Molecular Ecology 24: 1403–1418.

van Oosterhout C, Hutchinson WF, Wills DPM, Shipley P (2004) MICRO-CHECKER: software for identifying and correcting genotyping errors in microsatellite data. Molecular Ecology Notes 4: 535–538.

Veith M, Mayer C, Samraoui B, Barroso DD, Bogaerts S (2004) From Europe to Africa and vice versa: evidence for multiple intercontinental dispersal in ribbed salamanders (Genus *Pleurodeles*). Journal of Biogeography 31: 159–171.

Velo-Antón G, Godinho R, Harris DJ, *et al*. (2012) Deep evolutionary lineages in a Western Mediterranean snake (*Vipera latastei*/*monticola* group) and high genetic structuring in Southern Iberian populations. Molecular Phylogenetics and Evolution 65: 965–973.

Wang J (2004) Sibship reconstruction from genetic data with typing errors. Genetics 166: 1963–1979.

Weisrock DW, Janzen FJ (2000) Comparative molecular phylogeography of North American softshell turtles (*Apalone*): implications for regional and wide-scale historical evolutionary forces. Molecular Phylogenetics and Evolution 14: 152–164.

Wiens JJ (2007) Global patterns of diversification and species richness in amphibians. The American Naturalist 170: S86–S106.

Williams SE, Shoo LP, Isaac JL, Hoffmann AA, Langham G (2008) Towards an integrated framework for assessing the vulnerability of species to climate change. PLoS Biology 6: e325.

Wilson JS, Pitts JP (2012) Identifying Pleistocene refugia in North American cold deserts using phylogeographic analyses and ecological niche modelling. Diversity and Distributions 18: 1139–1152.

Zhang P, Liang D, Mao RL, *et al*. (2013) Efficient sequencing of anuran mtDNAs and a mitogenomic exploration of the phylogeny and evolution of frogs. Molecular Biology and Evolution 30: 1899–1915.

Supplementary

Table IV.S1. Locality information for samples used in this study, including latitude and longitude, sample codes, number of haplotypes, haplogroups and nucleotide diversity in mtDNA sequences, and genetic diversity based on 14 microsatellite loci: Nc = sample size after exclusion of potential siblings from the sample; Na = mean number of alleles per locus; Ho and He = observed and expected heterozygosity; Fis = inbreeding coefficient; Ar = allelic richness; P = private alleles. Locality ID corresponds to Fig. 1b.

ID	Locality	Longitude	Latitude	mtDNA				SSR								
				N	Sample Codes	Haplotypes	Haplogroup	(π)	N	Nc	Na	Ho	He	Fis	Ar	P
1	Tocha, Cantanhede, Coimbra, Portugal	-8.796	40.352	8	IMS3831A, IMS3831F, IMS3832, PC799- PC803	H3, H12	West	0.00029	9	9	2.357	0.315	0.278	-0.145	1.92	0.00004
2	Paramos, Espinho, Aveiro, Portugal	-8.644	40.981	4	PC679-PC682	H3	West	0	19	14	2.5	0.308	0.26	-0.184	1.861	0.00003
3	O Grove, Pontevedra, Spain	-8.874	42.45	4	PC721-PC724	H3	West	0	10	9	1.571	0.179	0.199	0.143	1.5	0
4	Bemposta, Mogadouro, Bragança, Portugal	-6.492	41.326	4	IMS2811-IMS2814	H2, H5	West	0.00057	10	10	2.429	0.271	0.268	-0.013	1.92	0.04123
5	Carpio de Azaba, Salamanca, Spain	-6.609	40.592	4	PC658-PC661	H2	West	0	10	10	3	0.321	0.307	-0.015	2.169	0.03469
6	Valdunciel, Salamanca, Spain	-5.697	41.129	4	IMS3083-IMS3086	H2, H3	West	0.00127	10	7	2.571	0.386	0.375	-0.058	2.215	0.04909
7	Izagre, León, Spain	-5.269	42.218	4	IMS3173-IMS3175, IMS3177	H2	West	0	10	9	1.929	0.34	0.265	-0.218	1.798	0.00469
8	Valdefinjas, Zamora, Spain	-5.467	41.435	4	IMS3117-IMS3120	H2, H6	West	0.00127	10	10	2.786	0.386	0.364	-0.036	2.222	0.03149
9	Aldeaseca de Alba, Salamanca , Spain	-5.46	40.808	4	PC605-PC608	H2, H32, H33	West	0.00127	10	10	2.857	0.414	0.409	-0.015	2.413	0.01809
10	Autilla del Pino, Palencia, Spain	-4.626	41.99	4	IMS3061-IMS3062, IMS3066-IMS3067	H2	West	0	10	10	1.429	0.137	0.108	-0.204	1.34	0.0023

11	Villamayor de los Montes, Burgos, Spain	-3.734	42.095	4	IMS4045-IMS4048	H2, H3, H13	West	0.00172	10	7	2.143	0.364	0.309	-0.146	1.964	0.00104
12	Boceguillas, Segovia, Spain	-3.618	41.33	4	IMS4074-IMS4077	H14	West	0.00115	10	9	2.857	0.343	0.363	0.065	2.414	0.0786
13	Montuenga de Soria, Arcos de Jalón, Soria, Spain	-2.21	41.225	1	IMS2612	H2	West	-	4	4	2.071	0.429	0.326	-0.249	2.071	0
14	Noviercas, Soria, Spain	-2.029	41.713	4	PC821-PC824	H1	East	0	10	9	2.786	0.414	0.425	0.08	2.413	0.00253
15	Fuendetodos, Zaragoza, Spain	-0.932	41.337	7	IMS2294-IMS2296, PC837-PC840	H1	East	0	13	13	3.214	0.473	0.504	0.062	2.657	0.00005
16	Arnedo, La Rioja, Spain	-2.036	42.288	4	IMS3886-IMS3888, IMS3890	H1	East	0	10	7	1.857	0.431	0.336	-0.283	1.896	0.00001
17	Cabanillas, Navarra, Spain	-1.488	42.06	4	IMS3896-IMS3899	H1	East	0	10	10	2.714	0.407	0.386	-0.015	2.281	0.001
18	Plage Biscarrosse, Landes, Aquitaine, France	-1.249	44.457	4	IMS3979-IMS3982	H1	East	0	10	8	1.286	0.086	0.071	-0.17	1.216	0
19	Valflaunes, Hérault, Languedoc-Roussillon, France	3.863	43.847	4	PC905-PC908	H1	East	0	10	7	1.643	0.252	0.184	-0.319	1.556	0.01253
20	Montblanc, Hérault, Languedoc-Roussillon, France	3.355	43.359	4	PC885-PC888	H1, H42	East	0.00057	10	7	1.643	0.164	0.152	-0.083	1.48	0.00637
21	Riudarenes, Girona, Spain	2.718	41.829	4	PC865-PC868	H41	East	0	9	8	1.786	0.346	0.242	-0.425	1.694	0
22	Lleida, Lleida, Spain	0.677	41.524	4	PC845-PC848	H1	East	0	10	10	2.857	0.371	0.368	0.02	2.42	0.04772
23	Tivissa, Tarragona, Spain	0.666	40.988	4	PC926-PC927, PC930- PC931	H1	East	0	8	7	1.5	0.179	0.166	-0.1	1.437	0
24	Banyeres de Mariola, Alicante, Spain	-0.737	38.75	4	IMS3162-IMS3165	H7	East	0	10	8	2.286	0.393	0.411	0.029	2.062	0.00767

ID	Locality	Longitude	Latitude	mtDNA				SSR								
				N	Sample Codes	Haplotypes	Haplogroup	(π)	N	Nc	Na	Ho	He	Fis	Ar	P
25	Sinarcas, Valencia, Spain	-1.239	39.763	4	IMS3329-IMS3332	H1, H3	East, West	0.00115	19	13	3.571	0.492	0.494	0.013	2.661	0.02377
26	La Parroquia, Lorca, Murcia, Spain	-1.943	37.749	3	IMS4385-IMS4387	H1, H15	East	0.00076	10	9	3.143	0.45	0.489	0.08	2.573	0.05304
27	Los Palancares, Cuenca, Spain	-1.984	40.024	3	IMS3349-IMS3351	H1, H9, H10	East, West	0.00382	10	10	2.714	0.521	0.455	-0.116	2.398	0
28	Gárgoles, Cifuentes, Guadalajara, Spain	-2.627	40.74	2	IMS2616, IMS2626	H1 H3	East, West	0.00229	6	5	2.5	0.393	0.387	0.026	2.365	0.07269
29	Bienservida, Albacete, Spain	-2.712	38.55	4	IMS3225-IMS3227, IMS3229	H1, H8, H9	East, West	0.00363	10	10	3.643	0.557	0.501	-0.121	2.761	0.0297
30	Valdemanco, Madrid, Spain	-3.645	40.853	3	PC0901-PC0903	H3, H9	West	0.00153	19	18	3.857	0.417	0.447	0.058	2.47	0.0615
31	Los Escoriales, Andújar, Jaén, Spain	-3.924	38.18	4	PC376-PC379	H20	East	0	10	6	3.071	0.443	0.404	-0.04	2.56	0.00551
32	Malagón, Ciudad Real, Spain	-3.91	39.179	4	PC650-PC653	H3, H35	West	0.00172	8	8	3.286	0.5	0.491	-0.026	2.727	0.03584
33	Cabezarrubias del Puerto, Ciudad Real, Spain	-4.257	38.569	2	IMS3419-IMS3420	H11	West	0	10	9	3.143	0.404	0.365	-0.053	2.321	0.02506
34	Menasalbas, Toledo, Spain	-4.357	39.662	4	PC627-PC630	H1, H3, H34	East, West	0.00268	10	10	3.786	0.475	0.452	-0.064	2.788	0.04154
35	Loja, Granada, Spain	-4.173	37.114	3	PC941-PC943	H1, H21	East, West	0.00306	10	10	2.357	0.379	0.367	-0.045	2.097	0.04284
36	Villanueva del Duque, Córdoba, Spain	-5.007	38.311	4	PC393-PC396	H11, H21,	West	0.00229	10	7	2.714	0.6	0.44	-0.363	2.375	0.04068
37	Navalmoral de la Mata, Cáceres, Spain	-5.547	39.908	4	IMS2799-IMS2802	H3, H4	West	0.00057	10	8	3.214	0.486	0.443	-0.086	2.588	0.01996
38	Malpartida de Cáceres, Cáceres, Spain	-6.505	39.463	4	PC778-PC781	H38, H39	West	0.00115	10	9	3.643	0.571	0.53	-0.073	2.84	0.11135

39	Don Benito, Badajoz, Spain	-5.845	38.962	4	PC585, PC587-PC589	H31	West	0	9	9	2.5	0.406	0.332	-0.191	2.063	0.00039
40	El Pedroso, Sevilla, Spain	-5.785	37.828	4	PC406-PC408, PC410	H1, H21, H22	East, West	0.00382	10	10	3.357	0.5	0.442	-0.134	2.562	0.01986
41	Benalup-Casas Viejas, Cádiz, Spain	-5.767	36.323	4	IMS4415-IMS4418	H16	West	0.00161	10	9	3	0.479	0.487	0.04	2.642	0.09998
42	Valencia de Alcántara, Cáceres, Spain	-7.225	39.444	4	PC808-PC811	H11, H40	West	0.00172	9	5	3.214	0.508	0.418	-0.189	2.883	0.08093
43	Burguillos del Cerro, Badajoz, Spain	-6.64	38.358	4	PC557-PC560	H29, H30	West	0.00306	10	9	2.857	0.443	0.416	-0.062	2.383	0.06092
44	Doñana, Almonte, Huelva, Spain	-6.455	36.989	4	PC700-PC703	H16	West	0	19	13	2.5	0.486	0.427	-0.136	2.136	0.10454
45	Redondo, Évora, Portugal	-7.653	38.65	4	PC737-PC740	H36	West	0.00092	10	7	1.786	0.393	0.27	-0.433	1.743	0.00815
46	Sedas, Espirito Santo, Mértola, Beja, Portugal	-7.599	37.537	4	PC448-PC451	H24, H23, H25, H26	West	0.00325	10	9	3.643	0.464	0.447	-0.017	2.862	0.08492
47	Boticos, Abela, Santiago do Cacém, Setúbal, Portugal	-8.492	38.005	4	PC469-PC472	H3, H23, H27, H28	West	0.00191	19	19	4.786	0.412	0.487	0.126	2.85	0.0316
48	Porto Covo, Sines, Setúbal, Portugal	-8.784	37.86	2	PC934-PC935	H3, H43	West	0.00191	7	7	2.857	0.439	0.413	-0.051	2.825	0.14205
49	Faro, Faro, Portugal	-7.979	37.051	4	PC757-PC760	H37	West	0	10	10	3.714	0.521	0.491	0.024	2.861	0.14931
50	Pataias, Alcobaça, Leiria, Portugal	-9.009	39.681	1	IMS2828	H3	West	-	-	-	-	-	-	-	-	-
51	Évora, Évora, Portugal	-7.928	38.556	1	PC492	H3	West	0.00092	-	-	-	-	-	-	-	-
52	Gaitán, Murcia, Spain	-1.409	38.595	2	M5120-M5121	H1	East	0	-	-	-	-	-	-	-	-
53	Valcárcel, Murcia, Spain	-1.622	38.147	1	M5122	H19	East	-	-	-	-	-	-	-	-	-
54	Tarifa, Cádiz, Spain	-5.618	36.027	2	M40282-M40283	H17, H18	West	0.00161	-	-	-	-	-	-	-	-

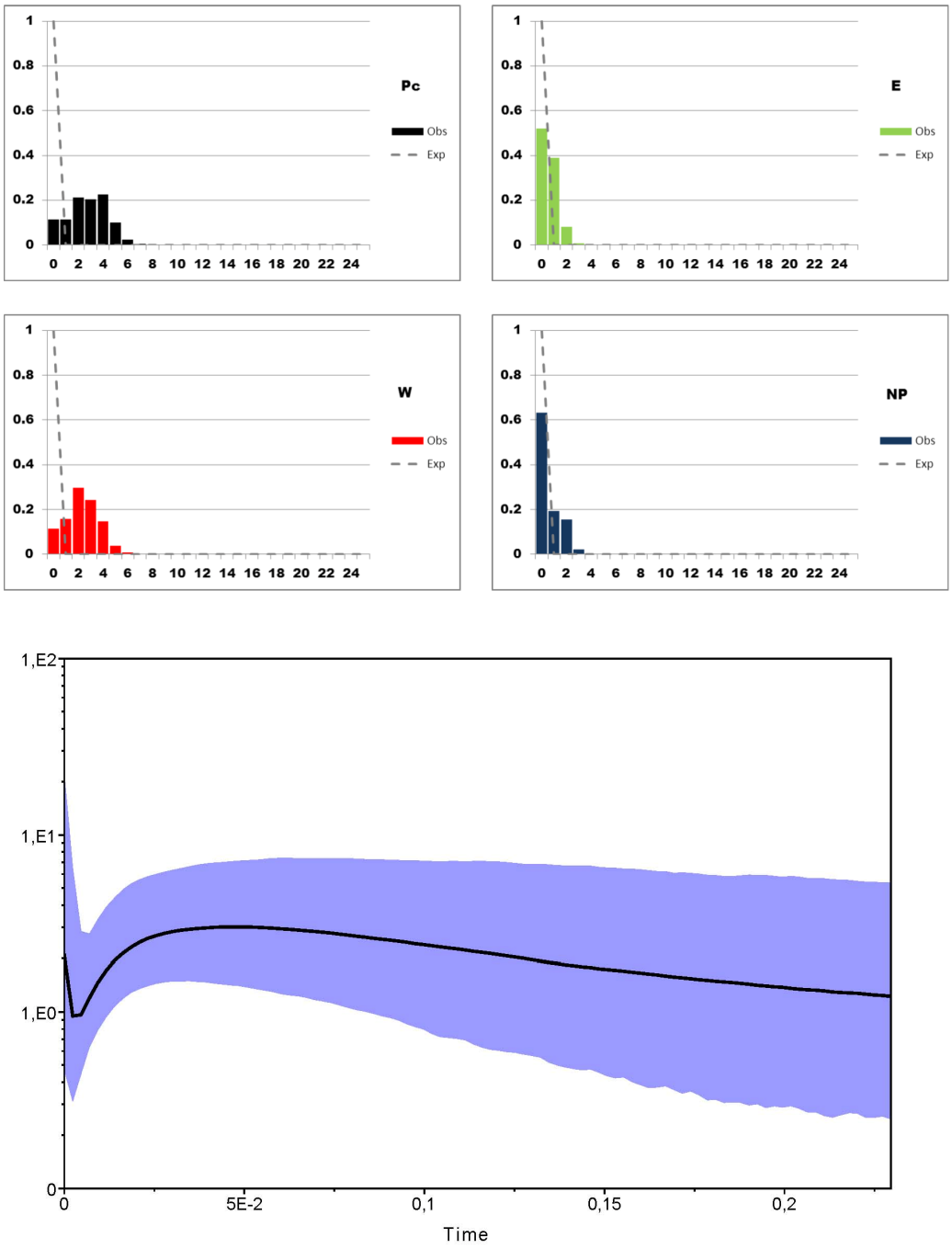

Figure IV.S1. Top: Mismatch distributions (expected vs. observed) for the species (Pc, *Pelobates cultripes*) and the two main haplogroups (East and West) and Northern-Plateau. The number of pairwise differences and their frequencies are shown on the horizontal and vertical axes, respectively. Bottom: Bayesian skyline plot showing changes in effective population size (vertical axis) through time (horizontal axis, in million years) in *P. cultripes*. Note the population decline starting around 25 ka and subsequent recovery about 5 ka.

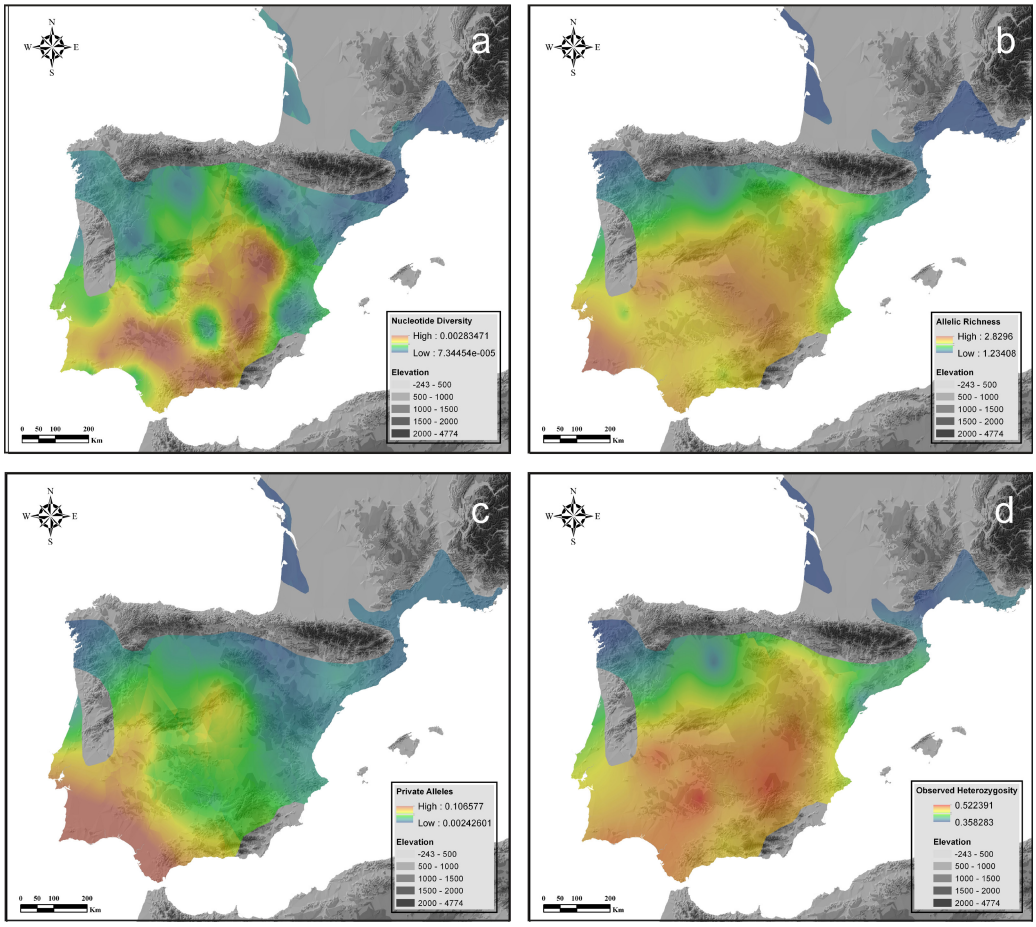

Figure IV.S2. Geographical patterns of genetic diversity in *P. cultripes*, based on: A) Nucleotide diversity, B) Allelic richness, C) Private alleles and D) Observed heterozygosity.

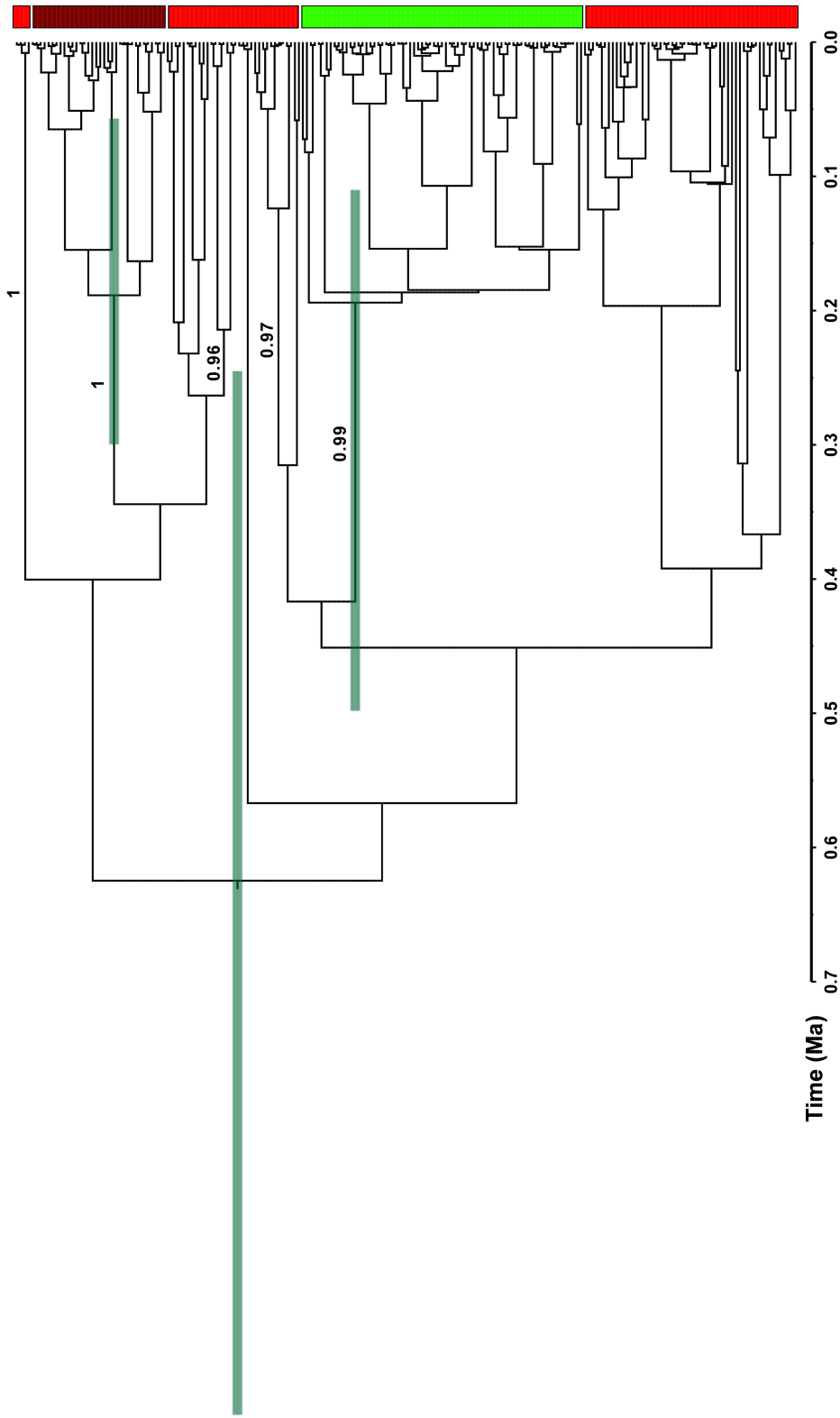

Figure IV.S3. Maximum clade credibility tree (MCCT) recovered in BEAST analyses of ND4 sequences in *P. cultripes*. Horizontal bars represent 95% HPDis for clades of interest. Support values (Bayesian Posterior Probabilities, shown only when >0.95) are shown above nodes. Correspondence with haplogroups in Fig. 1 is represented with vertical bars on the right.

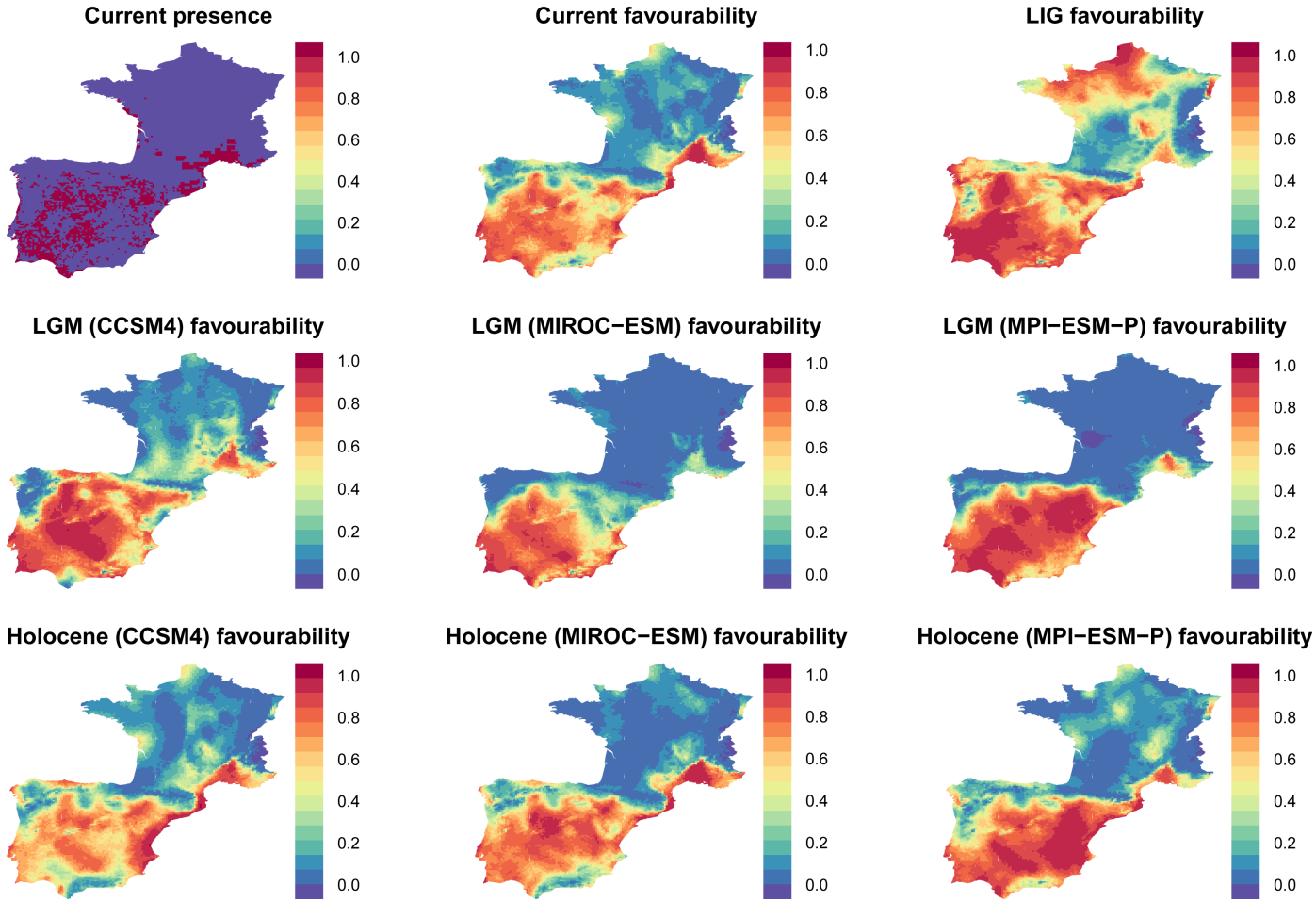

Figure IV.S4. Current distribution of *P. cultripes* on UTM 10x10 km cells, and climatic favourability according to the obtained distribution model, including the present, the Last Inter-Glacial (LIG), and 3 scenarios for the Last Glacial Maximum (LGM) and the Mid-Holocene.

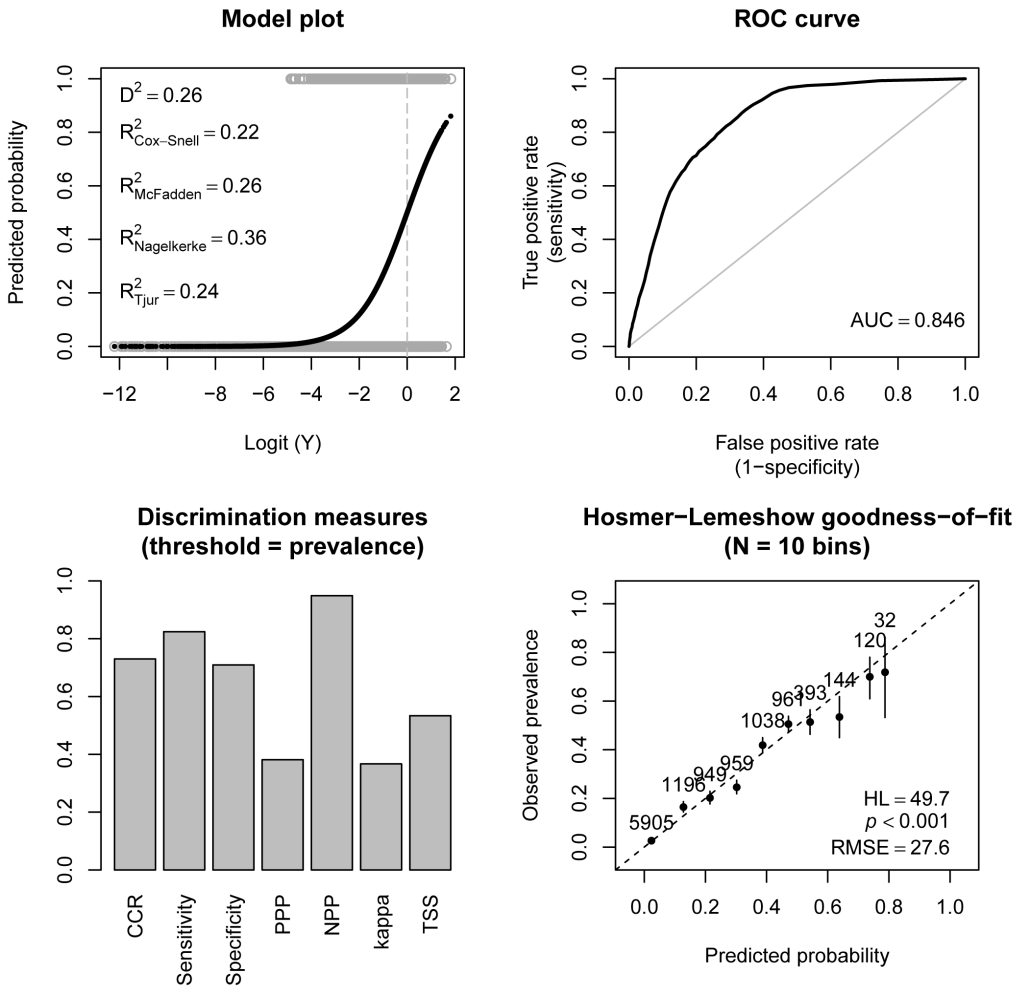

Figure IV.S5. Representation and evaluation of the distribution model built for *P. cultripes*, based on presence-absence on UTM 10x10 km cells of mainland Portugal, Spain and France (N = 11697, 2088 of which were presences). Measures and plots were obtained with the *modEvA* R package (Barbosa *et al*., 2013).

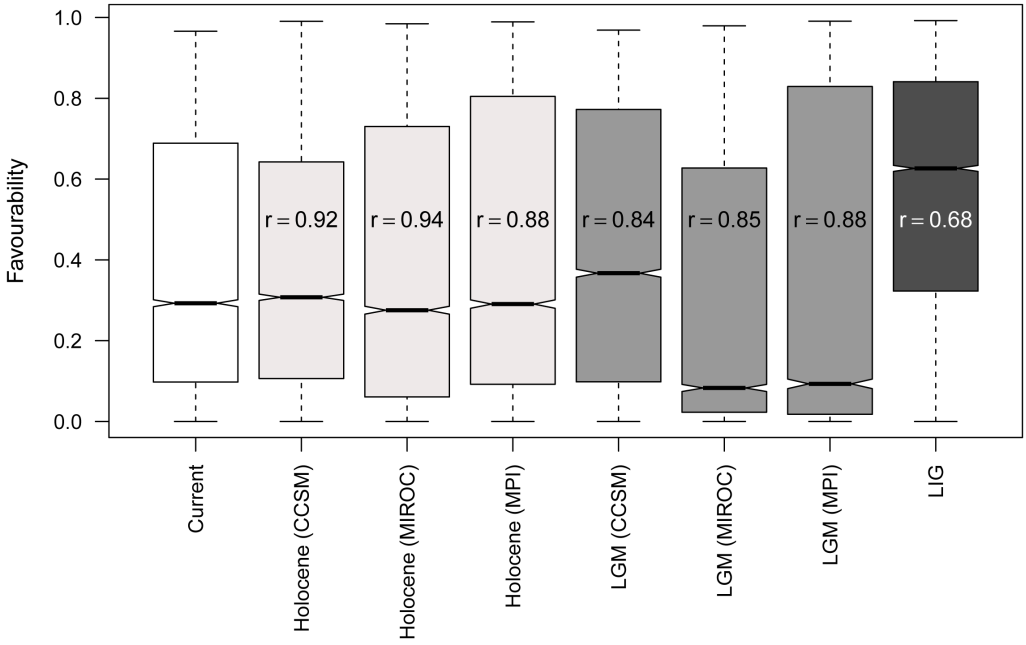

Figure IV.S6. Box plots of climatic favourability for *P. cultripes* under current climate, under three scenarios for the Mid Holocene and the Last Glacial Maximum (CCSM4, MIROC-ESM and MPI-ESM-P), and under the Last Inter-Glacial period (LIG). Darker colours indicate older periods. The values are the coefficients of Pearson's correlation (r) between favourability in each scenario and current favourability ($p < 0.001$ with 11695 degrees of freedom).

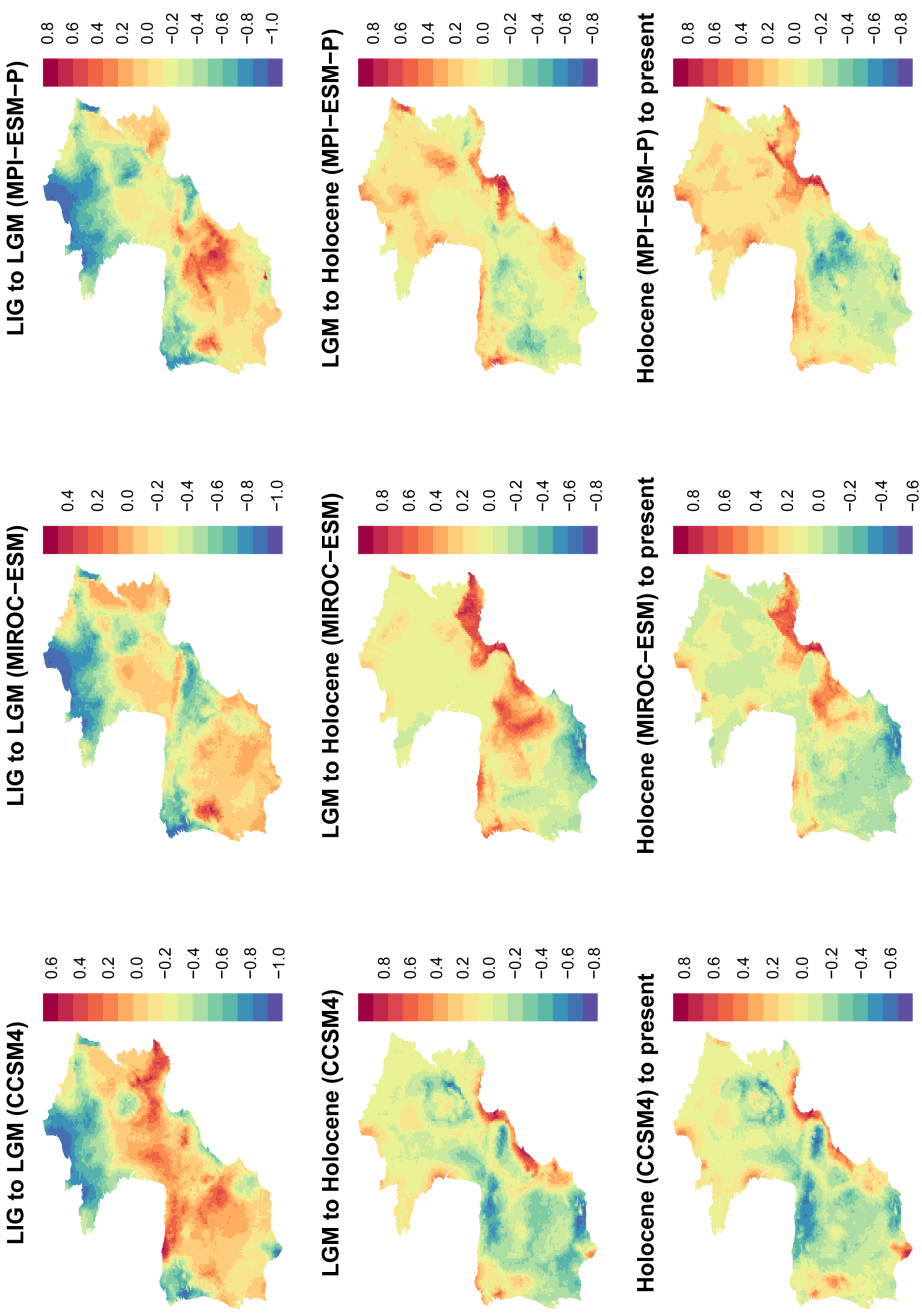

Figure IV.S7. Change (difference) in climatic favourability across the study area between different time periods, from the Last Inter-Glacial (LIG), to the Last Glacial Maximum (LGM), the Mid Holocene and the present, under the three hypothetical scenarios currently available across periods on WorldClim. Positive and negative values indicate increases and decreases in favourability, respectively.

Capítulo III

Escala regional

Artículo V: Genética del paisaje comparada de dos especies de anfibios mediterráneos: el papel favorable de la heterogeneidad estructural en la conectividad poblacional

Comparative landscape genetics of pond-breeding amphibians in Mediterranean temporal wetlands: the positive role of structural heterogeneity in promoting gene flow

J. Gutiérrez-Rodríguez, J. Gonçalves, E. Civantos, I. Martínez-Solano

En Revisión

Molecular Ecology

Abstract

Comparative landscape genetics studies can provide key information to implement cost-effective conservation measures favoring a broad set of taxa. These studies are scarce, particularly in Mediterranean areas, which include diverse but threatened biological communities. Here we focus on Mediterranean wetlands in central Iberia and perform a multi-level, comparative study of two endemic pond-breeding amphibians, a salamander (*Pleurodeles waltl*) and a toad (*Pelobates cultripes*). We genotyped 411 salamanders from 20 populations and 306 toads from 16 populations at 18 and 16 microsatellite loci, respectively, and identified major factors associated with population connectivity through the analysis of three sets of variables potentially affecting gene flow at increasingly finer levels of spatial resolution. Topographic, land use/cover, and remote-sensing vegetation/moisture indices were used to derive optimized resistance surfaces for the two species. We found contrasting patterns of genetic structure, with stronger, finer-scale genetic differentiation in *Pleurodeles waltl*, and notable differences in the role of fine-scale patterns of heterogeneity in vegetation cover and water content in shaping patterns of regional genetic structure in the two species. Overall, our results suggest a positive role of certain vegetation types and structural heterogeneity in population connectivity in pond-breeding amphibians, with habitat patches of Mediterranean scrubland and open oak woodlands ("dehesas") facilitating gene flow. Our study highlights the usefulness of remotely-sensed continuous variables of land cover, vegetation and water content (e.g., NDVI, NDMI) in conservation-oriented studies aimed at identifying major drivers of population connectivity.

Resumen

Los estudios de genética del paisaje comparada pueden proporcionar información clave para implementar medidas efectivas de conservación que favorezcan a un amplio conjunto de taxones. A día de hoy, estos estudios son escasos, particularmente en el área mediterránea, que incluye comunidades biológicas diversas y amenazadas. En este estudio nos hemos centrado en un área en el centro de la península ibérica y hemos llevado a cabo un estudio comparado a varias escalas de dos especies de anfibios endémicas: *Pleurodeles watlt* y *Pelobates cultripes*. Para ello, se genotiparon mediante 16 y 18 microsatélites un total de 411 ejemplares de 20 poblaciones de *P. waltl* y 306 ejemplares de 16 poblaciones de *P. cultripes*. Se identificaron los principales factores asociados a la conectividad poblacional a través del análisis de tres conjuntos de variables que potencialmente afectan al flujo génico a diferentes niveles de resolución espacial. Se encontraron diferentes patrones de estructura genética, siendo más marcada y a una escala más fina de diferenciación genética en *P. waltl*. En el modelado de la estructura genética de las dos especies se observaron similitudes en la influencia de la topografía a escala regional y se encontraron diferencias marcadas en el papel de la heterogeneidad y contenido en agua de la cubierta vegetal a una escala más fina. En general, los resultados sugieren un efecto favorable de ciertos tipos de vegetación y heterogeneidad estructural (principalmente matorral mediterráneo y dehesas) en la conectividad poblacional en ambas especies. Se discuten los resultados en el contexto de las características biológicas de las dos especies de estudio, resaltando la utilidad del uso de variables continuas de cobertura vegetal y contenido de agua (por ejemplo, NDVI, NDMI) en estudios orientados a la conservación que tienen como objetivo identificar los principales factores implicados en los patrones de conectividad poblacional.

Introduction

Comparative landscape genetics studies on co-distributed species have great potential to design cost-effective conservation plans focusing on measures favoring a wider set of taxa, but are still relatively scarce. So far, comparative studies have focused primarily on vertebrates, including amphibians (Richardson, 2012; Zancolli *et al*., 2014; Coster *et al*., 2015), mammals (Muscarella *et al*., 2011; Frantz *et al*., 2012; Dudaniec *et al*., 2016), and fishes (Olsen *et al*., 2011), and more occasionally on invertebrates (Engler *et al*., 2014; Ortego *et al*., 2015; Phillipsen *et al*., 2015). These multi-species studies may allow identifying inter-specific differences in the way landscape features influence connectivity and gene flow and provide general guidelines for land management programs aimed at protecting biological communities or ecosystems (Nicholson & Possingham, 2006; Goldberg & Waits, 2010a; Schwenk & Donovan, 2011; Keller *et al*., 2014). Additionally, by comparing spatial genetic patterns across syntopic species in a shared landscape, important yet often obscure aspects about species life-history traits can be inferred (Steele *et al*., 2009; Goldberg & Waits, 2010a; Richardson 2012; Igawa *et al*., 2013; Kurz *et al*., 2014; Coster *et al*., 2015).

Pond-breeding amphibians are a good study system for comparative landscape genetics studies because they form more or less complex communities of species that use to different extents both terrestrial and aquatic habitats. Due to their low dispersal abilities (Bowne & Bowers, 2004; Graeter *et al*., 2008), small effective population sizes (Funk *et al*., 1999), and the discontinuous distribution of their preferred breeding habitats (Jehle *et al*., 2005) they tend to form "patchy" breeding assemblages. Dispersal and the maintenance of gene flow between breeding ponds depends on the composition and configuration of the landscape (Coster *et al*., 2015), and studies focusing on functional connectivity have described different species responses to landscape features such as differences in soil moisture, clear-cut habitats, agriculture lands, riparian network, as well as differences in metamorphosis, philopatry, dispersal, selection of breeding sites, and post-breeding behavior (Steele *et al*., 2009; Goldberg & Waits, 2010a; Richardson, 2012; Coster *et al*., 2015; Peterman *et al*., 2015). Identification of the factors promoting or reducing gene flow is key to prevent local and regional extinctions in the long-term and to inform conservation management.

Most comparative amphibian landscape genetic studies have focused on North American communities with continental (Goldberg & Waits, 2010a; Richardson, 2012; Coster *et al*., 2015), temperate (Steele *et al*., 2009) or humid subtropical climates (Peterman *et al*., 2015), but little is known about factors shaping regional patterns of gene flow across taxa in Mediterranean wetlands, which are diverse and highly threatened ecosystems (Blondel & Aronson, 1999; Beja & Alcazar, 2003). The effects of unpredictability in hydroperiod, coupled with a continued decline in the number and extent of these wetlands (Doulgeris *et al*., 2016), challenge the survival of their rich amphibian and aquatic invertebrate communities. Assessing comparative patterns of regional gene flow can help in developing integrative management practices that preserve pond-breeding communities with explicit consideration of functional connectivity.

Landscape analysis methods allow simultaneously testing for the relative influence of different factors acting as potential barriers to dispersal at different spatial scales, at an increasingly finer resolution (Wulder *et al*., 2004; Greenberg *et al*., 2005). This allows linking genetic data with different potential response variables and explicitly quantifying the effects of landscape composition, configuration and matrix quality on gene flow and spatial genetic variation (Storfer *et al*., 2007). Here we perform a multi-level, comparative study focusing on two endemic pond-breeding amphibian species that are characteristic of Mediterranean wetlands in the Iberian Peninsula, *Pleurodeles waltl* Michahelles, 1830 and *Pelobates cultripes* (Cuvier, 1829). Both are usually syntopic but probably differ in their use of the available terrestrial and aquatic habitats, although much of their life-history remains little studied. In addition, both are facing a slow but continued decline mostly associated with habitat loss, invasive species and road mortality, and as a consequence they are listed with 'Near Threatened' (NT) status by the IUCN (Beja *et al*., 2009; Beja *et al*., 2016). We compared patterns of genetic diversity and structure and identified the key factors associated with gene flow and population connectivity in both species through the analysis of genotypic data from a suite of highly polymorphic microsatellites in a large sample of individuals of both species in a shared geographic setting.

We explored the relative contribution of landscape features, life-history traits (dispersal, philopatry) and density effects in shaping regional patterns of

genetic structure in the two species. We anticipated land cover-related variables to have a strong impact on population genetic structure in both species, since the study region (near the city of Madrid, central Spain) has experienced major land use changes in the last century (Hewitt & Escobar, 2011). Thus, in addition to maps with discrete land use/cover categories, we incorporated remote-sensing vegetation/moisture indices, which allow for detailed characterization of components of terrestrial habitats at scales relevant for low-dispersing taxa, to derive optimized resistance surfaces. A model ranking approach was then used to identify variables with greater influence on regional patterns of genetic structure.

Methods

Study area and sampling

The study area is bounded by -4.136º to -3.296º longitude and 40.131º to 41.416º latitude (Fig. V.1). Elevation ranges from 482 m up to 2403 m a.s.l. The two species are widely distributed in the study area, but their populations are fragmented due to the continued loss of terrestrial and aquatic habitats (Martínez-Solano, 2006).

We sampled 306 individuals of *P. cultripes* and 411 of *P. waltl* at 16 and 20 ponds, respectively (Fig. V.1, Table V.1). Average geographic distances between populations for both species were similar and ranged from 0.7 to 40 km between the closest sampled populations (Fig. V.1; Tables V.S1 and V.S2). The scale of analysis reflects uncertainty about actual dispersal potential in both species but includes minimum estimates of adult dispersal (700 meters) based on capture-mark-recapture studies (Gutiérrez-Rodríguez *et al*., 2017a). Tissues were obtained from tail tips of larvae (most samples) and toe clips of adults (only the *P. waltl* samples from populations W4 and W17). All sampled individuals were released back in their place of capture after sample collection.

Genetic analyses

Genomic DNA was extracted using NucleoSpin Tissue-Kits (Macherey-Nagel). A total of 16 previously characterized microsatellite markers for *P. cultripes* were amplified following the PCR conditions described in Gutiérrez-Rodríguez and Martínez-Solano (2013). For *P. waltl*, 18 previously published loci (van de Vliet

Table V.1. Locality information and genetic diversity estimates for sampled *Pelobates cultripes* (C) and *Pleurodeles waltl* (W) populations: N = sample size; Nc = sample size after exclusion of potential siblings from the sample; Na = mean number of alleles per locus; Ho: observed heterozygosity; He = expected heterozygosity; Fis = inbreeding coefficients; Nb = effective number of breeders.

ID	Locality	Longitude	Latitude	N	Nc	Na	Ho	He	Fis	Nb
C1	Segovia, Boceguillas	-3.618	41.330	10	9	2.857	0.341	0.364	0.121	30 (11-inf)
C2	Madrid, Buitrago de Lozoya	-3.644	40.974	20	16	2.857	0.341	0.362	0.088	68 (33-660)
C3	Madrid, Canencia, Prado Toril	-3.800	40.859	20	12	1.429	0.190	0.159	-0.154	17 (8-92)
C4	Madrid, Valdemanco	-3.645	40.853	19	18	3.786	0.437	0.460	0.080	68 (31-312)
C5	Guadalajara, El Cubillo de Uceda	-3.451	40.795	19	13	3.571	0.455	0.419	-0.043	23 (12-48)
C6	Madrid, El Vellón	-3.586	40.773	20	18	3.714	0.452	0.447	0.017	76 (35-528)
C7	Madrid, Guadalix de la Sierra, Medianillos	-3.676	40.756	20	15	3.786	0.367	0.380	0.070	38 (20-90)
C8	Madrid, Algete, Salomón	-3.561	40.648	18	14	3.286	0.436	0.410	-0.027	44 (21-150)
C9	Madrid, Colmenar Viejo	-3.786	40.628	20	14	3.857	0.413	0.407	0.021	54 (28-137)
C10	Madrid, Hoyo de Manzanares	-3.916	40.613	20	14	1.786	0.352	0.296	-0.151	16 (8-38)
C11	Madrid, Las Rozas	-3.923	40.509	20	16	3.786	0.424	0.427	0.039	54 (29-147)
C12	Madrid, Getafe, Camino de Preresa	-3.596	40.303	20	14	2.643	0.352	0.358	0.054	20 (10-43)
C13	Madrid, Fuenlabrada, Valdehondillo	-3.801	40.261	20	16	3.714	0.531	0.493	-0.045	42 (23-97)
C14	Madrid, Fuenlabrada, Camino de las Panaderas	-3.800	40.255	20	17	3.643	0.492	0.480	0.006	38 (20-105)
C15	Madrid, Batres, Soto del Endrinal	-3.950	40.238	20	16	2.286	0.330	0.323	0.009	27 (15-59)
C16	Madrid, Griñón, Cerro del Rayo	-3.821	40.223	20	18	4.143	0.552	0.526	-0.020	95 (45-752)
W1	Segovia, Santo Tomé del Puerto	-3.589	41.200	20	20	2.824	0.476	0.478	0.028	127 (55-Inf)
W2	Madrid, Gascones	-3.651	41.012	20	20	3.235	0.529	0.518	0.003	127 (55-inf)
W3	Madrid, Buitrago de Lozoya	-3.644	40.975	20	9	2.941	0.458	0.439	0.017	15 (7-32)
W4	Madrid, Bustarviejo, Fuente del Collado	-3.724	40.855	20	17	3.765	0.550	0.517	-0.034	76 (34-522)
W5	Madrid, Valdemanco	-3.645	40.853	33	28	5.118	0.610	0.583	-0.028	151 (86-428)
W6	Madrid, Torrelaguna	-3.573	40.830	20	12	2.647	0.490	0.456	-0.030	25 (14-50)

W7	Guadalajara, El Cubillo de Uceda	-3.451	40.795	20	17	4.059	0.578	0.596	0.060	95 (45-Inf)
W8	Madrid, El Vellón, Cotos de Monterrey	-3.603	40.786	20	14	4.059	0.558	0.595	0.101	29 (16-62)
W9	Madrid, El Vellón	-3.586	40.773	20	16	3.765	0.563	0.547	0.004	54 (29-163)
W10	Madrid, Guadalix de la Sierra, Medianillos	-3.676	40.756	18	16	4.588	0.652	0.593	-0.067	153 (55-Inf)
W11	Madrid, Colmenar Viejo	-3.786	40.628	20	17	4.353	0.612	0.603	0.015	95 (48-851)
W12	Madrid, Hoyo de Manzanares, La Berzosa	-3.928	40.603	20	18	4.471	0.592	0.573	-0.004	127 (57-inf)
W13	Madrid, Las Rozas	-3.923	40.509	20	18	3.824	0.526	0.526	0.028	95 (45-662)
W14	Madrid, Brunete	-4.000	40.413	20	16	3.765	0.500	0.533	0.094	42 (20-115)
W15	Madrid, San Fernando de Henares, La Guindalera	-3.504	40.409	20	17	3.059	0.554	0.504	-0.068	54 (27-180)
W16	Madrid, Fuenlabrada, Valdehondillo	-3.801	40.261	20	17	3.941	0.522	0.542	0.067	127 (57-Inf)
W17	Madrid, Fuenlabrada, Camino de las Panaderas	-3.800	40.255	20	19	4.000	0.563	0.560	0.021	76 (39-268)
W18	Madrid, Morata de Tajuña	-3.408	40.241	20	17	2.059	0.353	0.320	-0.066	27 (14-66)
W19	Madrid, Parla, Sancha Barca	-3.793	40.239	20	19	4.235	0.554	0.569	0.052	127 (58-Inf)
W20	Madrid, Griñón, Cerro del Rayo	-3.821	40.223	20	19	3.353	0.495	0.489	0.013	48 (26-117)

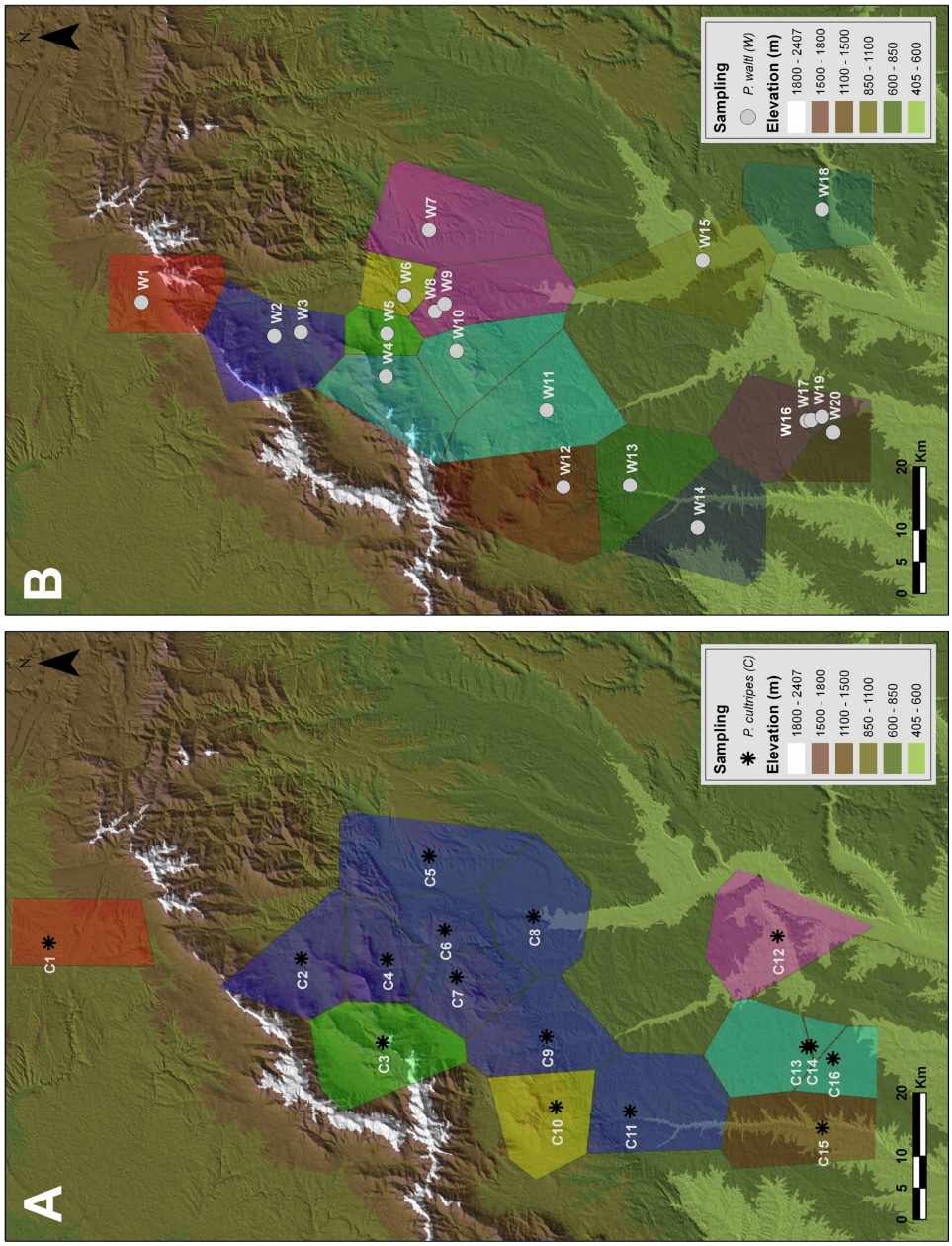

Figure V.1. Sampling locations for the two study species: *P. cultripes* (A) and *P. waltl* (B). Results of the optimal number of clusters for each species according to BAPS are also shown.

et al., 2009; Gutiérrez-Rodríguez *et al*., 2014) were grouped into six multiplex reactions (multiplex 1: Pleu2.3, Pleu2.19, Pleu2.34; multiplex 2: Pleu2.16, Pleu2.31, Pleu3.2; multiplex 3: Pleu3.5, Pleu4.1; multiplex 4: Ppl2, Ppl3, Ppl5; multiplex 5: Ppl1, Ppl12, Ppl13, Ppl14; and multiplex 6: Ppl6, Ppl7, Ppl10). PCR conditions and genotype calling followed Gutiérrez-Rodríguez *et al*. (2014).

The presence of possible null alleles, stuttering and large allele dropout was tested in microsatellite markers using MICROCHECKER v2.2.3 (van Oosterhout *et al*., 2004), with a 99% confidence interval and 1,000 randomizations. Since including sibs and half sibs in population samples can introduce undesired biases in the analyses (Goldberg & Waits, 2010b), we conducted genetic parentage analyses with software COLONY v2.0.5.1 (Jones & Wang, 2010). These analyses were carried out assuming a monogamous mating system for both sexes, with the full-likelihood method (Wang, 2004). Analyses consisted of ten independent runs, with medium-length likelihood precision and updated allele frequencies, and individuals identified as full-siblings with a probability of 0.8 or higher were discarded from subsequent analyses.

We tested for deviations from Hardy-Weinberg equilibrium (HWE) and evidence of linkage disequilibrium (LD) with the software GENEPOP (http://genepop.curtin.edu.au/; Raymond & Rousset, 1995; Rousset, 2008). The Markov chain was run with 10,000 dememorization steps, 1,000 batches and 10,000 iterations per batch. We applied the sequential Bonferroni correction (Rice,1989) to adjust significance values for multiple tests. Different estimates of genetic diversity were calculated for each population using GENALEX v6.5b5 (Peakall & Smouse, 2012), including the number of alleles (Na), observed (Ho) and expected heterozygosity (He). We also calculated the inbreeding coefficient (Fis) because it is an indirect measure of philopatry (more philopatric species will in principle have higher Fis values). The effective number of breeders (Nb) was also calculated with COLONY software.

The genetic structure of the populations was assessed with Bayesian spatial clustering methods, using program BAPS v6 (Corander *et al*., 2008; Cheng *et al*., 2013). We ran spatial genetic mixture analyses, with ten independent runs and a maximum number of groups equal to the number of sampled localities. Clusters resulting from each replicate run were compared based on their likelihood score

and the optimal clustering level was identified based on a stochastic optimization algorithm (Corander *et al*., 2008).

We calculated three estimates of genetic differentiation between populations, Fst (Weir & Cockerham, 1984), G''st (Meirmans & Hedrick, 2011) and Dest (Jost, 2008) using Genepop, GENODIVE v2.0b23 (Meirmans & van Tienderen, 2004) and SMOGD v1.2.5 (Crawford, 2010), respectively, to compare patterns of regional genetic structure across species and characterize genetic differentiation between populations. We used software CODIDI v1.0 (Wang, 2015) to determine if G''st provides an accurate estimate of genetic differentiation in our study. Analyses were carried out using with 100,000 permutations. We also estimated recent migration rates between localities using the software BAYESASS v3.0 (Wilson & Rannala, 2003). Three different replicates were run for each species with 50,000,000 iterations, a burn-in period of 2,000,000 and sampling frequency each 2000. We assessed convergence of results across runs and used those with the best likelihood in subsequent analyses.

Input data used for resistance surfaces and pre-processing

During pre-processing all raster variables were aggregated to a spatial resolution of 100m to make the optimization of resistance surfaces tractable and with the same raster support characteristics. Elevation data was obtained from ASTER Global Digital Elevation Model (GDEM v2; Tachikawa *et al*., 2011) with a spatial resolution of 30m later resampled to 100m (bilinear method). Percent slope, describing surface roughness, was calculated from elevation data and also the Topographic Wetness Index (TWI) describing the tendency of a cell to accumulate water (Quinn *et al*., 1995). Elevation, slope and TWI were all hypothesized as potential factors for explaining gene flow and genetic differences between sampled populations at a coarser regional scale (Table V.2).

Land use/cover (LUC) considering both composition (the amount of certain land cover categories) and configuration (referring mainly to the spatial distribution and diversity of land cover types) have been hypothesized to impact connectivity, species movements and gene flow (Pérez-Espona *et al*., 2008) at the landscape level. To assess this, two land use/cover datasets were used to derive resistance surfaces and test the effect of landscape matrix composition. The first

Table V.2. Input variables used to calculate resistance surfaces by level and data source. Summary statistics in brackets: minimum (min), average (avg), maximum (max) and standard-deviation (std).

Level	Variable acronym	Description	Source
Regional	elev	Elevation (meters a.s.l; min: 482.0, avg: 935.0, max: 2403.0, std: 326.1)	USGS/ASTER GDEM
	slope	Slope (%; min: 0.0, avg: 9.4, max: 121.2, std: 10.4)	
	twi	Topographic wetness index (unitless; min: 2.9, avg: 7.0, max: 12.6, std: 1.2)	
Local	clc06	Corine Land Cover class for year 2006 (15 classes)	EEA
	siose05	SIOSE 2005 Land cover class (resistance weights, unitless; min: 0.0, avg: 12.7, max: 100.0, std: 26.3)	CNIG/Spain
	rdens	Road density (m/ha; min: 0, avg: 27.5, max: 1272.5, std: 26.3)	
Habitat	ndvi_avg	Normalized Difference Vegetation Index (spatial average from 30m to 100m; vegetation biomass/greenness amount; $\times 10^{-4}$, unitless, min: -3013, avg: 3652, max: 8971, std: 1723)	Landsat 5 TM USGS/ESPA
	ndvi_std	Normalized Difference Vegetation Index (spatial standard-deviation from 30m to 100m; vegetation heterogeneity; $\times 10^{-4}$, unitless, min: 0, avg: 429, max: 5503, std: 310)	
	ndmi_avg	Normalized Difference Moisture Index (spatial average from 30m to 100m; vegetation water content; $\times 10^{-4}$, unitless, min: -4976, avg: -335, max: 5613, std: 1413)	
	ndmi_std	Normalized Difference Moisture Index (spatial standard-deviation from 30m to 100m; vegetation water content heterogeneity; $\times 10^{-4}$, unitless, min: 10, avg: 385, max: 3862, std: 277)	

dataset, Corine Land Cover (CLC), for 2006 with a spatial resolution of 100m, was used as a categorical map in optimization procedures to derive a resistance surface accounting for the different resistance of each land cover category. This dataset was previously reclassified from the original 30 classes into 15 broader categories (Table V.S3) to make it tractable by *ResistanceGA* package (Peterman 2014; Peterman *et al*., 2014); which allows a maximum of 15 categories. Given that CLC is a hierarchic dataset, we maintained some relevant classes maximally disaggregated (e.g., different types of vegetated areas), while others were merged into their broader supra-category (e.g., similar types of impervious or artificial areas).

A second fine-scale LUC dataset, SIOSE (Sistema de Información sobre Ocupación del Suelo de España), available from the Spanish Centro Nacional de Información Geográfica for year 2005 (CNIG; URL: http://centrodedescargas.cnig.es), was used for deriving a continuous resistance surface. Due to the large number of initial classes in the dataset (totaling 116) a reclassification was performed (with 54 aggregated new classes) based on similarities between classes. From the reclassified data, a total of 29 classes were found in the study area. An aprioristic resistance weight was initially attributed to each class reflecting the increased resistance to amphibian movement and higher mortality rates associated with artificial (urban habitats, roads) vs natural land cover/use classes observed in our study area (Martínez-Solano, 2006; see initial weights in Table V.S5). These a priori weights were later transformed by the resistance surface optimization procedure (see subsection below) to better reflect land use effects. Since SIOSE data also provides composite/multiclass patches with a proportion given for each class represented in a given patch, the total resistance weight of each LUC patch (t) was given by: $t = \sum p_c w_c$, with p_c, equal to the proportion of class c in the patch and w_c, equal to the weight attributed to that class (Tables V.S4 and V.S5).Values at patch-level were then averaged for each pixel at 100m.

Roads have also been hypothesized to impact species mortality, movements and gene flow (Pérez-Espona *et al*., 2008). Considering this, linear road data by Spanish Provinces were obtained from the Centro Nacional de Información Geográfica (CNIG; URL: http://centrodedescargas.cnig.es) and was used to calculate total road density for each 100m pixel (m/ha) in the study area.

Finally, the amount and spatial heterogeneity of vegetation cover and vegetation water content (VWC) were also hypothesized to affect genetic differentiation. Thus, pre-processed remote sensing image data for the Landsat 5 TM sensor, with a spatial resolution of 30m, were downloaded from the USGS/ESPA service (URL: http://espa.cr.usgs.gov/). One scene for each month of June, August and September 2009, coinciding with field surveys, was used to generate a single average composite image. The Normalized Difference Vegetation Index (NDVI), extensively used in ecological applications (Turner *et al*., 2003; Nagendra *et al*., 2013) was used to provide a continuous measure related to vegetation canopy characteristics such as biomass, leaf area index and percentage

of vegetation cover. This index varies from -1 (non-vegetated/artificial surfaces) to 1 (densely vegetated areas). Complementarily, the Normalized Difference Moisture Index (NDMI) was employed to characterize vegetation water content (VWC; Gao, 1996). NDMI also varies from -1 (indicative of low VWC) to 1 (high VWC).

Image data was aggregated to 100m to match the same spatial resolution of topographic and land cover data using the average (defining the amount of vegetation cover and VWC), and also, the standard-deviation (translating the spatial heterogeneity of vegetation cover and VWC).

Statistical modelling and resistance surface optimization

To assess the relative support of each variable to explain differences in patterns of genetic structure between sampled populations of *P. cultripes* and *P. waltl* we used the *ResistanceGA* package (Peterman 2014; Peterman *et al*., 2014) implemented in R v3.0.3 (R Core Team, 2014). This package implements a genetic algorithm that optimizes a set of equation parameters used to transform the initial values of each variable into resistance surfaces. This optimized surface is then used to calculate cost-based distances between sampled locations through least-cost path analyses using *gdistance* package (van Etten, 2015). A linear mixed effects model with the maximum likelihood population effects (MLPE) parameterization (Clarke *et al*., 2002) was used to relate the genetic and the cost-based distance matrices and to calculate the model Akaike Information Criterion (with a correction for finite sample size; AICc). The AICc value is the fitness function output used for iteratively improving the genetic algorithm. The MLPE allows accounting for the non-independence of values within pairwise distance matrices (Clarke *et al*., 2002; van Strien *et al*., 2012) and was fitted by maximum likelihood using R package *lme4* (Bates *et al*., 2014).

Pairwise genetic distances (measured by Fst, G’’st, and Dest), as well as migration rates between populations were used as the response variable, while scaled and centered effective cost-based resistance distances between populations were considered the independent variable. A maximum number of 250 rounds, or 20 rounds without performance improvement, were used by the genetic algorithm to determine the best set of parameters for optimizing the resistance surfaces.

We also used estimates of the effective number of breeders (Nb) as surrogates for species abundance and analyzed them using the same MLPE model with the expectation that larger populations will have higher net migration rates with neighboring populations (expressing a density-dependent effect), and thus inclusion of this variable may partially explain patterns of regional genetic structure in the two species. We implemented this analysis using Nb estimates from Colony and calculated a distance matrix based on index $I_{i,j}$' (Eqn. 1) taking values for each population pair i and j according to the equation:

$$I_{i,j}' = 1 / (Nb_i + Nb_j) \text{ (Eqn. 1)}$$

where the values between two populations would get smaller as the population sizes get larger. A second index, $I_{i,j}$'', (Eqn. 2) of similar characteristics but accounting for the distance between populations was also calculated. Our expectation was that if a density-dependent effect exists then net migration rates (triggered by this effect) would reflect more on closer populations than on distant ones.

$$I_{i,j}'' = D_{i,j} / (Nb_i + Nb_j) \text{ (Eqn. 2)}$$

Finally, to evaluate model performance, we compared AICc values between models generated with each optimized resistance surface to two baseline null-models: one based on a single intercept-term (IntOnly) and other including only Isolation-by-distance (IBD) effects. Each model was then ranked based on delta AICc values (ΔAICc) considering the confidence set determined by models with substantial or good support, i.e. with ΔAICc≤4. Akaike weights (wi) were calculated to quantitatively represent the strength of evidence or support of each tested model.

Dispersal distance estimation

The estimation of dispersal distance was based on Peterman *et al*. (2014). It starts by calculating the geometric mean of all pairwise Fst values to obtain a

unique, population-specific Fst value for each population (Eqn. 3) that represents the differentiation of a focal population to all other populations (Gaggiotti & Foll, 2010; Pflüger & Balkenhol, 2014). Then a connectivity index is calculated (Eqn. 4) which is based on the assumption that genetic connectivity is uniquely dependent on the distance between populations.

$$Fst_i = \frac{N}{\sum_{\substack{i=1 \\ if\ i \neq j}}^{N} \left(\frac{1}{Fst_{i,j}}\right)} \text{ (Eqn. 3)}$$

$$S_i = \sum_{if\ i \neq j} e^{(-k \cdot d_{i,j})} = \sum_{if\ i \neq j} e^{(-D^{-1} \cdot d_{i,j})}\,;\, k = \frac{1}{D} \text{ (Eqn. 4)}$$

$$O = \frac{1}{N} \sum_{i=1}^{N} (Fst_i - S_i)^2 \text{ (Eqn. 5)}$$

In Eqn. 4 $d_{i,j}$ equals the Euclidean distance between focal population *i* and other populations *j* summed across all populations (if $j \neq i$). The *k* is a scaling parameter equal to $k = 1/D$ where *D* is equal to the average dispersal distance (Moilanen & Nieminen, 2002). Since *D*, is unknown for both species we estimated it based on our data. To accomplish this, Brent's optimization algorithm implemented in R was used with an objective function (defined as *O*; Eqn. 5) expressing the average square sum of errors between the population-specific Fst and connectivity index estimates (Eqn. 5). The optimization routine was then used to minimize the result of the objective function, *O* by optimizing the average dispersal distance parameter. A bootstrap procedure (with 10 000 replicates) was implemented to estimate the average dispersal distance and 95% confidence intervals.

Results

Genotypes were amplified with a success rate of >99% for both species. Based on MICROCHECKER results, two microsatellite loci (Pc4.7 and Pc4.11) were discarded in *P. cultripes*, because of the possible presence of null alleles. In *P. waltl*, locus Pleu2.3 was monomorphic in all samples analyzed and was thus discarded. Sibship analyses in COLONY detected a low proportion of full-sibs in both species (see Table V.1), which were subsequently removed from the dataset,

leaving one representative per sibship group. No significant deviations from HWE and LD were detected, except in locus Pleu3.5 in Pop14 (Brunete) in *P. waltl*, which showed evidence of heterozygote deficit.

Descriptive statistics of genetic diversity for *P. cultripes* and *P. waltl* are shown in Table V.1. Estimates of genetic diversity were slightly higher in *P. waltl*. The mean number of alleles per population ranged from 1.43 (Pop3) to 4.14 (Pop16) in *P. cultripes* and from 2.06 (Pop18) to 5.12 (Pop5) in *P. waltl*. The observed heterozygosity ranged from 0.19 (Pop3) and 0.55 (Pop16) in *P. cultripes*, and from 0.35 (Pop18) to 0.65 (Pop10) in *P. waltl*. Average population inbreeding coefficients (Fis) were higher in *P. waltl* (0.01) than in *P. cultripes* (0.004). Estimates of the effective number of breeders (Nb) also differed among populations and species, with values between 16 to 95 in *P. cultripes* and 15 to 153 in *P. waltl* (Table V.1). Mean values of Nb were higher (almost double on average) in *P. waltl* (Nb= 83) than in *P. cultripes* (Nb=43).

The results of BAPS analyses supported optimal clustering levels at K=13 and K=7 for *P. waltl* and *P. cultripes*, respectively (Fig. V.1). The number of clusters was consistent across replicate runs. In *P. waltl*, inferred clusters included geographically close sampling locations, such as clusters (W2+W3), (W4+W10+W11), (W7+W8+W9), and (W16+W17+W19), whereas in *P. cultripes* some clusters included larger groups of populations, especially one cluster including locations: (C2+C4+C5+C6+C7+C8+C9+C11), distributed across medium elevations at the foothills of Sierra de Guadarrama, and the cluster (C13+C14+C16) in the south of our study area. This is consistent with resistance surfaces, where these areas generally show low resistance / higher connectivity (see below). Overall, there are clear differences between species, with a stronger signal of geographic structure in *P. waltl* (Fig. V.1).

Pairwise estimates of Fst, G''st, and Dest between populations of each species are presented Tables V.S6 to V.S11. Lower average values, indicating greater population connectivity, were found in *P. cultripes* (Fst = 0.117; G''st = 0.192; Dest = 0.044) than in *P. waltl* (Fst = 0.187; G''st = 0.402; Dest = 0.184). Analyses with CODIDI did not detect significant negative correlations between diversity (Hs) and G''st in either species (*P. cultripes*: r = 0.20, p = 0.73; *P. waltl*: r = -0.21, p = 0.21), indicating G''st estimates accurately describe population

differentiation and are comparable across species.

BAYESASS results indicate low migration rates across sites, except among geographically close localities (Tables V.S12 and V.S13), with higher average migration rates between populations of *P. cultripes* (mean = 0.0179) than in populations of *P. waltl* (mean = 0.0126).

Multi-model selection and ranking

For *P. cultripes* optimization and model selection showed similar and congruent results with low model uncertainty when comparing rankings obtained for distance matrices based on Dest, Fst and G''st (Table V.3). For this species, average NDVI (related to vegetation amount) was the most frequently selected variable for all distance matrices. Topographic variables related to elevation (selected for Dest matrix) and slope (selected for Fst and G''st distance matrices) were also important to explain genetic differentiation in *P. cultripes*.

Regarding *P. waltl* model selection also showed similar and coherent results with low model uncertainty across different genetic distances. For this species, spatial heterogeneity of vegetation (ndvi_std) and spatial heterogeneity in vegetation water content (ndmi_std), were the most frequently selected variables. These attained very high model support being selected for all genetic distances (Table V.3). Topographic resistance surfaces related to elevation (selected for Dest and Fst matrices) and slope (selected for Fst matrix) were also important to explain genetic differentiation for *P. waltl*.

For both species models related to landscape composition and structure (siose05) or road density showed very little to no support in explaining genetic differentiation (Table V.3). Overall, for both species and considering all genetic distance matrices, the IBD and the intercept-only models attained no relative support, showing a good relative performance of resistance surfaces to explain gene flow patterns. Likewise, we found no support for density-dependent effects on regional patterns of gene flow based on the analyses of our two indices (i.e., $I_{i,j}$', and $I_{i,j}$') based on Nb estimates (Table V.S14).

Overall, model selection results for migration rates (Table V.4) showed a strong coherence with model rankings obtained for genetic distance metrics. For *P. cultripes* average NDVI attained the largest support; for this species both the IBD

Table V.3. Model selection table for species *P. cultripes* (left) and *P. waltl* (right). Models highlighted in bold attained the highest relative support and were included in the confidence set (ΔAICc≤4). AICc – Akaike Information Criterion value (with a correction for finite sample size), ΔAICc – delta AIC value, wi – Akaike weights. IBD – Isolation-by-distance model. IntOnly – Intercept-only/null model.

Genetic distance metric	*Pelobates cultripes*				*Pleurodeles waltl*			
	Variable	**AICc**	**ΔAIC**	**wi**	**Variable**	**AICc**	**ΔAIC**	**wi**
Dest	**elev**	**-578.90**	**0.00**	**0.47**	**ndvi_std**	**-522.71**	**0.00**	**0.52**
	ndvi_avg	**-578.72**	**0.18**	**0.43**	**elev**	**-521.95**	**0.75**	**0.36**
	ndmi_avg	-573.38	5.52	0.03	**ndmi_std**	**-519.76**	**2.95**	**0.12**
	slope	-573.37	5.54	0.03	rdens	-511.89	10.81	0.00
	twi	-570.84	8.06	0.01	slope	-511.23	11.47	0.00
	ndmi_std	-570.48	8.43	0.01	twi	-509.96	12.74	0.00
	ndvi_std	-570.09	8.82	0.01	ndvi_avg	-508.57	14.14	0.00
	siose05	-569.66	9.24	0.00	siose05	-502.84	19.87	0.00
	rdens	-569.58	9.33	0.00	IBD	-502.24	20.46	0.00
	IntOnly	-569.46	9.44	0.00	ndmi_avg	-502.09	20.62	0.00
	clc06	-568.84	10.06	0.00	clc06	-488.00	34.70	0.00
	IBD	-567.70	11.20	0.00	IntOnly	-387.81	134.90	0.00
Fst	**ndvi_avg**	**-495.08**	**0.00**	**0.59**	**ndvi_std**	**-646.58**	**0.00**	**0.63**
	slope	**-492.48**	**2.60**	**0.16**	**slope**	**-643.24**	**3.35**	**0.12**
	twi	-490.29	4.79	0.05	**ndmi_std**	**-642.69**	**3.89**	**0.09**
	siose05	-490.29	4.80	0.05	**elev**	**-642.45**	**4.14**	**0.08**
	elev	-489.90	5.18	0.04	rdens	-641.74	4.84	0.06
	ndmi_std	-489.85	5.23	0.04	twi	-638.87	7.72	0.01
	rdens	-488.20	6.88	0.02	ndvi_avg	-638.44	8.14	0.01
	ndvi_std	-488.10	6.98	0.02	siose05	-636.99	9.60	0.01
	ndmi_avg	-487.73	7.35	0.01	clc06	-629.92	16.66	0.00
	IBD	-484.04	11.04	0.00	ndmi_avg	-624.61	21.98	0.00
	IntOnly	-482.72	12.36	0.00	IBD	-624.42	22.16	0.00
	clc06	-479.98	15.10	0.00	IntOnly	-516.03	130.55	0.00
G”st	**ndvi_avg**	-383.78	0.00	0.77	**ndvi_std**	**-364.56**	**0.00**	**0.74**
	slope	-381.21	2.57	0.21	**ndmi_std**	**-361.18**	**3.38**	**0.14**
	twi	-375.35	8.44	0.01	rdens	-358.92	5.64	0.04
	ndmi_std	-372.81	10.97	0.00	slope	-358.32	6.24	0.03
	elev	-372.58	11.20	0.00	elev	-357.48	7.08	0.02
	ndvi_std	-372.54	11.24	0.00	twi	-355.91	8.64	0.01
	ndmi_avg	-371.50	12.28	0.00	siose05	-355.15	9.41	0.01
	rdens	-369.93	13.85	0.00	ndvi_avg	-354.98	9.58	0.01
	siose05	-368.80	14.98	0.00	IBD	-343.12	21.44	0.00
	IBD	-364.43	19.35	0.00	ndmi_avg	-342.98	21.58	0.00
	clc06	-363.11	20.67	0.00	clc06	-340.58	23.98	0.00
	IntOnly	-360.67	23.11	0.00	IntOnly	-230.69	133.86	0.00

Table V.4. Model selection results for average migration rates for the test species *P. cultripes* (left) and *P. waltl* (right). Models highlighted in bold attained the highest relative support and were included in the confidence set (ΔAICc≤4). AICc – Akaike Information Criterion value (with a correction for finite sample size), ΔAICc – delta AIC value, wi – Akaike weights. IBD – Isolation-by-distance model. IntOnly – Intercept-only/null model.

Pelobates cultripes				***Pleurodeles waltl***			
Variable	**AICc**	**ΔAIC**	**wi**	**Variable**	**AICc**	**ΔAIC**	**wi**
ndvi_avg	**-606.05**	**0.00**	**0.93**	**ndvi_std**	**-1001.37**	**0.00**	**0.15**
slope	-600.77	5.28	0.07	**ndmi_std**	**-1001.28**	**0.09**	**0.14**
twi	-589.73	16.32	0.00	**slope**	**-1000.49**	**0.88**	**0.09**
ndmi_avg	-589.34	16.71	0.00	**ndmi_avg**	**-1000.46**	**0.91**	**0.09**
rdens	-586.68	19.37	0.00	**siose05**	**-1000.36**	**1.01**	**0.09**
ndmi_std	-586.32	19.73	0.00	**rdens**	**-1000.22**	**1.15**	**0.08**
elev	-585.07	20.98	0.00	**ndvi_avg**	**-1000.18**	**1.19**	**0.08**
ndvi_std	-585.05	21.00	0.00	**elev**	**-999.84**	**1.53**	**0.07**
siose05	-585.02	21.02	0.00	**clc06**	**-999.83**	**1.54**	**0.07**
IBD	-582.86	23.18	0.00	**twi**	**-999.79**	**1.58**	**0.07**
IntOnly	-576.18	29.87	0.00	**IBD**	**-999.42**	**1.95**	**0.06**
clc06	-574.94	31.11	0.00	IntOnly	-996.05	5.32	0.01

and the intercept-only models recorded no support, which means good relative performance of resistance-based surfaces to explain migration rates. In turn, *P. waltl* recorded much higher model uncertainty with several models entering the confidence set including the IBD model (Table V.4). This translates in relatively weaker performance of resistance-based variables to explain migration rates for *P. waltl*.

Resistance surfaces

Resistance surface optimization revealed several non-linearities regarding the way landscape features influence gene flow (Fig. V.2). Also, when considering model-selected variables (Tables V.3 and V.4), the transformations used for generating optimized resistance surfaces showed a very strong similarity of responses across different genetic distances translating a certain degree of stability between optimization rounds.

For *P. cultripes* lower resistance areas were found for below median elevations (with a minimum resistance around 870m) and moderate slopes (minimum 11.4%) corresponding to low- and midland areas. Vegetated areas

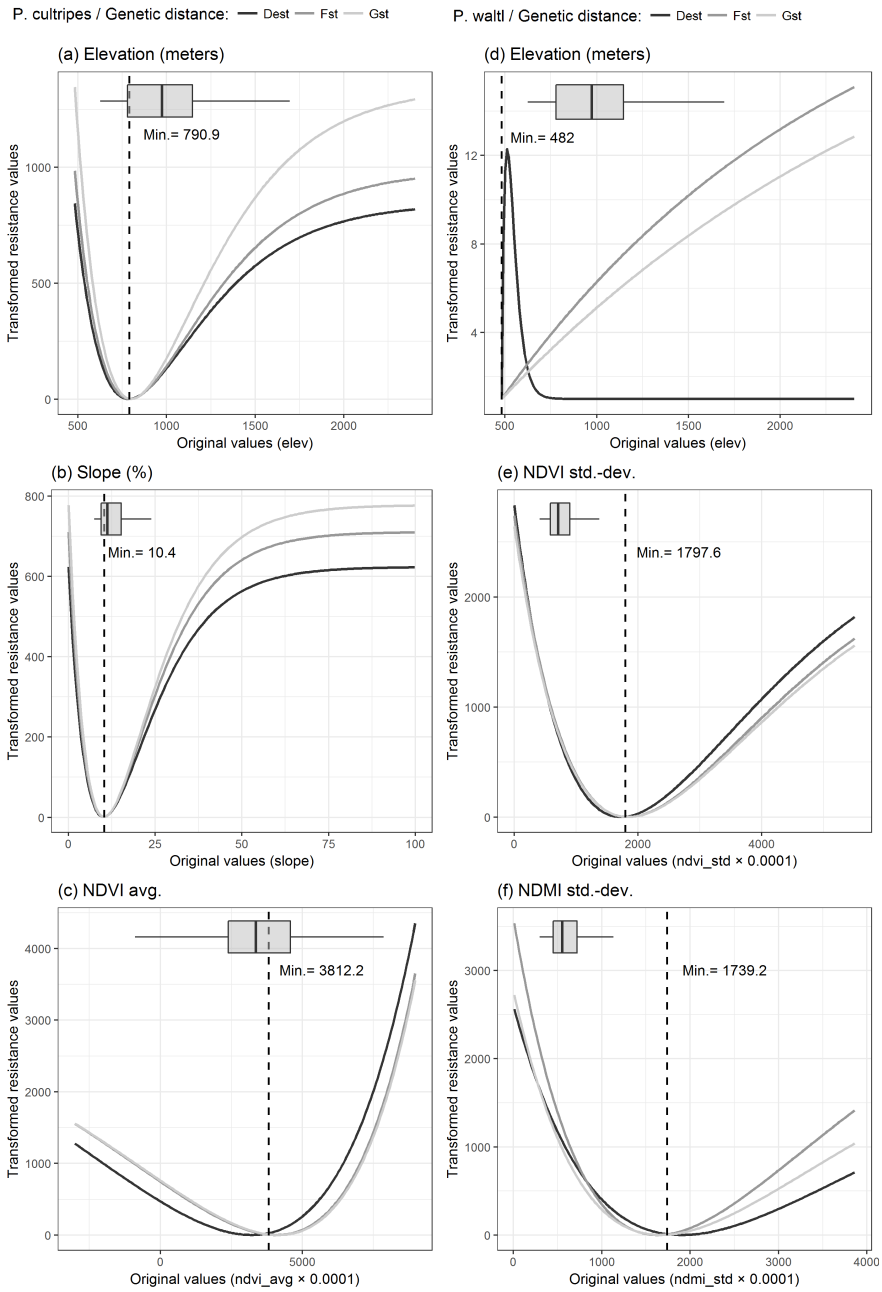

Figure V.2. Transformations applied to each variable (included in the most frequently selected models) to generate resistance surfaces for species *P. cultripes* (left-side) and *P. waltl* (right-side). Each curve represents a different transform parametrization optimized for Dest (black color), Fst (dark-grey) and G''st (light-grey). Original values are represented in the x-axis (including the full range of the variable) while transformed (resistance) values are shown in the y-axis and should be interpreted in relative fashion between variables. The dashed line shows the minimum resistance for the original values of each variable. The boxplot on top shows the distribution of the original untransformed variable (boxes are the 25%, 50% and 75% quartiles and whiskers show the smallest/largest observation greater/less than or equal to lower hinge -/+ 1.5 times the inter-quartile range). NDVI and NDMI values have a 10^{-4} scale factor.

Table V.5. Bootstrap estimation of dispersal distance (in meters) based on the Brent optimization method defined in Peterman *et al*. (2014). A total of 10 000 replicates were used. Notice the large right-tail in 95% confidence intervals. Overall *P. cultripes* consistently recorded higher values in comparison to *P. waltl.*

Species	Genetic distance metric	Dispersal distance estimate (meters)	95% CI (lower, upper limits)
Pelobates cultripes	Fst	154.0	[14.0, 1389.2]
	Gst	151.7	[14.1, 1673.2]
	Dest	154.5	[14.1, 1104.1]
	Average	**153.4**	**[14.1, 1388.9]**
Pleurodeles waltl	Fst	53.2	[13.8, 995.4]
	Gst	54.6	[13.0, 1559.7]
	Dest	53.2	[13.4, 975.2]
	Average	**53.7**	**[13.4, 1176.8]**

with above median NDVI values were found to have low resistance (minimum around 0.42; Fig. V.3) showing both an avoidance for artificialized areas (e.g., urban settlements, roads; typically, with very low or negative NDVI values) and strongly vegetated areas mostly related to elevated mountainous zones with forest cover.

For *P. waltl* two different (and complementary) transformations were found for elevation. When considering Fst and G''st, it was almost linear, i.e., with increasing resistance following the increase in altitude (Fig. V.3) while for Dest, strong resistance values were related to lowland areas. In addition, low resistance landscapes were found to have very-high NDVI / NDMI standard-deviation corresponding to heterogeneous and moderately disturbed areas with natural and/or semi-natural vegetation.

Estimation of dispersal distances

Both species revealed relatively low dispersal distances with *P. waltl* recording the lowest average estimates (*P. waltl* = 53.7m [13.4m, 1176.8m] vs. *P. cultripes* = 153.4m [14.1m, 1388.9m]) and also the lowest estimate variability across genetic difference metrics (Table V.5). Both species also showed widely asymmetric confidence intervals, with large upper values (in comparison to the estimated distance), and a relatively high overlap between the two intervals.

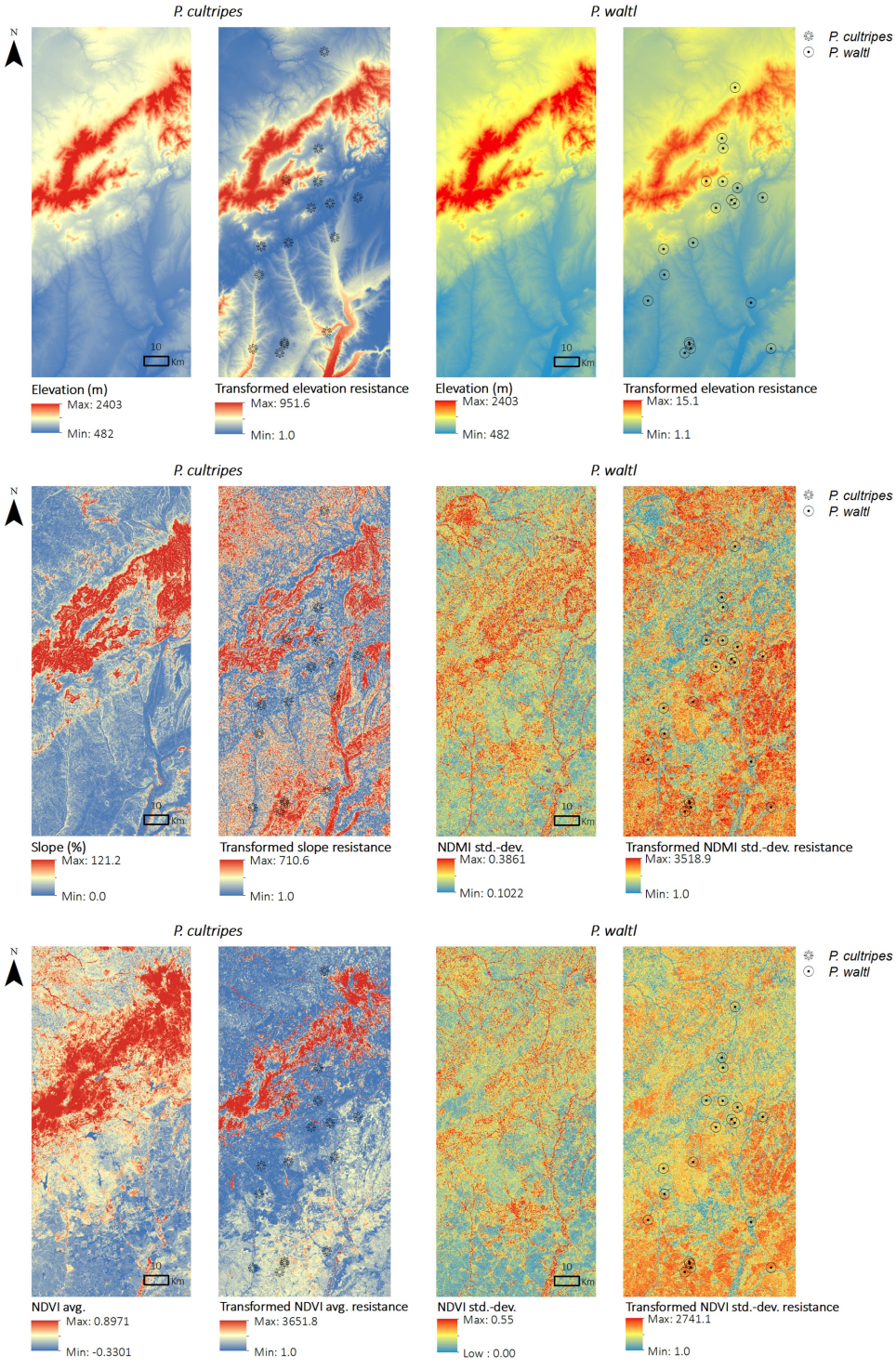

Figure V.3. Optimized resistance surfaces for *Pelobates cultripes* (left-side) and *Pleurodeles waltl* (right-side) based on the most frequently selected variables and considering Fst distances. For each species, left are maps showing the original continuous values for each variable; on the right, the resistance surface generated through optimization. Points represent sampling localities.

Discussion

Comparative studies based on molecular approaches hold great potential to improve our understanding on the effect of different landscape features on regional patterns of population connectivity across taxa. Here we anticipated land cover-related variables to have the most impact on genetic structure, and hypothesized remote-sensing data would provide a more accurate description of terrestrial habitats at the relevant spatial scale for low dispersing organisms than other traditionally used discrete categories of land use/cover. Our results support this notion, with genetic differentiation in the two species in the study area mainly associated to environmental factors related to land and vegetation cover (but in different ways between the two species).

Our comparative study revealed contrasting patterns of genetic structure in the two species, with stronger, finer-scale genetic differentiation in *Pleurodeles waltl* (see Fig. V.1). This difference can be associated to demographic (especially differences in dispersal rates) and life-history traits, density-dependent effects, or divergent habitat preferences, which in this case would refer to their terrestrial habitats, since both species usually breed in the same types of ponds (Recuero 2014). These factors are not mutually exclusive, and our resistance surfaces provide some keys to sort out their relative effects. Leaving aside the common effect of topography on both species (see below), land-cover related categorical variables did not have an important role in shaping genetic structure. Some studies have previously reported negative effects of roads on gene flow in anurans (Richardson, 2012) and salamanders (Coster *et al*., 2015). Nevertheless, models including road density as a variable were not well supported in either species (Table V.3). Instead, we found remarkable differences associated to the role of fine-scale patterns of vegetation cover, vegetation water content and their spatial heterogeneity in shaping patterns of regional genetic structure for the two species. These differences were better captured by fine-scale remotely-sensed spectral indices (NDVI/NDMI) portraying land cover, vegetation and moisture in a continuous fashion, highlighting their value in landscape genetics studies.

For *P. cultripes*, genetic differentiation increased with both high and low values of vegetation coverage (NDVI avg.), with medium values in this variable

associated with reduced resistance to gene flow (Table V.3). Patches with high resistance are typically related to urban/artificial areas and roads (low NDVI values) or high altitude forested areas (high values; Fig. V.3). Habitats with mid-range canopy cover have been reported as areas preferentially selected during dispersal in other species of anurans, such as *Bufo boreas* (Bartelt *et al*., 2004). In *P. waltl*, high or very high values in variables related to the spatial heterogeneity of vegetation cover (NDVI and NDVI std.-dev.), and the spatial heterogeneity in vegetation water content (NDMI std.-dev.), were associated with higher connectivity between populations. These values correspond to heterogeneous and moderately disturbed areas with different types of natural and/or semi-natural vegetation (Table V.3 and Fig. V.3). Thus, our results suggest a positive role of certain vegetation types and structural heterogeneity in population connectivity for the two species, with habitat patches of Mediterranean scrubland and open oak woodlands ("dehesas") facilitating gene flow.

Fine-scale aspects of the landscape, described by remote-sensing data, strongly influenced gene flow in both species, as anticipated. However, different variables were more important in shaping patterns of gene flow between species. This is surprising in view of the extensive overlap in their geographic ranges, probably reflecting similar ecological requirements at the macro (bioclimatic) scale (Sillero *et al*., 2009). Regionally, vegetation amount played a key role in *P. cultripes*, whereas in *P. waltl* the spatial heterogeneity in vegetation coverage and water content / water stress were more important. Since NDMI is an indicator of water stress, its presence in models for *P. waltl* may indicate that this species is more sensitive to drought conditions. With potential alterations in hydrologic regimes derived from climate change (affecting wetlands and ponds through changes in hydroperiod) this has important consequences for connectivity and conservation assessments. Also, low-resistance areas (with importance for connectivity) are less common in the landscape for *P. waltl* than for *P. cultripes* (notice the difference in resistance curves in Fig. V.2: in *P. waltl*, low-resistance conditions are pushed to the right-side, close to extreme data values; while in *P. cultripes* they are closer to the median). This observation, in conjunction with the inferred lower dispersal ability in *Pleurodeles*, probably make this species more vulnerable to the effects of fragmentation, whereas *Pelobates* could be

considered more of a generalist species, in the sense that it benefits from a higher availability of favorable areas for dispersal in the study area.

In addition to variables related with land and vegetation cover, our results also showed some effect of topography on regional patterns of genetic structure. Variables related to topography have been previously shown to explain genetic differentiation in a wide range of taxa (for examples in amphibians, see Funk *et al*., 2005; Giordano *et al*., 2007; Savage *et al*., 2010; Igawa *et al*., 2013; Zancolli *et al*., 2014; Funk *et al*., 2016). In our study area, we also found that neither elevation nor slope favor gene flow in the two species studied (Table V.3). Both are typical inhabitants of Mediterranean habitats at low and medium elevations, with upper altitudinal limits of up to 1480 meters in *P. waltl* and 1770 meters in *P. cultripes* (Cejudo 1990; Montori *et al*., 2002; Tejedo & Reques, 2002; García-París *et al*., 2004). Restrictions to population connectivity imposed by elevation and slope probably operate on deeper time scales than those related to land use/cover. Recent phylogeographic studies have shown that the Iberian Central System has acted as an historical barrier to gene flow in the two species, separating different evolutionary groups north and south of this mountain range (Gutiérrez-Rodríguez *et al*., 2017b,c). These groups would have experienced limited connectivity during the Last Glacial Maximum (21 ka), since glacial areas occupied lower altitudes around 1350 m in the study area (Bullón, 2016). In contrast, vegetation dynamics in the Central System mountains have been constantly changing during the Holocene due to human activities (López-Sáez *et al*., 2014). In addition, large water surfaces and rivers are also associated to potential barrier effects in areas of low elevation and slope, especially in *P. cultripes* (but also in *P. waltl*, see Fig. V.3).

Demographic and life history traits, such as dispersal, philopatry, population effective size, generation time, clutch size and larval phenology have been described as promoters of genetic differentiation in amphibians (Richardson, 2012; Whiteley *et al*., 2014; Nowakowski *et al*., 2015). One of the most important biological traits affecting the genetic structure of populations is dispersal capacity, which is fundamental to maintain gene flow between populations. Amphibians generally present limited dispersal and significant differences have been observed between anurans and salamanders (Smith & Green, 2005). In the

case of *P. cultripes* and *P. waltl*, there is no published information about dispersal distance or home range. Nonetheless, our analyses suggest low migration rates in both species (Table V.5), with slightly higher average values in *P. cultripes* but extensive overlap in the respective confidence intervals. In addition, the distribution of bootstrapped estimates of dispersal distances show large right-tails, potentially indicating the occurrence of long-distance dispersal events. These events, combined with low resistance of the landscape in certain areas, may help explain the existence of relatively large areas with little genetic differentiation in both species (but especially in *Pelobates*). At any rate, our estimates of similar but slightly higher dispersal potential in *Pelobates* are consistent with our own preliminary field data. Over an 8-year period, we recorded 0.5% vs 1.2% dispersal event rates involving distances over 250 meters of marked adult individuals of *Pleurodeles* (6 dispersal events per 1172 recaptures) and *Pelobates* (16 dispersal events per 1293), respectively (Gutiérrez-Rodríguez *et al*., 2017a). In turn, these results are in agreement with observed higher genetic differentiation between *P. waltl* populations. Other indirect evidence, like higher frequency of road-kills in *P. cultripe*s in areas where the two species co-occur (D'Amico *et al*., 2015) also suggest more dispersal capacity and propensity in *Pelobates*, in line with previous studies documenting higher migration potential in anurans compared to urodeles. Another life history trait linked to dispersal and population structure is breeding site philopatry, with the species with higher philopatry showing increased population genetic differentiation. Here, we inferred philopatry based on the comparison of inbreeding coefficients (Fis), with results in agreement with dispersal estimates: mean values of Fis in *P. waltl* (0.010) doubled those in *P. cultripes* (0.004), suggesting a more philopatric behavior of the former species.

Finally, density effects can also impact regional patterns of gene flow. Populations with a higher effective population size differentiate due to genetic drift at a slower rate than smaller populations (Charlesworth, 2009) and may also contribute more migrants to neighboring breeding ponds. In our case, mean estimated values of Nb were higher (almost double) in *P. waltl* than in *P. cultripes*, and thus we would expect higher dispersal and lower differentiation between populations in the former. However, our analyses did not find evidence for density dependent effects in any of the two species, in contrast to the results

of Coster *et al*. (2015), who found a negative correlation between Fst and the number of egg masses in *Ambystoma maculatum* and *Lithobates sylvaticus*. Gene flow between breeding ponds can be favored by large clutch sizes too, through increased recruitment and a higher probability of juvenile dispersal. In our case, differences in clutch sizes between the two species also parallel patterns of population genetic differentiation, with larger clutches in *P. cultripes* (1301-6882 eggs) than in *P. waltl* (150-1303 eggs) (González de la Vega, 1988; Lizana *et al*., 1994; García-París *et al*., 2004).

Our study represents a valuable contribution to the knowledge on the functioning and conservation of Mediterranean habitats, including the finding of a positive role of structural heterogeneity on gene flow in pond-breeding amphibians. More generally, it illustrates how remotely-sensed continuous variables of vegetation cover and water content (e.g., NDVI, NDMI) have great potential to offer relevant insights about major drivers of population connectivity in landscape genetics studies. In our study area, variables associated to fine-scale structural habitat heterogeneity/complexity proved to have a major impact on regional patterns of genetic differentiation in two syntopic pond breeding amphibians. This heterogeneity is a characteristic of Mediterranean landscapes with low/ medium elevations, which include extensively managed areas together with natural and/or semi-natural habitats. While it remains to be seen whether our results are generalizable to other taxa, like aquatic invertebrates, the differences observed in our comparison regarding two taxonomically and ecologically similar taxa highlight the conservation value of these areas and point to the need of considering species individually when identifying and designing corridors connecting local populations in Mediterranean habitats.

Acknowledgements

We thank Agentes Forestales de la Comunidad de Madrid and G. Astudillo, C. Grande, J.L. Gutiérrez, A. López, J.A. Lucas, L. Martín, B. Paños, R. Pereira, E. Recuero and G. Sánchez Montes for help in sampling. T. Cuartero and V. González (Laboratorio de Biogeografía Informática, MNCN-CSIC) for support with spatial data. JGR was supported by the Consejo Superior de Investigaciones Científicas of Spain (CSIC) and the European Social Fund (ESF) (JAE-pre PhD

fellowship). JG was financially supported by FCT (Portuguese Foundation for Science and Technology) through PhD grant SFRH/BD/90112/2012 funded by POPH-QREN (2007-2013). EC was also supported by FCT through Postdoctoral Grant SFRH/BPD/109182/2015 funded by CSF (2014-2020). This research was funded by grants CGL2008-04271-C02-01/BOS, and CGL2011-28300 (Ministerio de Ciencia e Innovación -MICINN-, Ministerio de Economía y Competitividad -MEC-, Spain, and FEDER) to IMS, who was also supported by funding from the Spanish Severo Ochoa Program (SEV-2012-0262).

References

Bartelt PE, Peterson CR, Klaver RW (2004) Sexual differences in the post-breeding movements and habitats selected by western toads (*Bufo boreas*) in southeastern Idaho. Herpetologica 60: 455–467.

Bates D, Maechler M, Bolker B, Walker S (2014) lme4: Linear mixed-effects models using Eigen and S4. R package version 1.1–7.

Beja P, Alcazar R (2003) Conservation of Mediterranean temporary ponds under agricultural intensification: an evaluation using amphibians. Biological Conservation 114: 317–326.

Beja P, Bosch J, Tejedo M *et al*. (2009) *Pleurodeles waltl*. The IUCN Red List of Threatened Species 2009.

Beja P, Bosch J, Tejedo M *et al*. (2016) *Pelobates cultripes*. The IUCN Red List of Threatened Species 2016.

Blondel J, Aronson J (1999) Biology and wildlife of the Mediterranean region. Oxford University Press, USA.

Bowne DR, Bowers MA (2004) Interpatch movements in spatially structured populations: a literature review. Landscape Ecology 19: 1–20.

Bullón T (2016) The upper Pleistocene on the northern face of the Guadarrama Mountains (central Spain): Palaeoclimatic phases and glacial activity. Geomorphology 268: 233–245.

Cejudo D (1990) Nueva altitud máxima para *Pelobates cultripes*. Boletín de la Asociación Herpetológica Española 1: 20.

Charlesworth B (2009) Effective population size and patterns of molecular evolution and variation. Nature Reviews Genetics 10: 195–205.

Cheng L, Connor TR, Sirén J, Aanensen DM, Corander J (2013) Hierarchical and spatially explicit clustering of DNA sequences with BAPS software. Molecular Biology and Evolution 30: 1224–1228.

Clarke RT, Rothery P, Raybould AF (2002) Confidence limits for regression relationships between distance matrices: Estimating gene flow with distance. Journal of Agricultural, Biological, and Environmental Statistics 7: 361–372.

Corander J, Sirén J, Arjas E (2008) Bayesian spatial modeling of genetic population structure. Computational Statistics 23: 111–129.

Coster SS, Babbitt KJ, Cooper A, Kovach AI (2015) Limited influence of local and landscape

factors on finescale gene flow in two pond-breeding amphibians. Molecular Ecology 24: 742–758.

Crawford NG (2010) SMOGD: software for the measurement of genetic diversity. Molecular Ecology Resources 10: 556–557.

D'Amico M, Román J, de los Reyes L, Revilla E (2015) Vertebrate road-kill patterns in Mediterranean habitats: Who, when and where. Biological Conservation 191: 234–242.

Doulgeris C, Papadimos D, Kapsomenakis J (2016) Impacts of climate change on the hydrology of two Natura 2000 sites in Northern Greece. Regional Environmental Change 16: 1941–1950.

Dudaniec RY, Worthington Wilmer J, Hanson JO *et al*. (2016) Dealing with uncertainty in landscape genetic resistance models: a case of three co-occurring marsupials. Molecular Ecology 25: 470–486.

Engler JO, Balkenhol N, Filz KJ, Habel JC, Rödder D (2014) Comparative landscape genetics of three closely related sympatric hesperid butterflies with diverging ecological traits. PLoS ONE 9: e106526.

Frantz AC, Bertouille S, Eloy MC *et al*. (2012) Comparative landscape genetic analyses show a Belgian motorway to be a gene flow barrier for red deer (*Cervus elaphus*), but not wild boars (*Sus scrofa*). Molecular Ecology 21: 3445–3457.

Funk WC, Blouin MS, Corn PS *et al*. (2005) Population structure of Columbia spotted frogs (*Rana luteiventris*) is strongly affected by the landscape. Molecular Ecology 14: 483–496.

Funk WC, Murphy MA, Hoke KL *et al*. (2016) Elevational speciation in action? Restricted gene flow associated with adaptive divergence across an altitudinal gradient. Journal of Evolutionary Biology 29: 241–252.

Funk WC, Tallmon DA, Allendorf FW (1999) Small effective population size in the long-toed salamander. Molecular Ecology 8: 1633–1640.

Gaggiotti OE, Foll M (2010) Quantifying population structure using the F-model. Molecular Ecology Resources 10: 821–830.

Gao B-C (1996) NDWI—A normalized difference water index for remote sensing of vegetation liquid water from space. Remote Sensing of Environment 58: 257–266.

García-París M, Montori A, Herrero P (2004) Fauna Iberica. Vol. 24. Amphibia: Lissamphibia. Museo Nacional de Ciencias Naturales, Consejo Superior de Investigaciones Científicas.

Giordano AR, Ridenhour BJ, Storfer A (2007) The influence of altitude and topography on genetic structure in the long-toed salamander (*Ambystoma macrodactulym*). Molecular Ecology 16: 1625–1637.

Goldberg CS, Waits LP (2010a) Comparative landscape genetics of two pond-breeding amphibian species in a highly modified agricultural landscape. Molecular Ecology 19: 3650–3663.

Goldberg CS, Waits LP (2010b) Quantification and reduction of bias from sampling larvae to infer population and landscape genetic structure. Molecular Ecology Resources 10: 304–313.

González de la Vega JP (1988) Anfibios y reptiles de la provincia de Huelva. ERTISA.

Graeter GJ, Rothermel BB, Gibbons JW (2008) Habitat selection and movement of pond-breeding amphibians in experimentally fragmented pine forests. The Journal of Wildlife Management 72: 473–482.

Greenberg JA, Dobrowski SZ, Ustin SL (2005) Shadow allometry: Estimating tree structural parameters using hyperspatial image analysis. Remote Sensing of Environment 97: 15–25.

Gutiérrez-Rodríguez J, Martínez-Solano Í (2013) Isolation and characterization of sixteen polymorphic microsatellite loci in the Western Spadefoot, *Pelobates cultripes* (Anura: Pelobatidae) via 454 pyrosequencing. Conservation Genetics Resources 5: 981–984.

Gutiérrez-Rodríguez J, Gonzalez EG, Martínez-Solano Í (2014) Development and characterization of twelve new polymorphic microsatellite loci in the Iberian ribbed newt, *Pleurodeles waltl* (Caudata: Salamandridae), with data on cross-amplification in *P. nebulosus*. Amphibia-Reptilia 35: 129–134.

Gutiérrez-Rodríguez J, Sánchez-Montes G, Martínez-Solano Í. (2017a) Effective to census population size ratios in two Near Threatened Mediterranean amphibians: *Pleurodeles waltl* and *Pelobates cultripes*. Conservation Genetics. In press.

Gutiérrez-Rodríguez J, Barbosa AM, Martínez-Solano Í. (2017b) Present and past climatic effects on the current distribution and genetic diversity of the Iberian spadefoot toad (*Pelobates cultripes*): an integrative approach. Journal of Biogeography 44: 245–258.

Gutiérrez-Rodríguez J, Barbosa AM, Martínez-Solano Í. (2017c) Integrative inference of population history in the Ibero-Maghrebian endemic *Pleurodeles waltl* (Salamandridae). Molecular Phylogenetics and Evolution 112: 122–137.

Hewitt R, Escobar F (2011) The territorial dynamics of fast-growing regions: Unsustainable land use change and future policy challenges in Madrid, Spain. Applied Geography 31: 650–667.

Igawa T, Oumi S, Katsuren S, Sumida M (2013) Population structure and landscape genetics of two endangered frog species of genus *Odorrana*: different scenarios on two islands. Heredity 110: 46–56.

Jehle R, Burke T, Arntzen JW (2005) Delineating fine-scale genetic units in amphibians: probing the primacy of ponds. Conservation Genetics 6: 227–234.

Jones OR, Wang J (2010) Molecular marker-based pedigrees for animal conservation biologists. Animal Conservation 13: 26–34.

Jost L (2008) Gst and its relatives do not measure differentiation. Molecular Ecology 17: 4015–4026.

Keller D, Holderegger R, Strien MJ, Bolliger J (2014) How to make landscape genetics beneficial for conservation management? Conservation Genetics 16: 503–512.

Kurz DJ, Nowakowski AJ, Tingley MW, Donnelly MA, Wilcove DS (2014) Forest-land use complementarity modifies community structure of a tropical herpetofauna. Biological Conservation 170: 246–255.

Lizana M, Márquez R, Martín-Sánchez R (1994) Reproductive biology of *Pelobates cultripes* (Anura: Pelobatidae) in central Spain. Journal of Herpetology 28: 19–27.

López-Sáez JA, Abel-Schaad D, Pérez-Díaz S *et al*. (2014) Vegetation history, climate and human impact in the Spanish Central System over the last 9000 years. Quaternary International 353: 98–122.

Martínez-Solano Í (2006) Atlas de distribución y estado de conservación de los anfibios de la Comunidad de Madrid. Graellsia 62: 253–291.

Meirmans PG, Van Tienderen PH (2004) genotype and genodive: two programs for the analysis of genetic diversity of asexual organisms. Molecular Ecology Notes 4: 792–794.

Meirmans PG, Hedrick PW (2011) Assessing population structure: Fst and related measures. Molecular Ecology Resources 11: 5–18.

Moilanen A, Nieminen M (2002) Simple connectivity measures in spatial ecology. Ecology 83: 1131–1145.

Montori A, Llorente GA, Santos X, Carretero MA (2002) *Pleurodeles waltl* Michahelles, 1830. Gallipato. In: Atlas y libro rojo de los anfibios y reptiles de España (eds. Pleguezuelos JM, Márquez R, Lizana M), pp. 51–54. Dirección General de Conservación de la Naturalez-Asociación Herpetológica Española, Madrid.

Muscarella RA, Murray KL, Ortt D, Russell AL, Fleming TH (2011) Exploring demographic, physical, and historical explanations for the genetic structure of two lineages of Greater Antillean bats. PLoS ONE 6: e17704.

Nagendra H, Lucas R, Honrado JP *et al*. (2013) Remote sensing for conservation monitoring: Assessing protected areas, habitat extent, habitat condition, species diversity, and threats. Ecological Indicators 33: 45–59.

Nicholson E, Possingham HP (2006) Objectives for multiple-species conservation planning. Conservation Biology 20: 871–881.

Nowakowski AJ, DeWoody JA, Fagan ME, Willoughby JR, Donnelly MA (2015) Mechanistic insights into landscape genetic structure of two tropical amphibians using field-derived resistance surfaces. Molecular Ecology 24: 580–595.

Olsen J, Crane P, Flannery B *et al*. (2011) Comparative landscape genetic analysis of three Pacific salmon species from subarctic North America. Conservation Genetics 12: 223–241.

Ortego J, García-Navas V, Noguerales V, Cordero PJ (2015) Discordant patterns of genetic and phenotypic differentiation in five grasshopper species codistributed across a microreserve network. Molecular Ecology 24: 5796–5812.

Peakall R, Smouse PE (2012) GenAlEx 6.5: genetic analysis in Excel. Population genetic software for teaching and research—an update. Bioinformatics 28: 2537–2539.

Pérez-Espona S, Pérez-Barbería FJ, McLeod JE *et al*. (2008) Landscape features affect gene flow of Scottish Highland red deer (*Cervus elaphus*). Molecular Ecology 17: 981–996.

Peterman WE (2014) ResistanceGA: An R package for the optimization of resistance surfaces using genetic algorithms. bioRxiv. doi: http://dx.doi.org/10.1101/007575

Peterman WE, Connette GM, Semlitsch RD, Eggert LS (2014) Ecological resistance surfaces predict fine-scale genetic differentiation in a terrestrial woodland salamander. Molecular Ecology 23: 2402–2413.

Peterman W, Anderson T, Ousterhout B *et al*. (2015) Differential dispersal shapes population structure and patterns of genetic differentiation in two sympatric pond breeding salamanders. Conservation Genetics 16: 59–69.

Pflüger FJ, Balkenhol N (2014) A plea for simultaneously considering matrix quality and local environmental conditions when analysing landscape impacts on effective dispersal. Molecular Ecology 23: 2146–2156.

Phillipsen IC, Kirk EH, Bogan MT *et al*. (2015) Dispersal ability and habitat requirements determine landscape-level genetic patterns in desert aquatic insects: Molecular Ecology 24, 54–69.

Quinn PF, Beven KJ, Lamb R (1995) The in(a/tan/β) index: How to calculate it and how to use it within the topmodel framework. Hydrological Processes 9: 161–182.

R Core Team (2014) R: A language and environment for statistical computing. R Foundation for Statistical Computing, Vienna, Austria.

Raymond M, Rousset F (1995) GENEPOP (Version 1.2): Population genetics software for exact tests and ecumenicism. Journal of Heredity 86: 248–249.

Recuero E (2014) Sapo de espuelas - *Pelobates cultripes*. In: Enciclopedia Virtual de los Vertebrados Españoles (eds. Salvador A, Martínez-Solano Í). Museo Nacional de Ciencias Naturales, Madrid.

Rice WR (1989) Analyzing tables of statistical tests. Evolution 43: 223–225.

Richardson JL (2012) Divergent landscape effects on population connectivity in two co-occurring amphibian species. Molecular Ecology 21: 4437–4451.

Rousset F (2008) genepop'007: a complete re-implementation of the genepop software for Windows and Linux. Molecular Ecology Resources 8: 103–106.

Savage WK, Fremier AK, Bradley Shaffer H (2010) Landscape genetics of alpine Sierra Nevada salamanders reveal extreme population subdivision in space and time. Molecular Ecology 19: 3301–3314.

Schwenk WS, Donovan TM (2011) A multispecies framework for landscape conservation planning. Conservation Biology 25: 1010–1021.

Sillero N, Brito JC, Skidmore AK, Toxopeus AG (2009) Biogeographical patterns derived from remote sensing variables: the amphibians and reptiles of the Iberian Peninsula. Amphibia-Reptilia 30: 185–206.

Smith MA, Green DM (2005) Dispersal and the metapopulation paradigm in amphibian ecology and conservation: are all amphibian populations metapopulations? Ecography 28: 110–128.

Steele CA, Baumsteiger J, Storfer A (2009) Influence of life-history variation on the genetic structure of two sympatric salamander taxa. Molecular Ecology 18: 1629–1639.

Storfer A, Murphy MA, Evans JS *et al*. (2007) Putting the "landscape" in landscape genetics. Heredity 98: 128–142.

Tachikawa T, Hato M, Kaku M, Iwasaki A (2011) Characteristics of ASTER GDEM version 2. 2011 IEEE International Geoscience and Remote Sensing Symposium, Vancouver, BC, pp. 3657–3660.

Tejedo M, Reques R (2002) *Pelobates cultripes* (Cuvier, 1829). Sapo de espuelas. In: Atlas y libro rojo de los anfibios y reptiles de España (eds. Pleguezuelos JM, Márquez R, Lizana M), pp. 94–96. Dirección General de Conservación de la Naturaleza-Asociación Herpetológica Española, Madrid.

Turner W, Spector S, Gardiner N *et al*. (2003) Remote sensing for biodiversity science and conservation. Trends in Ecology & Evolution 18: 306–314.

van de Vliet MS, Diekmann OE, Serrão EA, Beja P (2009) Isolation of highly polymorphic microsatellite loci for a species with a large genome size: sharp-ribbed salamander (*Pleurodeles waltl*). Molecular Ecology Resources 9: 425–428.

van Etten J (2015) gdistance: distances and routes on geographical grids. R package version 1.1-7.

van Oosterhout C, Hutchinson WF, Wills DPM, Shipley P (2004) MICRO-CHECKER: software for identifying and correcting genotyping errors in microsatellite data. Molecular Ecology Notes 4: 535–538.

van Strien MJ, Keller D, Holderegger R (2012) A new analytical approach to landscape genetic modelling: least-cost transect analysis and linear mixed models. Molecular Ecology 21: 4010–4023.

Wang J (2004) Sibship reconstruction from genetic data with typing errors. Genetics 166: 1963–1979.

Wang J (2015) Does Gst underestimate genetic differentiation from marker data? Molecular Ecology 24: 3546–3558.

Weir BS, Cockerham CC (1984) Estimating F-statistics for the analysis of population structure. Evolution: 1358–1370.

Whiteley A, McGarigal K, Schwartz M (2014) Pronounced differences in genetic structure despite overall ecological similarity for two *Ambystoma* salamanders in the same landscape. Conservation Genetics 15: 573–591.

Wilson GA, Rannala B (2003) Bayesian inference of recent migration rates using multilocus genotypes. Genetics 163: 1177–1191.

Wulder MA, Hall RJ, Coops NC, Franklin SE (2004) High spatial resolution remotely sensed data for ecosystem characterization. BioScience 54: 511–521.

Zancolli G, Rödel M-O, Steffan-Dewenter I, Storfer A (2014) Comparative landscape genetics of two river frog species occurring at different elevations on Mount Kilimanjaro. Molecular Ecology 23: 4989–5002.

Supplementary

Table V.S1. Geographic distances (in km) between sampled *P. cultripes* populations.

Pop/ km	C1	C2	C3	C4	C5	C6	C7	C8	C9	C10	C11	C12	C13	C14	C15	C16
C1	0.00															
C2	39.64	0.00														
C3	56.17	21.61	0.00													
C4	53.05	13.43	17.27	0.00												
C5	62.29	29.30	39.49	22.54	0.00											
C6	62.04	23.26	25.43	10.98	15.49	0.00										
C7	64.17	24.57	17.92	11.42	25.45	9.96	0.00									
C8	76.11	37.45	35.43	24.69	20.49	14.21	17.53	0.00								
C9	80.20	41.57	25.65	29.53	41.63	27.21	18.68	25.06	0.00							
C10	86.27	50.27	30.15	40.30	55.61	40.58	31.06	39.70	14.65	0.00						
C11	97.31	60.29	41.15	49.21	61.43	47.40	38.80	43.12	20.22	11.59	0.00					
C12	114.10	74.73	65.72	61.35	56.97	52.13	51.01	38.43	41.79	49.58	43.02	0.00				
C13	120.45	81.09	66.33	68.01	70.93	61.51	56.61	50.49	40.76	41.16	30.73	23.26	0.00			
C14	121.13	81.75	67.03	68.66	71.45	62.11	57.26	51.03	41.46	41.87	31.41	23.29	0.71	0.00		
C15	126.86	88.64	70.95	76.37	83.21	71.79	65.11	62.82	47.07	41.89	30.30	40.12	16.87	16.89	0.00	
C16	125.04	85.74	70.61	72.71	75.75	66.32	61.30	55.32	45.14	44.61	33.73	26.63	4.83	4.30	14.44	0.00

Table V.S2. Geographic distances (in km) between sampled *P. waltl* populations.

Pop/ km	W1	W2	W3	W4	W5	W6	W7	W8	W9	W10	W11	W12	W13	W14	W15	W16	W17	W18	W19	W20
W1	0.00																			
W2	21.90	0.00																		
W3	25.67	4.22	0.00																	
W4	41.18	19.36	16.12	0.00																
W5	38.95	17.68	13.52	8.83	0.00															
W6	41.14	22.09	17.99	17.08	8.45	0.00														
W7	47.47	32.82	29.33	31.13	22.54	14.10	0.00													
W8	45.95	25.70	21.49	15.53	8.84	5.85	16.91	0.00												
W9	47.43	27.54	23.33	17.67	10.98	6.56	15.49	2.20	0.00											
W10	50.28	28.68	24.67	12.24	11.42	14.14	25.45	8.87	9.96	0.00										
W11	67.16	45.27	41.67	26.08	29.53	32.60	41.63	26.90	27.21	18.68	0.00									
W12	76.25	54.95	52.04	35.97	42.01	46.84	57.20	41.52	42.22	32.73	16.06	0.00								
W13	85.24	63.60	60.39	44.30	49.21	52.80	61.43	47.12	47.40	38.80	20.22	10.43	0.00							
W14	98.65	77.13	74.00	57.88	62.92	66.38	74.44	60.65	60.82	52.44	33.79	22.61	13.70	0.00						
W15	88.32	68.99	64.77	55.21	51.79	47.34	43.31	43.30	41.45	42.98	39.65	51.82	47.94	55.20	0.00					
W16	106.85	85.08	81.19	66.44	68.01	68.02	70.93	62.32	61.51	56.61	40.76	40.50	30.73	27.88	36.82	0.00				
W17	107.51	85.75	81.85	67.12	68.66	68.63	71.45	62.94	62.11	57.26	41.46	41.20	31.41	28.40	37.04	0.71	0.00			
W18	108.33	89.82	85.63	76.67	72.93	67.87	61.71	64.28	62.32	64.44	60.09	70.42	64.61	68.61	21.49	43.75	43.60	0.00		
W19	109.05	87.32	83.40	68.76	70.17	69.99	72.53	64.32	63.45	58.78	43.18	43.09	33.31	30.08	37.23	2.59	1.90	42.83	0.00	
W20	111.51	89.71	85.84	70.96	72.71	72.82	75.75	67.11	66.32	61.30	45.14	43.82	33.73	28.99	40.88	4.83	4.30	46.05	3.66	0.00

Table V.S3. Reclassification table for Corine Land Cover 2006.

CLC code	Corine Land Cover class	New code	New category
111	Continuous urban fabric	1	Urban/artificial
112	Discontinuous urban fabric	1	Urban/artificial
121	Industrial or commercial units	1	Urban/artificial
122	Road and rail networks and associated land	1	Urban/artificial
124	Airports	1	Urban/artificial
131	Mineral extraction sites	1	Urban/artificial
132	Dump sites	1	Urban/artificial
133	Construction sites	1	Urban/artificial
141	Green urban areas	1	Urban/artificial
142	Sport and leisure facilities	1	Urban/artificial
211	Non-irrigated arable land	2	Non-irrigated arable land
212	Permanently irrigated land	3	Permanently irrigated land
221	Vineyards	4	Permanent crops
222	Fruit trees and berry plantations	4	Permanent crops
223	Olive groves	4	Permanent crops
231	Pastures	5	Pastures
242	Complex cultivation patterns	6	Complex cultivation patterns
243	Land principally occupied by agriculture and natural vegetation	7	Land principally occupied by agriculture and natural vegetation
244	Agro-forestry areas	8	Agro-forestry areas
311	Broad-leaved forest	9	Broad-leaved forest
312	Coniferous forest	10	Coniferous forest
313	Mixed forest	11	Mixed forest
321	Natural grasslands	12	Natural grasslands
322	Moors and heathland	13	Scrub and/or herbaceous vegetation
323	Sclerophyllous vegetation	13	Scrub and/or herbaceous vegetation
324	Transitional woodland-shrub	13	Scrub and/or herbaceous vegetation
332	Bare rocks	14	Open spaces with little or no vegetation
333	Sparsely vegetated areas	14	Open spaces with little or no vegetation
334	Burnt areas	14	Open spaces with little or no vegetation
512	Water bodies	15	Water bodies

Table V.S4. Full reclassification table for SIOSE 2005 considering all classes for Spain (total of 116 initial classes and 54 new).

SIOSE ID	SIOSE code	SIOSE class description	New class
831	PAG	Agrícola, Ganadero	Agriculture/livestock farm
103	LAA	Lámina de Agua Artificial	Artificial water line
331	PDA	Playas, dunas y arenales	Beach/sand dunes
311	-	Frondosas	Broadleaf
312	FDC	Frondosas Caducifolias	Broadleaf deciduous
313	FDP	Frondosas Perennifolias	Broadleaf evergreen
334	ZQM	Zonas Quemadas	Burnt areas
844	TCG	Camping	Camping
211	CHA	Arroz	Cereal crops
212	CHL	Cultivos Herbáceos distintos de Arroz	Cereal crops
521	ALC	Lagunas Costeras	Coastal lagoons
599	-	Compuestas	Composite types
316	CNF	Coniferas	Coniferous
413	HSA	Salinas Continentales	Continental salt pit
410	-	Humedales Continentales	Continental wetlands
336	RMB	Ramblas	Creek/stream bed
200	-	Cultivos	Crops
701	DHS	Dehesa	Dehesa
522	AES	Estuarios	Estuary
833	PMX	Minero Extractivo	Extractive mining
834	PPS	Piscifactoria	Fish farm
310	-	Arbolado Forestal	Forest tree cover
335	GNP	Glaciares y Nieves permanentes	Glaciers/permanent snow
859	ECG	Campo de Golf	Golf course
320	MTR	Matorral	Heathland/shrubland
210	-	Cultivos Herbáceos	Herbaceous crops
510	-	Aguas Continentales	Inland waters
513	ALG	Lagos y Lagunas	Lakes and lagoons
921	NVE	Vertederos y Escombreras	Landfills/slagheaps
422	HSM	Salinas Marinas	Marine salt pit
520	-	Aguas Marinas	Marine waters
420	-	Humedales Marinos	Marine wetlands
411	HPA	Zonas Pantanosas	Marshes/swamps
421	HMA	Marismas	Marshes/swamps
290	PRD	Prados	Meadows
412	HTU	Turberas	Mire/peatland
600	-	No Predefinida	Non-predefined
330	-	Terrenos sin Vegetación	Non-vegetated

SIOSE ID	SIOSE code	SIOSE class description	New class
333	SDN	Suelo Desnudo	Open soil
300	PST	Pastizal	Pastureland
700	-	Predefinida	Predefined
832	PFT	Forestal Primario	Production forest
880	-	Transporte	Roads/railways
881	NRV	Red Viaria	Roads/railways
882	NRF	Red Ferroviaria	Roads/railways
350	-	Roquedos	Rocky outcrops
351	ACM	Acantilados Marinos	Rocky outcrops
352	ARR	Afloramientos Rocosos y Roquedos	Rocky outcrops
353	CCH	Canchales	Rocky outcrops
354	CLC	Coladas Lávicas	Rocky outcrops
523	AMO	Mares y Océanos	Sea and ocean
99	-	Simples	Simple cover types
840	-	Terciario	Tertiary sector
102	ZAU	Zona Verde Artificial y Arbolado Urbano	Urban green/woodland
860	EPU	Parque Urbano	Urban park
100	-	Coberturas Artificiales	Urban/artificial
101	EDF	Edificación	Urban/artificial
104	VAP	Vial, Aparcamiento o Zona Peatonal sin Vegetación	Urban/artificial
111	OCT	Otras Construcciones	Urban/artificial
121	SNE	Suelo No Edificado	Urban/artificial
131	ZEV	Zonas de Extracción o Vertido	Urban/artificial
703	AAR	Asentamiento Agrícola Residencial	Urban/artificial
800	-	Artificial	Urban/artificial
810	-	Urbano Mixto	Urban/artificial
811	UCS	Casco	Urban/artificial
812	UEN	Ensanche	Urban/artificial
813	UDS	Discontinuo	Urban/artificial
820	-	Industrial	Urban/artificial
821	IPO	Polígono Industrial Ordenado	Urban/artificial
822	IPS	Polígono Industrial sin Ordenar	Urban/artificial
823	IAS	Industrial Aislada	Urban/artificial
830	-	Primario	Urban/artificial
841	TCO	Comercial y Oficinas	Urban/artificial
842	TCH	Complejo Hotelero	Urban/artificial
843	TPR	Parque Recreativo	Urban/artificial
850	-	Equipamiento Dotacional	Urban/artificial
851	EAI	Administrativo Institucional	Urban/artificial
852	ESN	Sanitario	Urban/artificial

SIOSE ID	SIOSE code	SIOSE class description	New class
853	ECM	Cementerio	Urban/artificial
854	EDU	Educación	Urban/artificial
855	EPN	Penitenciario	Urban/artificial
856	ERG	Religioso	Urban/artificial
857	ECL	Cultural	Urban/artificial
858	EDP	Deportivo	Urban/artificial
870	-	Infraestructuras	Urban/artificial
883	NPO	Portuario	Urban/artificial
884	NAP	Aeroportuario	Urban/artificial
890	-	Energía	Urban/artificial
891	NEO	Eólica	Urban/artificial
892	NSL	Solar	Urban/artificial
893	NCL	Nuclear	Urban/artificial
894	NEL	Eléctrica	Urban/artificial
895	NTM	Térmica	Urban/artificial
896	NHD	Hidroeléctrica	Urban/artificial
897	NGO	Gaseoducto Oleoducto	Urban/artificial
900	NTC	Telecomunicaciones	Urban/artificial
910	-	Suministro de Agua	Urban/artificial
911	NDP	Depuradoras y Potabilizadoras	Urban/artificial
912	NCC	Conducciones y Canales	Urban/artificial
913	NDS	Desalinizadora	Urban/artificial
920	-	Residuos	Urban/artificial
922	NPT	Plantas de Tratamiento	Urban/artificial
704	UER	Huerta Familiar	Urban/vegetable crops
514	AEM	Embalses	Water dam/reservoir
500	-	Coberturas de Agua	Water surface
511	ACU	Cursos de Agua	Water surface/line
512	-	Láminas de Agua	Water surface/line
400	-	Coberturas Húmedas	Wetlands
220	-	Leñosos	Woody crops
221	-	Frutales	Woody crops
222	LFC	Frutales Cítricos	Woody crops
223	LFN	Frutales No Cítricos	Woody crops
231	LVI	Viñedo	Woody crops
232	LOL	Olivar	Woody crops
241	LOC	Otros Leñosos	Woody crops
702	OVD	Olivar-Viñedo	Woody crops

Table V.S5. Resistance values/weights attributed to each new SIOSE class (total 29) in the study area.

SIOSE 2005 new class	Resistance weight
Agriculture/livestock farm	1
Artificial water line	1
Broadleaf deciduous	1
Broadleaf evergreen	1
Burnt areas	10
Camping	25
Cereal crops	1
Coniferous	1
Continental salt pit	50
Creek/stream bed	1
Dehesa	1
Extractive mining	25
Golf course	25
Heathland/shrubland	1
Landfills/slagheaps	25
Marshes/swamps	1
Meadows	1
Open soil	1
Pastureland	1
Production forest	1
Roads/railways	75
Rocky outcrops	25
Urban green/woodland	1
Urban park	25
Urban/artificial	100
Urban/vegetable crops	50
Water dam/reservoir	50
Water surface/line	1
Woody crops	25

Table V.S6. Pairwise Fst values between sampled *P. cultripes* populations.

Pop/ Fst	C1	C2	C3	C4	C5	C6	C7	C8	C9	C10	C11	C12	C13	C14	C15	C16
C1																
C2	0.166															
C3	0.394	0.231														
C4	0.136	0.066	0.239													
C5	0.130	0.036	0.246	0.021												
C6	0.100	0.046	0.200	0.032	0.021											
C7	0.132	0.036	0.246	0.047	0.019	0.031										
C8	0.097	0.089	0.273	0.034	0.030	0.023	0.049									
C9	0.101	0.040	0.240	0.053	0.028	0.043	0.016	0.050								
C10	0.305	0.149	0.359	0.196	0.133	0.174	0.130	0.212	0.146							
C11	0.137	0.073	0.283	0.073	0.043	0.045	0.039	0.048	0.030	0.189						
C12	0.211	0.143	0.230	0.145	0.138	0.087	0.149	0.153	0.130	0.270	0.150					
C13	0.126	0.077	0.240	0.052	0.052	0.044	0.076	0.050	0.041	0.204	0.049	0.122				
C14	0.131	0.111	0.271	0.066	0.062	0.068	0.080	0.054	0.058	0.208	0.061	0.155	0.001			
C15	0.163	0.147	0.341	0.145	0.098	0.108	0.086	0.125	0.083	0.208	0.113	0.211	0.136	0.132		
C16	0.114	0.079	0.225	0.044	0.054	0.065	0.054	0.051	0.026	0.171	0.041	0.123	0.011	0.017	0.120	

Table V.S7. Pairwise G''st values between sampled *P. cultripes* populations.

Pop/ G"st	C1	C2	C3	C4	C5	C6	C7	C8	C9	C10	C11	C12	C13	C14	C15	C16
C1	0.000															
C2	0.267	0.000														
C3	0.522	0.332	0.000													
C4	0.247	0.115	0.381	0.000												
C5	0.222	0.060	0.357	0.039	0.000											
C6	0.180	0.080	0.317	0.060	0.039	0.000										
C7	0.216	0.059	0.355	0.083	0.033	0.055	0.000									
C8	0.164	0.148	0.397	0.062	0.052	0.041	0.083	0.000								
C9	0.171	0.067	0.349	0.097	0.049	0.077	0.027	0.087	0.000							
C10	0.456	0.227	0.477	0.329	0.210	0.290	0.202	0.333	0.229	0.000						
C11	0.238	0.123	0.428	0.134	0.076	0.083	0.067	0.086	0.054	0.305	0.000					
C12	0.339	0.228	0.323	0.256	0.233	0.151	0.242	0.253	0.216	0.408	0.254	0.000				
C13	0.238	0.138	0.384	0.102	0.099	0.085	0.138	0.093	0.077	0.349	0.093	0.220	0.000			
C14	0.243	0.197	0.432	0.128	0.118	0.129	0.145	0.102	0.109	0.354	0.114	0.278	0.001	0.000		
C15	0.249	0.228	0.470	0.246	0.157	0.181	0.135	0.199	0.133	0.307	0.184	0.325	0.235	0.227	0.000	
C16	0.226	0.147	0.380	0.089	0.109	0.130	0.103	0.100	0.052	0.306	0.081	0.231	0.023	0.034	0.216	0.000

Table V.S8. Pairwise Dest values between sampled *P. cultripes* populations.

Pop/ Dest	C1	C2	C3	C4	C5	C6	C7	C8	C9	C10	C11	C12	C13	C14	C15	C16
C1	0.000															
C2	0.086	0.000														
C3	0.146	0.046	0.000													
C4	0.104	0.016	0.086	0.000												
C5	0.071	0.005	0.055	0.004	0.000											
C6	0.061	0.027	0.055	0.010	0.004	0.000										
C7	0.067	0.006	0.038	0.016	0.003	0.009	0.000									
C8	0.050	0.033	0.081	0.012	0.004	0.005	0.010	0.000								
C9	0.047	0.008	0.059	0.008	0.003	0.008	0.003	0.015	0.000							
C10	0.146	0.038	0.065	0.100	0.042	0.082	0.028	0.068	0.049	0.000						
C11	0.062	0.015	0.083	0.025	0.017	0.014	0.007	0.013	0.006	0.074	0.000					
C12	0.103	0.041	0.048	0.064	0.039	0.031	0.049	0.048	0.057	0.100	0.073	0.000				
C13	0.089	0.041	0.083	0.019	0.015	0.013	0.023	0.011	0.010	0.114	0.015	0.070	0.000			
C14	0.073	0.055	0.115	0.036	0.024	0.046	0.031	0.016	0.024	0.119	0.027	0.095	0.000	0.000		
C15	0.055	0.053	0.065	0.076	0.023	0.045	0.030	0.028	0.025	0.056	0.047	0.066	0.063	0.059	0.000	
C16	0.074	0.033	0.088	0.014	0.022	0.042	0.018	0.022	0.004	0.084	0.018	0.062	0.002	0.006	0.087	0.000

Table V.S9. Pairwise Fst values between sampled *P. waltl* populations.

Pop/ Fst	W1	W2	W3	W4	W5	W6	W7	W8	W9	W10	W11	W12	W13	W14	W15	W16	W17	W18	W19	W20
W1	0.000																			
W2	0.133	0.000																		
W3	0.189	0.004	0.000																	
W4	0.236	0.217	0.278	0.000																
W5	0.124	0.122	0.152	0.099	0.000															
W6	0.280	0.266	0.332	0.293	0.187	0.000														
W7	0.112	0.097	0.138	0.170	0.079	0.162	0.000													
W8	0.099	0.116	0.164	0.146	0.095	0.186	0.033	0.000												
W9	0.121	0.120	0.155	0.156	0.111	0.261	0.050	0.033	0.000											
W10	0.208	0.159	0.212	0.063	0.090	0.225	0.120	0.104	0.121	0.000										
W11	0.198	0.166	0.217	0.093	0.111	0.202	0.101	0.081	0.109	0.037	0.000									
W12	0.246	0.227	0.273	0.140	0.157	0.237	0.146	0.119	0.166	0.072	0.080	0.000								
W13	0.313	0.274	0.315	0.192	0.194	0.255	0.188	0.176	0.211	0.124	0.153	0.069	0.000							
W14	0.295	0.259	0.309	0.216	0.213	0.294	0.180	0.163	0.208	0.121	0.095	0.107	0.191	0.000						
W15	0.239	0.230	0.279	0.204	0.148	0.282	0.137	0.118	0.142	0.122	0.110	0.115	0.164	0.172	0.000					
W16	0.322	0.270	0.308	0.196	0.187	0.251	0.199	0.187	0.230	0.107	0.111	0.110	0.112	0.153	0.187	0.000				
W17	0.295	0.250	0.291	0.168	0.167	0.234	0.169	0.148	0.203	0.086	0.101	0.064	0.086	0.128	0.164	0.007	0.000			
W18	0.336	0.307	0.394	0.384	0.292	0.427	0.271	0.252	0.268	0.306	0.266	0.372	0.384	0.386	0.337	0.370	0.369	0.000		
W19	0.268	0.222	0.259	0.178	0.174	0.224	0.151	0.135	0.190	0.094	0.093	0.108	0.116	0.138	0.176	0.029	0.031	0.324	0.000	
W20	0.309	0.282	0.333	0.252	0.235	0.270	0.217	0.154	0.230	0.146	0.138	0.129	0.186	0.147	0.167	0.124	0.107	0.392	0.109	0.000

Table V.S10. Pairwise G''st values between sampled *P. waltl* populations.

Pop/ G''st	W1	W2	W3	W4	W5	W6	W7	W8	W9	W10	W11	W12	W13	W14	W15	W16	W17	W18	W19	W20
W1	0.000																			
W2	0.272	0.000																		
W3	0.366	0.010	0.000																	
W4	0.482	0.463	0.564	0.000																
W5	0.274	0.283	0.344	0.229	0.000															
W6	0.544	0.542	0.628	0.594	0.419	0.000														
W7	0.248	0.225	0.315	0.399	0.197	0.364	0.000													
W8	0.216	0.268	0.369	0.339	0.233	0.413	0.087	0.000												
W9	0.255	0.265	0.328	0.345	0.266	0.549	0.122	0.081	0.000											
W10	0.460	0.370	0.477	0.146	0.227	0.500	0.311	0.268	0.293	0.000										
W11	0.442	0.390	0.496	0.220	0.282	0.459	0.265	0.214	0.268	0.097	0.000									
W12	0.532	0.515	0.597	0.319	0.385	0.516	0.367	0.298	0.393	0.180	0.204	0.000								
W13	0.645	0.590	0.647	0.415	0.453	0.524	0.444	0.413	0.470	0.291	0.364	0.158	0.000							
W14	0.613	0.565	0.643	0.471	0.501	0.611	0.433	0.390	0.470	0.290	0.230	0.250	0.421	0.000						
W15	0.480	0.485	0.555	0.430	0.338	0.564	0.316	0.269	0.310	0.279	0.256	0.259	0.348	0.369	0.000					
W16	0.674	0.593	0.646	0.430	0.444	0.528	0.483	0.453	0.526	0.258	0.271	0.258	0.248	0.344	0.406	0.000				
W17	0.630	0.560	0.625	0.377	0.403	0.504	0.415	0.362	0.472	0.211	0.252	0.153	0.196	0.294	0.363	0.016	0.000			
W18	0.580	0.549	0.632	0.682	0.576	0.701	0.518	0.477	0.486	0.579	0.516	0.700	0.686	0.695	0.589	0.665	0.684	0.000		
W19	0.579	0.503	0.564	0.404	0.424	0.487	0.377	0.337	0.447	0.234	0.233	0.260	0.265	0.320	0.394	0.069	0.073	0.608	0.000	
W20	0.613	0.583	0.651	0.521	0.527	0.531	0.488	0.344	0.491	0.326	0.313	0.282	0.389	0.309	0.341	0.263	0.231	0.675	0.239	0.000

Table V.S11. Pairwise Dest values between sampled *P. waltl* populations.

Pop/ Dest	W1	W2	W3	W4	W5	W6	W7	W8	W9	W10	W11	W12	W13	W14	W15	W16	W17	W18	W19	W20
W1	0.000																			
W2	0.091	0.000																		
W3	0.141	0.000	0.000																	
W4	0.194	0.219	0.273	0.000																
W5	0.067	0.104	0.145	0.093	0.000															
W6	0.216	0.233	0.301	0.276	0.165	0.000														
W7	0.081	0.066	0.110	0.190	0.078	0.153	0.000													
W8	0.084	0.114	0.151	0.096	0.051	0.192	0.030	0.000												
W9	0.086	0.092	0.120	0.118	0.090	0.281	0.043	0.019	0.000											
W10	0.242	0.138	0.193	0.063	0.088	0.256	0.139	0.058	0.077	0.000										
W11	0.207	0.170	0.222	0.065	0.080	0.185	0.094	0.063	0.099	0.021	0.000									
W12	0.324	0.325	0.333	0.118	0.220	0.247	0.202	0.153	0.199	0.069	0.082	0.000								
W13	0.339	0.303	0.298	0.185	0.244	0.235	0.225	0.186	0.216	0.154	0.191	0.048	0.000							
W14	0.334	0.299	0.309	0.211	0.238	0.302	0.188	0.149	0.245	0.110	0.098	0.127	0.203	0.000						
W15	0.171	0.197	0.221	0.199	0.092	0.237	0.097	0.047	0.093	0.085	0.067	0.090	0.149	0.149	0.000					
W16	0.425	0.358	0.387	0.182	0.257	0.264	0.299	0.196	0.273	0.103	0.105	0.089	0.102	0.148	0.177	0.000				
W17	0.374	0.307	0.322	0.163	0.222	0.251	0.259	0.162	0.254	0.086	0.103	0.046	0.071	0.103	0.153	0.001	0.000			
W18	0.256	0.261	0.307	0.363	0.298	0.351	0.243	0.234	0.206	0.270	0.232	0.399	0.389	0.381	0.253	0.307	0.393	0.000		
W19	0.322	0.250	0.236	0.160	0.232	0.230	0.214	0.158	0.254	0.107	0.106	0.080	0.105	0.128	0.165	0.015	0.014	0.289	0.000	
W20	0.346	0.311	0.323	0.242	0.297	0.226	0.260	0.158	0.223	0.142	0.127	0.091	0.139	0.117	0.120	0.068	0.069	0.289	0.071	0.0000

Table V.S12. Pairwise migration rates between populations of *P. cultripes* as estimated by BayesAss. Direction of migration (from population X to population Y) indicated in rows. Population numbers as in Table 1.

Pc/Nm	C1	C2	C3	C4	C5	C6	C7	C8	C9	C10	C11	C12	C13	C14	C15	C16
C1	0.7878	0.0133	0.0136	0.0133	0.0134	0.0134	0.0133	0.0133	0.0180	0.0140	0.0132	0.0138	0.0158	0.0135	0.0168	0.0134
C2	0.0126	0.6771	0.0158	0.0105	0.0104	0.0103	0.0102	0.0106	0.1623	0.0122	0.0103	0.0112	0.0125	0.0106	0.0130	0.0104
C3	0.0121	0.0117	0.8193	0.0118	0.0121	0.0117	0.0118	0.0121	0.0129	0.0122	0.0123	0.0120	0.0120	0.0119	0.0121	0.0119
C4	0.0100	0.0098	0.0100	0.6766	0.0099	0.0098	0.0099	0.0097	0.1813	0.0099	0.0098	0.0118	0.0111	0.0099	0.0105	0.0100
C5	0.0121	0.0113	0.0117	0.0116	0.6784	0.0118	0.0114	0.0116	0.1386	0.0119	0.0114	0.0116	0.0162	0.0118	0.0273	0.0115
C6	0.0098	0.0099	0.0097	0.0098	0.0096	0.6765	0.0098	0.0098	0.1727	0.0098	0.0097	0.0104	0.0110	0.0098	0.0217	0.0100
C7	0.0110	0.0108	0.0189	0.0108	0.0110	0.0106	0.6775	0.0106	0.1473	0.0130	0.0107	0.0108	0.0167	0.0107	0.0190	0.0107
C8	0.0118	0.0111	0.0111	0.0112	0.0111	0.0109	0.0111	0.6777	0.1571	0.0122	0.0111	0.0110	0.0142	0.0111	0.0165	0.0110
C9	0.0246	0.0113	0.0199	0.0114	0.0110	0.0114	0.0111	0.0109	0.7299	0.0174	0.0111	0.0197	0.0445	0.0113	0.0428	0.0116
C10	0.0111	0.0111	0.0163	0.0113	0.0113	0.0110	0.0111	0.0110	0.0166	0.8156	0.0112	0.0116	0.0119	0.0112	0.0166	0.0112
C11	0.0117	0.0105	0.0105	0.0103	0.0103	0.0104	0.0105	0.0102	0.0919	0.0107	0.6770	0.0110	0.0621	0.0105	0.0418	0.0106
C12	0.0112	0.0111	0.0187	0.0110	0.0113	0.0113	0.0111	0.0109	0.0336	0.0155	0.0109	0.7950	0.0128	0.0111	0.0136	0.0111
C13	0.0109	0.0105	0.0116	0.0104	0.0103	0.0104	0.0105	0.0104	0.0258	0.0119	0.0106	0.0186	0.8137	0.0103	0.0137	0.0105
C14	0.0098	0.0101	0.0103	0.0098	0.0099	0.0101	0.0102	0.0101	0.0133	0.0102	0.0100	0.0105	0.1733	0.6769	0.0153	0.0102
C15	0.0106	0.0104	0.0106	0.0103	0.0102	0.0105	0.0103	0.0105	0.0129	0.0130	0.0105	0.0106	0.0112	0.0103	0.8380	0.0103
C16	0.0110	0.0099	0.0132	0.0098	0.0098	0.0098	0.0100	0.0098	0.0243	0.0109	0.0095	0.0112	0.1618	0.0099	0.0126	0.6765

Table V.S13. Pairwise migration rates between populations of *P. waltl* as estimated by BayesAss. Direction of migration (from population X to population Y) indicated in rows. Population numbers as in Table 1.

Pw/ Nm	W1	W2	W3	W4	W5	W6	W7	W8	W9	W10	W11	W12	W13	W14	W15	W16	W17	W18	W19	W20
W1	0.8296	0.0200	0.0083	0.0086	0.0087	0.0083	0.0084	0.0084	0.0085	0.0081	0.0083	0.0083	0.0082	0.0085	0.0084	0.0083	0.0083	0.0084	0.0082	0.0083
W2	0.0140	0.8284	0.0082	0.0116	0.0090	0.0083	0.0084	0.0085	0.0111	0.0083	0.0083	0.0083	0.0082	0.0082	0.0083	0.0084	0.0083	0.0091	0.0085	0.0085
W3	0.0114	0.1151	0.6780	0.0118	0.0114	0.0114	0.0113	0.0113	0.0116	0.0115	0.0116	0.0115	0.0116	0.0115	0.0113	0.0114	0.0115	0.0115	0.0116	0.0117
W4	0.0092	0.0094	0.0091	0.8212	0.0123	0.0092	0.0091	0.0090	0.0126	0.0089	0.0091	0.0089	0.0091	0.0089	0.0091	0.0090	0.0089	0.0091	0.0091	0.0089
W5	0.0132	0.0084	0.0070	0.0239	0.8223	0.0092	0.0070	0.0069	0.0247	0.0069	0.0069	0.0073	0.0070	0.0069	0.0073	0.0069	0.0070	0.0070	0.0072	0.0071
W6	0.0106	0.0105	0.0103	0.0113	0.0104	0.7980	0.0105	0.0102	0.0135	0.0103	0.0105	0.0103	0.0105	0.0104	0.0107	0.0103	0.0104	0.0103	0.0105	0.0105
W7	0.0091	0.0090	0.0091	0.0092	0.0095	0.0089	0.6757	0.0090	0.1614	0.0089	0.0090	0.0090	0.0091	0.0091	0.0091	0.0092	0.0089	0.0089	0.0089	0.0089
W8	0.0110	0.0181	0.0101	0.0217	0.0114	0.0100	0.0100	0.6768	0.1223	0.0099	0.0097	0.0099	0.0098	0.0100	0.0101	0.0097	0.0098	0.0101	0.0099	0.0098
W9	0.0204	0.0132	0.0093	0.0197	0.0133	0.0092	0.0092	0.0093	0.7902	0.0091	0.0094	0.0093	0.0092	0.0094	0.0136	0.0092	0.0092	0.0093	0.0094	0.0091
W10	0.0092	0.0094	0.0090	0.1561	0.0092	0.0092	0.0094	0.0095	0.0103	0.6759	0.0094	0.0094	0.0093	0.0091	0.0094	0.0093	0.0094	0.0091	0.0093	0.0093
W11	0.0090	0.0091	0.0090	0.1594	0.0090	0.0089	0.0089	0.0089	0.0110	0.0089	0.6757	0.0090	0.0089	0.0087	0.0097	0.0088	0.0092	0.0089	0.0097	0.0091
W12	0.0104	0.0093	0.0087	0.0640	0.0097	0.0088	0.0090	0.0085	0.0137	0.0089	0.0089	0.6929	0.0273	0.0118	0.0596	0.0087	0.0089	0.0087	0.0113	0.0109
W13	0.0087	0.0086	0.0089	0.0094	0.0090	0.0086	0.0087	0.0086	0.0088	0.0088	0.0089	0.0097	0.8301	0.0089	0.0091	0.0087	0.0087	0.0088	0.0096	0.0093
W14	0.0091	0.0094	0.0094	0.0110	0.0095	0.0093	0.0094	0.0095	0.0094	0.0092	0.0093	0.0108	0.0100	0.7868	0.0100	0.0093	0.0091	0.0093	0.0339	0.0162
W15	0.0091	0.0091	0.0089	0.0103	0.0115	0.0092	0.0090	0.0090	0.0140	0.0089	0.0090	0.0093	0.0093	0.0092	0.8188	0.0091	0.0089	0.0091	0.0090	0.0093
W16	0.0090	0.0091	0.0090	0.0090	0.0091	0.0089	0.0092	0.0091	0.0090	0.0091	0.0092	0.0093	0.0090	0.0090	0.0092	0.6757	0.0091	0.0090	0.1610	0.0091
W17	0.0086	0.0086	0.0088	0.0085	0.0086	0.0086	0.0085	0.0086	0.0086	0.0083	0.0087	0.0086	0.0087	0.0087	0.0087	0.0086	0.6751	0.0087	0.1684	0.0102
W18	0.0091	0.0089	0.0112	0.0091	0.0090	0.0089	0.0108	0.0110	0.0091	0.0114	0.0106	0.0089	0.0090	0.0091	0.0089	0.0102	0.0109	0.8159	0.0091	0.0089
W19	0.0085	0.0086	0.0087	0.0105	0.0085	0.0083	0.0085	0.0084	0.0087	0.0086	0.0087	0.0086	0.0098	0.0094	0.0088	0.0087	0.0087	0.0085	0.8317	0.0098
W20	0.0087	0.0087	0.0086	0.0138	0.0085	0.0085	0.0086	0.0085	0.0086	0.0084	0.0086	0.0089	0.0088	0.0093	0.0137	0.0085	0.0088	0.0086	0.0209	0.8130

Table V.S14. Model selection results for average effective population sizes (Nb) for the test species *P. cultripes* (top) and *P. waltl* (bottom). AICc – Akaike Information Criterion value (with a correction for finite sample size), IBD – Isolation-by-distance model. IntOnly – Intercept-only/ null model; IBD and IntOnly are used here for comparing the relative support of 'InvNbSum' and 'ModGeoInvNb' models which translate a density-dependent effect on connectivity (lower values represent greater support).

Species	Dist	AICc. Null	AICc. IBD	AICc. InvNbSum	AICc. ModGeoInvNb
P. cultripes	Dest	-569.3	-566.9	-569.8	-566.7
	FST	-482.5	-483.0	-480.4	-481.0
	Gst	-360.5	-363.6	-358.9	-358.7
	MigRate1	-530.2	-530.6	-527.5	-528.8
	MigRate2	-475.5	-475.9	-472.9	-473.7
	MigRate.avg	-576.0	-582.0	-573.6	-577.6
P. waltl	Dest	-387.6	-500.6	-387.3	-430.7
	FST	-515.8	-623.6	-516.0	-564.1
	Gst	-230.5	-342.3	-229.8	-275.0
	MigRate1	-876.4	-887.5	-875.2	-879.6
	MigRate2	-1054.9	-1058.7	-1052.9	-1054.7
	MigRate.avg	-995.8	-998.9	-993.9	-996.3

InvNbSum = 1 / (Nb_pop1 + Nb_pop2)

ModGeoInvNb = EucGeoDistance_pop1,2 / (Nb_pop1 + Nb_pop2)

Capítulo IV

Escala Local

Artículo VI: Los ratios entre el tamaño efectivo poblacional y el de censo en dos especies Casi Amenazadas de anfibios mediterráneos: *Pleurodeles waltl* y *Pelobates cultripes*

Effective to census population size ratios in two Near Threatened Mediterranean amphibians: *Pleurodeles waltl* and *Pelobates cultripes*

J. Gutiérrez-Rodríguez, G. Sánchez-Montes, I. Martínez-Solano

Publicado en

Conservation Genetics 2017 In Press

DOI: 10.1007/s10592-017-0971-5

Abstract

Efforts to mitigate amphibian declines are hindered by a lack of information about basic aspects of their biology and demography. The effective to census population size ratio (Ne/Nc) is one of the most important parameters for the management of wildlife populations because it combines information on population abundance and genetic diversity and helps predict population viability in the long term. Few studies have calculated this ratio in amphibians, which sometimes show low ratios, associated with a higher extinction risk. Here we integrate field-based (capture-mark-recapture studies, egg string counts) and molecular approaches (estimation of the effective number of breeders (Nb) and the effective population size (Ne) based on genotypes from larval cohorts and candidate parents) to produce the first estimates of the Ne/Nc and Nb/Nc ratios in two amphibians, the Iberian ribbed newt *Pleurodeles waltl* and the western spadefoot *Pelobates cultripes*. Additionally, we investigate sex-biased dispersal in both species based on direct (field observations) and indirect (genetic) evidence. Both species showed similar ratios, slightly lower in *Pleurodeles* (0.21-0.24) than in *Pelobates* (0.25-0.30). Observed displacement rates were low in both species (*P. waltl* = 0.51%; *P. cultripes* = 1.23%). We found no evidence for sex-biased dispersal in *P. cultripes*, but both direct and indirect evidences suggest a tendency for female-biased dispersal in *P. waltl*. We discuss differences in the genetic estimates of Ne and Nb provided by three inference methods and the implications of our findings for the management of these species, characteristic of Mediterranean wetlands in the Iberian Peninsula and listed as Near Threatened.

Resumen

Los esfuerzos para mitigar el declive de poblaciones de anfibios están limitados por la falta de información sobre aspectos básicos de su biología y demografía. La razón entre el tamaño efectivo y el tamaño de censo de la población (Ne/Nc) es uno de los parámetros más importantes para la gestión de poblaciones silvestres, porque combina información sobre la abundancia de la población y su diversidad genética, y ayuda por tanto a predecir la viabilidad de la población a largo plazo. Pocos estudios han calculado este ratio en anfibios, que generalmente presentan valores bajos, asociados a un mayor riesgo de extinción. En este estudio se han integrado datos tomados directamente en el campo (captura-marcaje-recaptura y conteos de puestas) y aproximaciones moleculares (estimas del número efectivo de reproductores (Nb) y del tamaño efectivo de la población (Ne), basados en genotipos de cohortes de larvas y de padres potenciales) para obtener las primeras estimas de los ratios Ne/Nc y Nb/Nc en dos especies de anfibios ibéricos, el gallipato (*Pleurodeles waltl*) y el sapo de espuelas (*Pelobates cultripes*). Además, se ha investigado la posible dispersión diferencial entre sexos en ambas especies, mediante evidencias directas (observaciones de campo) e indirectas (genéticas). Ambas especies mostraron ratios similares de Ne/Nc y Nb/Nc, ligeramente inferiores en *Pleurodeles* (0,21-0,24) que en *Pelobates* (0,25-0,30). Las tasas de dispersión observadas fueron bajas en ambas especies (*P. waltl* = 0,51%, *P. cultripes* = 1,23%). No se encontraron evidencias de dispersión diferencial entre sexos en *P. cultripes*, mientras que en *P. waltl* existen evidencias tanto directas como indirectas que sugieren una tendencia a una mayor tasa de dispersión en hembras. Finalmente, se discuten las diferencias en las estimas de Ne y Nb obtenidas a partir de tres métodos genéticos de inferencia y las implicaciones de los resultados obtenidos para el manejo de estas especies, catalogadas como Casi Amenazadas y características de sistemas acuáticos mediterráneos de la península ibérica.

Introduction

The effective population size (Ne) is an important parameter linking evolutionary and conservation biology. It is defined as the size of an 'ideal' population that experiences the same rate of change of allele frequencies or heterozygosity as the target population (Wright, 1931) and thus its estimation can help predict the long–term viability of populations (Luikart *et al*., 2010). Populations with a small size, in the absence of migration, experience a loss of genetic diversity determined by genetic drift, and are subject to increased inbreeding, making them more vulnerable to extinction due to stochastic processes (Frankham *et al*., 2002). Ne can be affected by several demographic factors: sex ratio, variation in offspring number, inbreeding, age and stage structure, changes in population size, and spatial and genetic structure (Charlesworth, 2009). As a consequence, direct estimates of Ne are hard to obtain for many species in the wild, and most studies have increasingly relied on the use of molecular approaches for indirect calculation of Ne (Wang *et al*., 2011; Baalsrud *et al*., 2014; Wilson *et al*., 2014; Kamath *et al*., 2015). Currently, several methods are able to estimate contemporary Ne based on samples from a single generation (e.g. Tallmon *et al*., 2008; Jones & Wang, 2010; Do *et al*., 2014), as opposed to the traditionally used two-sample method, that requires the use of time-distant samples (Fisher, 1930; Nei & Tajima, 1981; Turner *et al*., 2001).

From a conservation perspective, estimates of contemporary Ne provide very useful information on population status. In addition, calculation of the ratio between the effective and census population size (Nc) can provide more accurate forecasts of population viability (Nunney & Elam, 1994; Frankham, 1995). In fact, this ratio is considered one of the most important parameters for the management of wildlife populations (Luikart *et al*., 2010). The ratio Ne/Nc tends to be low in general, but shows wide variation across taxa (Frankham, 1995). Despite the importance of this parameter, most studies estimating Ne do not calculate Nc, mostly on account of logistic limitations related to obtaining sufficient and accurate demographic information from target species (Palstra & Fraser, 2012).

Amphibians are considered the most endangered group of vertebrates, with 41% of species included in some of the IUCN categories representing threat of extinction (Hoffmann *et al*., 2010). Causes of declines at the global level are multiple and, in some cases, poorly understood. At the base of this knowledge gap there is an incomplete understanding of basic aspects of the biology of most species, including demographic parameters like population sizes or migration rates. Previous studies analyzing the relationship Ne/Nc have found generally low ratios, although in some cases higher ratios have been found in small populations, which has been associated with mechanisms of genetic compensation (Gill, 1978; Easteal, 1985; Scribner *et al*., 1997; Jehle *et al*., 2001; Brede & Beebee, 2006; Beebee, 2009; Álvarez *et al*., 2015).

Studies in amphibians are still scarce, and results are difficult to compare due to differences in methodological approaches. For instance, amphibian populations often comprise overlapping generations, which complicates estimation of Ne. Some studies have estimated Ne by grouping samples from different cohorts, but this methodology has been criticized (Waples *et al*., 2014), since large biases can be introduced depending on two biological traits (maximum longevity and adult life span) that are usually not considered. Alternatively, other studies have estimated the effective number of breeders (Nb) based on sibship reconstruction, and used direct records of breeding activity (such as egg mass counts) to assess the reliability of results (Sánchez-Montes *et al*., in review). However, in many species eggs are laid individually rather than in masses and Nb can only be estimated via genetic methods. In spite of the difficulties, valuable insights on population demography to inform conservation programs can be obtained from the integration of field-based information (capture-mark-recapture data, counts of egg masses) and molecular approaches.

Amphibians in Mediterranean areas face a high extinction risk in the medium to long term (Araújo *et al*., 2011). Many species, including several geographically restricted endemics, depend on ephemeral water bodies for reproduction, which availability is expected to decrease due to increased aridification and changes in land use. Attempts to model potential responses of Mediterranean pond-breeding amphibians to future scenarios (e. g. Fortuna *et al*., 2006) are however hindered by the previously mentioned lack of information

on basic demographic parameters in most species. In this study, we provide new field- and molecular- based data on Ne, Nb and Nc for two syntopic, pond-breeding amphibians that are characteristic of Mediterranean wetlands: the Iberian ribbed newt, *Pleurodeles waltl* Michahelles, 1830 and the western spadefoot, *Pelobates cultripes* (Cuvier, 1829). In addition, we test for sex-biased dispersal in each species based on a combination of field observations and molecular tools. The two study species are broadly co-distributed across the Iberian Peninsula (García-París *et al*., 2004), but their populations are declining due to habitat fragmentation, aquatic habitat loss, road mortality and the introduction of invasive species (Montori *et al*., 2002; Tejedo & Reques, 2002), and consequently they are listed as Near Threatened (NT) by the IUCN (Beja *et al*., 2009; Beja *et al*., 2016). Our aim is to provide information to help design genetic monitoring programs accounting for patterns of local abundance and connectivity and prevent the loss of genetic diversity and evolutionary potential in the long term.

Methods

Study area, sampling, and adult population size estimates

The study area is a semi-permanent aquatic system comprising a large pond (Laguna de Valdemanco) and the surrounding flooded meadows, with a maximum extension of 12800 m^2, and a maximum depth of 1 meter (Sánchez-Montes & Martínez-Solano, 2011), and is located near Valdemanco (Madrid, central Spain). We estimated the annual adult population size (Na; Frankham, 1995), an approximation to Nc, for *P. cultripes* and *P. waltl* based on capture-mark-recapture (CMR) data. Capture sessions were performed during nocturnal surveys in the breeding seasons of 2010 to 2013. In *P. cultripes*, the breeding season usually extends from February to April, whereas in *P. waltl* it is a bit longer, from December to May. Adults of both species were captured by hand, sexed based on external morphological features and marked with subcutaneous PIT tags (8 mm AVID M.U.S.I.C. chips, EzID, Greeley, Colorado, USA) that provided them with an individual identifying code, readable with an AVID Minitracker II device. All specimens were released back into their place of capture after marking and we stored tissue samples from one toe clip of each specimen in 100% ethanol for subsequent genetic analyses.

CMR data were analyzed following Pollock's "Robust Design" procedure (Pollock, 1982) in program MARK 7 (White & Burnham, 1999). This multimodel approach is well suited to estimate Na in amphibians (see Sánchez-Montes *et al*., in review). It relies on some primary sampling periods (in this case, the different years) and some secondary periods within them (in this case, the capture sessions within each year's breeding season). Individual capture histories comprised thirteen capture sessions in the case of *P. cultripes*, and sixteen for *P. waltl*. Catchability parameters are modeled within each year provided that population closure can be assumed across all secondary sampling periods within each primary period. This information is then used to estimate the annual survival rate and Na.

We tested the likelihood of different models in which annual survival was modeled either as constant or as time and/or sex dependent. We also modeled the probability of individuals entering or exiting the "surveyable fraction of the population" (i. e. adult breeders) from year to year. This parameter accounts for individual migration in or out of the study area but also for the possibility that some adults might skip some breeding season (s). The probability of entering (or exiting) the adult breeding fraction was modeled either as random, dependent of the last state of the individual, or zero. All models were ranked based on their Akaike Information Criterion (AICc) (Akaike, 1974; Burnham & Anderson, 2002). Annual estimates of Na for each sex of each species were calculated as the weighted average of estimates from the candidate models.

Molecular methods and estimation of Nb and Ne

A subset of adult, marked individuals of the two species (55 males and 52 females for *P. waltl*; 47 males and 48 females in *P. cultripes*) as well as a sample of the offspring of each species (95 larvae of *P. waltl* collected in 2010 and 183 tadpoles of *P. cultripes* collected in 2013) were genotyped to estimate Nb and Ne. *Pleurodeles waltl* females lay eggs individually, attaching them to the vegetation, whereas *P. cultripes* females produce egg strings that can be counted and taken as a proxy for the number of breeding females, thus allowing calibration of genetic estimates of Nb. Particular care was devoted to ensuring that offspring samples provided an unbiased representation of most full sib and half sib families present

in the study area by comprehensive sampling throughout the pond (*P. waltl*) and by including samples from all recorded egg strings of *P. cultripes* in the season (75 in 2013).

Genomic DNA was extracted from tissue samples (tail tips of larvae and toe clips of adults) with NucleoSpin Tissue-Kits (Macherey-Nagel). Sixteen and 21 specific polymorphic microsatellite loci were used for genotyping individuals of *P. cultripes* and *P. waltl*, respectively (van de Vliet *et al*., 2009; Gutiérrez-Rodríguez & Martínez-Solano, 2013; Gutiérrez-Rodríguez *et al*., 2014; Álvarez *et al*., 2015, see Tables VI.S1 and VI.S2). PCR reactions were performed using Type-it Microsatellite PCR kits (Qiagen). All reactions were carried out in a total volume of 15 µl, containing 7.5 µl of Master Mix, 1.2 µl of primer mix (0.2 µM of each primer) and 25 ng of template DNA. Multiplex reactions have previously been described in Gutiérrez-Rodríguez and Martínez-Solano (2013) and Gutiérrez-Rodríguez *et al*. (2014). PCR products were genotyped on an ABI PRISM 3730 sequencer with the GeneScan 500 LIZ size standard (Applied Biosystems), and fragments were scored and binned using GENEMAPPER v4.0 (Applied Biosystems).

Micro-Checker v2.2.3 (van Oosterhout *et al*., 2004) was used to test for evidence of stuttering, large allele dropout and presence of null alleles in each species, using a 99% confidence interval and 1,000 randomizations. Deviations from Hardy-Weinberg equilibrium (HWE) and evidence of linkage disequilibrium (LD) were tested between all pairs of loci using Genepop on the Web (Raymond & Rousset, 1995). These analyses were carried out using only adult genotypes for each species. Significance values were adjusted for multiple testing by applying a sequential Bonferroni correction (Rice, 1989).

We estimated the mean number of alleles, observed and expected heterozygosities for each species with GenAlEx v6.5b5 (Peakall & Smouse, 2012). We also calculated the Probability of Identity with and without accounting for related individuals in the sample (PI and PISibs, respectively). The reciprocal of the mean squared deviations of relatedness estimates (RMSD) was calculated with KinInfor v1 (Wang, 2006) using one moment estimator (Wang, 2002). This method allows estimation of information content in the microsatellite markers used in each species.

We estimated Nb and Ne in *P. waltl* and *P. cultripes* with the single-sample methods implemented in programs Colony v2.0.6.2 (Jones & Wang, 2010), OneSamp v1.2 (Tallmon *et al*., 2008), and NeEstimator v2 (Do *et al*., 2014). These analyses were based on the full dataset in *P. waltl*, whereas for *P. cultripes* only fourteen loci were used in OneSamp and NeEstimator, because the potential presence of null alleles in two loci (see Results) may bias results obtained with these two programs. In contrast, we used the full marker set of *P. cultripes* in Colony analyses, since this program can accommodate genotyping errors such as those arising from the presence of null alleles.

Colony applies the sibship frequency (SF) method (Wang, 2009), where Nb is estimated using inferred family relationships between offspring samples as full-sibs, half-sibs or non-sibs, that is, individuals sharing two, one or zero parents, respectively (Jones & Wang, 2010). SF analyses were carried out including the offspring sample, and genotyped adults of both sexes as candidate parents. The average prior probability for genotyped adults actually siring some offspring was inferred from census estimates estimated by software Mark (see Results), as the ratio between the number of genotyped adults and the corresponding estimate of Na for each sex. Colony analyses were performed assuming a polygamous mating system in both species. For each species, one run was performed implementing the full-likelihood method of Wang (2004) with "very high" likelihood precision, "very long" run length and using the "weak" sibship size prior = 1.

Nb can also be calculated in iteroparous species using Onesamp and NeEstimator when all samples belong to a single cohort (Waples, 2005; Beebee, 2009), as is the case of our offspring samples of *P. waltl* and *P. cultripes*. Nb estimates were calculated in NeEstimator based on the bias-corrected version of the linkage disequilibrium method (LD) of Waples and Do (2008). Following the recommendations of Waples and Do (2010), rare alleles with a frequency of less than 0.02 were excluded. We also used the random mating prior and the parametric method to estimate confidence intervals.

To explore the effect of sample size on our final Nb estimates based on the SF and LD methods, we produced sets of subsampled data representing increasing proportions of our final offspring sample sizes and analyzed them in Colony and NeEstimator, with five and ten replicates per subsample, respectively.

The subsamples were produced using R v3.0.3 (R Core Team, 2014), and Nb estimates were calculated as in the full dataset, except for SF analyses, which were run with "medium" likelihood precision and "medium" run length. Mean Nb across replicates and percent root-mean-squared bias (RMSB; Waples *et al*., 2014) were estimated for each subsampled set.

We computed OneSamp estimates of Nb, which are based on the calculation of eight summary statistics using an approximate Bayesian computation (ABC) approach (Tallmon *et al*., 2008). We used default priors and defined different lower and upper bounds for Ne, informed by our Na estimates: 50-200 and 50-500 in *P. cultripes*, and 20-500 and 20-1000 in *P. waltl*. Three replicates were run for each prior combination, and mean values across runs were calculated and compared with the results of the SF and LD methods.

In addition to Nb, estimates of Ne in iteroparous species can be obtained by combining adult samples from different generations (Tallmon *et al*., 2008; Waples & Do, 2010). Thus, we calculated Ne using Onesamp and NeEstimator including only adult genotypes, with the same settings and priors described above. Recently, however, Waples *et al*. (2014) have criticized this approach, proposing several formulas to estimate Nb and Ne from single-cohort LD estimates using information about the adult life span (AL) and age at maturity (α) of the target species:

$$Nb(Adj2)=(\text{raw Nb})/(1.103-0.245\times\log(AL/\alpha))$$

$$Ne(Adj2)=(Nb(Adj2))/(0.485+0.758\times\log(AL/\alpha))$$

, where raw Nb is the unadjusted estimate obtained using the LD method from a single-cohort sample.

In the case of *P. cultripes*, data on age at maturity and adult life span have been estimated in two and twelve years, respectively, in a population near our study area in Madrid (Talavera, 1990). No published information is available for *P. waltl*, but skeletochronological studies in progress have produced preliminary values of two and eleven years in Valdemanco (Gutiérrez-Rodríguez *et al*., unpublished data). Thus, we used these values to apply Waples *et al*.'s (2014) formulas and calculate Ne in the two species.

Sex-biased dispersal

We used two different methods to test for differences in dispersal between sexes. First, an assignment index correction (AIc) developed by Favre *et al*. (1997) and extended by Mossman and Waser (1999) was calculated using Genalex v6.5b5. This analysis only accounts for complete genotypes, so individuals with missing data were excluded. Secondly, analyses comparing mean values of relatedness between sexes were carried out with Coancestry v1.0.1.5 (Wang, 2011) using five moment (Lynch, 1988; Queller & Goodnight, 1989: Ritland, 1996; Lynch & Ritland, 1999; Wang, 2002) and two likelihood estimators (Milligan, 2003; Wang, 2007). These analyses accounted for the possibility of inbreeding and assumed a 1 % genotyping error rate. We used 1,000 bootstraps to construct confidence intervals for the estimates. In both methods, statistically significant differences between sexes indicate higher dispersal of the sex exhibiting lower AIc or average relatedness values.

Finally, we used field observations of recorded displacements in the two species based on CMR monitoring data to compare with indirect (genetic) estimates of sex-biased dispersal. We performed nocturnal transects in an area of about 0.5 km^2 encompassing the main breeding site for the two species (Laguna de Valdemanco), surrounding terrestrial habitat, and additional minor breeding sites in the vicinities (see detailed description of the study area in Sánchez-Montes & Martínez-Solano, 2011). These transects were inspected on an opportunistic basis over an eight-year period (2009-2016), out of the main breeding season but when weather conditions (temperature, humidity) provided good conditions for amphibian activity.

Results

Na estimates

Between 2010 and 2013 we captured 356 adults of *P. waltl* (245 males and 111 females) and 385 adults of *P. cultripes* (242 males and 143 females). Recapture rates overall were 30.6% for male *P. waltl*; 23.4% for female *P. waltl*; 44.6% for male *P. cultripes*, and 32.2% for female *P. cultripes*.

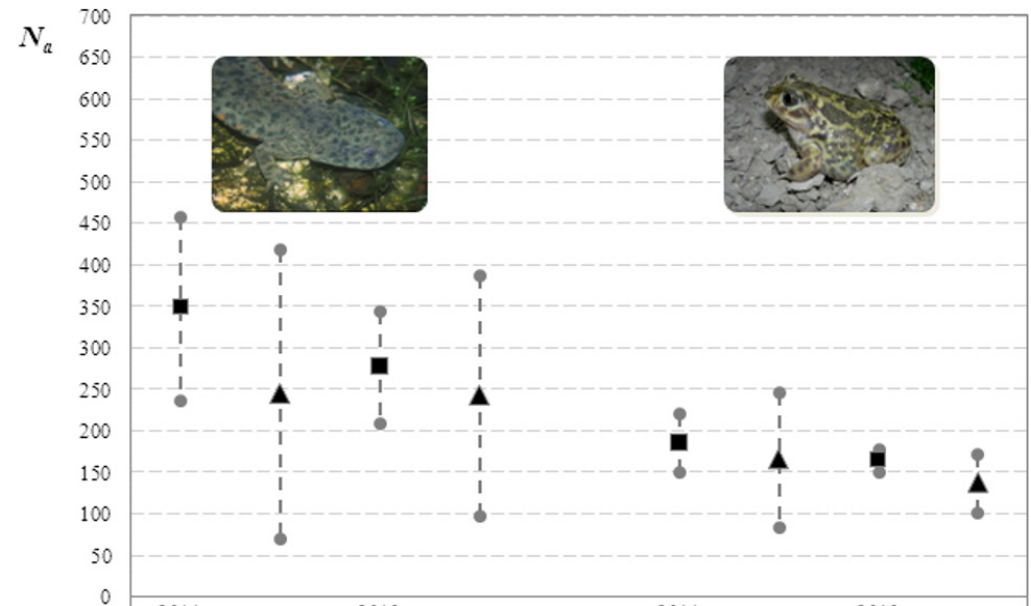

	2011		2013		2011		2013	
Max 95% IC	459	419	345	388	222	247	180	174
Min 95% IC	238	71	210	98	151	85	152	102
N	349	245	278	243	186	166	166	138

Figure VI.1. Estimates of the annual number of adults (Na, separately for each sex) in *P. waltl* (left) and *P. cultripes* (right) in 2011 and 2013. Squares and triangles represent males and females, respectively. Mean values are shown in black dots and 95% confidence intervals (IC) in grey dashed lines.

Na estimates for 2011 and 2013 obtained with program Mark are shown in Figure VI.1. Unfortunately, we could not obtain precise estimates in 2010 (the first year of marking) and 2012, an unusually dry year (see also Sánchez-Montes *et al*. in review). The precision of estimates of Na for both species increased over the years. In the two years with estimable parameters, estimates of the number of *P. waltl* males ranged between 278 and 349, and the number of females, between 243 and 245. In *P. cultripes*, estimates ranged between 166 and 186 males, and between 138 and 166 females in 2011 and 2013, respectively.

Estimates of Nb and Ne

Possible null alleles were detected for *P. cultripes* in loci Pc3.3, Pc4.3, Pc4.7 and Pc4.11. Of these, only loci Pc4.7 and Pc4.11 were discarded for subsequent analyses (except those in Colony, as indicated), because they have also been shown to present possible null alleles in other populations (Gutiérrez-Rodríguez *et al*. in review). We found no potential null alleles in loci used for genotyping in *P. waltl*,

but there were significant deviations from Hardy–Weinberg equilibrium (HWE) in loci Pleu2.35 and Pleu3.14. We also found evidence of linkage disequilibrium (LD) between loci Ppl7 - Pleu3.5, and Ppl5 - Pleu2.35. These disequilibria did not affect other populations (Gutiérrez-Rodríguez *et al*. in review) and thus are considered to represent population-specific processes rather than physical linkage.

The mean number of alleles, observed and expected heterozygosity were 4.238, 0.419 and 0.440 in *P. cultripes* and 5.127, 0.551 and 0.543 in *P. waltl*. Individual identification was possible in both species, since all adults, larvae and tadpoles presented exclusive genotypes. In *P. waltl*, individual identification with 95% confidence only required two loci (four when accounting for possible relatives in the sample), whereas two (five) loci were necessary in *P. cultripes* (see Figure VI.S1). Using the complete marker sets, the probability of two specimens having the same genotype was 3.0×10^{-14} (and 1.7×10^{-6} when accounting for relatives in the sample) in *P. waltl* and 2.6×10^{-7} (and 10^{-3}) for *P. cultripes*. The estimated RMSD values were 46.1 in the *P. waltl* microsatellite set and 26.1 in *P. cultripes*.

Estimates of Nb and Ne are shown in Table VI.1. In *P. waltl*, Nb estimates ranged from 96 to 123, with overall congruence across methods and most estimates slightly underestimating Nb as compared to the adjusted (Nb(Adj2)) formula. In *P. cultripes*, Nb estimates ranged from 84 to 230, with estimates based on the ABC method showing strong upward deviations with respect to the adjusted Nb(Adj2) estimate.

Replicate analyses performed to explore the effect of offspring sample size on final Nb estimates showed stabilization of LD-based estimates with 40 and 50% of total sample sizes in *P. cultripes* and *P. waltl*, respectively (Figure VI.S2). In the case of the SF method, Nb estimates increased with increasing sample size, and showed lower variance between replicates than in the LD method.

Estimates of Ne from samples combining individuals from different cohorts differed across methods. In *P. waltl*, the ABC method produced an estimate of 42, whereas the LD method estimated 153. The latter was closer, but upwards biased by 28% with respect to the adjusted Ne(Adj2) (Table VI.1). In *P. cultripe*s, estimates based on the ABC method were also lower than those

Table VI.1. Estimates of Nb and approximation to Ne for *P. waltl* (top) and *P. cultripes* (bottom) in Laguna de Valdemanco. For a description of the different priors used see Methods. The ratios Nb/Na and Ne/Na are calculated for two different years (2011 and 2013). P-P indicates the assumption of polygamy for both males and females, and Weak = weak sibship size prior in SF analyses. Adj. = adjusted estimate.

		Nb		Nb/Na		Ne		Ne/Na	
Method	**Priors**	**Estimate**	**95 % CI**	**2011**	**2013**	**Estimate**	**95 % CI**	**2011**	**2013**
P. waltl									
ABC (Onesamp)	20-500	100	84-157	0.17	0.19	42	36-55	0.07	0.08
	20-1000	109	72-219	0.18	0.21	42	38-59	0.07	0.08
LD (NeEstimator)	0.02	115	89-160	0.19	0.22	153	119-208	0.26	0.29
	Adj	123		0.21	0.24	122		0.21	0.23
SF (Colony)	P-P Weak	96	72-132	0.16	0.18				
P. cultripes									
ABC (Onesamp)	50-200	195	145-241	0.55	0.64	78	59-107	0.22	0.26
	50-500	230	167-400	0.65	0.76	84	64-133	0.24	0.28
LD (NeEstimator)	0.02	84	67-108	0.24	0.28	136	84-281	0.39	0.45
	Adj	91		0.26	0.30	87		0.25	0.29
SF (Colony)	P-P Weak	93	71-126	0.26	0.31				

from the LD method, which was upwards biased by over 50%. In this species, however, ABC-based estimates were closer to the adjusted Ne estimate, with a slight downward bias.

Adjusted values of Nb and Ne were similar within each species (123 and 122 in *P. waltl* and 91 and 87 in *P. cultripes*). The resulting Nb/Na ratios were similar across species, although slightly lower in *P. waltl* (0.21-0.24 vs 0.25-0.30).

Sex-biased dispersal

AIc estimates were different between sexes in *P. waltl* (see Figure VI.2), but results were not statistically significant. Mean bias assignment was lower in females than in males, indicating a tendency to female-biased dispersal. In the case of *P. cultripes*, no differences between sexes were observed. On the other hand, four out of the seven relatedness estimators calculated by Coancestry showed statistically significant differences between sexes in *P. waltl*. In all cases, the results showed higher relatedness in males than in females, also supporting female-biased dispersal. In *P. cultripes*, there were no significant differences

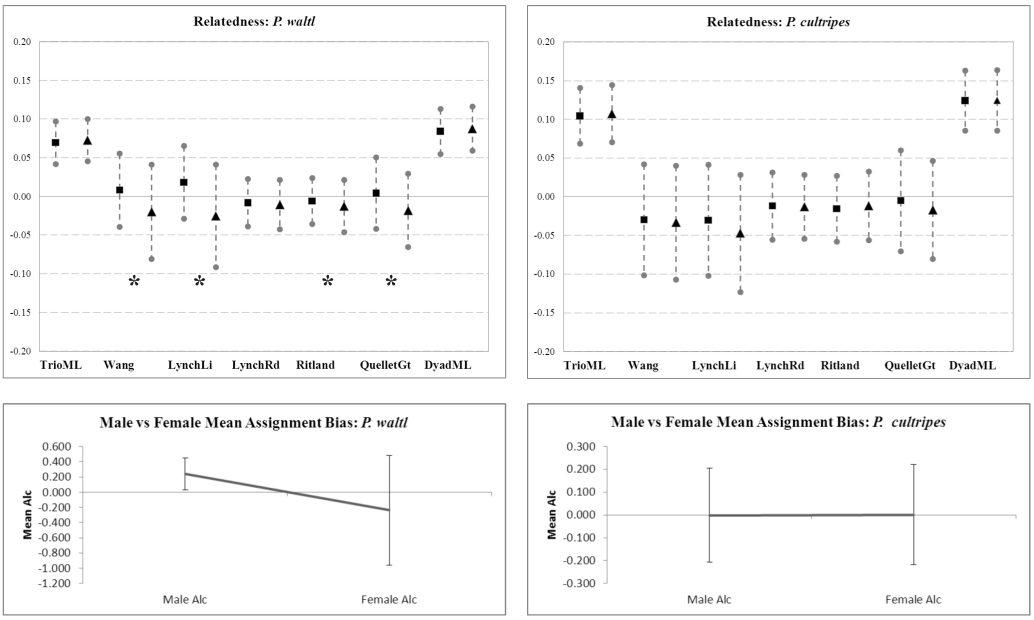

Figure VI.2. Mean and 95 % CI values of seven estimators of Relatedness (Top), and mean and standard error of Assignment Index correction (AIc) values (Bottom) in *P. waltl* (left) and *P. cultripes* (right). Squares and triangles represent males and females, respectively. Significant differences are marked with asterisks.

between sexes in average relatedness.

Over an eight-year period (2009-2016), out of a total of 1172 and 1293 recapture events, we recorded six (frequency = 0.51%) and sixteen (frequency = 1.23%) movements longer than 250 meters in *P. waltl* and *P. cultripes*, respectively. Four of these displacements (three females and one male) exceeded 700 meters in *P. waltl*. In the case of *P. cultripes*, eight displacements to nearby breeding sites were recorded, with five of them (two females and three males) involving distances longer than 700 meters.

Discussion

We present the first estimates of the effective to census population size ratio in two pond-breeding amphibians characteristic of Mediterranean wetlands. Prior to our study there was little information on their population biology or demography, so our results are a valuable contribution towards evidence-based conservation actions directed to minimize local extinction risk in these species. In this regard, a potential limitation of our results is to what extent they are generalizable to

other populations and regions, since variation in Nb, Ne and their ratio with Na is expected, especially in widespread species. While it is hard to anticipate the magnitude of differences in these parameters across populations, here we focused on large (hundreds of adults) and apparently healthy (with no record of the presence of exotic species or infectious diseases) populations. Furthermore, sampling took place in years with optimal conditions for breeding success (based on our field observations, including a long hydroperiod maximizing survival to metamorphosis and low egg mortality). This is an important factor, since the ephemeral ponds in which both species usually breed are subject to strong variation in hydroperiod across years, with dry years typically resulting in reduced breeding and recruitment (and therefore in lower Nb or Ne estimates). Therefore, our results should be representative of populations of both species in good conservation status and comparable to those from other locations. Smaller, isolated populations should also be studied to search for evidence of genetic compensation effects and quantify their magnitude with respect to large, healthy populations. Additionally, the obtained Nb/Na ratios could be used to approximate abundance (Na) based on Nb estimates, which are easier to obtain, given that Na estimates usually require years of mark-recapture efforts.

Considering the effect of sample size is critical to obtain accurate estimates of Ne and Nb based on LD methods (Waples & Do, 2010; Kamath *et al*., 2015), especially if sample sizes are lower than the actual values of Ne and Nb. In our case, Nb estimates from subsampled datasets based on the SF method increased linearly without reaching stabilization. However, differences between replicates were smaller than across Nb estimates based on the LD method, which stabilized at around 40% - 50% of the final sample size for both species (Figure VI.S2). This represents minimum sample sizes of around 70 (*P. cultripes*) and 50 (*P. waltl*) single-cohort offspring samples, higher values than those previously recommended (Waples, 2006; Waples & Do, 2010). This is probably caused by lower levels of polymorphism in our marker sets (RMSD: *P. waltl*: 46.1 and *P. cultripes*: 26.1) in comparison to those usually employed in simulations.

In iteroparous species with overlapping generations, Nb estimates have been more generally applied than Ne, because most methods attempting to estimate the latter rely on the assumption of discrete, non overlapping generations. This

assumption does not apply for the estimation of Nb, which partially summarizes the effects of the sizes of age classes and the variance in reproductive success within and among age and sex classes on inbreeding and drift in a population with overlapping generations (Wang, 2016). Here we used three different methods (LD, ABC and SA methods) to estimate Nb using single-cohort samples. The results were consistent across methods, except for estimates obtained with Onesamp for *P. cultripes*, which doubled LD and SA estimates (Table VI.1). The ABC method is sensitive to priors (Pérez-Figueroa *et al*., 2015), but adjusting the prior to reflect realistic estimates has been shown to improve estimates (Holleley *et al*., 2014). Here we specified boundaries for the priors based on our Na estimates, but perhaps they were still too wide to provide accurate estimates (although wider prior boundaries in *P. waltl* did not affect precision of Nb estimates).

Estimates based on the LD method with single cohort samples relate to Nb (Waples, 2005). However, Waples *et al*. (2014) have suggested that Nb estimates using this method in iteroparous species may present biases due to unaccounted age structure (Waples *et al*., 2013). Thus, we adjusted our LD-based estimates using the equations in Waples *et al*. (2014). By accounting for information on the adult life span and age at maturity of both species, we obtained slightly higher values compared to unadjusted LD estimates (7.0 % in *P. waltl* and 8.3 % in *P. cultripes*). The adjusted LD estimate of Nb was very similar to the SF estimate in *P. cultripes*, but slightly larger in the case of *P. waltl*. Wang (2009) suggested that the SF method could underestimate Nb when markers are less informative and sample size is small, especially in polygamous systems (Wang, 2016), whereas Nb estimates are more accurate when sample size is large relative to Nb (Wang 2009). Our markers are more informative in *P. waltl* (RMSD = 46.1) than in *P. cultripes* (RMSD = 26.1), but sample size in the former was about half of that in *P. cultripes*, which could partially explain this underestimation.

Studies estimating Nc in some explosive-breeding amphibians have used counts of egg strings as a proxy for the adult census size (number of egg strings x 2 = Nc), which is based on the assumptions that 1) most females in the population breed and they do so only once during the season, and 2) there is a balanced sex ratio (Beebee, 2009). It is worth asking whether a similar inference could be made for *P. cultripes*, because egg strings are easy to find and count

exhaustively in this species. In 2013 we counted 75 egg strings, but estimated an adult population size of around 140 females, suggesting a relatively low female breeding success, which contrasts with the high success recorded in other species in the same area (close to unity in *B. calamita*, in line with the findings of Beebee, 2009, see Sánchez-Montes *et al*. in review). The corresponding Nb estimate for *Pelobates* in 2013 was around 90 according to the LD and SF methods. Consistency across both methods supported the reliability of the estimates, in contrast to that obtained with the ABC method. This result suggests some degree of polygamy in this species, as also shown by family relationships reconstructed with software Colony. This is surprising in view of the short breeding season of the species, which provides few opportunities for multiple matings, and the mating behavior, in which amplectant males fertilize the eggs as they are released by the female. A question worth further exploration is the possibility of multiple fertilization of different egg strings by the sperm of several males meeting in breeding aggregations in small pools; these aggregations are often observed in our study area.

Several methods have been proposed to estimate Ne with single-sample estimators in iteroparous species: the LD method (Waples *et al*., 2014; Waples & Do, 2010), an ABC-based approach (Tallmon *et al*., 2008), the estimator by parentage assignments (EPA) (Wang *et al*., 2010), and the method implemented in software AgeNe (Waples *et al*., 2011). The last two methods could not be applied here, since information on the individual age, age-specific survival rates or relative fecundity was unavailable for both species. Thus, we focused on the LD and ABC methods, which produced different results. Mixed cohort adult samples produced strongly upwards-biased results compared to the adjusted estimates of Ne: 28 % in *P. waltl* and 56 % in *P. cultripes*. These results contrast with those obtained by Waples *et al*. (2014), where uncorrected estimates of Ne based on mixed cohorts were lower than adjusted ones in all species analyzed. However, Ruzzante *et al*. (2016) found a wider ratio of adjusted to unadjusted estimates based on mixed adult samples, ranging from 0.69 to 4.77.

On the other hand, the ABC method implemented in Onesamp has been also applied to estimate Ne with multiple-cohort samples in iteroparous species (Tallmon *et al*., 2008; Phillipsen *et al*., 2011). In our study, estimates of

Ne based on mixed cohort adult samples in Onesamp were similar to adjusted LD estimates in *P. cultripes*, but very different (less than half than adjusted LD estimates) in *P. waltl*. These discrepancies are hard to interpret, but may reflect the different timescales associated with ABC and LD-based estimates (Wang, 2016; Wang *et al*., 2016). For instance, one of the statistics used to estimate Ne with the ABC approach is the M-ratio, which is able to detect demographic changes in the previous 100 generations (Garza & Williamson, 2001), so it is hardly comparable to estimates based on the LD method, which estimates Ne in the parental generation for sampled individuals (Waples, 2005).

Keeping in mind the reported differences across methods, the Nb/Na and Ne/Na ratios obtained in the two species were similar (range: 0.21-0.30 considering LD estimates), and near the average estimate (0.22-0.23) calculated by Palstra and Fraser (2012) across disparate taxa. In amphibians, strong differences have been observed between species with different life-history traits. For instance, in anurans, Rowe and Beebee (2004) reported ratios of 0.02-0.17 in *Bufo calamita*, whereas Schmeller and Merilä (2007) estimated ratios between 0.23–1.67 in *Rana temporaria*. Similar variation has been reported in urodeles, with low ratios in *Triturus marmoratus* (0.09; Jehle *et al*., 2001) contrasting with high ratios in *Salamandra salamandra* (0.8; Álvarez *et al*., 2015), although in the latter case genetic compensation effects were invoked.

How do our estimated ratios relate to population viability? First, our results suggest that adult abundance may be a poor surrogate of population status, with populations with hundreds of breeding adults having an effective population size close to 100 individuals in the two species (around 90 in *Pelobates* and 120 in *Pleurodeles*). Frankham *et al*. (2014) proposed a minimum value of Ne of 100 to avoid or minimize problems of inbreeding depression in wild populations. If large and healthy populations such as those in our study area are characterized by Ne estimates below or barely above that critical value, the situation is probably much worse for smaller populations, although in these cases there may be genetic compensation mechanisms at play. In any case, additional estimates of the Na/Ne ratio in other populations are required for a better understanding of the actual range of variation in this key parameter.

Finally, our results also provide some insights on dispersal in the two species, which may be helpful when designing management strategies to revert the effects of habitat fragmentation. The observed rates of long displacement events were quite low in both species (*P. waltl* = 0.51%; *P. cultripes* = 1.23%), in line with the low general dispersal capacity of amphibians and their tendency to philopatry, suggesting high vulnerability to natural or artificial fragmentation of their habitats. The higher frequency of displacements in *P. cultripes* is consistent with their more terrestrial behaviour and with the higher dispersal capacity of anurans compared to urodeles (Smith & Green, 2005). On the other hand, our genetic-based results regarding sex-biased dispersal suggest a tendency for female-biased dispersal in *P. waltl* (Fig. VI.2). The same tendency was also suggested by our direct observations of dispersive individuals, in which three out of four recorded long-distance movements were performed by females. This result contrasts with general reports of male biased dispersal in urodeles (Liebgold *et al*., 2006; Helfer *et al*., 2012), but similar observations of female-biased dispersal have been recently reported in the newt *Triturus marmoratus* (Trochet *et al*., 2017). These authors hypothesize that this bias may result from the territorial behaviour of males during their aquatic phase and /or from a tendency of females to move further away from breeding sites in search of high quality terrestrial foraging grounds with reduced intraspecific competition. Both explanations may also apply to *Pleurodeles*, but need to be tested with field and experimental evidence. At any rate, low dispersal rates combined with low Ne values increase the risk of inbreeding (Johnson *et al*., 2007). Considering in addition that habitat fragmentation is one of the major threats identified in the two species, we argue that conservation measures should focus on improving population connectivity to minimize the risk of loss of genetic diversity and evolutionary potential.

Acknowledgements

We thank J. Agüera, F. Alda, R. Álvarez, S. Barrionuevo, P. Cabezas, M. Casal, E. Garrandés, J.L. Gutiérrez, E. Iranzo, I. Irisarri, D. Llusia, P. Pavón, C. Pedraza, J. Pérez, E. Recuero, G. Rodríguez, A. Sabalza, D. Salvi, L. San José, C. Settanni, I. Urbán and M. Peñalver for help during field work, P. Arntzen for constructive comments on a previous draft, and S. Abalde for help with R scripts for analyses

on replicate subsamples. JGR was supported by the Consejo Superior de Investigaciones Científicas of Spain (CSIC) and the European Social Fund (ESF) (JAE-pre PhD fellowship). GSM is funded by a predoctoral grant provided by the Asociación de Amigos de la Universidad de Navarra. This research was funded by grants CGL2008-04271-C02-01/BOS, and CGL2011-28300 (Ministerio de Ciencia e Innovación -MICINN-), Ministerio de Economía y Competitividad -MEC-, Spain, and FEDER) to IMS, who was supported by funding from the Spanish "Ramón y Cajal" and Severo Ochoa (SEV-2012-0262) programs.

References

Akaike H (1974) A new look at the statistical model identification. IEEE Transactions on Automatic Control 19: 716–723.

Álvarez D, Lourenço A, Oro D, Velo-Antón G (2015) Assessment of census (N) and effective population size (Ne) reveals consistency of Ne single-sample estimators and a high Ne/N ratio in an urban and isolated population of fire salamanders. Conservation Genetics Resources 7: 705–712.

Araújo MB, Guilhaumon F, Neto DR, Pozo IO, Calmaestra RG (2011) Impactos, vulnerabilidad y adaptación al cambio climático de la biodiversidad española. 2. Fauna de Vertebrados. Ministerio de Medio Ambiente, Madrid

Baalsrud HT, Sæther B-E, Hagen IJ, Myhre AM, Ringsby TH, Pärn H, Jensen H (2014) Effects of population characteristics and structure on estimates of effective population size in a house sparrow metapopulation. Molecular Ecology 23: 2653–2668.

Beebee TJC (2009) A comparison of single-sample effective size estimators using empirical toad (*Bufo calamita*) population data: genetic compensation and population size-genetic diversity correlations. Molecular Ecology 18: 4790–4797.

Beja P, Bosch J, Tejedo M *et al*. (2009) *Pleurodeles waltl*. The IUCN Red List of Threatened Species 2009. http://www.iucnredlist.org. Accessed 15 July 2016

Beja P, Bosch J, Tejedo M *et al*. (2016) *Pelobates cultripes*. The IUCN Red List of Threatened Species 2016. http://www.iucnredlist.org. Accessed 15 July 2016

Brede EG, Beebee TJC (2006) Large variations in the ratio of effective breeding and census population sizes between two species of pond-breeding anurans. Biological Journal of the Linnean Society 89: 365–372.

Burnham KP, Anderson DR (2002) Model selection and multimodel inference: a practical information-theoretic approach. 2nd edition edn. Springer-Verlag, New York

Charlesworth B (2009) Effective population size and patterns of molecular evolution and variation. Nature Reviews Genetics 10: 195–205.

Do C, Waples RS, Peel D, *et al*. (2014) NeEstimator v2: re-implementation of software for the estimation of contemporary effective population size (Ne) from genetic data. Molecular Ecology Resources 14: 209–214.

Easteal S (1985) The ecological genetics of introduced populations of the giant toad *Bufo marinus*. II. Effective population size. Genetics 110: 107–122.

Favre L, Balloux F, Goudet J, Perrin N (1997) Female-biased dispersal in the monogamous mammal *Crocidura russula*: evidence from field data and microsatellite patterns. Proceedings of the Royal Society B: Biological Sciences 264: 127–132.

Fisher RA (1930) The genetical theory of natural selection. Oxford University Press, Oxford

Fortuna MA, Gómez-Rodríguez C, Bascompte J (2006) Spatial network structure and amphibian persistence in stochastic environments. Proceedings of the Royal Society B: Biological Sciences 273: 1429–1434.

Frankham R (1995) Effective population size/adult population size ratios in wildlife: a review. Genetics Research 66: 95–107.

Frankham R, Bradshaw CJA, Brook BW (2014) Genetics in conservation management: Revised recommendations for the 50/500 rules, Red List criteria and population viability analyses. Biological Conservation 170: 56–63.

Frankham R, Briscoe DA, Ballou JD (2002) Introduction to conservation genetics. Cambridge University Press, Cambridge

García-París M, Montori A, Herrero P (2004) Fauna Iberica. Vol. 24. Amphibia: Lissamphibia. Museo Nacional de Ciencias Naturales, Consejo Superior de Investigaciones Científicas, Madrid

Garza JC, Williamson EG (2001) Detection of reduction in population size using data from microsatellite loci. Molecular Ecology 10: 305–318.

Gill DE (1978) Effective population size and interdemic migration rates in a metapopulation of the red-spotted newt, *Notophthalmus viridescens* (Rafinesque). Evolution 32: 839–849.

Gutiérrez-Rodríguez J, Gonçalves J, Civantos E, Martínez-Solano Í (in review) Comparative landscape genetics of pond-breeding amphibians in Mediterranean temporal wetlands: the positive role of structural heterogeneity in promoting gene flow. Molecular Ecology

Gutiérrez-Rodríguez J, Gonzalez EG, Martínez-Solano Í (2014) Development and characterization of twelve new polymorphic microsatellite loci in the Iberian ribbed newt, *Pleurodeles waltl* (Caudata: Salamandridae), with data on cross-amplification in *P. nebulosus*. Amphibia-Reptilia 35: 129–134.

Gutiérrez-Rodríguez J, Martínez-Solano Í (2013) Isolation and characterization of sixteen polymorphic microsatellite loci in the Western Spadefoot, *Pelobates cultripes* (Anura: Pelobatidae) via 454 pyrosequencing. Conservation Genetics Resources 5: 981–984.

Helfer V, Broquet T, Fumagalli L (2012) Sex-specific estimates of dispersal show female philopatry and male dispersal in a promiscuous amphibian, the alpine salamander (*Salamandra atra*). Molecular Ecology 21: 4706–4720.

Hoffmann M, Hilton-Taylor C, Angulo A *et al*. (2010) The Impact of Conservation on the Status of the World's Vertebrates. Science 330: 1503–1509.

Holleley C, Nichols R, Whitehead M, *et al*. (2014) Testing single-sample estimators of effective population size in genetically structured populations. Conservation Genetics 15: 23–35.

Jehle R, Arntzen JW, Burke T, Krupa AP, Hödl W (2001) The annual number of breeding adults and the effective population size of syntopic newts (*Triturus cristatus*, *T. marmoratus*). Molecular Ecology 10: 839–850.

Johnson JR, Knouft JH, Semlitsch RD (2007) Sex and seasonal differences in the spatial terrestrial distribution of gray treefrog (*Hyla versicolor*) populations. Biological Conservation 140: 250–258.

Jones OR, Wang J (2010) COLONY: a program for parentage and sibship inference from multilocus genotype data. Molecular Ecology Resources 10: 551–555.

Kamath PL, Haroldson MA, Luikart G, *et al*. (2015) Multiple estimates of effective population size for monitoring a long-lived vertebrate: an application to Yellowstone grizzly bears. Molecular Ecology 24: 5507–5521.

Liebgold EB, Cabe PR, Jaeger RG, Leberg PL (2006) Multiple paternity in a salamander with socially monogamous behaviour. Molecular Ecology 15: 4153–4160.

Luikart G, Ryman N, Tallmon D, Schwartz M, Allendorf F (2010) Estimation of census and effective population sizes: the increasing usefulness of DNA-based approaches. Conservation Genetics 11: 355–373.

Lynch M (1988) Estimation of relatedness by DNA fingerprinting. Molecular Biology and Evolution 5: 584–599.

Lynch M, Ritland K (1999) Estimation of pairwise relatedness with molecular markers. Genetics 152: 1753–1766.

Milligan BG (2003) Maximum-Likelihood Estimation of Relatedness. Genetics 163: 1153–1167.

Montori A, Llorente GA, Santos X, Carretero MA (2002) *Pleurodeles waltl* Michahelles, 1830. Gallipato. In: Pleguezuelos JM, Márquez R, Lizana M (eds) Atlas y Libro Rojo de los Anfibios y Reptiles de España. 2nd edn. Dirección General de Conservación de la Naturaleza-Asociación Herpetológica Española, Madrid, pp 51–54

Mossman CA, Waser PM (1999) Genetic detection of sex-biased dispersal. Molecular Ecology 8: 1063–1067.

Nei M, Tajima F (1981) Genetic drift and estimation of effective population size. Genetics 98: 625–640.

Nunney L, Elam DR (1994) Estimating the effective population size of conserved populations. Conservation Biology 8: 175–184.

Palstra FP, Fraser DJ (2012) Effective/census population size ratio estimation: a compendium and appraisal. Ecology Evolution 2: 2357–2365.

Peakall R, Smouse PE (2012) GenAlEx 6.5: genetic analysis in Excel. Population genetic software for teaching and research—an update. Bioinformatics 28: 2537–2539.

Pérez-Figueroa A, Fernández C, Amaro R, Hermida M, San Miguel E (2015) Population structure and effective/census population size ratio in threatened three-spined stickleback populations from an isolated river basin in northwest Spain. Genetica 143: 403–411.

Phillipsen IC, Funk WC, Hoffman EA, Monsen KJ, Blouin MS (2011) Comparative analyses of effective population size within and among species: ranid frogs as a case study. Evolution 65: 2927–2945.

Pollock KH (1982) A capture-recapture design robust to unequal probability of capture. Journal of Wildlife Management 46: 752–757.

Queller DC, Goodnight KF (1989) Estimating relatedness using genetic markers. Evolution 43: 258–275.

R Core Team (2014) R: A language and environment for statistical computing. R Foundation for Statistical Computing, Vienna, Austria.

Raymond M, Rousset F (1995) GENEPOP (Version 1.2): Population genetics software for exact tests and ecumenicism. Journal of Heredity 86: 248–249.

Rice WR (1989) Analyzing tables of statistical tests. Evolution 43: 223–225.

Ritland K (1996) Estimators for pairwise relatedness and individual inbreeding coefficients. Genetics Research 67: 175–185.

Ruzzante DE, McCracken GR, Parmelee S, Hill K, Corrigan A, MacMillan J, Walde SJ (2016) Effective number of breeders, effective population size and their relationship with census size in an iteroparous species, *Salvelinus fontinalis*. Proceedings of the Royal Society B: Biological Sciences 283: 1823.

Sánchez-Montes G, Martínez-Solano Í (2011) Population size, habitat use and movement patterns during the breeding season in a population of Perez's frog (*Pelophylax perezi*) in central Spain. Basic and Applied Herpetology 25: 81–96.

Sánchez-Montes G, Wang J, Ariño A, Vizmanos JL, Martínez-Solano Í (in review) Reliable effective/census population size ratios in seasonal-breeding species: opportunity for integrative demographic inferences based on capture-mark-recapture data and multilocus genotypes. Ecology and Evolution.

Scribner KT, Arntzen JW, Burke T (1997) Effective number of breeding adults in *Bufo bufo* estimated from age-specific variation at minisatellite loci. Molecular Ecology 6: 701–712.

Smith MA, Green DM (2005) Dispersal and the metapopulation paradigm in amphibian ecology and conservation: are all amphibian populations metapopulations? Ecography 28: 110–128.

Talavera RR (1990) Evolución de Pelobátidos y Pelodítidos (Amphibia: Anura): morfología y desarrollo del sistema esquelético. Ph. D. Dissertation, Universidad Complutense de Madrid

Tallmon DA, Koyuk A, Luikart G, Beaumont MA (2008) ONESAMP: a program to estimate effective population size using approximate Bayesian computation. Molecular Ecology Resources 8: 299–301.

Tejedo M, Reques R (2002) *Pelobates cultripes* (Cuvier, 1829). Sapo de espuelas. In: Pleguezuelos JM, Márquez R, Lizana M (eds) Atlas y Libro Rojo de los Anfibios y Reptiles de España. 2nd edn. Dirección General de Conservación de la Naturaleza-Asociación Herpetológica Española, Madrid, pp 94–96

Trochet A, Le Chevalier H, Calvez O, *et al*. (2017) Postbreeding movements in marbled newts (Caudata, Salamandridae): a comparative radiotracking study in two habitat types. Herpetologica 73: 1–9.

Turner TF, Salter LA, Gold JR (2001) Temporal-method estimates of Ne from highly polymorphic loci. Conservation Genetics 2: 297–308.

van de Vliet MS, Diekmann OE, Serrão EA, Beja P (2009) Isolation of highly polymorphic microsatellite loci for a species with a large genome size: sharp-ribbed salamander (*Pleurodeles waltl*). Molecular Ecology Resources 9: 425–428.

van Oosterhout C, Hutchinson WF, Wills DPM, Shipley P (2004) MICRO-CHECKER: software for identifying and correcting genotyping errors in microsatellite data. Molecular Ecology Notes 4: 535–538.

Wang I, Johnson J, Johnson B, Shaffer H (2011) Effective population size is strongly correlated with breeding pond size in the endangered California tiger salamander, *Ambystoma californiense*. Conservation Genetics 12: 911–920.

Wang J (2002) An estimator for pairwise relatedness using molecular markers. Genetics 160: 1203–1215.

Wang J (2004) Sibship reconstruction from genetic data with typing errors. Genetics 166: 1963–1979.

Wang J (2006) Informativeness of genetic markers for pairwise relationship and relatedness inference. Theoretical Population Biology 70: 300–321.

Wang J (2007) Triadic IBD coefficients and applications to estimating pairwise relatedness. Genetics Research 89: 135–153.

Wang J (2009) A new method for estimating effective population sizes from a single sample of multilocus genotypes. Molecular Ecology 18: 2148–2164.

Wang J (2011) COANCESTRY: a program for simulating, estimating and analysing relatedness and inbreeding coefficients. Molecular Ecology Resources 11: 141–145.

Wang J (2016) A comparison of single-sample estimators of effective population sizes from genetic marker data. Molecular Ecology 25: 4692–4711

Wang J, Brekke P, Huchard E, Knapp LA, Cowlishaw G (2010) Estimation of parameters of inbreeding and genetic drift in populations with overlapping generations. Evolution 64: 1704–1718.

Wang J, Santiago E, Caballero A (2016) Prediction and estimation of effective population size. Heredity 117: 193–206.

Waples RS (2005) Genetic estimates of contemporary effective population size: to what time periods do the estimates apply? Molecular Ecology 14: 3335–3352.

Waples RS (2006) A bias correction for estimates of effective population size based on linkage disequilibrium at unlinked gene loci. Conservation Genetics 7: 167.

Waples RS, Antao T, Luikart G (2014) Effects of overlapping generations on linkage disequilibrium estimates of effective population size. Genetics 197: 769–780.

Waples RS, Do C (2010) Linkage disequilibrium estimates of contemporary Ne using highly variable genetic markers: a largely untapped resource for applied conservation and evolution. Evolutionary Applications 3: 244–262.

Waples RS, Do C, Chopelet J (2011) Calculating Ne and Ne/N in age-structured populations: a hybrid Felsenstein-Hill approach. Ecology 92: 1513–1522.

Waples RS, Do C (2008) LDNE: a program for estimating effective population size from data on linkage disequilibrium. Molecular Ecology Resources 8: 753–756.

Waples RS, Luikart G, Faulkner JR, Tallmon DA (2013) Simple life-history traits explain key effective population size ratios across diverse taxa. Proceedings of the Royal Society B: Biological Sciences 280: 1768.

White GC, Burnham KP (1999) Program MARK: survival estimation from populations of marked animals. Bird Study 46: S120–S139.

Wilson CC, McDermid JL, Wozney KM, Kjartanson S, Haxton TJ (2014) Genetic estimation of evolutionary and contemporary effective population size in lake sturgeon (*Acipenser fulvescens* Rafinesque, 1817) populations. Journal of Applied Ichthyology 30: 1290–1299.

Wright S (1931) Evolution in Mendelian populations. Genetics 16: 97–159.

Supplementary

Table VI.S1. Loci used to genotype *P. cultripes* samples in this study. Locus name, multiplex reaction, mean number of alleles per locus (na), observed (Ho) and expected heterozygosity (He) and studies where loci were originally characterized.

Locus	Multiplex reaction	na	Ho	He	References
Pc3.25	Multiplex1	2.35	0.611	0.575	Gutiérrez-Rodríguez and Martínez-Solano 2013
Pc4.1	Multiplex1	2.16	0.621	0.537	Gutiérrez-Rodríguez and Martínez-Solano 2013
Pc3.2	Multiplex1	3.42	0.642	0.708	Gutiérrez-Rodríguez and Martínez-Solano 2013
Pc3.9	Multiplex1	1.84	0.463	0.455	Gutiérrez-Rodríguez and Martínez-Solano 2013
Pc3.1	Multiplex2	2.66	0.653	0.624	Gutiérrez-Rodríguez and Martínez-Solano 2013
Pc4.4	Multiplex2	1.01	0.011	0.010	Gutiérrez-Rodríguez and Martínez-Solano 2013
Pc3.23	Multiplex2	2.81	0.621	0.644	Gutiérrez-Rodríguez and Martínez-Solano 2013
Pc4.5	Multiplex3	1.59	0.200	0.372	Gutiérrez-Rodríguez and Martínez-Solano 2013
Pc3.3	Multiplex3	1.73	0.411	0.421	Gutiérrez-Rodríguez and Martínez-Solano 2013
Pc4.3	Multiplex3	1.49	0.200	0.327	Gutiérrez-Rodríguez and Martínez-Solano 2013
Pc3.7	Multiplex4	1.68	0.337	0.403	Gutiérrez-Rodríguez and Martínez-Solano 2013
Pc4.11	Multiplex4	1.75	0.266	0.428	Gutiérrez-Rodríguez and Martínez-Solano 2013
Pc4.9	Multiplex4	1.85	0.479	0.458	Gutiérrez-Rodríguez and Martínez-Solano 2013
Pc3.24	Multiplex5	1.06	0.032	0.053	Gutiérrez-Rodríguez and Martínez-Solano 2013
Pc4.7	Multiplex5	3.10	0.447	0.678	Gutiérrez-Rodríguez and Martínez-Solano 2013
Pc3.4	Multiplex5	2.10	0.574	0.523	Gutiérrez-Rodríguez and Martínez-Solano 2013

Table VI.S2. Loci used to genotype *P. waltl* samples in this study. Locus name, multiplex reaction, mean number of alleles per locus (na), observed (Ho) and expected heterozygosity (He) and studies where loci were originally characterized.

Locus	Multiplex reaction	na	Ho	He	References
Pleu2.19	Multiplex1	2.32	0.538	0.569	Gutiérrez-Rodríguez *et al*., 2014
Pleu2.34	Multiplex1	1.88	0.393	0.468	Gutiérrez-Rodríguez *et al*., 2014
Pleu2.16	Multiplex2	1.987	0.570	0.497	Gutiérrez-Rodríguez *et al*., 2014
Pleu2.31	Multiplex2	1.932	0.495	0.483	Gutiérrez-Rodríguez *et al*., 2014
Pleu3.2	Multiplex2	2.154	0.570	0.536	Gutiérrez-Rodríguez *et al*., 2014
Pleu3.5	Multiplex3	1.078	0.075	0.072	Gutiérrez-Rodríguez *et al*., 2014
Pleu4.1	Multiplex3	1.966	0.514	0.491	Gutiérrez-Rodríguez *et al*., 2014
Pleu2.35	Multiplex4	1.029	0.028	0.028	Gutiérrez-Rodríguez *et al*., 2014
pleu3.14	Multiplex4	1.314	0.196	0.239	Gutiérrez-Rodríguez *et al*., 2014
Pleu3.11	Multiplex4	1.939	0.523	0.484	Gutiérrez-Rodríguez *et al*., 2014
Pleu2.21	Multiplex4	2.503	0.626	0.600	Gutiérrez-Rodríguez *et al*., 2014
Ppl2	Multiplex5	5.303	0.802	0.811	van de Vliet *et al*., 2009
Ppl3	Multiplex5	3.32	0.736	0.699	van de Vliet *et al*., 2009
Ppl5	Multiplex5	3.551	0.748	0.718	van de Vliet *et al*., 2009
Ppl1	Multiplex6	5.229	0.813	0.809	van de Vliet *et al*., 2009
Ppl12	Multiplex6	3.875	0.738	0.742	van de Vliet *et al*., 2009
Ppl13	Multiplex6	3.16	0.692	0.684	van de Vliet *et al*., 2009
Ppl14	Multiplex6	3.998	0.776	0.750	van de Vliet *et al*., 2009
Ppl6	Multiplex7	3.106	0.702	0.678	van de Vliet *et al*., 2009
Ppl7	Multiplex7	1.595	0.364	0.373	van de Vliet *et al*., 2009
Ppl10	Multiplex7	4.963	0.738	0.798	van de Vliet *et al*., 2009

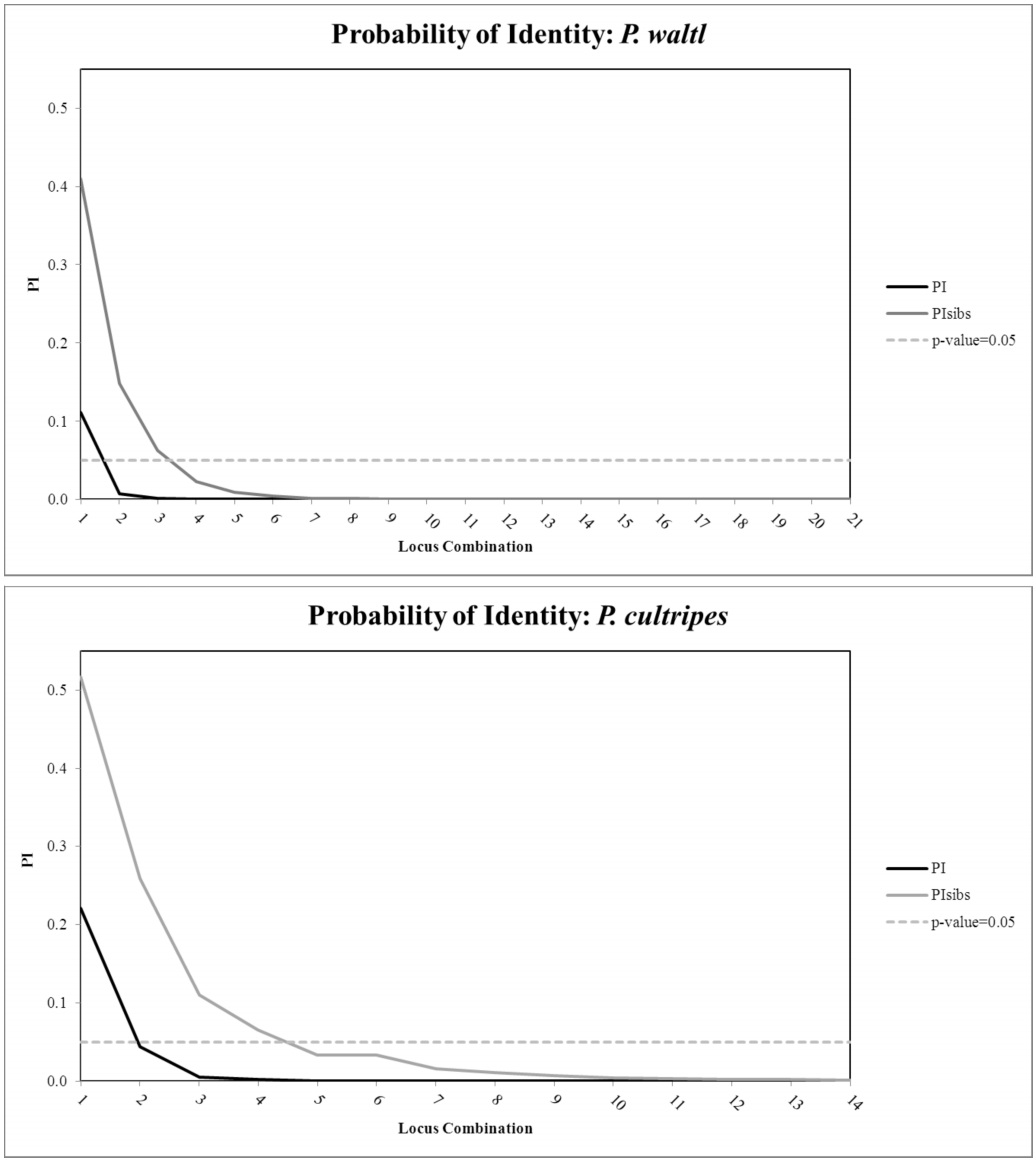

Figure VI.S1. Probability of Identity (with and without related individuals in the sample) as a function of the number of microsatellite loci used for genotyping. The broken line represents the threshold probability that two genotypes are identical at p = 0.05.

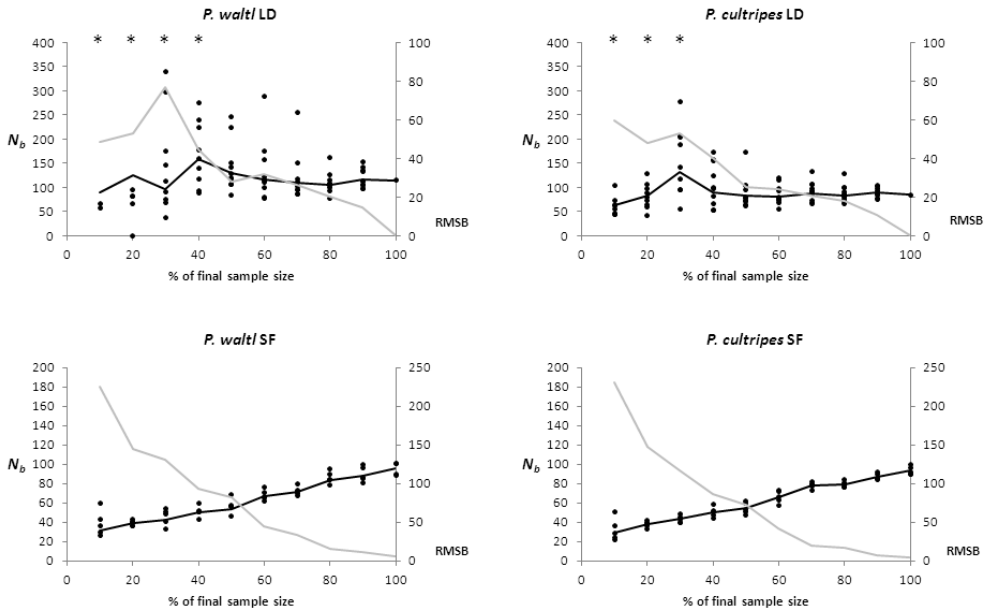

Figure VI.S2. Estimates of Nb based on the LD (top) and SF (bottom) methods with subsamples including increasing proportions of the final offspring sample size in *P. waltl* (left) and *P. cultripes* (right). The black dots and lines represent the values of each replicate and averaged Nb estimates, respectively. The grey lines show the decreasing bias in estimates (represented by RMSB) with increasing sample size. Infinite values are marked with asterisks.

Discusión general

El estudio comparado y multiescala realizado en la presente tesis doctoral ha permitido caracterizar las similitudes y discordancias en los patrones de diversidad y estructura genética de dos especies de anfibios a diferentes niveles de detalle, lo que permite evaluar el papel relativo de los factores demográficos, ecológicos e históricos en su historia evolutiva y comprender mejor su distribución actual. Las diferencias encontradas en la capacidad de dispersión, la respuesta a variables ecológicas asociadas al paisaje que determinan la conectividad poblacional y la escala temporal en la cual se produjeron los procesos antiguos de diversificación en ambas especies contribuyen a explicar las diferencias observadas en su diversidad y estructura genética. El análisis conjunto abarcando diferentes escalas espaciales y temporales ha aportado mayor solidez a la interpretación de las hipótesis propuestas para explicar los resultados obtenidos en cada nivel de análisis que si se hubieran analizado independientemente. Esto es una ventaja asociada a la visión de la filogeografía como una disciplina iterativa (Buckley, 2009), en la que las hipótesis resultantes de la interpretación de los resultados en cada nivel de análisis sirven de punto de partida para diseñar nuevos estudios a otros niveles, con muestreos y herramientas analíticas en ocasiones muy diferentes. Además, los resultados obtenidos tienen importantes implicaciones para el diseño de estrategias de conservación de las dos especies estudiadas, *P. waltl* y *P. cultripes*, también a varios niveles. En primer lugar, mediante la identificación de unidades evolutivamente significativas (ESUs) en ambas especies. Por otro lado, la identificación de los factores ambientales que determinan la conectividad entre sus poblaciones puede ser aplicada en el diseño de corredores naturales. Este punto es muy importante para la viabilidad de las poblaciones de estas especies, ya que los bajos tamaños efectivos poblacionales estimados llevan asociado un alto riesgo de extinción local por problemas de endogamia, entre otros factores.

El papel de los factores paleogeográficos y paleoclimáticos en el modelado de la diversidad genética actual

La península ibérica ha sido identificada como un centro importante de diversificación de especies desde el Mioceno hasta la actualidad, debido a su compleja historia geológica y a las fluctuaciones climáticas ocurridas en el Pleistoceno (Gómez y Lunt, 2007). Buena parte de las especies de la batracofauna

ibérica ha evolucionado *in situ* durante todo este tiempo (Barbadillo *et al*., 1997), por lo que han existido múltiples oportunidades para que eventos paleogeográficos y cambios climáticos tuviesen un efecto similar en comunidades enteras, aunque en la práctica a menudo se han documentado respuestas individuales de diferentes especies en respuesta a estos eventos (Lobo *et al*., 2016). En el caso que nos ocupa, hemos encontrado tanto similitudes como discordancias en los patrones históricos de diversificación de las dos especies estudiadas.

El origen de ambas especies es antiguo (Mioceno), y el proceso de especiación está posiblemente relacionado con eventos de vicarianza asociados a la formación y evolución tectónica del arco bético rifeño durante el Mioceno (Martín *et al*., 2009). Sin embargo, las estimas temporales asociadas a estos eventos de especiación difieren ligeramente. De acuerdo a nuestros resultados, la separación entre *P. waltl* y su grupo hermano, el ancestro de (*P. nebulosus* + *P. poireti*), se ha estimado en unos 18 Ma (Fig. III.S3), mientras el tiempo de divergencia de *P. cultripes* con respecto a su especie hermana *P. varaldii* es de unos 13 Ma (Fig. 5), aunque existe cierto solapamiento en las edades estimadas cuando se toman en consideración los intervalos de confianza de dichas estimas. Estas estimas temporales son algo más antiguas que las propuestas por Carranza y Arnold (2004) y Veith *et al*. (2004) para *Pleurodeles* (5,3-14 Ma) y que las de Busack *et al*. (1985) o García-París *et al*. (2003) en el caso de *Pelobates* (5,5-11 Ma), pero serían consistentes con eventos paleotectónicos en el Burdigaliense y Serravalliense, respectivamente (Rosenbaum *et al*., 2002).

Por otro lado, a nivel intraespecífico se observa una mayor diversidad genética en *P. waltl*, con un TMRCA estimado en unos 3 Ma, mientras que en *P. cultripes* toda la diversidad mitocondrial actual se habría originado dentro del último millón de años, y probablemente en los últimos 500.000 años. Dado el origen Mioceno de ambas especies, esta diferencia podría estar asociada a la existencia de extinciones masivas de linajes más antiguos en *P. cultripes* durante las glaciaciones del Plioceno y Pleistoceno, que contrastaría con una historia evolutiva ininterrumpida (o con una incidencia menor de procesos de extinción) desde el Plioceno en *P. waltl*. Aunque ambas especies presentan un patrón similar de distribución de su diversidad genética en sentido este-oeste en la península ibérica (ver por ej. Figs. III.1 y IV.1), el origen temporal de estos patrones es

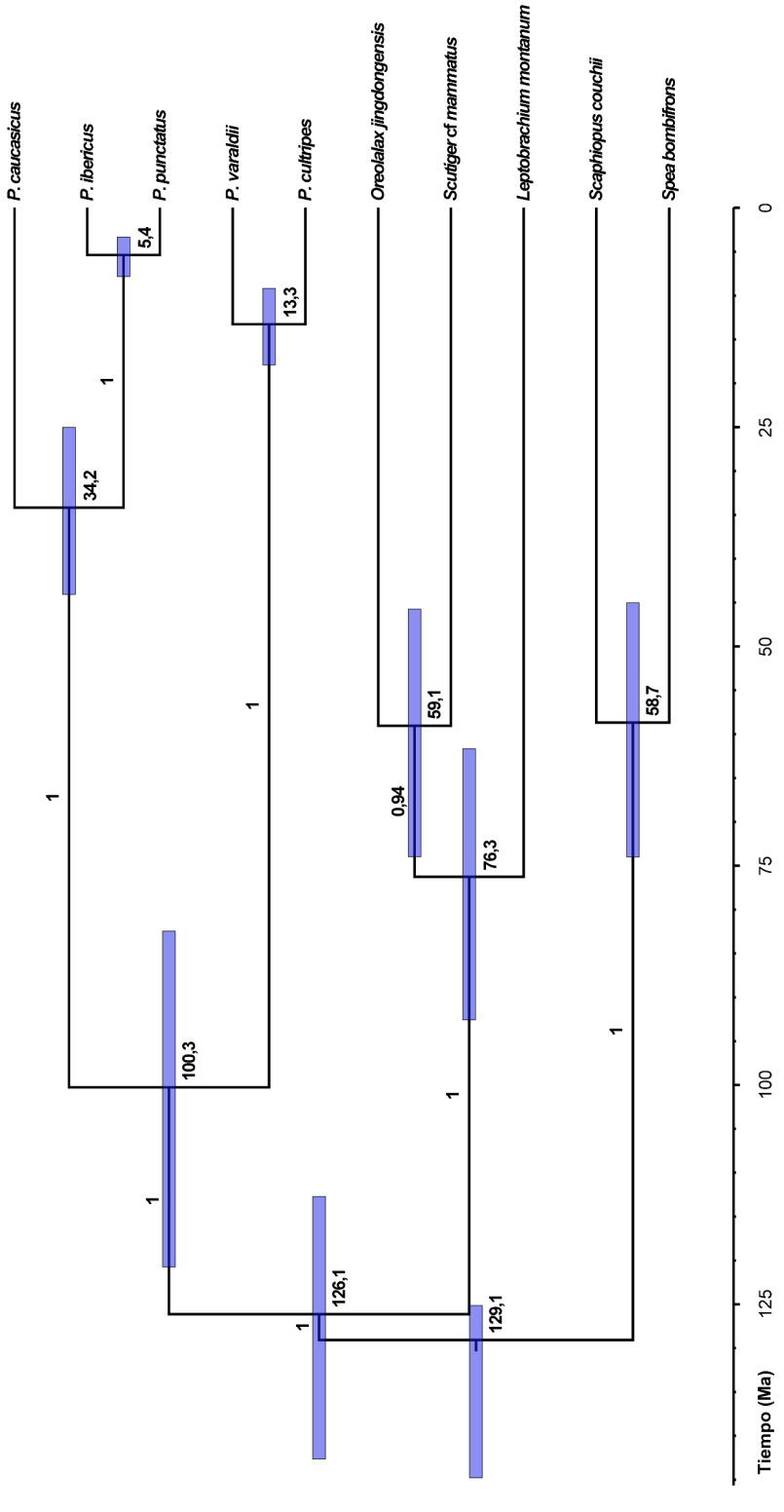

Figura 5. Árbol calibrado obtenido mediante el análisis en BEAST de secuencias del gen mitocondrial ND4. Los valores sobre las ramas muestran las probabilidades posteriores bayesianas (BPPs). Las barras moradas representan el intervalo de confianza al 95% de máxima densidad posterior de las estimas de tiempo (HPDis; valores de la mediana debajo de las barras). Escala en millones de años (Ma).

diferente. En *P. waltl* la separación entre los dos principales linajes intraespecíficos se ha estimado en el Plioceno, hace unos 3,5 Ma (Fig. III.2A), y posiblemente esté asociada a la formación de la cuenca actual del río Guadalquivir (Doadrio, 1988). Este evento paleogeográfico ha sido asociado con anterioridad a procesos de vicarianza en otros organismos con capacidad de dispersión limitada, como anfibios y reptiles, por ejemplo en los géneros *Discoglossus* (Martínez-Solano, 2004) y *Vipera* (Velo-Antón *et al*., 2012), respectivamente. En cambio, en el caso de *P. cultripes*, el patorón de diferenciación genética este-oeste se habría originado durante el Pleistoceno, debido probablemente a la fragmentación de sus poblaciones asociada a refugios glaciares en diferentes áreas dentro de la península ibérica.

Dentro de cada uno de estos linajes o haplogrupos mitocondriales que encontramos en ambas especies también existen diferencias en su estructura y diversidad genética. En el caso de *P. waltl*, el linaje "Oeste" está subdividido en dos: un sublinaje restringido al Algarve portugués y otro que ocupa el oeste y centro de la península ibérica (Figs. III.1A y 2A-B). Esta diferenciación de las poblaciones del suroeste portugués ya ha sido descrita en otros taxones de invertebrados y vertebrados como anfibios y reptiles (Serrano, 1995; Martínez-Solano *et al*., 2006; Godinho *et al*., 2008) y se ha asociado a la formación de la Serra do Caldeirão durante el Plioceno Temprano (Gonçalves *et al*., 2009), entre otros posibles factores (van de Vliet *et al*., 2014). Sin embargo, en *P. cultripes*, el haplogrupo "Oeste" está subdividido en dos grupos formados por las poblaciones al norte y al sur del Sistema Central, es decir, por un lado las que ocupan la Meseta Norte y por otro, las poblaciones distribuidas al sur de esta cadena montañosa, que al oeste se extienden también a lo largo de la costa atlántica hacia el norte hasta Galicia (Fig. IV.1). El linaje "Este" de *P. waltl* se subdivide en tres subclados bien diferenciados y apoyados estadísticamente, lo que sugiere la existencia de varios eventos de vicarianza que según nuestras dataciones se habrían producido durante el Pleistoceno (Fig. III.2A-B). Uno de estos linajes se distribuye por las cuencas hidrográficas del este de la península ibérica, otro por la cuenca hidrográfica del Guadalquivir y el último agrupa a las poblaciones de Marruecos (Fig. III.1A). Por el contrario, el haplogrupo "Este" de *P. cultripes* presenta una gran homogeneidad genética a lo largo de su amplia distribución en

el este ibérico y costas atlántica y mediterránea francesas (Fig. IV.1).

Una de las aportaciones novedosas al conocimiento de la historia evolutiva de *P. waltl* en esta tesis es la monofilia de las poblaciones del norte de África de acuerdo a los datos de ADNmit, que no había sido recuperada en estudios previos. Este nuevo resultado, junto con los resultados obtenidos con marcadores de evolución más rápida (microsatélites), sugiere que las poblaciones marroquíes se habrían originado por un evento de dispersión a través del mar desde la península ibérica durante el Pleistoceno, con flujo génico posterior en tiempos más recientes, lo que implica que al menos se produjeron dos eventos de dispersión transmarina. Tanto las poblaciones del norte de Marruecos como las de la cuenca del Guadalquivir se caracterizan por su alta diversidad genética (Figs. III.3 y III.S1), lo que asociado a la estabilidad climática inferida para estas áreas a lo largo del tiempo refuerza la interpretación de su papel como reservorios históricos de la diversidad genética de la especie.

Los resultados obtenidos con marcadores de tipo microsatélite son en general congruentes con los resultados de ADNmit (Figs. III.1C y IV.4A). Este tipo de marcadores de evolución rápida generalmente reflejan la estructura genética de las poblaciones a una escala temporal más reciente que los marcadores mitocondriales. Las principales discordancias entre marcadores nucleares y mitocondriales fueron detectadas en *P. waltl*, ya que los microsatélites identificaron un grupo genético bien diferenciado al norte del Sistema Central sin correspondencia con los datos de ADNmit (Figs. III.1A y III.1C). En ambas especies, las poblaciones de la Meseta Norte se caracterizan por presentar muy baja diversidad genética, lo que sugiere una colonización reciente de las áreas localizadas al norte del Sistema Central. Sin embargo, los análisis de difusión continua realizados con Beast apoyan una colonización más reciente en el caso de *P. waltl*, que se habría producido durante el último interglaciar (88 ka), mientras que en *P. cultripes* este evento se habría producido hace al menos unos 130 ka (Figs. III.S9 y IV.2). Esta estima es consistente con la presencia de un haplogrupo mitocondrial exclusivo de esta área en esta especie, lo que apoyaría el asentamiento de poblaciones de *P. cultripes* en la Meseta Norte desde más antiguo.

En el caso de *P. waltl*, la mayor parte de los linajes o grupos genéticos están bien delimitados y se caracterizan por tener poco flujo génico entre ellos (Figs. III.1A y III.1C). En general, se encuentran restringidos a las grandes cuencas hidrográficas de la península ibérica: el grupo Meseta Norte en la cuenca de Duero, el grupo Suroeste en las cuencas del Tajo y Guadiana, el grupo Sur en la cuenca del Guadalquivir, y por último, el grupo Mediterráneo principalmente restringido a las cuencas del Segura y del Levante. En cambio, en *P. cultripes* se observan amplias áreas donde hay flujo génico entre los diferentes grupos (Figs. IV.1B y IV.4A), probablemente debido unas mayores tasas de migración históricas o procesos de diferenciación más recientes.

Los cambios climáticos ocurridos durante los periodos glaciares e interglaciares del Pleistoceno produjeron grandes cambios en la distribución y diversidad genética de múltiples especies en ambientes templados, ocasionando la extinción de linajes, la fragmentación de poblaciones mediante eventos de vicarianza, o fuertes cuellos de botella (Hewitt, 1996; Provan y Bennett, 2008). En esta tesis hemos mostrado cómo la integración de modelos de distribución de especies proyectados al pasado junto con inferencias filogeográficas basadas en datos moleculares permite plantear hipótesis robustas sobre los procesos demográficos a los que han estado sometidas las especies durante los últimos 130.000 años. Este análisis integrador ha permitido inferir respuestas desiguales de *P. waltl* y *P. cultripes* a las oscilaciones climáticas del Pleistoceno Superior.

En el caso de *P. cultripes*, los resultados muestran una gran estabilidad de la favorabilidad climática en gran parte de su distribución, aunque con decrecimientos significativos en el noroeste de la península ibérica y costa atlántica francesa desde el LIG (Figs. IV.S4 y S7). En estas regiones se encuentran poblaciones en áreas ecológicamente marginales y con una diversidad genética muy reducida (Figs. IV.S2 y S4). La correlación significativa entre las áreas estables entre el LIG-LGM y la diversidad genética actual apoyan la existencia de refugios glaciares en el suroeste y sureste de la península ibérica, la Meseta Norte y posiblemente en el sureste de Francia (Figs. IV.3B-D). En combinación con los análisis de difusión continua, los modelos climáticos permiten inferir la colonización reciente de áreas de la costa atlántica de la península ibérica y de la costa atlántica francesa.

En *P. waltl*, los resultados muestran una estabilidad climática aún mayor desde el último periodo interglaciar hasta la actualidad (Fig. III.3). La favorabilidad climática durante el LGM está significativamente correlacionada con la actual (Fig. III.S12), aunque con un moderado decrecimiento de la favorabilidad en la transición LIG-LGM en el este de la península ibérica (Fig. III.3). Esta pérdida de áreas potencialmente favorables para la especie podría haber ido acompañada de reducciones en los tamaños efectivos poblacionales históricos. Esta pérdida de áreas potencialmente favorables para la especie podría haber ido acompañada de reducciones en los tamaños efectivos poblacionales históricos, algo que parecen apoyar, al menos parcialmente, los datos moleculares.

La presencia actual de las dos especies al norte del Sistema Central, en la Meseta Norte, está asociada con bajos niveles de diversidad genética. Varias líneas de evidencia sugieren que esto puede ser la consecuencia de ciclos de extinción y re-colonización durante el Pleistoceno. Por ejemplo, ambas especies están presentes en yacimientos del Pleistoceno Inferior en la Meseta Norte (Martín & Sanchiz, 2013). Estos yacimientos son más antiguos que las estimas moleculares (TMRCAs) asociadas a los haplogrupos presentes en esta zona. Los cambios de favorabilidad climática desde el LIG en la Meseta Norte y la evidencia (aunque limitada) de cambios demográficos recientes en las poblaciones en esta zona apoyarían también esta posible dinámica de colonización-extinción-recolonización de los territorios localizados al norte del Sistema Central.

En resumen, a pesar de presentar distribuciones sintópicas a lo largo de la mayor parte de la península ibérica, la diversidad genética actual de las dos especies es el resultado de procesos acontecidos a diferentes escalas temporales, con eventos de diferenciación genética desde el Plioceno-Pleistoceno en *P. waltl*, que contrastan con otros más recientes en *P. cultripes*, concentrados en los últimos 500 ka. Los patrones de diversidad genética global presentan similitudes a nivel espacial, con un patrón Este-Oeste en las dos especies cuyo origen no obstante estaría asociado a procesos evolutivos distintos. En el caso de *P. waltl*, la división Este-Oeste se produjo como resultado de los eventos paleogeográficos asociados a la formación de la cuenca del Guadalquivir, en el Plioceno, mientras que en *P. cultripes* fueron eventos más recientes, probablemente asociados a las oscilaciones climáticas ocurridas en el Pleistoceno. Dentro de cada uno de estos

grupos Este-Oeste los procesos de diversificación fueron también diferentes, siendo las poblaciones de *P. cultripes* en general más homogéneas y con mayor grado de mezcla desde un punto de vista genético que las de *P. waltl*. Estas diferencias en los patrones de diversidad genética pueden estar relacionadas, entre otros factores, con diferencias en la capacidad de dispersión de las dos especies, así como en sus respuestas frente a variables ambientales y topográficas asociadas al paisaje que condicionan los patrones de conectividad regional. Estas cuestiones han sido analizadas en los correspondientes niveles de análisis, como se discute a continuación.

Principales factores que condicionan los patrones de conectividad y estructura genética contemporánea

El estudio comparado realizado para evaluar el efecto de las características del paisaje en los patrones de diferenciación y estructura genética ha contribuido de manera relevante al conocimiento de la conectividad funcional en hábitats mediterráneos como los ocupados por ambas especies. Las características del paisaje que determinan los procesos de diferenciación genética en *P. waltl* y *P. cultripes* están asociadas a la topografía/elevación (a macroescala) y a los patrones de heterogeneidad del hábitat (a microescala), pero estas características inciden de manera diferente en las dos especies estudiadas (Tabla V.3). Cabe destacar también que el uso de variables continuas de cobertura vegetal y contenido en agua obtenidas mediante técnicas de teledetección ha aportado información clave a la hora de comprender el efecto de variables asociadas al paisaje en los patrones de conectividad entre poblaciones.

Los patrones de diferenciación genética de ambas especies a escala regional muestran gran congruencia con los resultados a escala filogeográfica, ya que en el caso de *P. waltl* se observa una estructura genética más marcada tanto a escala regional como filogeográfica que en el caso de *P. cultripes* (Figs. III.1C, IV.4A y V.1). A escala filogeográfica, en ambas especies se ha podido documentar la diferenciación genética entre las poblaciones localizadas al norte y sur del Sistema Central (Figs. III.1C, IV.1B y IV.4A). En este sentido, la hipótesis de que el Sistema Central haya podido actuar como una barrera histórica al flujo génico en ambas especies es apoyada por los resultados de los análisis de genética del

paisaje. Tanto en *P. waltl* como en *P. cultripes*, los análisis de resistencia al flujo génico mostraron el efecto negativo de la altitud y la pendiente en la conectividad entre poblaciones (Tabla V.3; Fig. V.3). Estos datos son congruentes con la información existente sobre el rango altitudinal que ocupan ambas especies a lo largo de sus áreas de distribución. Generalmente, las dos especies ocupan hábitats mediterráneos en altitudes bajas o medias, con poblaciones escasas a partir de los 1000 metros (García-París *et al*., 2004). Los procesos de diferenciación genética modulada por la topografía (elevación y pendiente) probablemente tienen consecuencias a escalas temporales mayores, de decenas o centenas de miles de años, debido a su mayor estabilidad en estos marcos temporales con respecto a otro tipo de variables. Por ejemplo, hay constancia de que durante el LGM las áreas cubiertas por glaciares descendieron a altitudes de unos 1350 m (Bullón, 2016), lo que muy probablemente habría limitado la conectividad entre poblaciones de ambas especies localizadas en diferentes vertientes de este sistema montañoso.

Por otro lado, de acuerdo a nuestros resultados, los factores que determinan la conectividad entre las poblaciones de las dos especies a una escala temporal más reciente (contemporánea) están asociados a cambios en los patrones de cobertura vegetal, su contenido en agua y la heterogeneidad espacial a escala fina del paisaje (Tabla V.3; Fig. V.3). A lo largo del tiempo, los cambios en la vegetación son más dinámicos en escalas temporales más breves, y por ejemplo en el área de estudio hay constancia de que han estado cambiando constantemente desde el Holoceno debido a actividades humanas (López-Sáez *et al*., 2014). Debido a la frecuente sintopía observada en las dos especies, cabría esperar similitudes en su respuesta a las variables analizadas a escala de paisaje. No obstante, se han observado diferencias significativas en el papel que juega la vegetación en el modelado de la estructura genética de las dos especies.

En el caso de *P. waltl*, la diferenciación genética a pequeña escala está asociada a variables relacionadas con la heterogeneidad espacial de la vegetación, mientras que en *P. cultripes* estaría determinada fundamentalmente por la cantidad de cobertura vegetal (Tabla V.3). La conectividad entre las poblaciones de *P. waltl* aumenta con valores altos de heterogeneidad de la cobertura vegetal (variables NDVI y NDVI std.-dev.) y de la heterogeneidad del contenido de agua

de la vegetación (NDMI std.-dev.), mientras que en *P. cultripes*, la diferenciación genética se incrementa a valores bajos y altos de cobertura vegetal (Fig. V.2). Estos resultados indican que a pesar de presentar requerimientos ecológicos similares a macroescala (Sillero *et al*., 2009), existen diferencias importantes en la selección de microhábitats en las dos especies. Estas diferencias estarían relacionadas con los hábitats terrestres que ocupan, ya que ambas se suelen reproducir en los mismos puntos de agua (Recuero, 2014). En el caso de *P. waltl*, los hábitats heterogéneos y moderadamente alterados con vegetación natural o seminatural favorecen la conectividad entre las poblaciones. En contraste, en *P. cultripes* los microhábitats que favorecen la conectividad y dispersión estarían asociados a valores medios de cobertura vegetal, con valores de alta resistencia al flujo génico en áreas urbanas o antropizadas, como carreteras (bajos valores de NDVI), aunque también en áreas forestales de alta montaña (altos valores de NDVI). Las características de los hábitats favorables para las dos especies son propias de paisajes mediterráneos de altitudes bajas o medias, que incluyen tanto áreas manejadas extensivamente, como pueden ser las dehesas, como hábitats naturales o seminaturales ocupados por matorral y/o bosque mediterráneo.

Además de las variables relacionadas con la vegetación, las grandes superficies de agua y los ríos parecen actuar como barreras potenciales al flujo génico en áreas de baja altitud y pendiente, especialmente en *P. cultripes* y en menor medida en *P. waltl* (Fig. V.3). Sin embargo, algunas variables que determinan la estructura genética en otras especies de anfibios, como la red de carreteras o los tipos de usos del suelo (Richardson, 2012; Coster *et al*., 2015), no parecen tener un papel significativo en la conectividad de las poblaciones de las dos especies estudiadas (Tabla V.3). En parte, esto podría ser debido a que la mayoría de los cambios en los usos del suelo y la construcción de la red de carreteras en el área de estudio se produjo recientemente, a partir de las décadas de los años cincuenta y sesenta del siglo pasado. Se han descrito casos donde las restricciones al flujo génico pueden tardar varias generaciones en modificar la estructura genética de las especies (Safner *et al*., 2011), aunque este desfase depende del tipo de hábitat y del tiempo de generación de las especies implicadas (Landguth *et al*., 2010).

En resumen, aunque ambas especies tienen requerimientos ecológicos similares a macroescala, a nivel regional nuestros resultados muestran diferencias en su estructura genética posiblemente asociadas a la selección de microhábitats terrestres. Estas diferencias determinan los patrones de conectividad entre poblaciones, aunque existen otros factores adicionales como las diferencias en la capacidad de dispersión entre anuros y urodelos, y/o en los tamaños efectivos poblacionales que deben ser analizados a una escala más detallada. Si bien a escala regional no se ha encontrado un efecto de la densidad (representada por el tamaño efectivo, Ne) en los patrones de conectividad de las dos especies, es importante llevar a cabo estudios demográficos detallados que permitan relacionar las estimas de Ne con el tamaño de censo de la población y contrastar las estimas indirectas (genéticas) de flujo génico con observaciones directas basadas en estudios de captura-marcaje-recaptura.

Relación entre demografía y biología de las especies con los patrones de diversidad y estructura genética

Además de las diferencias en la selección de microhábitats, existen otros factores asociados a la demografía o a la biología de las especies que pueden tener un efecto importante en los patrones de diversidad y estructura genética a diferentes escalas espaciales y temporales y que pueden contribuir por tanto a explicar las diferencias observadas en nuestro sistema de estudio. En el caso concreto de los anfibios, se ha descrito por ejemplo que diferencias entre especies en ciertas características biológicas, como por ejemplo la filopatría, la capacidad de dispersión, el tamaño efectivo poblacional o el tiempo de generación, entre otros, pueden promover la aparición de diferencias en los patrones de diferenciación genética (Richardson, 2012; Whiteley *et al*., 2014; Nowakowski *et al*., 2015). En la presente tesis doctoral nos hemos centrado en el estudio a escala regional y local de dos de estos parámetros: la filopatría y la capacidad de dispersión.

En primer lugar, una mayor filopatría tiene como consecuencia una estructura genética más marcada, ya que al haber menos flujo génico entre poblaciones, aumenta la diferenciación por deriva genética. En este sentido, las estimas del coeficiente de endogamia (Fis) obtenidas en el Capítulo III sugieren un mayor comportamiento filopátrico en *P. waltl*, ya que los valores medios

estimados en poblaciones de esta especie duplican a los de *P. cultripes* (0.01 y 0.004, respectivamente). En cuanto a la capacidad de dispersión, a pesar de ser uno de los factores más determinantes en el mantenimiento del flujo génico entre poblaciones, existe un gran vacío en la literatura, y de hecho con anterioridad a nuestro estudio no se disponía de estimas de dispersión para ninguna de las dos especies seleccionadas. Los resultados obtenidos a escala regional sugieren bajas tasas de migración en las dos especies, con gran solapamiento en los intervalos de confianza, pero con valores medios superiores en *P. cultripes* (Tabla V.5). Además, los intervalos de confianza incluyen valores altos (>1 km), lo que podría sugerir que las dos especies son capaces de dispersarse a grandes distancias, aunque con baja frecuencia (dando lugar a las típicas curvas leptokúrticas de dispersión, ver Smith y Green, 2005). Estas estimas, junto con la presencia de áreas amplias de baja resistencia al flujo génico en la zona de estudio, pueden contribuir a explicar la existencia de zonas caracterizadas por una escasa diferenciación genética entre poblaciones, especialmente en el caso de *P. cultripes* (Fig. V.1), tanto a escala regional como filogeográfica.

A escala local, las observaciones directas obtenidas mediante métodos de captura-marcaje-recaptura en las proximidades de la laguna de Valdemanco (Madrid) muestran que los eventos de dispersión son bastante limitados en las dos especies, aunque ligeramente más frecuentes en *P. cultripes*. Las tasas de dispersión a escala local fueron del 1,2% en *P. cultripes* y del 0,5% en *P. waltl*, con una mayor frecuencia de desplazamientos superiores a 250 metros en *P. cultripes* que en *P. waltl*. Las diferencias observadas son consistentes con la información disponible para otras especies de anfibios, que muestran una capacidad de dispersión generalmente mayor en anuros que en urodelos (Smith y Green, 2005). Las diferencias en las estimas directas e indirectas en la capacidad de dispersión, tanto a escala regional como local, unidas a la mayor filopatría en *P. waltl* son consistentes y contribuirían a explicar las diferencias en los patrones de diferenciación genética a escala regional y filogeográfica entre las dos especies estudiadas.

Aplicaciones para la conservación

Una de las prioridades en biología de la conservación es predecir la respuesta de las especies ante amenazas como la fragmentación del hábitat, los cambios de usos del suelo, la contaminación, el cambio climático, etc., para poder implementar medidas eficaces de conservación que aseguren su viabilidad a largo plazo. Para diseñar planes de conservación efectivos es necesario un conocimiento detallado de la biología de las especies, de su interacción con el medio y de su diversidad genética. Los anfibios son uno de los grupos de vertebrados más amenazados globalmente, ya que más de un tercio de las especies conocidas están incluidas en alguna categoría de amenaza según los criterios de la IUCN (2007). Además, en la cuenca Mediterránea, muchos de sus ecosistemas se encuentran amenazados (Blondel y Aronson, 1999; Beja y Alcazar, 2003). La supervivencia de muchas poblaciones está en peligro debido a la pérdida y degradación de los medios acuáticos en que se reproducen y a los efectos impredecibles del cambio climático en su hidroperiodo (Doulgeris *et al*., 2016). En este sentido, algunos de los resultados obtenidos en esta tesis doctoral pueden resultar relevantes para implementar estrategias eficientes para la conservación de las especies de anfibios aquí estudiadas, a varios niveles:

- **A escala filogeográfica:** para el desarrollo de estrategias globales de conservación, incluida la elaboración de listas rojas nacionales y regionales de especies amenazadas, es fundamental describir patrones de diversidad genética intraespecífica y delimitar unidades evolutivas (ESUs) (Moritz, 1994). En este sentido, los estudios filogeográficos desarrollados en esta tesis han permitido delimitar diferentes grupos con una historia evolutiva común en *P. cultripes* y, especialmente, en *P. waltl* (los linajes Este y Oeste), que pueden considerarse por tanto ESUs y ser objeto de planes de conservación específicos. Además, cabe destacar que ambas especies muestran una menor diversidad genética en latitudes más altas, mientras que las áreas con mayor riqueza genética se encuentran concentradas en el sur de la península ibérica y (en el caso de *P. waltl*) en el norte de África. Debido a su mayor diversidad genética y estabilidad histórica frente a cambios climáticos en el pasado, estas áreas deberían ser prioritarias

para la conservación de las dos especies, ya que históricamente ya han mostrado tener un papel importante como reservorios en periodos climáticamente desfavorables. En cambio, las poblaciones situadas en la mitad septentrional de la península ibérica y las costas mediterráneas y atlánticas francesas podrían ser más vulnerables a largo plazo, debido a su menor diversidad genética y a la menor favorabilidad climática actual de las zonas que ocupan, que las harían más vulnerables frente a cambios climáticos a medio o largo plazo.

- **A escala regional:** conocer cuáles son las factores que condicionan o determinan la conectividad de las poblaciones es fundamental para planificar su gestión (Gonçalves *et al*., 2016). Para ello, en esta tesis se ha adoptado la aproximación de cuantificar la resistencia relativa que plantean diferentes variables ambientales y topográficas, que promueven o dificultan la dispersión de los individuos de distintas especies (Spear *et al*., 2010). Estos análisis de genética del paisaje permiten mejorar el diseño de corredores naturales, que son fundamentales para la toma de decisiones relativas a la conservación de poblaciones y especies (Dennis *et al*., 2013; Nuñez *et al*., 2013). Además, la realización de estudios comparados con especies codistribuidas permite en principio diseñar planes de conservación eficaces y eficientes para un conjunto de taxones mediante la identificación de variables importantes para la conectividad en múltiples especies (Schwenk y Donovan, 2011; Keller *et al*., 2014). En el caso de las especies aquí estudiadas, se ha mostrado cómo las variables asociadas a la complejidad o heterogeneidad de la estructura del hábitat a escala fina, asociadas a la cobertura y al contenido de agua de la vegetación (ej. NDVI, NDMI), favorecen la conectividad entre sus poblaciones (Tabla V.3 y Fig. V.3). El diseño de corredores potenciales de dispersión debería considerar por tanto como áreas prioritarias aquellos hábitats a baja o media altitud ocupados por áreas de matorral mediterráneo natural o seminatural más o menos densas, incluyendo dehesas. Esto facilitaría la dispersión y la conectividad entre poblaciones de ambas especies y contribuiría a asegurar la viabilidad de sus poblaciones a largo plazo (Bennett y Saunders, 2010). Además, nuestros resultados también permitirían diseñar planes específicos para

cada especie, teniendo en cuenta las diferencias observadas en la selección de microhábitats.

- **A escala local:** disponer de estimas del tamaño efectivo poblacional es fundamental para determinar la viabilidad de las poblaciones a medio o largo plazo. Frankham *et al*. (2014) propusieron un valor mínimo de Ne de unos 100 individuos para asegurar la supervivencia de las poblaciones y evitar o minimizar problemas de depresión endogámica en poblaciones naturales en ausencia de migración con poblaciones próximas. En el caso de las especies aquí estudiadas, a pesar de ser a priori poblaciones en buen estado de conservación, los valores de Ne obtenidos son próximos a este mínimo, alrededor de 120 en *P. waltl* y de 90 en *P. cultripes* (Tabla VI.1). Estos valores tan bajos sugieren que es determinante facilitar y garantizar la conectividad entre poblaciones para asegurar su viabilidad y potencial evolutivo a largo plazo y evitar posibles procesos de depresión genética por endogamia (Johnson *et al*., 2007). Esto requiere la adopción de medidas específicas, puesto que tanto en el caso de *P. waltl* como en *P. cultripes*, las tasas de dispersión estimadas y observadas fueron bajas (Tabla V.5). En conjunto, estos parámetros (bajo tamaño efectivo y capacidad de dispersión) hacen que estas especies sean de por sí muy sensibles a la fragmentación; por ello las medidas de conservación a adoptar deberían ir enfocadas a mejorar la conectividad de sus poblaciones. Para ello, además de la identificación de variables del paisaje asociadas a la conectividad, a la hora de diseñar corredores es importante tener en cuenta las diferencias en la capacidad de dispersión de las especies al considerar las distancias relativas de las poblaciones cuya conectividad se pretende mejorar o reforzar.

Referencias

Barbadillo L, García-París M, Sanchiz B (1997) Orígenes y relaciones evolutivas de la herpetofauna ibérica. In: Distribución y biogeografía de los anfibios y reptiles en España y Portugal (ed. Pleguezuelos JM), pp. 47–100. Universidad de Granada, Asociación Herpetológica Española, Granada.

Beja P, Alcazar R (2003) Conservation of Mediterranean temporary ponds under agricultural intensification: an evaluation using amphibians. Biological Conservation 114: 317–326.

Bennett AF, Saunders DA (2010) Habitat fragmentation and landscape change. In: Conservation biology for all (eds. Sodhi NS, Ehrlich PR), pp. 88–106. Oxford University Press, New York.

Blondel J, Aronson J (1999) Biology and wildlife of the Mediterranean region. Oxford University Press, USA.

Buckley D (2009) Toward an organismal, integrative, and iterative phylogeography. BioEssays 31: 784–793.

Bullón T (2016) The upper Pleistocene on the northern face of the Guadarrama Mountains (central Spain): Palaeoclimatic phases and glacial activity. Geomorphology 268: 233–245.

Coster SS, Babbitt KJ, Cooper A, Kovach AI (2015) Limited influence of local and landscape factors on finescale gene flow in two pond-breeding amphibians. Molecular Ecology 24: 742–758.

Dennis RLH, Dapporto L, Dover JW, Shreeve TG (2013) Corridors and barriers in biodiversity conservation: a novel resource-based habitat perspective for butterflies. Biodiversity and Conservation 22: 2709–2734.

Doadrio I (1988) Delimitation of areas in the Iberian Peninsula on the basis of freshwater fishes. Bonner Zoologische Beiträge 39: 113–128.

Doulgeris C, Papadimos D, Kapsomenakis J (2016) Impacts of climate change on the hydrology of two Natura 2000 sites in Northern Greece. Regional Environmental Change 16: 1941–1950.

Frankham R, Bradshaw CJA, Brook BW (2014) Genetics in conservation management: Revised recommendations for the 50/500 rules, Red List criteria and population viability analyses. Biological Conservation 170: 56–63.

García-París M, Montori A, Herrero P (2004) Fauna Iberica. Vol. 24. Amphibia: Lissamphibia. Museo Nacional de Ciencias Naturales, Consejo Superior de Investigaciones Científicas, Madrid.

Godinho R, Crespo EG, Ferrand N (2008) The limits of mtDNA phylogeography: complex patterns of population history in a highly structured Iberian lizard are only revealed by the use of nuclear markers. Molecular Ecology 17: 4670–4683.

Gómez A, Lunt D (2007) Refugia within Refugia: patterns of phylogeographic concordance in the Iberian Peninsula. In: Phylogeography of Southern European Refugia (eds. Weiss S, Ferrand N), pp. 155–188. Springer Netherlands.

Gonçalves H, Martínez-Solano I, Pereira RJ, *et al*. (2009) High levels of population subdivision in a morphologically conserved Mediterranean toad (*Alytes cisternasii*) result from recent, multiple refugia: evidence from mtDNA, microsatellites and nuclear genealogies. Molecular Ecology 18: 5143–5160.

Gonçalves J, Honrado JP, Vicente JR, Civantos E (2016) A model-based framework for assessing the vulnerability of low dispersal vertebrates to landscape fragmentation under environmental change. Ecological Complexity 28: 174–186.

Hewitt GM (1996) Some genetic consequences of ice ages, and their role, in divergence and speciation. Biological Journal of the Linnean Society 58: 247–276.

IUCN (2007) 2007 IUCN Red List of Threatened Species.

Johnson JR, Knouft JH, Semlitsch RD (2007) Sex and seasonal differences in the spatial terrestrial

distribution of gray treefrog (*Hyla versicolor*) populations. Biological Conservation 140: 250–258.

Keller D, Holderegger R, Strien MJ, Bolliger J (2014) How to make landscape genetics beneficial for conservation management? Conservation Genetics 16: 503–512.

Landguth E, Cushman S, Schwartz M, *et al*. (2010) Quantifying the lag time to detect barriers in landscape genetics. Molecular Ecology 19: 4179–4191.

Lobo JM, Martínez–Solano I, Sanchiz B (2016) A review of the palaeoclimatic inference potential of Iberian Quaternary fossil batrachians. Palaeobiodiversity and Palaeoenvironments 96: 125–148.

Martín JM, Braga JC, Aguirre J, Puga-Bernabéu Á (2009) History and evolution of the North-Betic Strait (Prebetic Zone, Betic Cordillera): A narrow, early Tortonian, tidal-dominated, Atlantic-Mediterranean marine passage. Sedimentary Geology 216: 80–90.

Martín C, Sanchiz B (2013). Lisanfos KMS. Version 1.2. Museo Nacional de Ciencias Naturales, MNCN-CSIC. Madrid, Spain. Disponible: http:// www.lisanfos.mncn.csic.es Acceso 15 octubre de 2015.

Martínez-Solano I (2004) Phylogeography of Iberian *Discoglossus* (Anura: Discoglossidae). Journal of Zoological Systematics and Evolutionary Research 42: 298–305.

Martínez-Solano I, Teixeira J, Buckley D, García–París M (2006) Mitochondrial DNA phylogeography of *Lissotriton boscai* (Caudata, Salamandridae): evidence for old, multiple refugia in an Iberian endemic. Molecular Ecology 15: 3375–3388.

Moritz C (1994) Defining 'evolutionarily significant units' for conservation. Trends in Ecology & Evolution 9: 373–375.

Nowakowski AJ, DeWoody JA, Fagan ME, Willoughby JR, Donnelly MA (2015) Mechanistic insights into landscape genetic structure of two tropical amphibians using field–derived resistance surfaces. Molecular Ecology 24: 580–595.

Nuñez TA, Lawler JJ, McRae BH, *et al*. (2013) Connectivity planning to address climate change. Conservation Biology 27: 407–416.

Provan J, Bennett KD (2008) Phylogeographic insights into cryptic glacial refugia. Trends in Ecology & Evolution 23: 564–571.

Recuero E (2014) Sapo de espuelas – *Pelobates cultripes* (Cuvier, 1829). In: Enciclopedia Virtual de los Vertebrados Españoles (eds. Salvador A, Martínez–Solano I). Museo Nacional de Ciencias Naturales, Madrid.

Richardson JL (2012) Divergent landscape effects on population connectivity in two co–occurring amphibian species. Molecular Ecology 21: 4437–4451.

Rosenbaum G, Lister GS, Duboz C (2002) Reconstruction of the tectonic evolution of the western Mediterranean since the Oligocene. Journal of the Virtual Explorer 8: 107–130.

Safner T, Miaud C, Gaggiotti O, *et al*. (2011) Combining demography and genetic analysis to assess the population structure of an amphibian in a human-dominated landscape. Conservation Genetics 12: 161–173.

Schwenk WS, Donovan TM (2011) A multispecies framework for landscape conservation planning. Conservation Biology 25: 1010–1021.

Serrano A (1995) Description and natural history of tiger beetles larvae (Coleoptera: Cicindelidae) from Castro Marim-Vila Real de Santo António Region (Algarve, Portugal). Arquivos

do Museu Bocage 2: 555–606.

Sillero N, Brito JC, Skidmore AK, Toxopeus AG (2009) Biogeographical patterns derived from remote sensing variables: the amphibians and reptiles of the Iberian Peninsula. Amphibia-Reptilia 30: 185–206.

Smith MA, Green DM (2005) Dispersal and the metapopulation paradigm in amphibian ecology and conservation: are all amphibian populations metapopulations? Ecography 28: 110–128.

Spear SF, Balkenhol N, Fortin M–J, McRae BH, Scribner K (2010) Use of resistance surfaces for landscape genetic studies: considerations for parameterization and analysis. Molecular Ecology 19: 3576–3591.

van de Vliet MS, Diekmann OE, Machado M, *et al*. (2014) Genetic divergence for the amphibian *Pleurodeles waltl* in southwest Portugal: dispersal barriers shaping geographic patterns. Journal of Herpetology 48: 38–44.

Velo-Antón G, Godinho R, Harris DJ, *et al*. (2012) Deep evolutionary lineages in a Western Mediterranean snake (*Vipera latastei*/*monticola* group) and high genetic structuring in Southern Iberian populations. Molecular Phylogenetics and Evolution 65: 965–973.

Whiteley A, McGarigal K, Schwartz M (2014) Pronounced differences in genetic structure despite overall ecological similarity for two *Ambystoma* salamanders in the same landscape. Conservation Genetics 15: 573–591.

Conclusiones generales

1. Se han caracterizado 12 y 16 nuevos marcadores microsatélites polimórficos en *Pleurodeles waltl* y en *Pelobates cultripes*, respectivamente. Algunos de estos marcadores amplificaron con éxito también en otras especies de los géneros *Pleurodeles* y *Pelobates* (8 en *P. nebulosus* y 8 en *P. varaldii*).

2. Se ha identificado mediante datos genéticos mitocondriales y nucleares un patrón genético común en las dos especies ibéricas, con una división "Este-Oeste" de sus poblaciones. En *P. waltl*, el evento vicariante responsable de esta división se produjo durante el Plio-Pleistoceno (alrededor de 3,5 Ma), mientras que en *P. cultripes* los procesos de diversificación se concentraron en los últimos 500 ka.

3. En contraste con estudios previos, las poblaciones de *P. waltl* del norte de África forman un clado bien diferenciado dentro del linaje "Este" ibérico. Las poblaciones marroquíes se habrían originado por un evento de dispersión desde la península ibérica a través del estrecho de Gibraltar durante el Pleistoceno. También se ha documentado evidencia de flujo génico post-divergencia en tiempos más recientes, lo que implica que al menos se produjeron dos eventos de dispersión transmarina en la historia evolutiva de esta especie.

4. La diversidad genética actual de *P. waltl* y *P. cultripes* está significativa y positivamente correlacionada con la intersección de los valores de favorabilidad climática entre el LIG y el LGM, de manera que las áreas históricamente más estables y favorables han funcionado como reservorios de diversidad genética.

5. En ambas especies, las poblaciones localizadas cerca del límite norte de su área de distribución presentan baja diversidad genética y ocupan zonas marginalmente favorables y caracterizadas por una menor estabilidad climática a lo largo del tiempo, especialmente en *P. cultripes*, lo que las hace más vulnerables frente a cambios climáticos a largo plazo.

6. A pesar de su elevada diferenciación genética, se encontraron pocas diferencias en la favorabilidad climática en los dos linajes intraespecíficos en *P. waltl*, consistentes con la conservación de su nicho ecológico a escala evolutiva.

7. A escala regional, se encontraron diferencias en la estructura genética de las dos especies, siendo esta más marcada y a una escala espacial más fina en *P. waltl*.

8. Tanto la altitud como la pendiente tienen un efecto de resistencia al flujo génico en las dos especies, limitando la conectividad regional entre poblaciones. Este efecto es aparente tanto a la escala filogeográfica como a la de paisaje.

9. A escala fina, en el modelado de la estructura genética de las dos especies se encontraron diferencias marcadas en el papel de la heterogeneidad y contenido en agua de la cubierta vegetal. Los resultados sugieren una cierta favorabilidad para la conectividad poblacional de ciertos tipos de vegetación y heterogeneidad estructural, ocupados principalmente por matorral mediterráneo y dehesas.

10. Las tasas de dispersión observadas a escala local resultaron bajas para las dos especies (*P. waltl* = 0,51%, *P. cultripes* = 1,23%), lo que es consistente con las diferencias observadas en la estructura genética de ambas especies a diferentes escalas.

11. No se hallaron diferencias significativas en los patrones de dispersión entre sexos en *P. cultripes*, mientras que en *P. waltl* existen evidencias tanto directas como indirectas que sugieren una mayor tasa de dispersión en hembras.

12. Se han obtenido las primeras estimas de los ratios Ne/Nc y Nb/Nc en *P. waltl* y *P. cultripes* mediante la combinación de observaciones directas de campo y aproximaciones moleculares. Ambas especies mostraron ratios similares, siendo ligeramente inferiores en *Pleurodeles* (0,21-0.24) que en *Pelobates* (0,25-0,30).

13. Los resultados obtenidos permiten sustentar medidas de conservación orientadas al diseño de corredores naturales que tengan en cuenta las características biológicas de las dos especies, sus preferencias en la selección de hábitat y su historia evolutiva, con objeto de garantizar la conservación de su diversidad genética y potencial evolutivo.

General conclusions

1. Twelve and sixteen novel microsatellite loci were isolated and characterized for *Pleurodeles waltl* and *Pelobates cultripes*, respectively. Some of these loci were also successfully amplified in other species of the genus *Pleurodeles* and *Pelobates* (8 in *P. nebulosus* and 8 in *P. varaldii*).

2. We identified a common genetic break in these two Iberian species using a mitochondrial and nuclear genetic dataset, with an "East-West" division of their populations. In *P. waltl*, this phylogeographic split occurred during the Plio-Pleistocene (about 3.5 Mya), while in *P. cultripes*, the diversification processes dated back to the Pleistocene, around 500 ka.

3. In contrast with previous studies, populations of *P. waltl* in North Africa formed a monophyletic group within the Eastern Iberian lineage. Moroccan populations would have originated after an overseas dispersal event from the Iberian Peninsula in the Pleistocene. We also found evidence of post-divergence gene flow in more recent times, implying at least two trans-marine dispersal events during the evolutionary history of this species.

4. The current genetic diversity in *P. waltl* and *P. cultripes* is significantly and positively correlated with the intersection of climatic favourability in the LIG and LGM, indicating historically stable favourable areas acted as reservoirs of genetic diversity through time.

5. In both species, populations at the northern end of their distribution show lower genetic diversity and occupy marginally favourable areas, which are characterized by low climatic stability through time. This is especially the case of *P. cultripes*, which makes this species more vulnerable to long-term climate change.

6. We found relatively minor differences in climatic favourability across intraspecific lineages in *P. waltl* is spite of deep genetic differentiation, suggesting niche conservatism on an evolutionary scale.

7. At the regional scale, differences in genetic structure were found across species, with stronger, finer-scale genetic structure in *P. waltl*.

8. Altitude and slope have a resistance effect on gene flow patterns in the two species, limiting connectivity between populations at the regional level. This effect can be detected at the phylogeographic and landscape scales.

9. At a finer scale, patterns of genetic structure in the two species were differentially affected by the heterogeneity and water content of the vegetation. We found a positive role of certain vegetation types and structural heterogeneity (mainly habitat patches of Mediterranean scrubland and open oak woodlands, or "dehesas") in facilitating population connectivity in both species.

10. We found overall congruence between the genetic structure of the two species at different spatial scales and observed dispersal rates, which were generally low (*P. waltl* = 0.51%, *P. cultripes* = 1.23%).

11. We found both direct and indirect evidence for female-biased dispersal in *P. waltl* and no evidence for sex-biased dispersal in *P. cultripes*.

12. We produced the first estimates of the Ne/Nc and Nb/Nc ratios in *P. waltl* and *P. cultripes* through the integration of field-based and molecular approaches. Both species showed similar ratios, although slightly lower in *Pleurodeles* (0.21-0.24) than in *Pelobates* (0.25-0.30).

13. Our findings can be used to design corridors connecting populations of both species, taking into account their biological characteristics, preferences in habitat selection and evolutionary history, to help preserve their genetic diversity and evolutionary potential.